TECHNICAL REPORT STANDARD TITLE PAGE

1. Report No. FHWA/TX-89+1126-3	**2. Government Accession No.**	**3. Recipient's Catalog No.**

4. Title and Subtitle

BEHAVIOR AND DESIGN OF DUCTILE MULTIPLE-ANCHOR STEEL-TO-CONCRETE CONNECTIONS

5. Report Date

March 1989

6. Performing Organization Code

7. Author(s)

R. A. Cook and R. E. Klingner

8. Performing Organization Report No.

Research Report 1126-3

9. Performing Organization Name and Address

Center for Transportation Research
The University of Texas at Austin
Austin, Texas 78712-1075

10. Work Unit No.

11. Contract or Grant No.

Research Study 3-5-87-1126

12. Sponsoring Agency Name and Address

Texas State Department of Highways and Public Transportation; Transportation Planning Division
P. O. Box 5051
Austin, Texas 78763-5051

13. Type of Report and Period Covered

Interim

14. Sponsoring Agency Code

15. Supplementary Notes

Study conducted in cooperation with the U. S. Department of Transportation, Federal Highway Administration

Research Study Title: "Design Guide for Short Anchor Bolts"

16. Abstract

The connection of steel members to concrete is a common structural feature, with applications in both highway and building construction. A typical steel-to-concrete connection includes the following: a steel attachment consisting of a baseplate welded to the attached member; the anchors that actually do the connecting; and an embedment of the anchors into the concrete. The behavior and design of these connections is not well defined by existing design standards. Steel-to-concrete connections can be divided into two categories: connections whose strength is controlled by the strength of the anchor steel; and connections whose strength is controlled by the strength of the embedment.

Based on experimental research conducted at the University of Texas at Austin, the behavior and design of steel-to-concrete connections whose strength is controlled by the strength of the anchor steel is addressed. An analytical model for calculating the strength of these connections is presented. The model is developed from experimental results and is based on limit design theory. Experimental results are reported for 44 friction tests and 46 ultimate-load tests of multiple-anchor steel-to-concrete connections loaded monotonically by various combinations of moment and shear. Test specimens included steel attachments with rigid and flexible baseplates, connected to concrete with threaded cast-in-place or retrofit (undercut and adhesive) anchors. The results of this study are incorporated into a *Design Guide for Steel-to-Concrete Connections.*

17. Key Words connection, steel-to-concrete, member, strength, attachment, structural, anchor, embedment	**18. Distribution Statement** No restrictions. This document is available to the public through the National Technical Information Service, Springfield, Virginia 22161.

19. Security Classif. (of this report) Unclassified	**20. Security Classif. (of this page)** Unclassified	**21. No. of Pages** 214	**22. Price**

Form DOT F 1700.7 (8-69)

BEHAVIOR AND DESIGN OF DUCTILE MULTIPLE-ANCHOR STEEL-TO-CONCRETE CONNECTIONS

by

R. A. COOK AND R. E. KLINGNER

Research Report No. 1126-3
Research Project 3-5-83-1126
"Design Guide for Short Anchor Bolts"

Conducted for

Texas
State Department of Highways and Public Transportation

In Cooperation with the
U.S. Department of Transportation
Federal Highway Administration

by
CENTER FOR TRANSPORTATION RESEARCH
BUREAU OF ENGINEERING RESEARCH
THE UNIVERSITY OF TEXAS AT AUSTIN

March 1989

The contents of this report reflect the views of the authors who are responsible for the facts and accuracy of the data presented herein. The contents do not necessarily reflect the official views or policies of the Federal Highway Administration. This reports does not constitute a standard, specification, or regulation.

PREFACE

Many structural details in current use by the Texas State Department of Highways and Public Transportation (SDHPT) involve the use of anchor bolts, sometimes in retrofit applications. Examples are attachment of traffic barriers to structures, attachment of bridge girders to bearing blocks, attachment of end fixtures to precast concrete components, and attachment of steel members to existing concrete. Anchors are of different types: cast-in-place, grouted, adhesive, expansion, or undercut. These anchors are now designed using procedures which are outdated and often erroneous. Recent investigations have suggested that various Texas SDHPT designs involving anchor bolts are inconsistent and possibly unconservative.

In developing more rational design procedures for such connections, it was necessary to study the behavior of multiple-anchor connections involving flexible as well as rigid baseplates. This report describes such a study. Based on the results of this study, recommendations are given for the design of ductile multiple-anchor connections to concrete.

SUMMARY

The connection of steel members to concrete is a common structural feature, with applications in both highway and building construction. A typical steel-to-concrete connection includes the following: a steel attachment consisting of a baseplate welded to the attached member; the anchors that actually do the connecting; and an embedment of the anchors into the concrete. The behavior and design of these connections is not well defined by existing design standards. Steel-to-concrete connections can be divided into two categories: connections whose strength is controlled by the strength of the anchor steel; and connections whose strength is controlled by the strength of the embedment.

Based on experimental research conducted at the University of Texas at Austin, the behavior and design of steel-to-concrete connections whose strength is controlled by the strength of the anchor steel is addressed. An analytical model for calculating the strength of these connections is presented. The model is developed from experimental results and is based on limit design theory. Experimental results are reported for 44 friction tests and 46 ultimate-load tests of multiple-anchor steel-to-concrete connections loaded monotonically by various combinations of moment and shear. Test specimens included steel attachments with rigid and flexible baseplates, connected to concrete with threaded cast-in-place or retrofit (undercut and adhesive) anchors. The results of this study are incorporated into a *Design Guide for Steel-to-Concrete Connections.*

IMPLEMENTATION

This report concerns a study of the behavior and design of ductile multiple-anchor steel-to-concrete connections. The results of this report have already been incorporated into the draft of Research Report 1126-4F *(Design Guide).* That *Design Guide* should be used by the Texas SDHPT for design, qualification, and evaluation of connections involving short anchor bolts.

TABLE OF CONTENTS

Chapter Page

1. INTRODUCTION 1
  - 1.1 General 1
  - 1.2 Scope 1
  - 1.3 Objectives 3
  - 1.4 Historical Development 4

2. BACKGROUND: BEHAVIOR AND DESIGN OF DUCTILE CONNECTIONS . . . 7
  - 2.1 Introduction 7
  - 2.2 Ductile Single-Anchor Connections 7
    - 2.2.1 Single-Anchor Connections in Tension 7
    - 2.2.2 Single-Anchor Connections in Shear 9
    - 2.2.3 Single-Anchor Connections with Tension and Shear 12
  - 2.3 Ductile Multiple-Anchor Connections 16
    - 2.3.1 Multiple-Anchor Connections with Moment and Axial Load 16
    - 2.3.2 Multiple-Anchor Connections in Shear 20
    - 2.3.3 Multiple-Anchor Connections with Moment and Shear 20
    - 2.3.4 Multiple-Anchor Connections with Moment, Axial Load, and Shear 23
  - 2.4 Design Requirements for Baseplates 23
    - 2.4.1 Baseplate Flexure 23
    - 2.4.2 Baseplate Shear 25
    - 2.4.3 Anchor/Baseplate Bearing 26
    - 2.4.4 Anchor Holes 26

3. BACKGROUND: EMBEDMENT REQUIREMENTS FOR DUCTILE CONNECTIONS 27
  - 3.1 Introduction 27
  - 3.2 Embedment Design Criteria for Ductile Connections 27
  - 3.3 Tensile Strength of the Embedment 28
    - 3.3.1 Cast-in-Place Anchors 28
    - 3.3.2 Undercut Anchors 34
    - 3.3.3 Adhesive Anchors 35
    - 3.3.4 Grouted Anchors 36
    - 3.3.5 Expansion Anchors 37
  - 3.4 Shear Strength of the Embedment 37
  - 3.5 Bearing Strength of the Embedment 41
    - 3.5.1 Anchor Bearing 41
    - 3.5.2 Baseplate Bearing 41

4. DEVELOPMENT OF EXPERIMENTAL PROGRAM 43
4.1 Objectives of Experimental Program 43
4.2 Scope 44
4.3 Development of Friction Tests 44
4.4 Development of Ultimate Load Tests 47
4.4.1 Two-Anchor Rigid Baseplate Tests 47
4.4.2 Four-Anchor Rigid Baseplate Tests 48
4.4.3 Six-Anchor Rigid Baseplate Tests 48
4.4.4 Six-Anchor Flexible Baseplate Tests 49
4.5 Development of Test Specimens 50
4.5.1 Materials 50
4.5.2 Anchor Pattern 51
4.5.3 Embedment Design Basis 53
4.5.4 Test Block Design Basis 53
4.5.5 Rigid Baseplate Design Basis 53
4.5.6 Flexible Baseplate Design Basis 53
4.6 Development of Test Setup 58
4.6.1 Description of Test Setup 58
4.6.2 Shear Load Eccentricities 59
4.6.3 Test Frame and Loading System 60
4.7 Development of Test Instrumentation 62
4.7.1 Load Measurement 62
4.7.2 Displacement and Rotation Measurement 64

5. IMPLEMENTATION OF EXPERIMENTAL PROGRAM 67
5.1 Introduction 67
5.2 Test Matrix and Test Designations 67
5.2.1 Test Matrix 67
5.2.2 Test Designations 67
5.3 Concrete Casting 67
5.4 Materials 68
5.4.1 Concrete 68
5.4.2 Anchors 69
5.5 Anchor Installation 70
5.5.1 Cast-in-Place Anchors 70
5.5.2 Undercut Anchors 70
5.5.3 Adhesive Anchors 71

5.6 Test Equipment 72
    5.6.1 Test Setup 72
    5.6.2 Instrumentation 74
    5.6.3 Data Acquisition and Reduction 74
5.7 Test Procedures 76
    5.7.1 Friction Tests 76
    5.7.2 Ultimate Load Tests 77

6. TEST RESULTS 79
6.1 Introduction 79
6.2 Friction Tests 79
6.3 Ultimate Load Tests 80
    6.3.1 Two-Anchor Rigid Baseplate Tests 87
    6.3.2 Four-Anchor Rigid Baseplate Tests 88
    6.3.3 Six-Anchor Rigid Baseplate Tests 90
    6.3.4 Six-Anchor Flexible Baseplate Tests 92

7. DISCUSSION OF TEST RESULTS 99
7.1 Introduction 99
7.2 Coefficient of Friction 99
    7.2.1 Comparison and Analysis of Test Results 99
    7.2.2 Summary: Coefficient of Friction 102
7.3 Tension/Shear Interaction Relationships 102
    7.3.1 Comparison and Analysis of Test Results 102
    7.3.2 Summary: Tension/Shear Interaction Relationships 105
7.4 Distribution of Tension and Shear among Anchors 106
    7.4.1 Comparison and Analysis of Results 106
    7.4.2 Summary: Distribution of Tension and Shear 107
7.5 Effect of Baseplate Flexibility 109
    7.5.1 Comparison and Analysis of Test Results 109
    7.5.2 Summary: Effect of Baseplate Flexibility 112

8. THEORETICAL STRENGTH OF DUCTILE MULTIPLE-ANCHOR CONNECTIONS . . . 113
8.1 Introduction . . . 113
8.2 Behavioral Model for Ductile Multiple-Anchor Connections . . . 113
8.3 Analytical Development of the Behavioral Model . . . 115
8.3.1 Critical Eccentricities . . . 116
8.3.2 Distribution of Tension . . . 118
8.3.3 Maximum Predicted Strength for Connections Dominated by Moment ($e \geq e''$) . . . 125
8.3.4 Maximum Predicted Strength for Connections Dominated by Shear ($e < e''$) . . . 126
8.3.5 Summary: Analytical Development of Behavioral Model . . . 127
8.4 Assessment of Behavioral Model . . . 127
8.4.1 Two-Anchor Pattern . . . 128
8.4.2 Four-Anchor Pattern . . . 128
8.4.3 Six-Anchor Pattern . . . 130
8.4.4 Summary: Assessment of Behavioral Model . . . 132

9. SUMMARY, CONCLUSIONS, AND RECOMMENDATIONS . . . 135
9.1 Summary . . . 135
9.2 Conclusions . . . 136
9.2.1 Conclusions from Friction Tests . . . 136
9.2.2 Conclusions from Ultimate-Load Tests . . . 136
9.3 Design Recommendations . . . 138
9.4 Recommendations for Further Research . . . 138

APPENDIX A . . . 141

APPENDIX B . . . 147

APPENDIX C . . . 169

REFERENCES . . . 191

LIST OF FIGURES

Figure Page

1.1 Typical Steel-to-Concrete Connection 2
1.2 Types of Anchors 2
2.1 Anchor Yielded in Tension 7
2.2 Anchor Yielded in Shear 9
2.3 Deformations of Welded Studs and Threaded Anchors in Shear 11
2.4 Design Approaches for Shear Transfer 13
2.5 Anchor Yielded by Combined Tension and Shear 14
2.6 Interaction Equations for Combined Tension and Shear 15
2.7 Procedure based on Working - Stress Concrete Beam Design 17
2.8 Procedure based on Linear Compressive Stress Distribution with an Assumed Maximum Compressive Stress 17
2.9 Procedure Based on Linear Compressive Stress Distribution with Compressive Reaction at the Centroid of the Compression Elements of the Attached Member . . 18
2.10 Procedure Based on Ultimate Strength Concrete Beam Design 19
2.11 Procedure Based on Baseplate Thickness 20
2.12 Probable Locations of the Compressive Reaction 21
2.13 Possible Forces on Multiple-Anchor Connections with One Row of Anchors in the Tension Zone 22
2.14 Typical Deformed Shape of "Reasonably" Flexible Baseplate to Prevent Prying . . 24
3.1 Pullout-Cone Failure 29
3.2 Blowout-Cone Failure 30
3.3 Design Pullout Cone for Cast-in-Place Anchors 30
3.4 Design Pullout Cone Limited by Free Edge 31
3.5 Projected Areas for Overlapping Cones 32
3.6 Projected Areas as Limited by Concrete Thickness 32
3.7 Design Blowout Cone 33
3.8 Design Pullout Cone for Undercut Anchors 34
3.9 Plug/Cone-Pullout Failure 35
3.10 Plug-Pullout Failure 36
3.11 Excessive Slip Failure with Shallow Pullout Cone 38
3.12 Pryout Cone Failure 38
3.13 Pushout Cone Failure 39
3.14 Design Pushout Cone 40
4.1 Typical loading condition and measured values 45

4.2 Frictional forces on the baseplate prior to anchor bearing 46
4.3 Free body diagram of a two-anchor rigid baseplate specimen 47
4.4 Free body diagram of a four-anchor rigid baseplate specimen 48
4.5 Free body diagram of a six-anchor rigid baseplate specimen 49
4.6 Free body diagram of a six-anchor flexible baseplate test 50
4.7 General anchor pattern and baseplate dimensions (all dimensions in inches) 52
4.8 Typical test block 54
4.9 Steel attachment for rigid baseplate tests 55
4.10 Steel attachment for flexible baseplate tests 56
4.11 Design basis for flexible baseplate tests 57
4.12 Schematic Diagram of Test Setup 58
4.13 Schematic diagram of anchor load cell and adapter 63
4.14 Schematic diagram of slip measurement 64
4.15 Schematic diagram of rotation measurement for rigid baseplate tests 65
4.16 Schematic diagram of vertical displacement measurement for flexible baseplate tests 66
5.1 Test Block and Forms 69
5.2 Template and Bracing for Cast-in-Place Specimens 71
5.3 Test Setup for a Typical Rigid Baseplate Test 73
5.4 Schematic Diagram of Hydraulic Loading System 73
5.5 Anchor Load Cell and Adapter 74
5.6 Instrumentation used for rigid-baseplate tests 75
5.7 Instrumentation used for flexible baseplate tests 75
6.1 Typical Results for Mu-vs-Slip Recorded by the HP DAS and by the HP Plotter Data Acquisition Systems 81
6.2 Typical High and Low Values for the Coefficient of Friction 83
6.3 Typical Anchor Deformations for Multiple-Anchor Baseplate Tests 85
6.3 – continued 86
6.4 Severe Surface Spalling for Adhesive Anchors 87
6.5 Typical Surface Spalling for Undercut Anchors 88
6.6 Sleeves from Undercut anchors Failing in Shear 89
6.7 Typical Load-Displacement Diagram for Two-Anchor Rigid Baseplate Test Dominated by Anchor Shear 91
6.8 Typical Load-Displacement Diagram for Two-Anchor Rigid Baseplate Test Dominated by Anchor Tension 91
6.9 Typical Load-Displacement Diagram for Four-Anchor Rigid Baseplate Test Dominated by Anchor Shear 93
6.10 Typical Load-Displacement Diagram for Four-Anchor Rigid Baseplate Test Dominated by Anchor Tension 93

6.11 Typical Load-Displacement Diagram for Six-Anchor Rigid Baseplate Test Dominated by Anchor Shear . . . 95
6.12 Typical Load-Displacement Diagram for Six-Anchor Rigid Baseplate Test Dominated by Anchor Tension . . . 95
6.13 Typical Load-Displacement Diagram for Six-Anchor Flexible Baseplate Test . . . 96
6.14 Typical Vertical Displacements Along the Centerline of a Flexible Baseplate . . . 97
6.15 Typical Contact Zone for Flexible Baseplate Test . . . 97
7.1 Frequency Distribution for Friction Tests . . . 100
7.2 Effect of Compressive Force on the Coefficient of Friction . . . 100
7.3 Effect of Previous Testing on the Coefficient of Friction . . . 101
7.4 Tension/Shear Interaction for Cast-in-Place Anchors . . . 103
7.5 Tension/Shear Interaction for Adhesive Anchors . . . 104
7.6 Tension/Shear Interaction for Undercut Anchors . . . 105
7.7 Typical Results for Distribution of Tensile Forces Prior to Redistribution . . . 108
7.8 Calculated Location of the Compressive Reaction for Flexible Baseplate Tests . . . 110
7.9 Effect of Baseplate Flexibility on the Location of the Compressive Reaction . . . 111
8.1 Possible Distribution of Forces on a Multiple-Anchor Connection . . . 113
8.2 Ranges of Behavior for Ductile Multiple-Anchor Connections . . . 115
8.3 Forces on a Multiple-Anchor Connection with Shear Load Eccentricity Equal to e' . 116
8.4 Forces on a Multiple-Anchor Connection with Shear Load Eccentricity Equal to e'' . 117
8.5 Limiting Location for Tension Anchors . . . 119
8.6 Example of Connection Used to Assess the Maximum Predicted Strength . . . 120
8.7 Comparison of Predicted Strengths with Elliptical Tension/Shear Interaction . . . 123
8.8 Comparison of Predicted Strengths with Linear Tension/Shear Interaction . . . 124
8.9 Possible Distribution of Forces on a Multiple-Anchor Connection for Maximum Predicted Strength . . . 125
8.10 Test Results Versus Predicted Strengths for Two-Anchor Rigid Baseplate Specimens 129
8.11 Test Results Versus Predicted Strengths for Four-Anchor Rigid Baseplate Specimens 131
8.12 Test Results Versus Predicted Strengths for Six-Anchor Rigid Baseplate Specimens 133
A.1 Approximate Projected Areas for Overlapping Cones . . . 142
A.2 Typical Quadrant of Overlap for Closely Spaced Anchors . . . 144
A.3 Reduction Factor for Overlapping Failure Cones . . . 145

LIST OF TABLES

Table Page

2.1 Summary of Procedures for Calculating the Design Tensile Strength of the Steel . . 9

2.2 Summary of Previous Experimental Results for Average Shear Strength of the Steel 10

2.3 Summary of Procedures for Calculating the Design Shear Strength of the Steel 14

2.4 Summary of Published Values for the Coefficient of Friction between Steel and Concrete 23

4.1 Design Loads for Test Frame and Loading System 61

5.1 Test Matrix 68

5.2 Concrete Cylinder Strengths 69

5.3 Anchor Tensile Strength from Universal Testing Machine 70

6.1 Maximum Coefficent of Friction Recorded on Separate Data Acquisition Systems . 80

6.2 Summary of Friction Tests 82

6.3 Maximum Recorded Applied Load on Separate Data Acquisition Systems 84

6.4 Two-Anchor Rigid Baseplate Test Results 90

6.5 Four-Anchor Rigid Baseplate Test Results 92

6.6 Six-Anchor Rigid Baseplate Test Results 94

6.7 Six-Anchor Flexible Baseplate Test Results 96

7.1 Maximum Anchor Tension in Six-Anchor Tests 107

8.1 Test Results versus Predicted Strengths for Two-Anchor Specimens 130

8.2 Test Results versus Predicted Strengths for Four-Anchor Specimens 132

8.3 Test Results versus Predicted Strengths for Six-Anchor Specimens 134

1. INTRODUCTION

1.1 General

The connection of steel members to concrete is a common structural feature, with applications in both highway and building construction. A typical steel-to-concrete connection includes a steel attachment consisting of a baseplate welded to the attached member, the anchors that actually do the connecting, and an embedment of the anchors into the concrete. Figure 1.1 shows a typical steel-to-concrete connection. The anchors used in the connection can be either cast-in-place or retrofit. A typical cast-in-place anchor is a headed anchor installed in position before the concrete is placed. Retrofit anchors are installed after the concrete has hardened, and can be either undercut, adhesive, grouted, or expansion. Figure 1.2 shows typical types of anchors.

The procedures currently used by the Texas State Department of Highways and Public Transportation (SDHPT) and other organizations for the design of steel-to-concrete connections are varied and inconsistent. A consistent, rational design procedure for steel-to-concrete connections that covers both cast-in-place and retrofit anchors is needed.

1.2 Scope

To determine the ultimate strength of a steel-to-concrete connection, two separate strengths must be considered:

1) The strength of the steel

2) The strength of the embedment

The lesser of these two strengths represents the ultimate strength of the connection. In the simple case of a single cast-in-place headed anchor loaded in tension, the strength of the steel is the tensile strength of the anchor itself; the strength of the embedment is related to the embedded length of the anchor and the tensile strength of the concrete. If the anchor is embedded far enough into the concrete, the strength of the steel controls, and the anchor can be described as ductile.

For the purposes of this study, ductility is defined as the ability of a structural component to undergo significant inelastic deformation at predictable loads, and without significant loss of strength. A connection to concrete is ductile if its ultimate strength is controlled by the strength of the steel. A ductile connection to concrete fails by yielding and fracture of the anchors. A connection to concrete is non-ductile if its ultimate strength is controlled by the strength of the embedment. Non-ductile connections fail by brittle fracture of the concrete in tension, and by unpredictable concrete- related failure modes such as anchor slip without steel fracture.

To develop a comprehensive design procedure for steel-to-concrete connections, rational methods must be developed for calculating the strength of the steel and of the embedment.

This study is part of the Texas SDHPT Project 1126, "Design Guide for Short Anchor Bolts." The purpose of Project 1126 was to develop a design guide covering all aspects of design for steel-to-concrete connections using both cast-in-place and retrofit anchors. The project was divided into four parts:

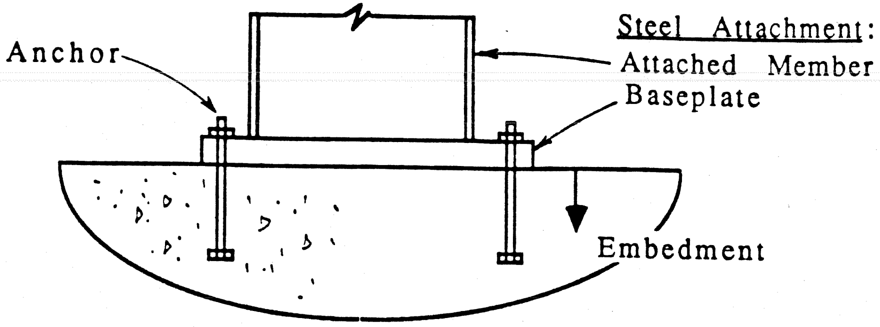
Anchor
Steel Attachment:
Attached Member
Baseplate
Embedment

Figure 1.1 Typical Steel-to-Concrete Connection

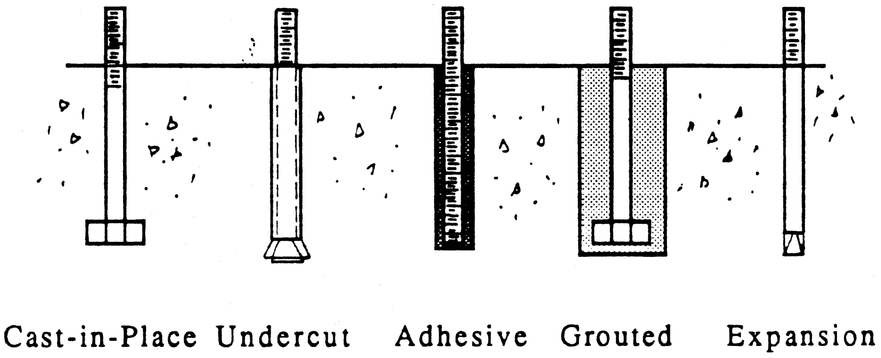
Cast-in-Place
Undercut
Adhesive
Grouted
Expansion

Figure 1.2 Types of Anchors

1) Behavior of single cast-in-place and retrofit anchors in tension [1].
2) Behavior and design of single and multiple adhesive anchors in tension [2].
3) Behavior and design of ductile multiple-anchor connections to concrete under combined loads.
4) Design guide for steel-to-concrete connections [3].

The first part of the project [1] dealt with defining what types of single anchors are capable of ductile behavior. Cast-in-place and retrofit anchors were embedded based on existing design procedures for cast-in-place headed anchors [4,5]. The results of the first part of the project indicated that cast-in-place, grouted, undercut, and some adhesive and expansion anchors could be considered ductile, but that existing design procedures for calculating the strength of the embedment for cast-in-place headed anchors were not applicable to adhesive anchors.

The second part of the project [2] concerned the tensile behavior of both single and multiple adhesive anchors. The results of that study provided methods for evaluating the strength of the embedment for adhesive anchors.

This part of the project dealt with the behavior and design of ductile multiple-anchor connections to concrete under combined loads. In this study, only ductile (ultimate strength controlled by the strength of the steel) multiple-anchor connections to concrete were considered. All non-ductile failure modes were precluded based on existing design procedures for cast-in-place multiple-anchor connections [4,5], and on information obtained from the first part of the project [1].

The fourth and final part of the project [3] incorporated the results of the first three parts, plus information from other design documents [4,5,6], into a design guide for steel-to-concrete connections using cast-in-place or retrofit anchors.

1.3 OBJECTIVES

The overall objectives of this study were:

1) To determine the characteristic behavior of ductile multiple- anchor connections to concrete.
2) To develop a rational design procedure for calculating the strength of the steel in multiple-anchor connections to concrete.

For single-anchor connections in tension, the strength of the steel is simply the tensile strength of the anchor. In a multiple-anchor connection subjected to combined loads the strength of the steel is dependent on many variables, such as the following, each of which was considered in this study:

- loading (axial,moment,shear)
- size of the steel attachment
- size, number, location, and type of anchors
- coefficient of friction between the baseplate and the concrete

- tension/shear interaction for an anchor
- distribution of shear among the anchors
- distribution of tension among the anchors
- flexibility of the baseplate

1.4 Historical Development

Historically, the design of steel-to-concrete connections has occupied a "no-man's land" between steel design codes and concrete design codes. Although steel-to-concrete connections occur in many types of construction, attempts to define rational design procedures did not begin until about 1960. Prior to 1960 the main research dealing with steel-to-concrete connections was a study conducted by Abrams [7] in 1913 which involved embedded length requirements for plain reinforcing bars anchored with threaded nuts.

During the 1960's the majority of the research on steel-to-concrete connections dealt with connections using welded studs [8-11]. Design procedures developed from this research were included in the 1971 Prestressed Concrete Institute (PCI) *Design Handbook* [12], the 1973 PCI *Manual on Design of Connections* [13], and in a 1971 report by KSM Welding Systems [14]. Other research performed during the 1960's on steel-to-concrete connections [15-17] dealt with various types of cast-in-place anchors loaded in tension and shear.

In the early 1970's, further research [18,19] on steel-to-concrete connections using welded studs led to more comprehensive design procedures. These were published in 1974 in the form of a design report by TRW Nelson Division [20]. Most of the design provisions in this report were incorporated into later PCI design documents [21,22]. These design provisions are still in use today for steel-to-concrete connections using welded studs, and are given in the 1985 PCI *Design Handbook* [23].

By the mid 1970's, steel-to-concrete connections utilizing various types of cast-in-place and expansion anchors were being used extensively in critical applications at nuclear power facilities. Safety concerns at these facilities led to research [24,25] into the behavior of steel-to-concrete connections using various types of threaded anchors. Two design documents were issued as a result of this research and of the previous research on welded studs. In 1975 the Tennessee Valley Authority (TVA) issued a design guide, *TVA DS- C6.1* [26], for connections to concrete. In 1979 a supplement to *ACI 349- 76* [27] was issued which contained an appendix for the design of connections to concrete (*ACI 349 Appendix B*). Each of these documents covered cast- in-place and expansion anchors. Both documents recognized the fact that ductile failure modes were preferred, although non-ductile failure modes were acceptable if high factors of safety were used in the design. A modified version of *ACI 349-76 (Appendix B)* for non-nuclear applications was published as a "Guide to the Design of Anchor Bolts and Other Steel Embedments" [28] in the July 1981 edition of *Concrete International.*

Most of the research conducted prior to 1980 [8-11,15-19,24,25,29- 31] dealt with single-anchor and multiple-anchor connections loaded in pure tension, in pure shear, or combined tension and shear. Two papers by Klingner and Mendonca [32,33], published in 1982, compared the strength formulas for tension and shear in the existing design documents [20,21,22,26,27] with actual test results from much of the previous research [8-10,18,19,24,25,29,31]. They concluded that the best procedures for calculating the strength of the steel were those found in the 1977 PCI *Manual for Structural Design* [21] while the strength of the embedment could best be calculated from the procedures in *ACI 349-76* [27].

Since the late 1970's additional types of retrofit anchors have been introduced, most noticeably undercut anchors, adhesive anchors, and improved expansion anchors. Additional research [34-46] has been performed on cast-in- place, undercut, and expansion anchors loaded in tension, shear, and combined tension and shear. Some of the results of this research led to revisions of both *TVA DS-C6.1* [26] and *ACI 349-76* [27]. The current revisions of these documents are *TVA DS-C1.7.1* [5] and *ACI 349-85* [4]. Both of these documents were developed for application in nuclear facilities where environmental concerns preclude the use of adhesive anchors. Neither document addresses this type of anchor. Recent research [1,2] has shown that adhesive anchors are suitable for steel-to-concrete connections. Adhesive anchors have applications in both highway and building construction.

During the late 1970's and 1980's several research projects [47-56] dealt with multiple-anchor steel-to-concrete connections subjected to moment and shear, or moment and axial load. The significant aspect of these studies was their deviation from the pure tension, pure shear, and combined tension and shear loadings of previous research. This research considered either connections between concrete and a steel cantilever beam with an eccentric shear load at a large eccentricity and no axial load [47-51], or connections between concrete and a steel column with an eccentric axial compression load and no shear [52,53]. Two of the research programs studied both types of connection [54,55]. A notable exception to these two types of connection was tested in a research project conducted by Hawkins, Mitchell, and Roeder [56]. This project studied welded stud connections between concrete and a cantilever steel beam, loaded by an eccentric shear acting at various eccentricities.

Two papers discussing the behavior and design of steel-to-concrete connections were published in the mid 1980's. In 1985 Marsh and Burdette [57] published a paper which discussed the behavior and design of single-anchor steel- to-concrete connections. In 1987 DeWolf [58] published a paper which discussed the behavior and design of steel column-to-concrete connections.

2. BACKGROUND: BEHAVIOR AND DESIGN OF DUCTILE CONNECTIONS

2.1 Introduction

The strength of a ductile connection is controlled by the strength of the steel. In this chapter, previous research and current design procedures dealing with the strength of the steel in steel-to-concrete connections are discussed. Background information related to the embedment requirements for ductile connections is presented in Chapter 3.

2.2 Ductile Single-Anchor Connections

In this section; the failure mechanisms, average strengths, and design strengths of the steel for single-anchor connections are discussed. The design strengths presented in this section are taken from *ACI 349-85* [4], *TVA DS-C6.1* [26], the 1985 PCI *Design Handbook* [23], and the AISC *LRFD Specification* [6]. These specifications are based on ultimate strength design procedures, sometimes referred to as strength design, or as load and resistance factor design.

2.2.1 Single-Anchor Connections in Tension. The steel failure mechanism for single-anchor connections in tension is usually characterized by yielding and fracture of the threaded portion of the anchor. Fig. 2.1 shows the deformed shape of an anchor that has yielded in tension. Anchors without threads (such as welded studs) and anchors with upset threads typically fail in the shank of the anchor.

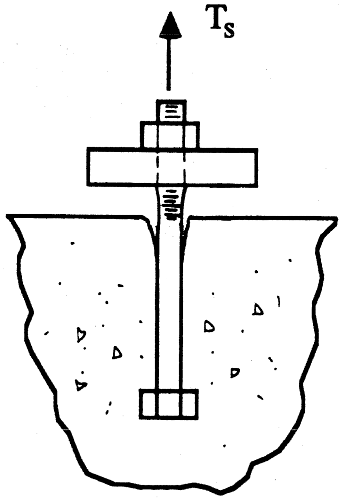

Figure 2.1 Anchor Yielded in Tension

The average tensile strength of the steel for single-anchor connections is dependent on the effective stress area of the anchor and the tensile strength of the type of steel used for the anchor:

$$T_{ut} = A_s F_{ut} \tag{2-1}$$

where: T_{ut} = average tensile strength of the steel

A_s = effective stress area of the anchor

F_{ut} = average tensile strength of the type of steel used for the anchor

The effective stress area of the anchor is the gross area of the anchor shank for welded studs and anchors with upset threads. The effective stress area for threaded anchors is the tensile stress area as defined by Slaughter [59] and adopted by the American National Standards Institute (ANSI) in *ANSI B1.1*. The tensile stress area is based on a mean area using the average of the root and pitch diameters of the threads. The tensile stress area for threaded anchors as given in *ANSI B1.1* is:

$$\textit{Tensile stress area} = 0.7854(d_b - 0.9743/n)^2 \tag{2-2}$$

where: d_b = nominal anchor diameter

n = number of threads per inch

It should be noted that there were slight changes in the basic root and pitch diameters of threads between *ANSI B1.1-1960* and *ANSI B1.1-1974*. The tensile stress area as given in Eq. (2-2) is no longer exactly equal to an average area based on the mean of the root and pitch diameters, but the difference is insignificant.

The average tensile strength of steel exceeds the minimum specified tensile strength given in the applicable American Society for Testing and Materials (ASTM) Specifications. Kulak, Fisher, and Struik [60] report that for ASTM A325 bolts (1/2- through 1-inch diameter) the average tensile strength exceeds the minimum specified tensile strength by 18%, with a standard deviation of 4.5%. They also report that for ASTM A490 bolts the average tensile strength exceeds the minimum specified tensile strength by 10%, with a standard deviation of 3.5%. The ASTM A490 bolts have a smaller difference between the minimum specified strength and the average tensile strength than the ASTM A325 bolts, since the ASTM A490 specification includes a maximum as well as a minimum limit on tensile strength. Tests results reported by Collins and Klingner [1] and Doerr and Klingner [2] indicate that for 5/8-inch ASTM A193-B7 threaded rods the average tensile strength exceeds the minimum specified tensile strength by 10%, with a standard deviation of 3.0%.

Table 2.1 Summary of Procedures for Calculating the Design Tensile Strength of the Steel

Reference	Type of Anchor	Nominal Strength[12] T_n	Strength Reduction Factor ϕ
PCI[3] [23]	Stud	$0.9\ A_s\ F_y$	1.00
ACI [4]	Threaded or Stud	$A_s\ F_y$	0.90
TVA [26]	Threaded or Stud	$A_s\ F_y$	0.90
AISC[4] [6]	Threaded	$A_s\ F_u$	0.75

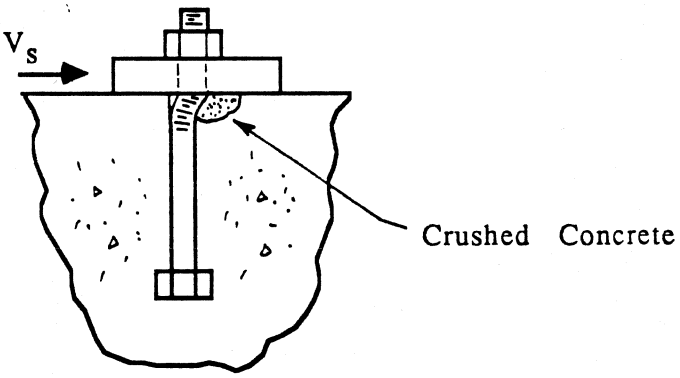

Figure 2.2 Anchor Yielded in Shear

Current procedures to determine the design tensile strength of the steel, $\phi\ T_n$, using ultimate strength design are summarized in Table 2.1.

2.2.2 Single-Anchor Connections in Shear. The steel failure mechanism for single-anchor connections in shear is usually characterized by yielding and fracture of the anchor at the shear plane due to kinking and bending. Local crushing of the concrete occurs but does not limit the strength of the anchor. Fig. 2.2 shows the deformed shape of an anchor, with threads in the shear plane, that has yielded in shear.

Welded studs and threaded anchors behave differently from one another in shear. Fig. 2.3 shows the differences in deformations for threaded anchors and welded studs. The difference in behavior is due to the fixity provided by the weld between the stud and the baseplate.

Table 2.2 provides a summary of previous experimental results for the average shear strength of the steel, V_{ut}. The average shear strength of the steel, V_{ut}, may be expressed as:

Table 2.2 Summary of Previous Experimental Results for Average Shear Strength of the Steel

Reference	Shear Plane	Average Strength[1,2] V_{ut}	Test Method[3]
Shoup, et al. [11]	Shank	$A_s\ F_{ut}$	Stud Steel/Conc.
McMackin, et al. [19]	Shank	$A_s\ F_{ut}$	Stud Steel/Conc.
Klingner, et al. [31]	Shank	$0.75\ A_s\ F_{ut}$	Steel/Conc.
Chesson, et al. [61]	Threads Threads	$0.64\ A_s F_{ut}$ $0.55\ A_s\ F_{ut}$	Steel/Steel A325 A354 BD
Kulak, et al. [60]	Threads	$0.62\ A_s\ F_{ut}$	Steel/Steel
TVA [24]	Unknown	$0.53\ A_s\ F_{ut}$	Steel/ Grout/Conc.
Burdette, et al. [42]	Threads	$0.65\ A_s\ F_{ut}$	Steel/Conc. Undercut Anc.

Note:

1. The average shear strength given in this table is based on the area of the anchor in the shear plane. For the shear plane in the shank this is the gross area of the anchor. For the shear plane in the threads this is the tensile stress area as given in *ANSI B1.1*.
2. F_{ut} is the average tensile strength of the anchor steel.
3. Steel/Conc. represents tests with the shear plane between a steel plate and concrete. Steel/Steel represents tests with the shear plane between two steel plates. Steel/Grout/Conc. represents tests with a grout layer between the steel plate and concrete.

$$V_{ut} = \gamma\ A_s\ F_{ut} \qquad (2-3)$$

$$V_{ut} = \gamma\ T_{ut}$$

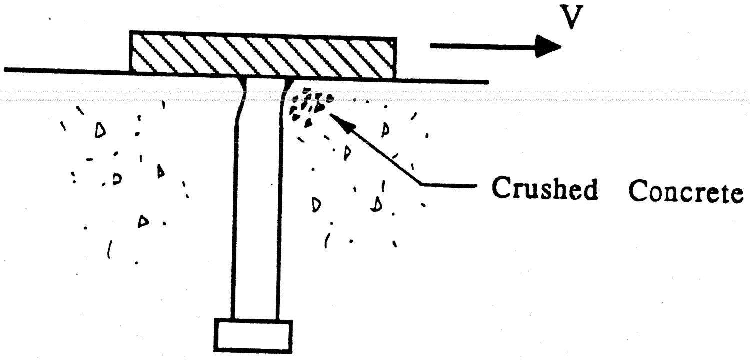
V
Crushed Concrete

WELDED STUDS

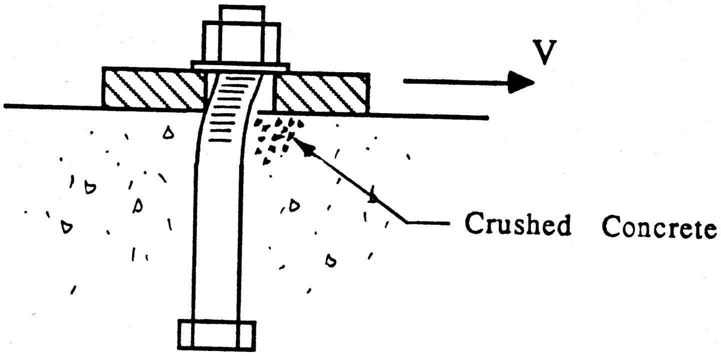
V
Crushed Concrete

THREADED ANCHORS

Figure 2.3 Deformations of Welded Studs and Threaded Anchors in Shear

As indicated by Table 2.2, the ratio, γ, of the average shear strength of the steel, V_{ut}, to the average tensile strength of the steel, T_{ut}, has been reported as 1.0 for welded studs, 0.75 for threaded anchors with the shear plane in the shank, and 0.55 to 0.65 for threaded anchors with the shear plane in the threads.

Two design approaches exist for shear transfer in single-anchor connections (Fig. 2.4):

1) *Shear Transfer by Bearing on the Anchor*: This approach is based on the assumption that shear is transferred directly by bearing on the anchor (sometimes called "dowel action"). This approach is used by *TVA DS-C6.1* [26], the 1985 PCI *Design Handbook* [23], and the AISC *LRFD Specification* [6].

2) *Shear Transfer by Shear Friction*: This approach is based on the assumption that shear is transferred by a frictional force which develops between the steel plate and the concrete surface. The frictional force is caused by the anchor pushing a spalled wedge of concrete upward against the steel plate. This upward movement causes tension in the anchor, which produces a compressive force and therefore a frictional force at the wedge/plate interface. The frictional force is equal to the tensile force in the anchor multiplied by the shear-friction coefficient. The anchor is assumed to carry tension only. This approach is used by *ACI 349-85* [4].

The shear-friction mechanism, as described above, has not been observed in experimental studies of steel-to-concrete connections with anchors. Klingner, Mendonca, and Malik [31] found that the plate rotated away from the concrete and prevented the confinement required for the shear-friction mechanism as described above.

The reason for this discrepancy is apparent when the basis for the shear- friction coefficients used by *ACI 349-85* [4] is considered. The shear- friction design approach was developed by Birkeland and Birkeland [62] as a design aid for precast concrete connections, such as corbels and ledger beam bearings. Hofbeck, Ibrahim, and Mattock [63] and Mattock and Hawkins [64] performed several tests of concrete specimens with cracked and uncracked concrete in the shear plane. Reinforcement was provided normal to the shear plane. The shear-friction coefficient was determined by dividing the shear strength of the specimen by the yield strength of the reinforcement. No separation of frictional shear resistance and shear resistance by dowel action was attempted. The resulting shear-friction coefficient determined by these tests is an "apparent" coefficient of friction that includes the effects both of dowel action and frictional resistance.

The shear-friction coefficients used by *ACI 349-85* [4] were determined in this manner. They are not the same as the coefficient of friction between two materials. Both experimental studies [63,64] indicate that dowel action is significant for pre-existing cracks in the shear plane. This would be especially true when the pre-existing crack is between a steel plate and hardened concrete. In this case dowel action is dominant, and the apparent coefficient of friction is really a measure of the shear strength of the anchors.

Current procedures to determine the design shear strength of the steel, ϕV_n, using ultimate strength design are summarized in Table 2.3.

2.2.3 Single-Anchor Connections with Tension and Shear. The steel failure mechanism for single-anchor connections in combined tension and shear is characterized by yielding and fracture

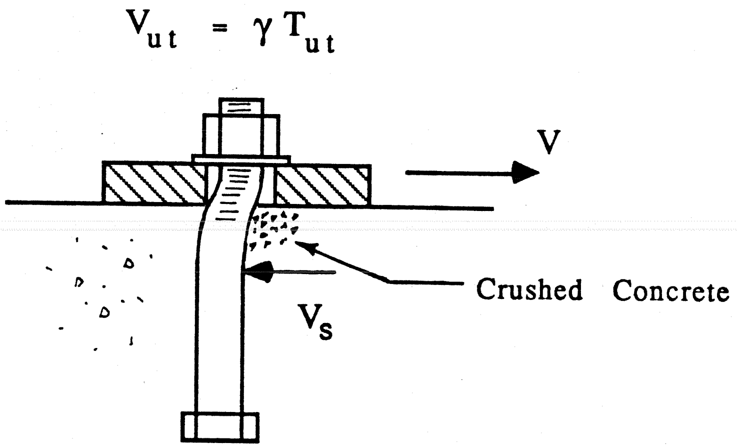
Vut = γ Tut
V
Crushed Concrete
Vs

SHEAR TRANSFER BY BEARING ON THE ANCHOR

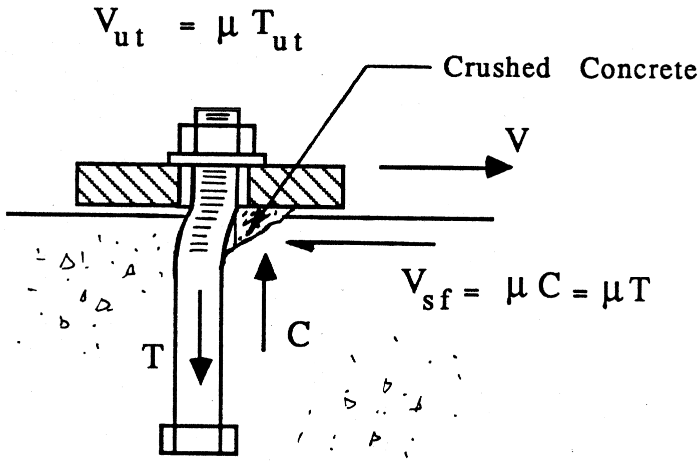
Vut = μ Tut
Crushed Concrete
V
Vsf = μ C = μ T
T
C

SHEAR TRANSFER BY SHEAR FRICTION

Figure 2.4 Design Approaches for Shear Transfer

Table 2.3 Summary of Procedures for Calculating the Design Shear Strength of the Steel

Reference	Shear Plane	Nominal Strength[12] V_n	Strength Reduction Factor ϕ
PCI[3] [23]	Shank	$0.75\ A_s\ F_y$	1.00
ACI[4] [4]	Threads or Shank	$0.7\ A_s\ F_y$	0.85
TVA[5] [26]	Threads or Shank	$0.67\ A_s\ F_y$	0.90
AISC[6] [6]	Threads or Shank	$0.6\ A_s\ F_u$	0.65

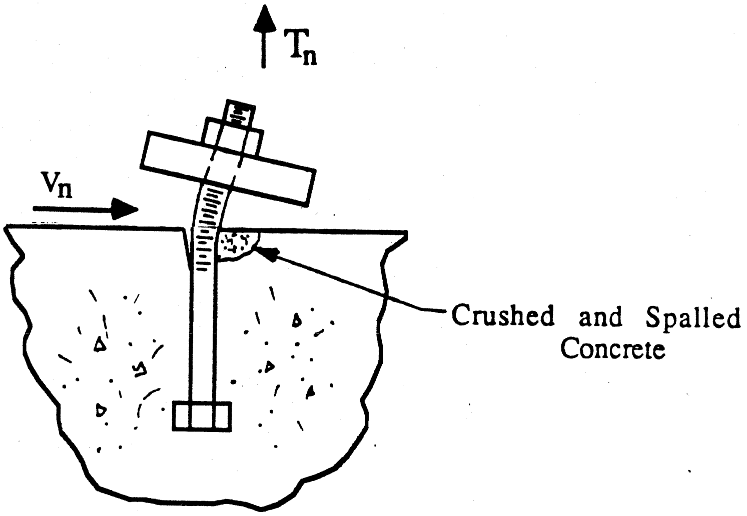

Figure 2.5 Anchor Yielded by Combined Tension and Shear

of the anchor due to tension, kinking, and bending. Fig. 2.5 shows a typical deformed shape for a threaded anchor in tension and shear.

The general form of the tension/shear interaction equation is:

$$(T\ /\ T_{ut})^n \quad + \quad (V\ /\ V_{ut})^n \quad = \quad 1 \tag{2-4}$$

where: $T =$ the tension load on the anchor

V = the shear load on the anchor

T_{ut} = the average tensile strength of the anchor

V_{ut} = the average shear strength of the anchor

n = an empirically determined exponent, equal to 1 for linear interaction, and 2 for elliptical interaction.

For welded studs, McMackin, Slutter, and Fisher [19] found that an interaction equation between linear and elliptical ($n = 5/3$) provided the best fit to the test data. For anchors tested in steel-to-steel connections, Chesson, Faustino, and Munse [61] and Kulak, Fisher, and Struik [60] determined that an elliptical interaction equation ($n = 2$) was appropriate. For anchors tested in steel-to-concrete connections, TVA *CEB 75-32* [24] and Burdette [36] found that a linear interaction ($n = 1$) produced a conservative fit to the test data.

Fig. 2.6 shows the curves of Eq. (2-4) for $n = 1, 5/3$, and 2.

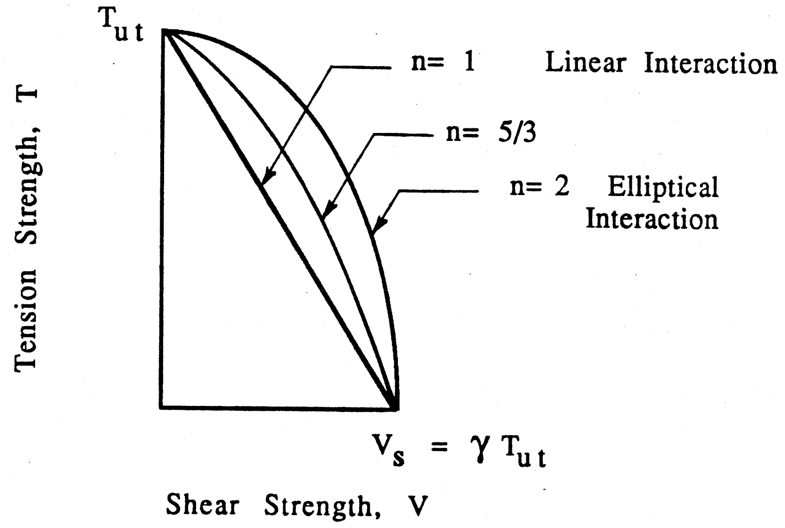

Figure 2.6 Interaction Equations for Combined Tension and Shear

Current procedures for evaluating the design strength of the steel for single-anchor connections in combined tension and shear are based on the interaction equation given by Eq. (2-4), except that the design strengths for tension, $\phi\ T_n$, and for shear, $\phi\ V_n$, are used in place of the average strengths, T_{ut} and V_{ut}. The design procedures are:

1) *1985 PCI Design Handbook [23]*: For welded studs in steel- to-concrete connections an elliptical tension/shear interaction ($n = 2$) is used.

2) *ACI 349-85 [4]*: For welded studs and threaded anchors in steel-to-concrete connections a linear tension/shear interaction (n = 1) is used.

3) *TVA DS-C6.1 [26]*: For welded studs and threaded anchors in steel-to-concrete connections a linear tension/shear interaction (n = 1) is used.

4) *AISC LRFD Specification [6]*: For threaded anchors in steel-to-steel connections, an elliptical tension/shear interaction (n = 2) provides the basis for the tri-linear design provisions given in the *Specification*.

2.3 Ductile Multiple-Anchor Connections

In this section, various procedures for calculating the strength of the steel in multiple-anchor connections are discussed. Several procedures have been proposed, but few experimental results are available to verify the procedures. The purpose of this study was to obtain experimental results that would define the behavior of ductile multiple-anchor connections, and which could be used to develop design guidelines for calculating the strength of the steel in this type of connection.

2.3.1 Multiple-Anchor Connections with Moment and Axial Load. This deals with evaluating the forces normal to the steel/concrete interface. The most important part of the normal force evaluation is to determine the tensile forces in the anchors. The tensile forces in the anchors are dependent on the location of the compressive reaction due to the applied moment and axial load. In connections with more than one row of tension anchors, the tensile forces in the anchors are also dependent on the distribution of tension among the rows. Several procedures have been proposed:

1) *Procedure Based on Working-Stress Concrete Beam Design*: This procedure assumes a linear variation of stress and strain at the steel/concrete interface. This is shown schematically in Fig. 2.7 for the case of moment only. This procedure has been proposed by Blodgett [65]. In experimental work on cantilever beams, Hawkins, Mitchell, and Roeder [56] found that this procedure is likely to overestimate the tensile forces in the anchors at failure. This procedure can be applied to connections with more than one row of tension anchors.

2) *Procedure Based on Linear Compressive Stress Distribution with an Assumed Maximum Compressive Stress*: This procedure assumes a linear compressive stress distribution, with the compressive stress at the toe of the baseplate equal to the allowable compressive stress. This is shown schematically in Fig. 2.8 for the case of moment only. This procedure has been proposed by Gaylord and Gaylord [66], Tall et al. [67], and Miatra [68]. In experimental work on eccentrically loaded columns, DeWolf and Sarisley [52] and Thambiratnam and Paramasivam [53] found that this procedure produced conservative results in the working load range. DeWolf and Sarisley [52], who tested their specimens to failure of either the anchor steel or the concrete in bearing, preferred the ultimate strength concrete beam design procedure for calculating the ultimate strength of the connection. It is not clear how to apply this procedure to connections with more than one row of tension anchors.

3) *Procedure Based on Linear Compressive Stress Distribution with Compressive Reaction at the Centroid of the Compression Elements of the Attached Member*: This procedure is

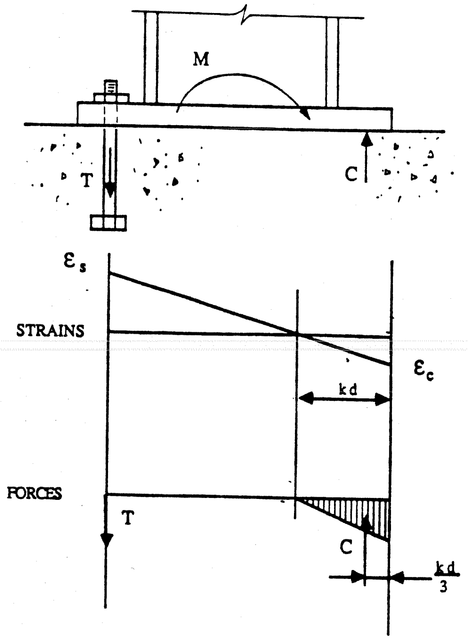
M
T
C
ε_s
STRAINS
ε_c
kd
FORCES
T
C
$\frac{kd}{3}$

Figure 2.7 Procedure based on Working - Stress Concrete Beam Design

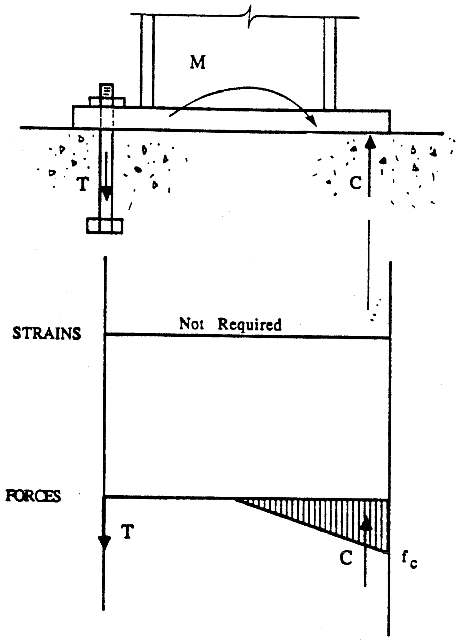
M
T
C
STRAINS
Not Required
FORCES
T
C
f_c

Figure 2.8 Procedure based on Linear Compressive Stress Distribution with an Assumed Maximum Compressive Stress

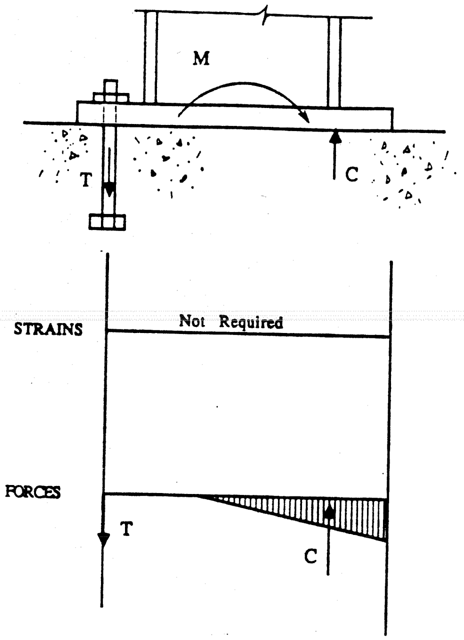

Figure 2.9 Procedure Based on Linear Compressive Stress Distribution with Compressive Reaction at the Centroid of the Compression Elements of the Attached Member

based on the assumption that the compressive reaction is located at the centroid of the compression elements of the attached member. This is shown schematically in Fig. 2.9 for the case of moment only. This procedure has been proposed by Blodgett [65], Salmon and Johnson [69], and Shipp and Haninger [70]. No experimental work has been correlated with this procedure. It is not clear how to apply this procedure to connections with more than one row of tension anchors.

4) *Procedure Based on Ultimate Strength Concrete Beam Design*: This procedure is based on the assumption of a linear variation of strain with a compressive stress distribution, the same as that used for the ultimate-strength design of reinforced concrete. This is shown schematically in Fig. 2.10 for the case of moment only. This procedure has been proposed by Gaylord and Gaylord [66] and Armstrong, Klingner, and Steves [51]. This procedure is suggested by some current design standards including *ACI 349-85* [4] and the 1985 PCI *Design Handbook* [23]. In experimental work on cantilever beams, Picard and Beaulieu [55] found that this procedure produced conservative results. In experimental work on eccentrically loaded columns, DeWolf and Sarisley [52] found that this procedure provided reasonable results for ultimate load prediction if the assumed bearing stress is not limited to 0.85 f'_c when the baseplate is away from a free edge of the concrete. They suggest

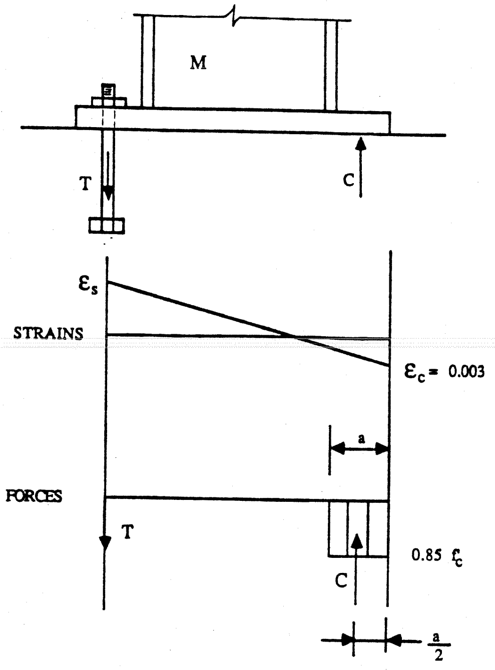

Figure 2.10 Procedure Based on Ultimate Strength Concrete Beam Design

that the effects of concrete confinement be included in the design. This procedure can be applied to connections with more than one row of tension anchors.

5) *Procedure Based on Baseplate Thickness*: In this procedure, the compressive reaction is located based on the flexibility of the baseplate. This procedure has been proposed by TVA [48,49,50] as a result of experimental work on cantilever beams. TVA *CEB 78-21* [48] provides a detailed equation based on elastic behavior of the anchors and the portions of the baseplate extending past the attached member. The concrete and portion of the baseplate welded to the attached member are considered to be rigid in this formulation. The equation is not applicable if the anchors or baseplate yield. TVA *CEB 79-18* [49] and TVA *CEB 80-1* [50] locate the compressive reaction 2 plate thicknesses from the edge of the compression element of the attached member. This is an empirical procedure based on tests of cantilever beams with flexible baseplates. This procedure is suggested by *TVA DS-C1.7.1* [5]. The procedure is shown schematically in Fig. 2.11 for the case of moment only. It is not clear how to apply this procedure to connections with more than one row of tension anchors.

All of the procedures listed above require that equilibrium conditions be satisfied at the steel/concrete interface. None of these procedures are theoretically correct since the exact strain compatibility relationship at the steel/concrete interface is not satisfied. The procedure proposed by TVA *CEB 78-21* [48] does make an attempt at satisfying the strain compatibility relationship at the steel/concrete interface, but the procedure is limited to elastic behavior and is based on simplified assumptions. The other procedures either ignore the actual strain compatibility relationship at the steel/concrete interface, or assume a linear strain distribution as predicted by beam theory. Since

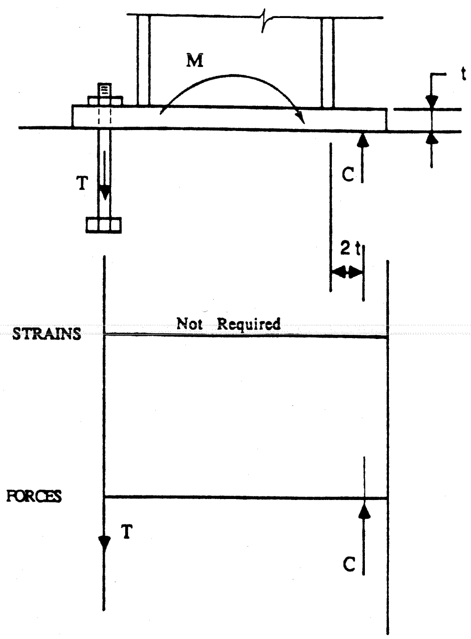

Figure 2.11 Procedure Based on Baseplate Thickness

plane sections do not necessarily remain plane at the steel/concrete interface, and since the relative stiffnesses of the anchors, baseplate, and concrete are highly indeterminate, the assumption of a linear strain distribution as predicted by beam theory for both working stress design and ultimate strength design is not justifiable.

One important aspect of the these procedures is the assumed location of the compressive reaction, since this directly affects the calculated tensile forces in the anchors. The actual compressive stress distribution is unimportant and impossible to determine analytically, due to unknown variations of the actual contact surface at the steel/concrete interface caused by the finish of the concrete and the warping of the baseplate. The compressive reaction should be located in a conservative manner based on the flexibility of the baseplate. Fig. 2.12 shows the likely locations of the compressive reaction for a rigid baseplate and a flexible baseplate.

2.3.2 Multiple-Anchor Connections in Shear. The results of tests on four-anchor connections in pure shear, reported in TVA *CEB 75-32* [24] show that shear forces redistribute in the connection prior to failure. These results indicate that sufficient inelastic deformation occurs in these connections so that each anchor achieves its single-anchor connection shear strength. These tests were performed on connections with welded studs, and on connections with threaded anchors.

2.3.3 Multiple-Anchor Connections with Moment and Shear. The distribution of shear in a ductile multiple-anchor connection with moment and shear is not obvious. Present design procedures do not adequately address this problem. Fig. 2.13 shows the possible forces on a multiple-anchor connection with one row of anchors in the tension zone loaded in moment, M, and shear, V. In Fig. 2.13 the tensile force, T_1, and the compressive force, C, result from the internal couple required to resist the applied moment, M. The frictional force, V_μ, is equal to the compressive

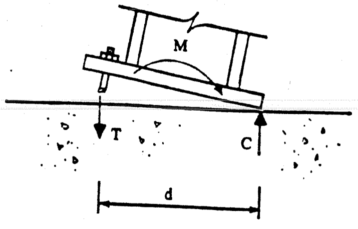

RIGID BASEPLATE

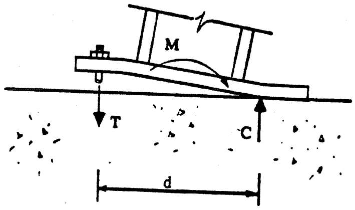

FLEXIBLE BASEPLATE

Figure 2.12 Probable Locations of the Compressive Reaction

force, C, multiplied by the coefficient of friction between steel and concrete, μ. The anchor shear forces, V_1 and V_2, may or may not be present depending on the magnitude of the frictional force, V_μ and the applied shear, V.

Table 2.4 provides a summary of the published values for the coefficient of friction between steel and concrete, μ. Results of the 27 tests cited in Table 2.4 show that the coefficient of friction between steel and concrete, μ, ranges from about 0.35 to about 0.65, with a mean of 0.50.

Extensive testing has previously been conducted on multiple-anchor connections having one row of anchors in the tension zone and subjected to eccentric shear loads at high eccentricities (large M/V ratios). TVA [48,49,50], Mahoney and Burdette [47], Armstrong, Klingner, and Steves [51], Hilti [54], and Picard and Beaulieu [55] have performed studies for this type of connection and loading. In this situation, the compressive reaction from the internal couple is so large that the frictional shear strength, V_μ, exceeds the applied shear, V. In this situation the anchors transfer no shear load; that is V_1 and V2, as shown in Fig. 2.13, are zero.

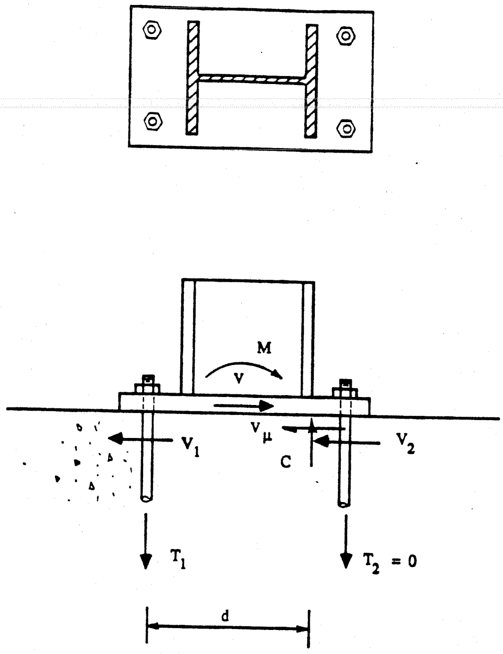

Figure 2.13 Possible Forces on Multiple-Anchor Connections with One Row of Anchors in the Tension Zone

The only previous study involving multiple-anchor connections subjected to eccentric shear loads at various eccentricities was a study by Hawkins, Mitchell, and Roeder [56]. This study investigated the behavior of multiple-anchor connections with welded studs and one row of anchors in the tension zone. As a result of that study, the following behavioral model was proposed:

1) If the shear strength provided by anchors in the compression zone, V_2, exceeds the applied shear, V, the anchors in the tension zone can be assumed to develop their full tensile strength for moment resistance.

2) If the shear strength provided by anchors in the compression zone, V_2, is less than the applied shear, V, the anchors in the tension zone can be assumed to transfer the excess shear load. The shear strength of the anchors in the tension zone, V_1 is limited by the strength of the anchors in combined tension and shear. The tension zone anchors contribute to both moment resistance and shear resistance.

Table 2.4 Summary of Published Values for the Coefficient of Friction between Steel and Concrete

Reference	Surface Condition[1]	Coefficient of Friction μ	Basis
TVA DS-C1.7.1 [5]	Unknown	0.50	Unknown
AISC [6]	Unknown	0.70[2]	Unknown
KSM [14]	Dry	0.40	Unknown
PCI [23]	Dry	0.40	Unknown
Hilti [54]	Dry	0.54	4 Tests
Holmes, et al. [71]	Unknown	0.30	Unknown
TVA CEB 77-46 [72]	Dry	0.34	7 Tests
	Wet	0.39	4 Tests
Rabbat, et al.[3] [73]	Dry	0.57	3 Tests
	Wet	0.65	9 Tests

Hawkins, Mitchell, and Roeder [56] call this the "plastic distribution" method and found that it provided the best fit to test data. This method assumes that sufficient inelastic deformation occurs in the connection so that each anchor achieves its single-anchor connection strength. For anchors in combined tension and shear an interaction equation lying between linear and elliptical was proposed ($n = 5/3$ in Eq. 2-3).

The study by Hawkins, Mitchell, and Roeder [56] did not consider the contribution of the frictional force between the baseplate and the concrete, V_μ. This may have led to an overestimation of the shear forces in the anchors, and in the amount of shear redistribution at failure. Their study did not include multiple-anchor connections with more than one row of anchors in tension.

2.3.4 Multiple-Anchor Connections with Moment, Axial Load, and Shear. No experimental results or published design procedures are available for this type of loading. It is generally believed that this loading condition is an extension of the moment and shear loading condition. In practice, a designer normally uses one of the procedures in Subsection 2.3.1 for moment and axial load design, and then adds a sufficient number of anchors to transfer the applied shear.

2.4 Design Requirements for Baseplates

In this section, the design requirements for baseplates in ductile multiple-anchor connections are discussed. The design requirements given in this section are based on ultimate strength design.

2.4.1 Baseplate Flexure. Baseplates should be of a sufficient thickness so that prying action at the tension anchors is precluded.

As noted by TVA *CEB 78-21* [48], prying action is not as critical in steel-to-concrete connections as it is in steel-to-steel connections. This is principally due to the differences in flexibility between an anchor in a steel-to-steel connection and an anchor in a steel-to-concrete connection. The anchors in steel-to-concrete connections are more flexible since they are usually longer and their flexibility is a function of the combined effect of the properties of the concrete and the anchor steel. The increased flexibility of the anchors helps prevent prying action. In tests on baseplates which were flexible enough to develop some prying action, Mahoney and Burdette [47] found that prying action was lost when the tension anchors began to yield.

A general guideline for the prevention of prying action in baseplates is to design the baseplate with enough flexural strength to prevent the formation of a plastic hinge in the baseplate between the tension anchors and the attached member. This is shown schematically in Fig. 2.14. This goal can be accomplished using the design provisions of the AISC *LRFD Specifications* [6]:

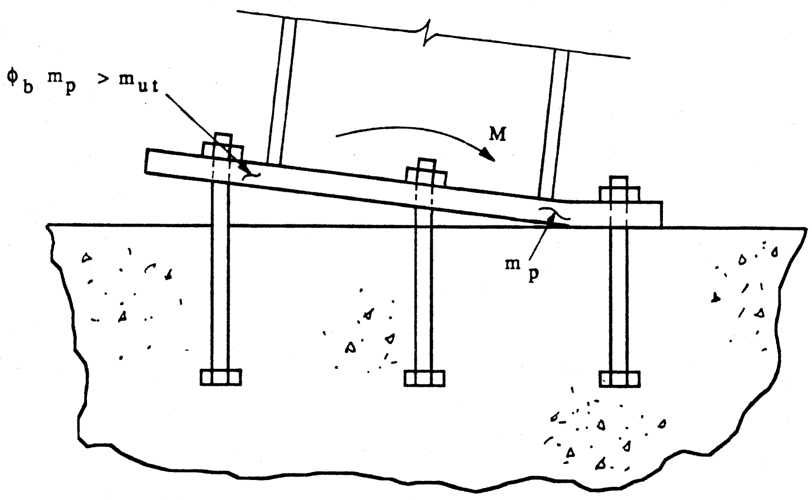

Figure 2.14 Typical Deformed Shape of "Reasonably" Flexible Baseplate to Prevent Prying

$$\phi\, m_p \quad \geq \quad m_{ut} \qquad (2-4)$$

where: ϕ = strength reduction factor for baseplate steel in flexure (equal to 0.90)

m_p = nominal flexural capacity per unit width, of a baseplate, based on the plastic section modulus

m_{ut} = maximum moment per unit width induced in a baseplate by the tension anchors, based on the average tensile strength, T_{ut}, of the tension anchors

Several methods are available in steel design texts for evaluating m_{ut} in baseplates. These procedures include yield line analysis, which is appropriate for baseplate design in steel-to-concrete connections given the myriad of anchor patterns that a designer could elect to use. Any rational design procedure could be used to evaluate m_{ut}.

By equating the design moment capacity, $\phi\ m_p$, to the maximum moment induced in the baseplate by the tension anchors, m_{ut}, the minimum required plate thickness, t, for flexure can be calculated:

$$\phi\ m_p \geq m_{ut}$$

$$\phi\ F_y\ t^2\ /\ 4 \geq m_{ut}$$

$$t \geq \sqrt{(4\ m_{ut})\ /\ (\phi\ F_y)} \qquad (2-5)$$

where: $F_y =$ specified minimum yield strength of baseplate steel

2.4.2 Baseplate Shear. To prevent the development of prying action, the formation of a shear hinge between the tension anchors and the attached member should also be prevented. This can be accomplished using the design provisions of the AISC *LRFD Specifications* [6]:

$$\phi\ v_n \geq v_{ut} \qquad (2-6)$$

where: $\phi =$ strength reduction factor for baseplate steel in shear (equal to 0.90)

$v_n =$ nominal shear strength per unit width, of a baseplate

$v_{ut} =$ maximum shear per unit width induced in a baseplate by the tension anchors, based on T_{ut} of the anchors

Any rational design procedure could be used to evaluate v_{ut}.

By equating the design shear strength, $\phi\ v_n$, to the maximum shear induced in the baseplate by the tension-anchors, v_{ut}, the minimum required plate thickness, t, for shear can be calculated:

$$\phi\ v_n \geq v_{ut}$$

$$\phi\ 0.6\ F_y t \geq v_{ut}$$

$$t \geq v_{ut}/(\phi\ 0.6\ F_y) \qquad (2-7)$$

where: $F_y =$ specified minimum yield strength of baseplate steel

2.4.3 Anchor/Baseplate Bearing. The following design requirement is based on the provisions of the AISC *LRFD Specification* [6]:

The design bearing strength of an anchor hole in the baseplate, m P_n, should exceed the average shear strength of an anchor, V_{ut}:

$$\phi \, P_n \quad \geq \quad V_{ut} \tag{2-8}$$

The design bearing strength of an anchor hole in the baseplate, $\phi \, P_n$, is given by:

$$\phi \, P_n \quad = \quad \phi \, 2.4 \, d_b \, t \, F_u \tag{2-9}$$

where: $\phi =$ strength reduction factor for baseplate steel in bearing (equal to 0.75)

$d_b =$ nominal diameter of an anchor

$t =$ thickness of baseplate

$F_u =$ specified minimum tensile strength of baseplate steel

By equating the design bearing strength, $\phi \, P_n$, to the average shear strength of an anchor, V_{ut}, the minimum required baseplate thickness, t, for bearing can be calculated:

$$\phi \, 2.4 \, d_b \, t \, F_u \quad \geq \quad V_{ut}$$

$$t \quad \geq \quad V_{ut} \, / \, (\phi \, 2.4 \, d_b \, F_u) \tag{2-10}$$

2.4.4 Anchor Holes. The following design requirements are based on the provisions of the AISC *LRFD Specification* [6]:

1) Anchor hole oversize should not exceed 3/16 inch for anchors 7/8 inch and less in diameter, 1/4 inch for 1-inch diameter anchors, and 5/16" for larger anchors.

2) The minimum edge distance from the centerline of an anchor hole to the edge of the baseplate should not be less than 1.75 times the anchor diameter for baseplates with sheared edges, and 1.25 times the anchor diameter for other baseplates.

3) The center-to-center distance between anchor holes should not be less than 3 times the anchor diameter.

3. BACKGROUND:
EMBEDMENT REQUIREMENTS FOR DUCTILE CONNECTIONS

3.1 Introduction

In this chapter, embedment design criteria for ductile connections, embedment failure mechanisms, and recommended procedures for evaluating the strength of the embedment are discussed. The recommended procedures for evaluating the strength of the embedment are based on the provisions of *ACI 349-85* [4] and *TVA DS-C1.7.1* [5], and on the recommendations of Doerr and Klingner [2].

This chapter is not meant to provide an extensive review of the results from previous experimental studies dealing with the strength of embedments. The evaluation of the strength of the embedment was not the objective of this study. Previous experimental studies dealing with the strength of the embedment are noted in this chapter, but specific results are not discussed.

3.2 Embedment Design Criteria for Ductile Connections

A ductile connection is a connection that is sufficiently embedded so that failure occurs by yielding and fracture of the steel. Although existing design documents [4,5] agree with this statement, specific embedment design criteria for ductile connections are not well defined.

In this study, the embedment design criterion for ductile connections is to require that the design strength of the embedment exceed the average strength of the steel.

For a single-anchor connection in tension this criterion is represented by:

$$\phi \, T_e \quad > \quad T_{ut} \tag{3-1}$$

where: $\phi =$ strength reduction factor applied to the nominal strength of the embedment

$T_e =$ nominal tensile strength of the embedment, as defined in Section 3.3

$T_{ut} =$ $A_s \, F_{ut}$, average tensile strength of the steel as defined by Eq. (2-1)

For a single-anchor connection in shear this criterion is represented by:

$$\phi V_e \; > \; V_{ut} \tag{3-2}$$

where: $\phi =$ strength reduction factor applied to the nominal strength of the embedment

$V_e =$ nominal shear strength of the embedment as defined in Section 3.4

$V_{ut} =$ $\tau \, A_s \, F_{ut}$, average shear strength of the steel as defined by Eq. (2-3)

For a multiple-anchor connection subjected to moment, axial load, and shear the application of embedment design criteria for ductile connections is not obvious. The embedment design criteria represented by Eq. (3-1) and Eq. (3-2) can be applied to both single-anchor and multiple-anchor connections if anchors are separated into two categories:

1) *Tension-Anchors*: A tension-anchor is any anchor that is assumed to transfer tensile forces from the steel to the concrete.
2) *Shear-Anchors*: A shear-anchor is any anchor that is assumed to transfer shear forces from the steel to the concrete.

An individual anchor in a connection can be a tension-anchor, a shear-anchor, or both. This applies to both single-anchor connections and multiple-anchor connections.

The embedment design criterion for ductile connections with tension, as represented by Eq. (3-1), can be applied to both single-anchor and multiple- anchor connections if the nominal tensile strength of the embedment, T_e, and the average tensile strength of the steel, T_{ut}, are computed based on all the tension-anchors in the connection.

The embedment design criterion for ductile connections with shear, as represented by Eq. (3-2), can be applied to both single-anchor and multiple- anchor connections if the nominal shear strength of the embedment, V_e, and the average tensile strength of the steel, V_{ut}, are computed based on all the shear-anchors in the connection.

Section 3.3 details the procedures for calculating the nominal tensile strength of the embedment for both single-anchor and multiple-anchor connections. Section 3.4 details the procedures for calculating the nominal shear strength of the embedment for both single-anchor and multiple-anchor connections. The average strength of the steel is determined by Eq. (2-1) and Eq. (2-3) based on the number of tension-anchors and shear-anchors in the connection.

The embedment design criteria for ductile connections as represented by Eq. (3-1) and Eq. (3-2) ensures steel failure prior to embedment failure. As discussed in Section 1.2, steel failure is preferred since it permits load redistribution and energy absorption prior to failure.

3.3 Tensile Strength of the Embedment

The following subsections describe the failure modes and recommended procedures for evaluating the nominal tensile strength of the embedment for connections with different types of tension-anchors.

3.3.1 Cast-in-Place Anchors. Two embedment failure mechanisms are possible for connections with cast-in-place tension-anchors:

1) *Pullout-Cone Failure*: This embedment failure mechanism is characterized by pullout of a cone of concrete radiating from the bearing surface at the head of the anchor to the surface of the concrete. The pullout-cone failure occurs when the applied tension load exceeds the

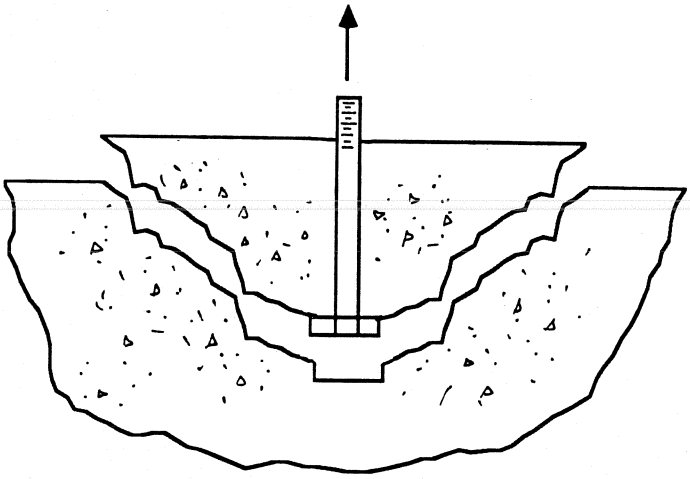

Figure 3.1 Pullout-Cone Failure

tensile strength of the concrete cone. Fig. 3.1 shows a typical pullout-cone failure for a connection with a single cast-in-place tension-anchor.

2) *Blowout-Cone Failure*: This embedment failure mechanism is characterized by blowout of a cone of concrete radiating from the embedded head of the anchor to the free edge of the concrete. The blowout-cone failure occurs when the radial bursting forces developed at the embedded anchor head exceed the lateral resistance of the concrete, bursting or splitting the concrete adjacent to the embedded head of the anchor. Fig. 3.2 shows a typical blowout- cone failure for a connection with a single cast-in-place tension-anchor.

Pullout-Cone Failure

Previous experimental studies of the pullout failure mode for cast- in-place anchors include Nelson Stud Welding Company [8-10], Shoup and Singleton [11], Ollgaard, Slutter, and Fisher [18], McMackin, Slutter, and Fisher [19], TVA *CEB 75-32* [24], Bode and Roik [40], and Hawkins [45].

For design purposes the apex of the pullout cone is taken as the intersection of the anchor centerline with the far side of the anchor head. Fig. 3.3 shows the design pullout cone for a connection with a single cast-in-place tension-anchor. The nominal tensile strength of the embedment is determined by applying a nominal concrete tensile strength to the projected area, A_p, of the pullout cone at the surface of the concrete. The area of the anchor head is not subtracted from the projected area of the cone unless its area exceeds the area of a standard bolt head as given in *ANSI B18.2.1*, or of a standard nut as given in *ANSI B18.2.2*. The projected area of the pullout cone is limited by thee intersection of the cone with any free edge of concrete. Fig. 3.3 and Fig. 3.4 show projected areas of the design pullout cone for a connection with a single tension-anchor.

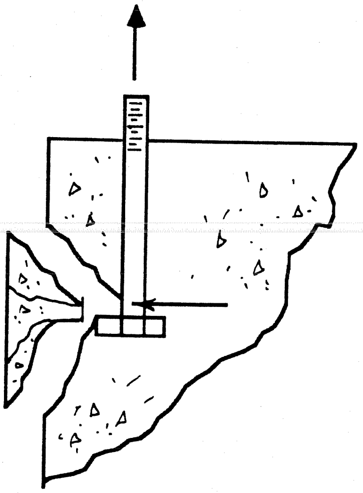

Figure 3.2 Blowout-Cone Failure

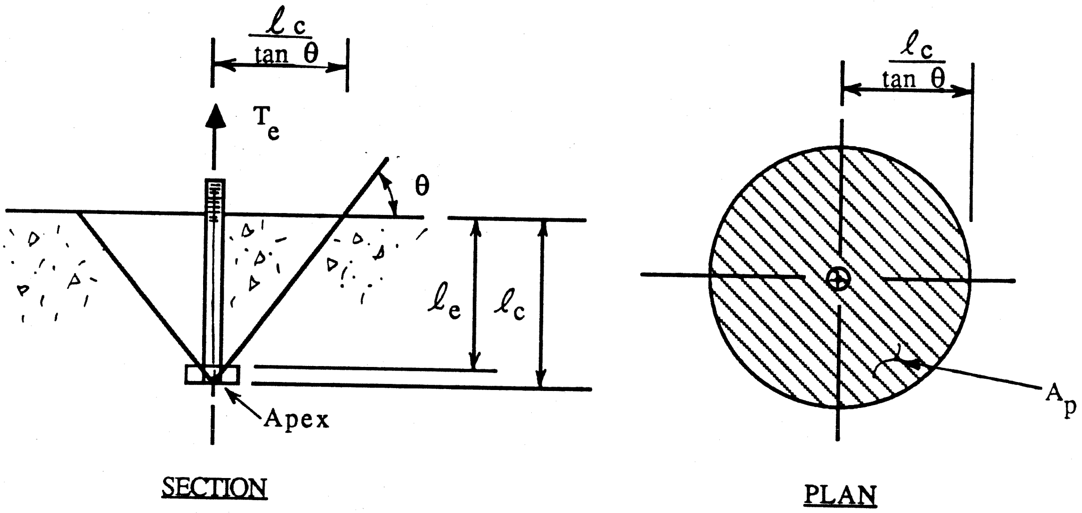

$\frac{\ell_c}{\tan\theta}$
T_e
θ
ℓ_e
ℓ_c
Apex
SECTION
$\frac{\ell_c}{\tan\theta}$
A_p
PLAN

Figure 3.3 Design Pullout Cone for Cast-in-Place Anchors

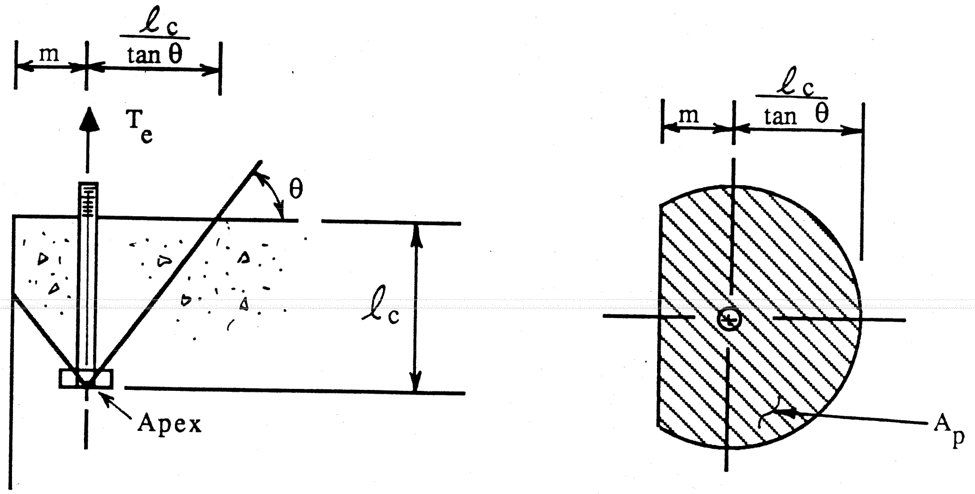

SECTION

PLAN

Figure 3.4 Design Pullout Cone Limited by Free Edge

The base angle, Θ, of the pullout cone is given by:

$$\Theta \quad = \quad 45^\circ \; for \; l_e \quad \geq \quad 5 inches$$

$$\Theta \quad = \quad 28^\circ \; + \; (3.4 l_e)^\circ \; for \; l_e \quad < \quad 5 inches$$

where: $l_e =$ embedded length of the anchor; distance from concrete surface to bearing surface of anchor head

For pullout failure of a group of cast-in-place tension-anchors the projected area of the failure surface, A_p, is limited by the overlap of individual tension-anchor pullout cones, by the intersection of the individual tension-anchor pullout cones with any free edge of concrete, and by the overall thickness of the concrete. Fig. 3.5 shows projected areas for overlapping cones. Fig. 3.6 shows the projected area as limited by the concrete thickness.

An exact calculation of the projected area of the pullout failure surface for overlapping failure cones is difficult, tedious, and not justified given the inexact nature of other parameters in the embedment design. Marsh and Burdette [74] and Siddiqui and Beseler [75] provide design aids for calculating the projected area for overlapping failure cones. Appendix A provides an approximate method for calculating the projected area for overlapping failure cones.

The nominal tensile strength of the embedment, T_e, for connections with cast-in-place tension-anchors as governed by pullout-cone failure is given by:

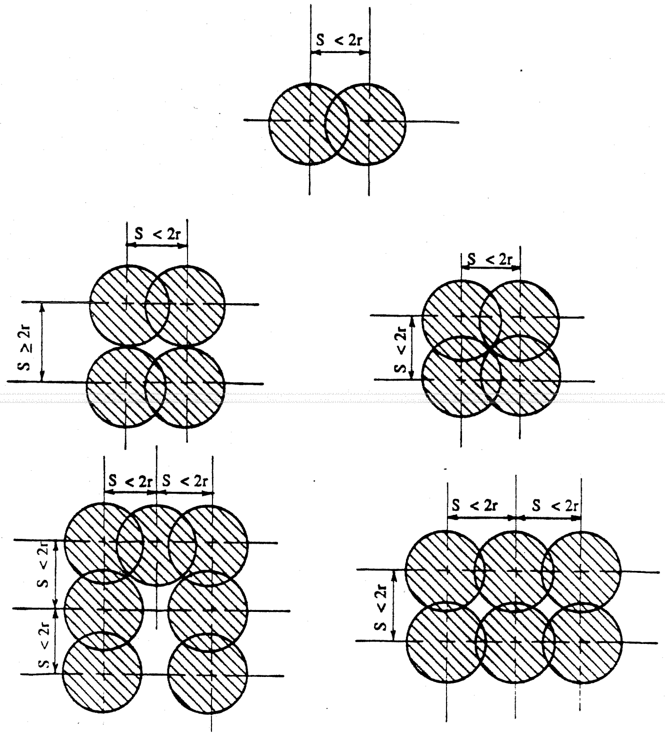
S < 2r
S < 2r
S ≥ 2r
S < 2r
S < 2r
S < 2r S < 2r
S < 2r
S < 2r
S < 2r S < 2r
S < 2r

Figure 3.5 Projected Areas for Overlapping Cones

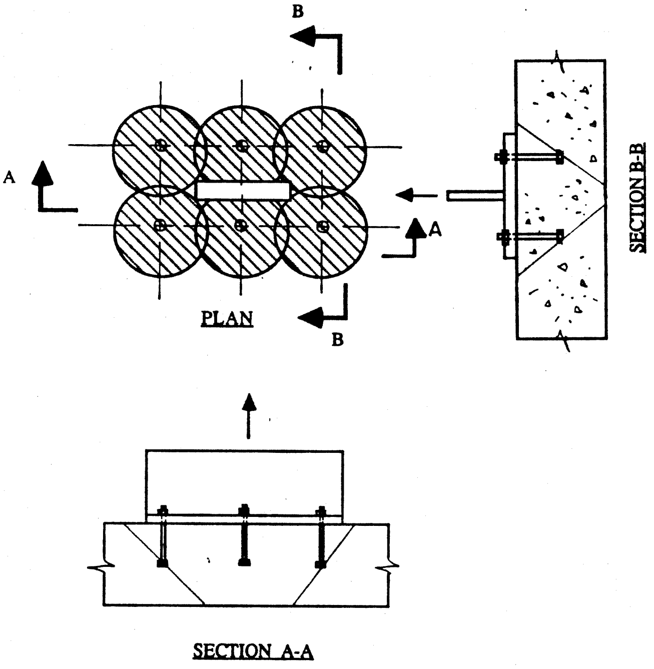
B
A
A
PLAN
B
SECTION B-B
SECTION A-A

Figure 3.6 Projected Areas as Limited by Concrete Thickness

$$T_e = 4\sqrt{f'_c}\,A_p \tag{3-3}$$

where:

$\sqrt{f'_c}$ = square root of specified compressive strength of concrete, psi

A_p = projected area of the failure surface as described above

Blowout-Cone Failure

Previous experimental studies of the blowout failure mode include Breen [15], Lee and Breen [16], Bailey and Burdette [25], and Hasselwander, Jirsa, and Breen [44].

For design purposes the apex of the blowout cone is taken as the intersection of the anchor centerline and the bearing surface of the anchor head. The base angle, Θ, of the blowout cone is taken as 45°. Fig. 3.7 shows the design blowout cone for a connection with a single cast-in-place tension-anchor. The ratio of the lateral blowout force to the applied tensile force in the anchor is assumed to be the same as the ratio of the lateral strain in the concrete to the longitudinal strain in the concrete. The ratio of lateral force to longitudinal force is conservatively taken as 0.25. The nominal tensile strength of the embedment is determined by applying a nominal concrete tensile strength to the projected area, A_p, of the blowout cone on the free-edge surface of the concrete.

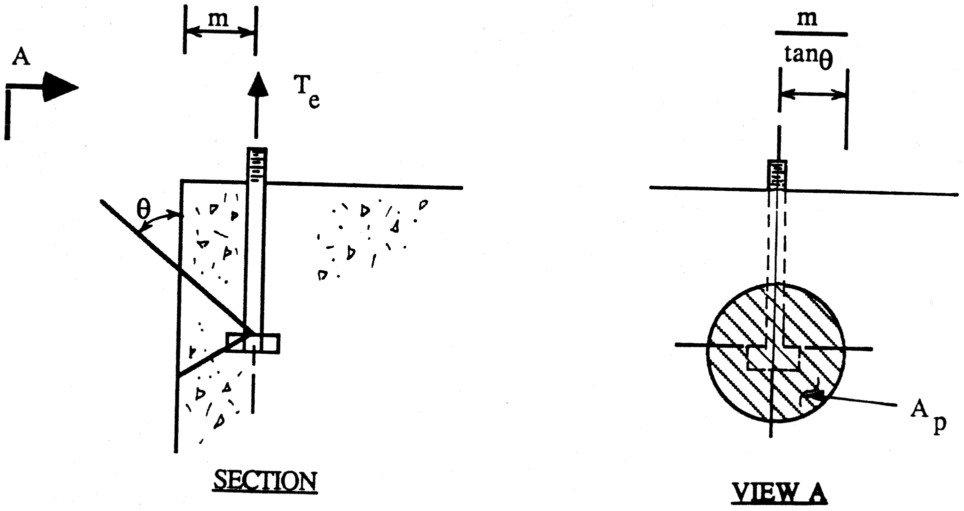

Figure 3.7 Design Blowout Cone

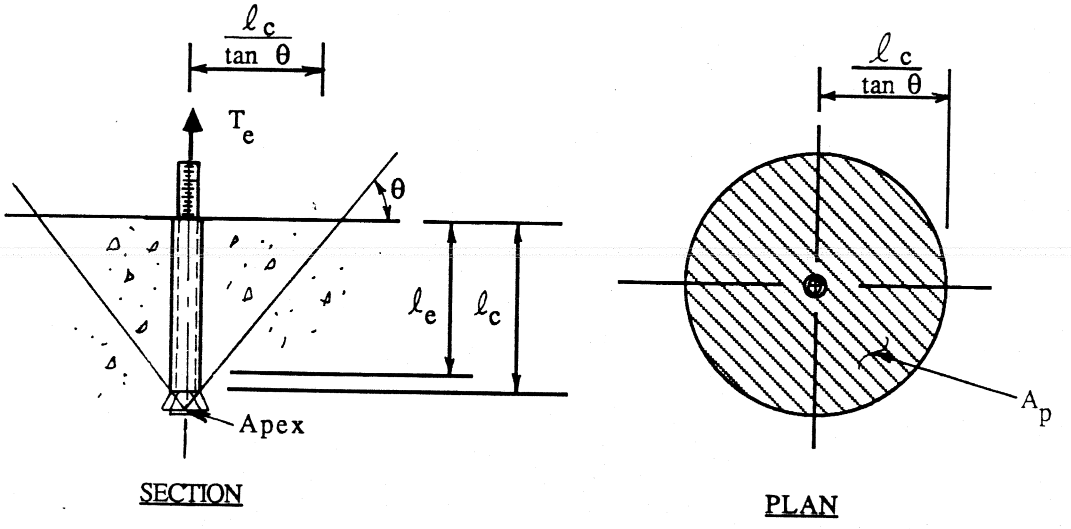

Figure 3.8 Design Pullout Cone for Undercut Anchors

For blowout failure of a group of cast-in-place tension-anchors the projected area, A_p, of the failure surface is limited by the overlap of individual tension-anchor blowout cones and by the intersection of the individual tension-anchor blowout cones with any free edge of concrete.

The nominal tensile strength of the embedment, T_e, for a connection with cast-in-place tension-anchors as governed by blowout-cone failure is given by:

$$0.25\, T_e = 4\sqrt{f'_c}\, A_p$$

$$T_e = 16\sqrt{f'_c}\, A_p \qquad (3-4)$$

where:
$\sqrt{f'_c}$ = square root of specified compressive strength of concrete, psi
A_p = projected area of the failure surface as described above

3.3.2 Undercut Anchors. Previous experimental studies of undercut anchors in tension include Collins and Klingner [1], TVA *CEB 80-64* [34], Stethen and Burdette [35], Burdette [36], and Burdette, Perry, and Funk [42].

The embedment failure mechanisms for connections with undercut tension-anchors are the same as for connections with cast-in-place tension- anchors. For design purposes the apex of the pullout cone for undercut anchors is taken as the intersection of the anchor centerline with the far side of the expansion device. Fig. 3.8 shows the design pullout cone for a connection with a single undercut tension-anchor. The provisions of Subsection 3.3.1 are used to determine the nominal tensile strength of the embedment for connections with undercut tension-anchors.

3.3.3 Adhesive Anchors. Previous experimental studies of adhesive anchors in tension include Collins and Klingner [1], Doerr and Klingner [2], TVA CEB 80-64 [34], and Stethen and Burdette [35].

Two embedment failure mechanisms are possible for connections with adhesive tension-anchors:

1) *Plug/Cone-Pullout Failure*: For fully bonded anchors the embedment failure mechanism is characterized by pullout of an adhesive plug with a shallow concrete cone. A fully bonded anchor is bonded along the entire embedded length of the anchor. Fig. 3.9 shows a typical plug/cone-pullout failure for a connection with a single adhesive tension-anchor.

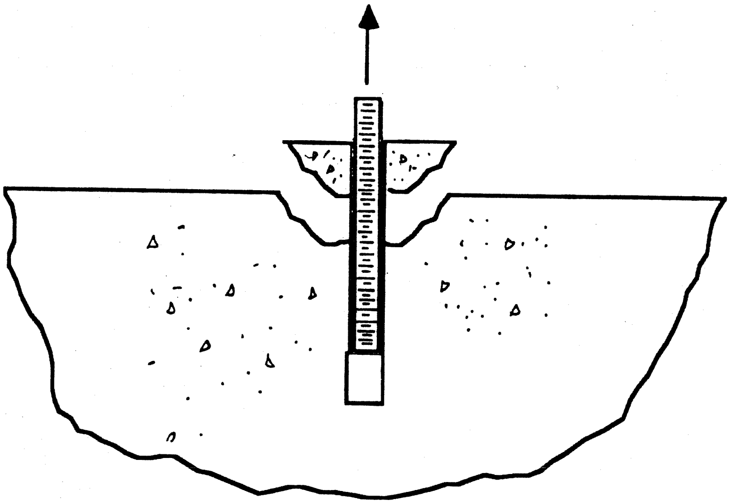

Figure 3.9 Plug/Cone-Pullout Failure

2) *Plug-Pullout Failure*: For partially bonded anchors the embedment failure mechanism is characterized by pullout of an adhesive plug. A partially bonded anchor is intentionally debonded at the top portion of its embedded length (usually over a length of about 2"). This type of failure can also occur when the adhesive is improperly mixed or cured. If proper adhesive preparation is ensured by field testing and inspection, a plug-pullout failure should not occur for a fully bonded anchor. Fig. 3.10 shows a typical plug- pullout failure for a connection with a single adhesive tension-anchor.

There is virtually no difference between the strength of a fully bonded anchor failing by plug/cone-pullout, and that of a partially bonded anchor of the same embedment depth failing by plug-pullout.

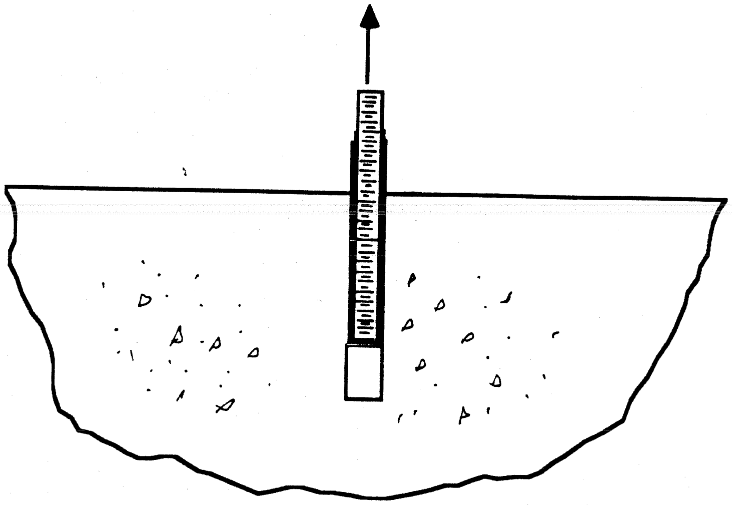

Figure 3.10 Plug-Pullout Failure

The nominal tensile strength of the embedment, T_e, for a connection with adhesive tension-anchors spaced greater than or equal to 8 inches apart is given by:

$$T_e = n(\pi\, d_h^{1.5}\, u_0 \,/\, \lambda')\, tanh(\lambda'\, (l_e - 2) \,/\, \sqrt{d_h}) \qquad (3-5)$$

where: n = number of adhesive tension-anchors in the connection

d_h = nominal diameter of the hole

u_0 = specified bond strength of adhesive, psi

λ' = specified elastic property of adhesive, psi.

l_e = embedded length of the anchor

NOTE: For $s < 8''$, $T_e = 85\%$ of that given by Eq. (3-5)

3.3.4 Grouted Anchors. Previous experimental studies of grouted anchors in tension include Collins and Klingner [1], Conrad [17], Cones [37], and Elfgren, Broms, Cederwall, and Gylltoft [39].

Four embedment failure mechanisms are possible for connections with grouted tension-anchors:

1) Pullout of a concrete cone, as with a pullout-cone failure of a connection with cast-in-place tension-anchors.

2) Blowout of a concrete cone, as with a blowout-cone failure of a connection with cast-in-place tension-anchors.

3) Pullout of a grout plug and shallow cone of concrete, as with a plug/cone-pullout failure of a connection with adhesive tension-anchors.

4) Pullout of the grout plug, as with a plug-pullout failure of a connection with adhesive tension-anchors.

The provisions of Subsection 3.3.1 and Subsection 3.3.3 are used to determine the nominal tensile strength of the embedment for connections with grouted tension-anchors.

3.3.5 *Expansion Anchors.*

Previous experimental studies of expansion anchors in tension include Collins and Klingner [1], TVA CEB 75-32 [24], TVA CEB 80-64 [34], Stethen and Burdette [35], Ghodsi and Breen [38], Schwartz [41], Eligehausen [43], and Dusel and Harrington [46]. A paper by Meinheit and Heidbrink [76] provides a general discussion of the behavior of expansion anchors.

Three embedment failure mechanisms are possible for connections with expansion tension-anchors:

1) Pullout of a concrete cone, as with a pullout-cone failure of a connection with undercut tension-anchors.

2) Blowout of a concrete cone, as with a blowout-cone failure of a connection with cast-in-place tension-anchors.

3) Excessive slip of the anchor followed by pullout of a shallow cone of concrete. Fig. 3.11 shows a typical slip/cone failure for a connection with a single expansion tension-anchor. Excessive slip of the anchor is defined as a slip greater than 5% of the embedded length after installation. A slip greater than 5% reduces the pullout-cone strength as defined in Subsection 3.3.1 by more than 10%

All expansion anchors must be tested to determine the governing embedment failure mechanism. Only those expansion anchors which can be shown to fail by pullout-cone failure are acceptable for use in ductile connections.

For expansion anchors which can be shown to fail by pullout-cone failure, the nominal tensile strength of the embedment is calculated by the methods of Subsection 3.3.1 using the same design pullout cone as for an undercut tension-anchor.

3.4 Shear Strength of the Embedment

The shear strength of the embedment is determined in the same manner for all types of anchors. Two embedment failure mechanisms are possible for connections with shear-anchors:

1) *Pryout-Cone Failure*: This embedment failure mechanism occurs when anchors are loaded in shear away from a free edge of concrete. This embedment failure mechanism is characterized by prying loose a cone of concrete on the side of the anchor away from the load. Fig. 3.12 shows a typical pryout- cone failure for a connection with a single shear-anchor.

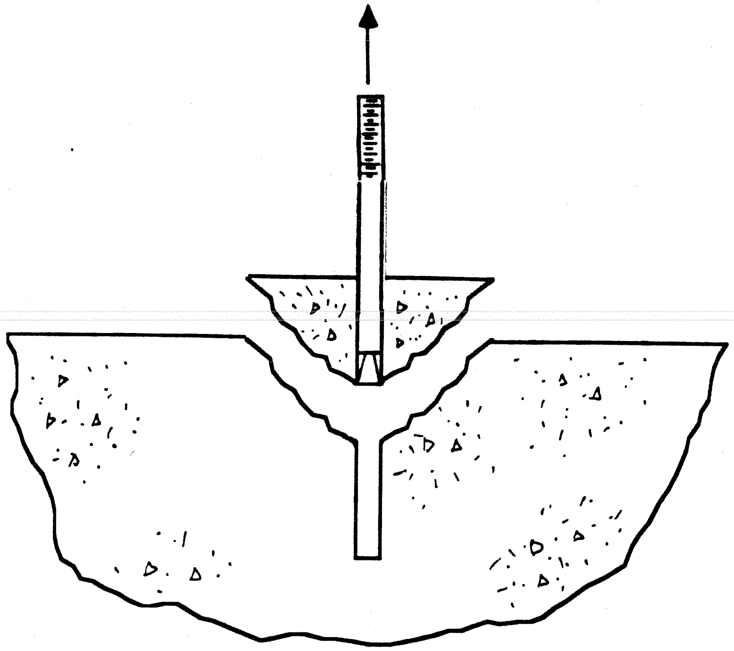

Figure 3.11 Excessive Slip Failure with Shallow Pullout Cone

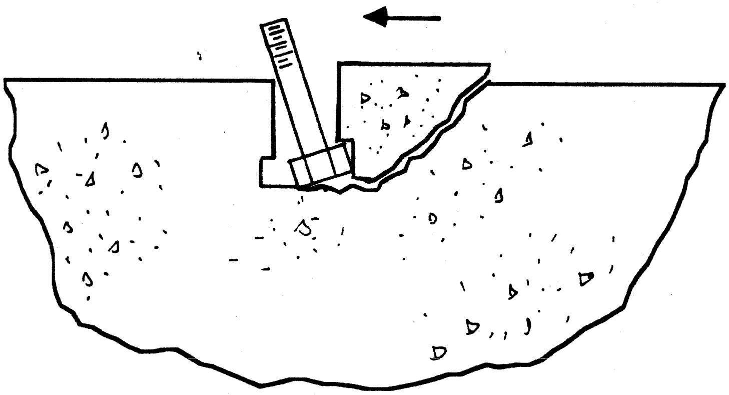

Figure 3.12 Pryout Cone Failure

2) *Pushout-Cone Failure*: This embedment failure mechanism occurs when anchors are loaded in shear near a free edge of concrete. This embedment failure mechanism is characterized by pushout of a cone of concrete radiating from the centerline of the anchor at the surface of the concrete to the free edge. Fig. 3.13 shows a typical pushout-cone failure for a connection with a single shear-anchor.

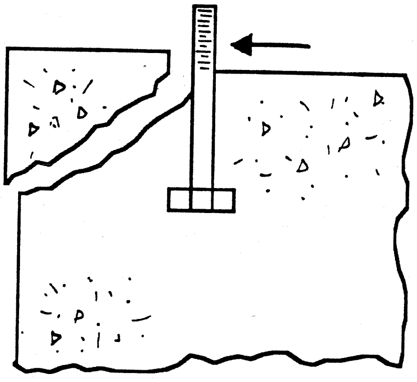

Figure 3.13 Pushout Cone Failure

Pryout-Cone Failure

Previous experimental studies of the pryout-cone failure mechanism include Shoup and Singleton [11], Ollgaard, Slutter, and Fisher [18], McMackin, Slutter, and Fisher [19], TVA *CEB 75-32* [24], and Hawkins [35].

The nominal shear strength of the embedment, V_e, as governed by pryout-cone failure, is assumed to equal the nominal tensile strength of the embedment, T_e, as determined by Eq. (3-3) or Eq. (3-5) as applicable:

$$V_e \quad = \quad T_e \qquad (3-6)$$

Pushout-Cone Failure

Previous experimental studies of the pushout-cone failure mechanism include Bailey and Burdette [25], Swirsky, Dusel, Crozier, Stoker, and Nordlin [29], Klingner, Mendonca, and Malik [31], and Armstrong, Klingner, and Steves [51].

For design purposes the apex of the pushout cone is taken as the intersection of the anchor centerline with the surface of the concrete. The base angle, Θ, of the pushout cone is taken as 45°. Fig. 3.14 shows the design pushout cone for a single shear-anchor near a free edge. The nominal shear strength of the embedment is determined by applying a nominal concrete tensile strength to the projected area, A_p, of the pushout cone at the free- edge surface of the concrete. The projected area of the pushout cone is limited by the intersection of the cone with any other free edges of the concrete.

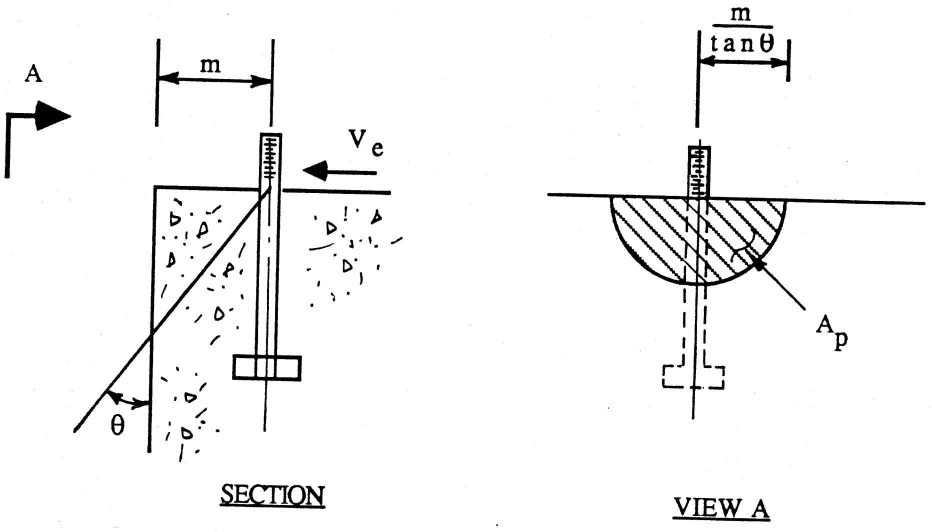

Figure 3.14 Design Pushout Cone

For pushout failure of a group of shear-anchors the projected area, A_p, of the failure surface is limited by the overlap of individual anchor pushout cones and by the intersection of the individual anchor pushout cones with any free edge of concrete.

The nominal shear strength of the embedment, V_e, for connections with shear-anchors as governed by pushout-cone failure is given by:

$$V_e = 4\sqrt{f'_c}\,A_p \qquad (3-7)$$

where: $\sqrt{f'_c}$ = square root of specified compressive strength of concrete, psi

A_p = projected area of the failure surface as described above

3.5 Bearing Strength of the Embedment

The bearing strength of the embedment refers to the bearing strength of the concrete. It can be divided into two categories:

1) *Anchor Bearing*: This includes bearing of the embedded head of the anchor against the surrounding concrete, and bearing of the anchor shank against the concrete near the surface of the concrete for anchors in shear. Anchor bearing is discussed in Subsection 3.5.1.

2) *Baseplate Bearing*: This involves the bearing of the baseplate on the surface of the concrete due to moment and axial load. Baseplate bearing is discussed in Subsection 3.5.2.

3.5.1 Anchor Bearing. The results of numerous experimental studies have shown that bearing at the embedded head of an anchor is not a design consideration if the size of the anchor head is no less than that of a standard bolt head as given in *ANSI B18.2.1* or standard nut as given in *ANSI B18.2.2.* The effect of concrete confinement allows very high bearing forces to develop with no adverse affect on the strength of the anchor.

Experimental studies of anchors in shear have shown that bearing failure of the embedment (concrete) near the surface of the concrete occurs but does not limit the shear strength of the anchor. As noted by Marsh and Burdette [74] bearing failure of the concrete is confined to a depth of roughly one-fourth the anchor diameter. The bearing failure is characterized by crushing and spalling of the concrete within this limited depth. Fig. 2.2 shows this type of bearing failure in the concrete. The shear force in the anchor is transferred to the embedment below the zone of crushed and spalled concrete.

3.5.2 Baseplate Bearing. Bearing of the baseplate on the surface of the concrete should not cause failure of the supporting concrete. For maintaining the overall bearing integrity of the supporting concrete, the actual distribution of bearing stress is much less important than the requirement that the compressive reaction not cause splitting failure of unconfined concrete. Current design procedures do not adequately address this failure mode for steel- to-concrete connections with moment or moment and axial load.

Although experimental results from tests on baseplates with moment or moment and axial load are available [47-56], very little correlation of the results with the bearing strength of the embedment have been made. DeWolf and Sarisley [52], who did investigate bearing, conclude that the effects of concrete confinement and baseplate flexibility are important but that further research is necessary.

ACI 349-85 [4] and the AISC *LRFD Specification* [6] use the same procedure for evaluating bearing strength of the embedment for baseplates. This procedure was developed for checking bearing of axially loaded column baseplates on piers. The design bearing strength of the embedment is given by:

$$\phi\, P_n \quad = \quad \phi\, 0.85 f'_c\, A_1\, \sqrt{A_2/A_1} \qquad (3-8)$$

where: $\sqrt{A_2/A_1} \leq 2$

$\phi =$ strength reduction factor for concrete in bearing

$f'_c =$ specified compressive strength of concrete, psi

$A_1 =$ loaded area

$A_2 =$ maximum area of the portion of the supporting surface that is geometrically similar to and concentric with the loaded area

For connections with moment or moment and axial load the loaded area, A_1, is not explicitly defined. Currently, the designer must use judgment in evaluating the bearing strength of the embedment for these connections. This study did not specifically address this problem but test results are correlated with Eq. (3-8).

The tests performed in this study were developed to preclude any type of failure in the supporting concrete, including failure modes associated with baseplate bearing.

4. DEVELOPMENT OF EXPERIMENTAL PROGRAM

4.1 Objectives of Experimental Program

The behavior of a ductile multiple-anchor connection to concrete depends on a number of variables, including the following:

- loading (axial load, moment, shear)
- size of the steel attachment
- size, number, location, and type of anchors
- coefficient of friction between the baseplate and the concrete
- tension/shear interaction for a single anchor
- distribution of shear among the anchors
- distribution of tension among the anchors
- flexibility of the baseplate

In a typical design situation only the loading is known. The job of the designer is to determine the size of the steel attachment and the size, number, location, and type of anchors. In order to complete this task, the designer must consider the effects of the last five variables. Present design standards [4,5,23] do not adequately address these variables. The purpose of the experimental program was to quantify and define these five variables for multiple-anchor connections to concrete.

The objectives of the experimental program were:

1) To determine the coefficient of friction between a surface mounted steel baseplate and hardened concrete in multiple- anchor connections.
2) To determine tension/shear interaction relationships for cast- in-place anchors, undercut anchors, and adhesive anchors in multiple-anchor connections.
3) To determine the distribution of shear forces among anchors in multiple-anchor connections.
4) To determine the distribution of tension forces among anchors in multiple-anchor connections.
5) To determine the effect of baseplate flexibility on the behavior and design of multiple-anchor connections.

4.2 Scope

To complete the objectives of the experimental program it was necessary to control the variables not being investigated. The loading, the size of the steel attachment, and the size, number, location, and type of anchors were controlled in all tests. Since each of the variables being investigated could be studied in the absence of any externally applied axial load, the experimental program was limited to the study of multiple-anchor connections subjected to moment and shear only. This was accomplished by applying an eccentric shear load to several types of multiple-anchor connections at various load eccentricities.

The experimental program included the following types of tests:

1) Friction tests
2) Ultimate load tests:
    a) Two-anchor rigid baseplate tests
    b) Four-anchor rigid baseplate tests
    c) Six-anchor rigid baseplate tests
    d) Six-anchor flexible baseplate tests

Each type of test was developed to investigate one or more of the unknown variables.

Fig. 4.1 shows the basic loading condition used for all types of tests. In each test, measurements were made of the eccentric shear load, V, the eccentricity of the shear load, e, the individual anchor tension, T, the baseplate slip, δ_h, and the baseplate rotation, Θ. For the ultimate load tests, connection failure was defined as the fracture of any anchor.

4.3 Development of Friction Tests

The purpose of the friction tests was to determine the coefficient of friction, μ, between a steel attachment and hardened concrete in a multiple-anchor connection.

In previous research [54,72,73], the coefficient of friction was evaluated by applying a known external compressive load to the attachment, and then pulling on the attachment in pure shear until slip occurred. In this procedure the external compressive load moves with the attachment and the only frictional force is that existing between the baseplate and the concrete. The coefficient of friction is calculated as the shear load which produces slip, divided by the applied compression force.

The test procedure used in this study differed from the procedure used in the previous research. In this study, the coefficient of friction was evaluated by applying the compressive load to the attachment via tensile forces in the anchors, and then pulling on the attachment with an eccentric shear load until slip occurred. The tensile forces in the anchors were produced by anchor preload and/or by the forces developed to resist the external moment induced by the eccentric shear load. Oversized holes were provided to allow the plate to slip between the washers under the anchor nuts and the concrete as the eccentric shear load was applied.

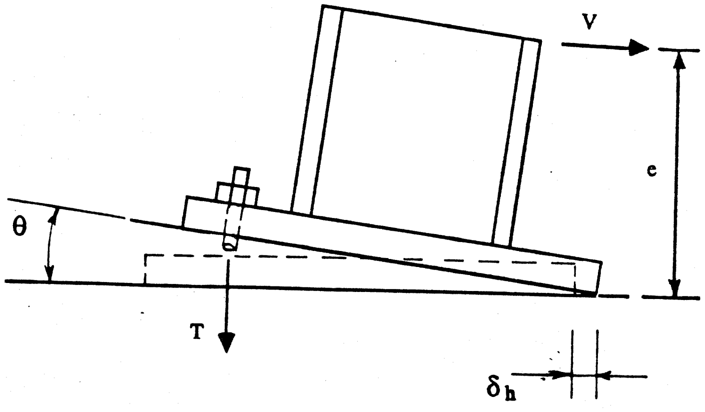

Figure 4.1 Typical loading condition and measured values

In this test procedure, the total shear resistance comes from two frictional forces, shown in Fig. 4.2. One frictional force occurs between the washers and the baseplate, and is equal to the coefficient of friction between the washer and the baseplate, μ_s, multiplied by the total tensile force in all the anchors, ΣT. The other frictional force develops between the baseplate and the concrete, and is equal to the coefficient of friction between the baseplate and the concrete, μ, multiplied by the total compressive force across the steel/concrete interface.

The basic principle behind the test procedure is that knowing the tension force in the anchors, ΣT, then the total compression force, C, across the steel/concrete interface is also known regardless of the eccentricity of the applied shear load. The condition of normal force equilibrium is given by:

$$C = \Sigma T \tag{4-1}$$

Since the applied shear, V, and the total anchor tension, ΣT, are measured as the steel attachment slips, the coefficient of friction between the baseplate and concrete, μ, is determined by the condition of shear force equilibrium as:

$$V = \mu C + \mu_s \Sigma T$$

Substituting Eq. (4-1) gives:

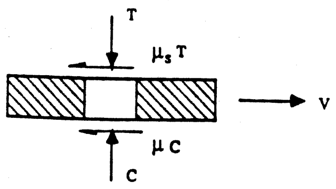

(a) Free Body Diagram of Baseplate

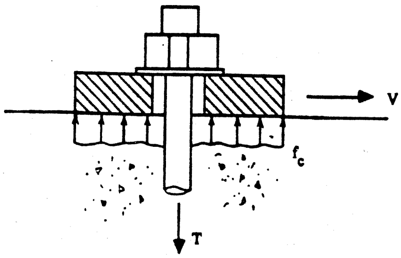

(b) Free Body Diagram of Baseplate with Anchor

Figure 4.2 Frictional forces on the baseplate prior to anchor bearing

$$V = \mu\,\Sigma T + \mu_s\,\Sigma T$$

$$\mu = \left(V/\Sigma T\right) - \mu_s \qquad (4-2)$$

where: $\mu =$ coefficient of friction between the baseplate and the concrete

$\mu_s =$ coefficient of friction between the washers and the baseplate

The coefficient of friction between the baseplate and the concrete, μ, was determined by using a material with a known coefficient of friction between the washer and the baseplate, μ_s, in the friction tests.

The coefficient of friction between the baseplate and the concrete, μ, is applicable to connections where the anchors bear against the baseplate.

In this situation the anchors displace with the baseplate and the only frictional force is between the baseplate and the concrete.

The anchors begin to bear on the baseplate when the applied shear load exceeds the effective frictional force of the connection. The ultimate load tests were all in this category. To analyze this type of connection the coefficient of friction for steel on concrete, μ, must be evaluated.

A friction test was conducted before every ultimate load test so that a unique coefficient of friction could be determined for each ultimate load test.

4.4 Development of Ultimate Load Tests

4.4.1 Two-Anchor Rigid Baseplate Tests. The purpose of the two-anchor rigid baseplate tests was to determine the tension/shear interaction relationship for various types of anchors. Fig. 4.3 shows a free-body diagram of a typical two-anchor rigid baseplate specimen.

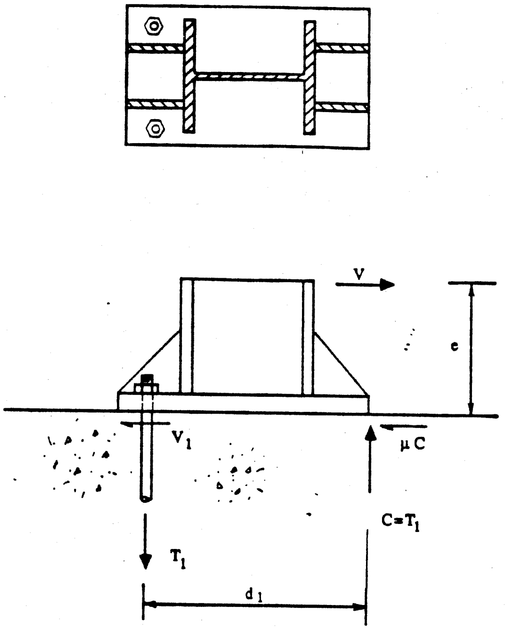

Figure 4.3 Free body diagram of a two-anchor rigid baseplate specimen

Using the coefficient of friction determined by the friction test, μ, the anchor tension, T_1, and applied shear, V, the amount carried by the anchors, V_1, is calculated as:

$$V_1 = V - \left(\mu\, T_1\right) \qquad (4-3)$$

where: $\mu\, T_1 \leq V$

By loading at different eccentricities, several combinations of anchor tension and anchor shear were recorded. The results were used to determine the tension/shear interaction relationship for the anchors.

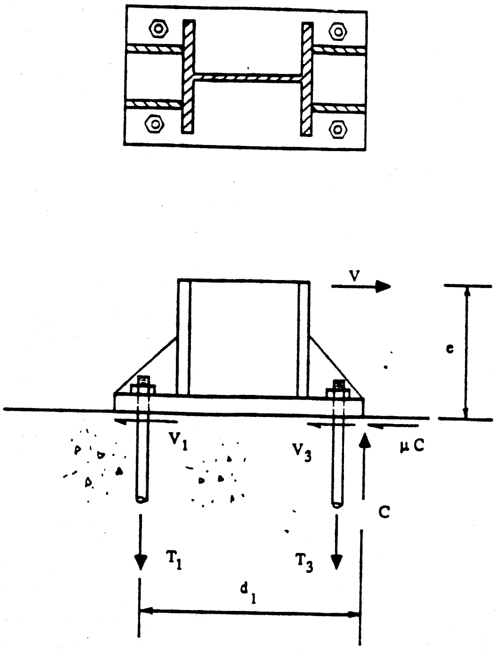

Figure 4.4 Free body diagram of a four-anchor rigid baseplate specimen

4.4.2 Four-Anchor Rigid Baseplate Tests. The four-anchor rigid baseplate tests were developed to determine the distribution of shear among anchors. Fig. 4.4 shows a free-body diagram of a typical four-anchor rigid baseplate specimen.

The difference between the two-anchor tests and the four-anchor tests is the contribution of the shear strength of the anchors on the compression side of the steel attachment.

Individual anchor shear was not measured. By using the coefficient of friction from the friction test, the tension/shear interaction relationship developed from the two-anchor tests, and the measured values of anchor tension, the amount of shear redistribution in the connection at failure can be evaluated.

For example: If the total applied shear load at failure is equal to the sum of the frictional force between the concrete and the steel, plus the pure shear strength of the anchors on the compression side of the connection, plus the residual shear strength of the tension-side anchors based on their tension/shear interaction, then full redistribution of shear has occurred in the connection.

4.4.3 Six-Anchor Rigid Baseplate Tests. The six-anchor rigid baseplate tests were developed to determine the distribution of tension among the anchors, and to verify if the method of shear distribution determined from the four-anchor tests could be extended to a six-anchor configuration. Fig. 4.5 shows a free body diagram of a typical six-anchor rigid baseplate specimen.

The difference between the six-anchor tests and the four-anchor tests was the addition of a middle row of anchors. From a design viewpoint this is a very inefficient location for additional anchors. For additional moment capacity the anchors should be placed toward the tension side of the

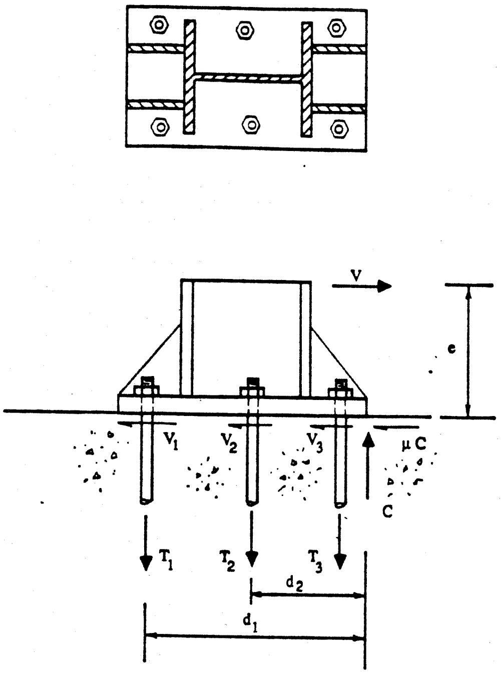

Figure 4.5 Free body diagram of a six-anchor rigid baseplate specimen

of the connection. Because the purpose of these tests was to determine the distribution of tension and shear in an extreme situation, the anchors were placed at the centerline of the connection. Since the anchor tension was measured for all anchors, the distribution of tensile forces in the connection was known throughout the test.

4.4.4 Six-Anchor Flexible Baseplate Tests. The primary purpose of the six-anchor flexible baseplate tests was to evaluate the effects of baseplate flexibility on the location of the compressive resultant. A secondary purpose was to determine if the methods of predicting shear and tension distribution developed in the rigid baseplate tests could be extended to connections with flexible baseplates.

In a rigid baseplate test there is no flexibility in the steel attachment, and the compressive reaction from applied moment is located at the leading edge of the plate. In a flexible baseplate loaded with applied moment, the portion of the baseplate extending beyond the attached member bends and causes the compressive reaction to shift inward from the leading edge. Fig. 4.6 shows a free-body diagram of a typical six-anchor flexible baseplate specimen. Since the applied moment, $(V x e)$, and the anchor tensions, T_1 and T_2, were measured, the internal moment arm for the outer row of tension anchors, d_1, is calculated by the condition of moment equilibrium as:

$$V\,e = T_1\,d_1 + T_2\left(d_1 - s\right)$$

$$d_1 = \left(V\,e - T_2\,s\right) / \left(T_1 + T_2\right) \tag{4-4}$$

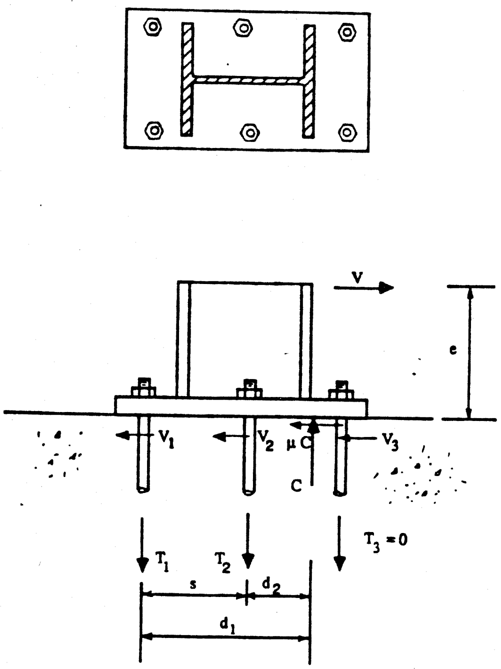

Figure 4.6 Free body diagram of a six-anchor flexible baseplate test

The location of the compressive reaction, as determined by Eq. (4-4), can be compared to what would be predicted by the various procedures given in Subsection 2.3.1. The appropriate method of analysis for determining the internal moment arm and the location of the compressive resultant for flexible baseplates can then be determined.

4.5 Development of Test Specimens

To study the behavior of ductile multiple-anchor connections, the test specimens were developed so that steel failure would occur. Anchors tested in this study included cast-in-place anchors, undercut anchors, and six types of adhesive anchors. Anchor material, anchor diameter, anchor patterns, and baseplate size were consistent with what might typically be used to connect a W12 steel beam to concrete. Embedment failure was precluded by using the embedment design provisions of *ACI 349-85* [4] for cast-in-place and undercut anchors, and the results of the study by Collins and Klingner [1] for adhesive anchors. The provisions of ACI *349-85* [4] were also used to prevent flexural or shear failure of the test blocks.

In the following subsections, information is presented on the materials, anchor patterns, embedment design basis, test block design basis, and baseplate design basis used in the experimental program.

4.5.1 Materials. The design basis for selecting the particular anchor material, baseplate material, and concrete used in this study are given below:

1) *Anchors*: To produce a probable worst-case condition for redistribution of shear and tension, the anchor material chosen was a high-strength steel with no yield plateau. The material used for all types of anchors conformed to ASTM A193-B7. This material is commonly used by retrofit anchor manufacturers, and is mechanically equivalent to other high- strength steels used for connecting steel members, such as ASTM A325 and ASTM A354. All anchors were 5/8-inch diameter.

   The minimum specified tensile strength of the anchor material is 125 ksi, the minimum specified yield strength determined at a 0.2% offset is 105 ksi, and the minimum specified elongation in 2 inches is 16%. The average tensile strength of the material as determined from 24 tests by Collins and Klingner [1] and Doerr and Klingner [2] is 31.0 kips, or 137.2 ksi on the tensile stress area.

2) *Baseplates*: The baseplate material for the rigid baseplate tests was ASTM A572 Grade 50. The baseplate material for the flexible baseplate tests was ASTM A36. Both of these materials are commonly specified for baseplates. The important aspect of the baseplates was the surface condition of the bottom of the plates. To produce a probable lower bound to the coefficient of friction between the baseplates and the concrete, the bottom surface of the plates was chosen to be clean mill scale.

3) *Concrete*: The concrete chosen for the experimental program was a ready-mix concrete designed to meet Texas SDHPT Specifications for Class C concrete. Minimum design compressive strength was 3600 psi at 28 days, and minimum tensile strength (midpoint modulus of rupture) was 600 psi at 7 days for moist-cured specimens.

4.5.2 Anchor Pattern. The anchor pattern chosen for the experimental study was consistent with what is required to develop the plastic moment capacity of a W12 steel beam with a yield strength of 36 ksi using 5/8- inch diameter ASTM A193-B7 anchors.

The anchor patterns and baseplate dimensions were developed to provide adequate clearance for a wrench or tensioning device, and to meet the minimum edge distance requirements of the AISC *LRFD Specification* [6]. The minimum distance between the steel member and the centerline of the 5/8-inch diameter anchors was taken as 2 inches based on the clearance requirements for wrenches and tensioning devices. The minimum edge distance required for 5/8- inch diameter anchors by the AISC *LRFD Specification* [6] is 7/8 inch; 1 inch was used. The edge distances between the centerline of the anchors and the edge of the baseplate were differed slightly for the rigid baseplate tests and flexible baseplate tests. Fig. 4.7 shows the general anchor pattern and dimensions of the rigid and flexible baseplate with a W12 steel beam.

The maximum design moment capacity of the six-anchor rigid baseplate (Fig. 4.5), as limited by the strength of the anchor steel, was determined using the following assumptions:

1) The compressive reaction from the applied moment was assumed to be at the toe of the plate.

2) The tensile forces, T_3, in the anchors on the compression side of the plate were assumed to be zero.

3) The tensile forces in the extreme tension anchors, T_1, and the middle row of anchors, T_2, were assumed to be at their design tensile strength.

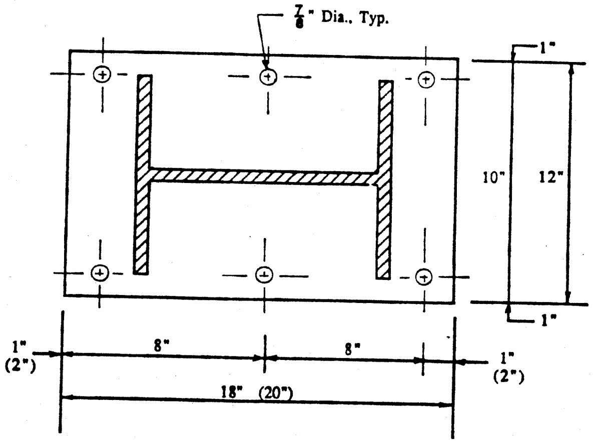

NOTE: DIMENSIONS IN PARENTHESES ARE FOR THE FLEXIBLE BASEPLATE

Figure 4.7 General anchor pattern and baseplate dimensions (all dimensions in inches

4) The design tensile strength of the anchors was determined using the procedures of the AISC *LRFD Specification* as given in Table 2.1.

The maximum design moment capacity of the connection as limited by the strength of the anchor steel was calculated as:

$$\phi M = \phi T_1 d_1 + \phi T_2 d_2$$

$$\phi M = \phi A_s F_u \left(d_1 + d_2\right)$$

$$\phi M = (0.75) \left[(2)(0.226)\right] (125)(17 + 9)$$

$$\phi M = 1102 \; in - k = 91.8 \; k - ft$$

This design moment capacity is sufficient to develop the plastic moment capacity of a W12x22 steel beam.

4.5.3 Embedment Design Basis. The embedded length of the anchors was determined using the provisions of *ACI 349-85* [4] for cast- in-place and undercut anchors, and using the results of the study by Collins and Klingner [1] for adhesive anchors.

For the cast-in-place and undercut anchors, the required embedded length necessary to develop the six-anchor pattern was determined to be 11 inches by the procedures of *ACI 349-85* [4].

The required embedded length for adhesive anchors was determined by applying a capacity reduction factor, ϕ, of 0.65 to the embedded length which typically failed the steel for single 5/8-inch diameter ASTM A193-B7 adhesive anchors in the tests reported by Collins and Klingner [1]. The corresponding required embedded length was determined to be 11 inches.

Therefore an 11 inch embedded length was used for all types of anchors in all types of tests.

4.5.4 Test Block Design Basis. As shown in Fig. 4.8, a typical test block was 42 inches wide by 56 inches long by 24 inches deep, and was reinforced with 7-#6 bars in both the top and bottom face, and 12-#4 U- shaped stirrups. Cast-in-place and retrofit anchors were installed in the blocks on the top surface for some of the tests, and on the bottom surface for other tests. The anchor pattern centerline coincided with the centerline of the block.

The blocks were designed to satisfy the minimum edge distance requirements of the anchors as determined by the provisions of *ACI 349-85* [4]. The blocks were also designed to transfer load from the steel attachment to the test frame and tie-down anchors in the laboratory floor. The procedures of *ACI 349-85* [4] were used to evaluate the flexural and shear reinforcement requirements for the blocks. PVC sleeves were cast into the ends of the block to accommodate the tie-down anchors.

4.5.5 Rigid Baseplate Design Basis. Although the anchor patterns were developed to be consistent with connecting a W12 steel beam, it was not possible, using a W12 member, to obtain rigid baseplate behavior, and also provide an adequate interface with the test frame. To provide a steel attachment that would rotate as a rigid body, the attached member was constructed of two 1 inch plates separated by 3-1/4 inches, extending the full length of the baseplate, and welded to the baseplate with full-penetration welds. The plate separation was required for attaching the horizontal loading arm of the test frame. Fig. 4.9 shows the steel attachment used for the rigid baseplate tests. The eccentricities shown in Fig. 4.9 are discussed in Subsection 4.6.2.

The overall thickness of the baseplate was 2 inches, sufficient to prevent yielding of the baseplate near the attached member. The baseplate was counterbored 1/2 inch deep by 2-1/4-inches diameter around the anchor hole centerlines, reducing the baseplate thickness to 1-1/2 inches at the anchors. This provided a reasonable projected anchor length above the surface of the concrete.

The anchor holes were 7/8-inches diameter. This corresponded to a 1/4 inch oversize hole for the 5/8-inch diameter anchors, which is larger than the 3/16 inch oversize permitted by the AISC *LRFD Specification* [6]. The large oversize was to accommodate construction tolerances and to provide a probable worst case for redistribution of shear in the connection.

4.5.6 Flexible Baseplate Design Basis. The flexible baseplate was designed to yield on the compression side of the baseplate, and be at or just above yield on the tension side of the baseplate at anchor failure. The particular design chosen was meant to represent a reasonable limit on plate

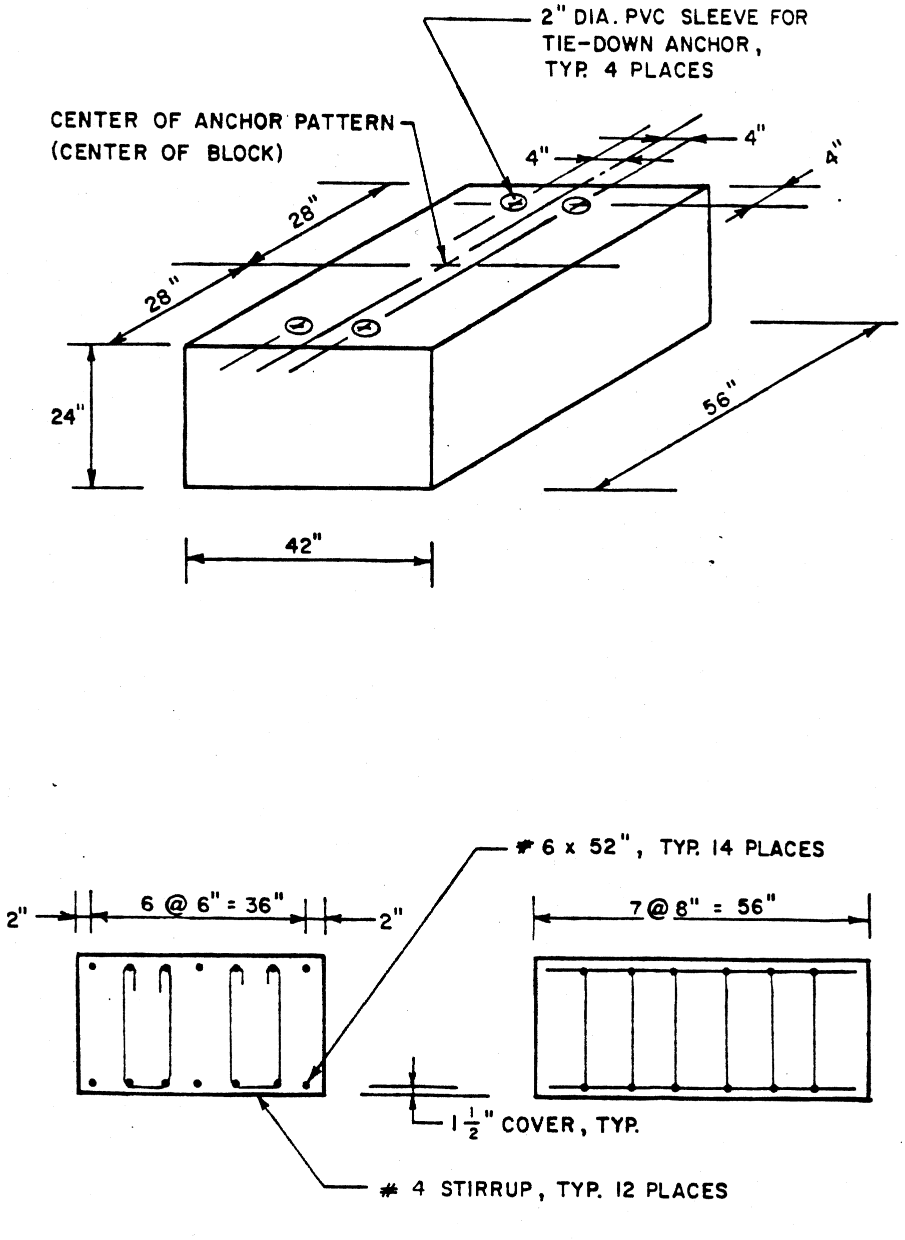
2" DIA. PVC SLEEVE FOR TIE-DOWN ANCHOR, TYP. 4 PLACES
CENTER OF ANCHOR PATTERN (CENTER OF BLOCK)
4"
4"
4"
28"
28"
24"
56"
42"
# 6 x 52", TYP. 14 PLACES
2"
6 @ 6" = 36"
2"
7 @ 8" = 56"
1 1/2" COVER, TYP.
# 4 STIRRUP, TYP. 12 PLACES

END VIEW

SIDE VIEW

Figure 4.8 Typical test block

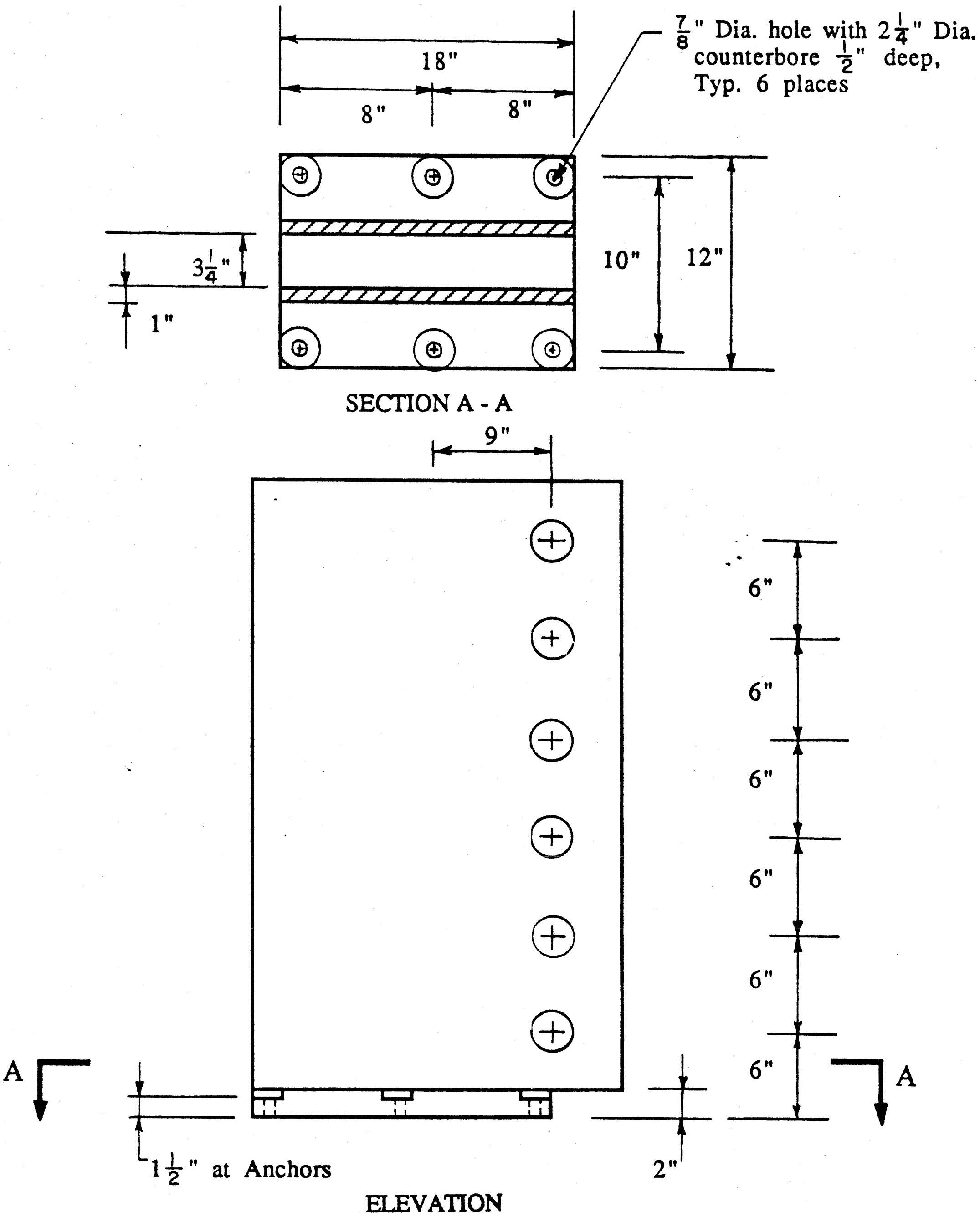

7/8" Dia. hole with 2 1/4" Dia. counterbore 1/2" deep, Typ. 6 places
18"
8"
8"
3 1/4"
1"
10"
12"
SECTION A - A
9"
6"
6"
6"
6"
6"
6"
A
A
1 1/2" at Anchors
2"
ELEVATION

Figure 4.9 Steel attachment for rigid baseplate tests

flexibility. If the plate were more flexible (thinner), a plastic hinge would form on the tension side of the baseplate, possibly causing prying forces in the anchors.

The six-anchor flexible baseplate dimensions were chosen based on using a 12 inch deep member on a 20 inch deep baseplate with the same anchor pattern as the rigid baseplate tests. The flexible baseplate was 2 inches longer than the rigid baseplate. The extra 2 inches in length was provided to increase the flexibility of the baseplate. The attached member was constructed using two 12 inch channel sections separated by 5-1/4 inches. The channel separation was required for two 1 inch plates and the horizontal loading arm of the test frame. Fig. 4.10 shows the steel attachment used for the flexible baseplate tests. The eccentricity shown in Fig. 4.10 is discussed in Subsection 4.6.2.

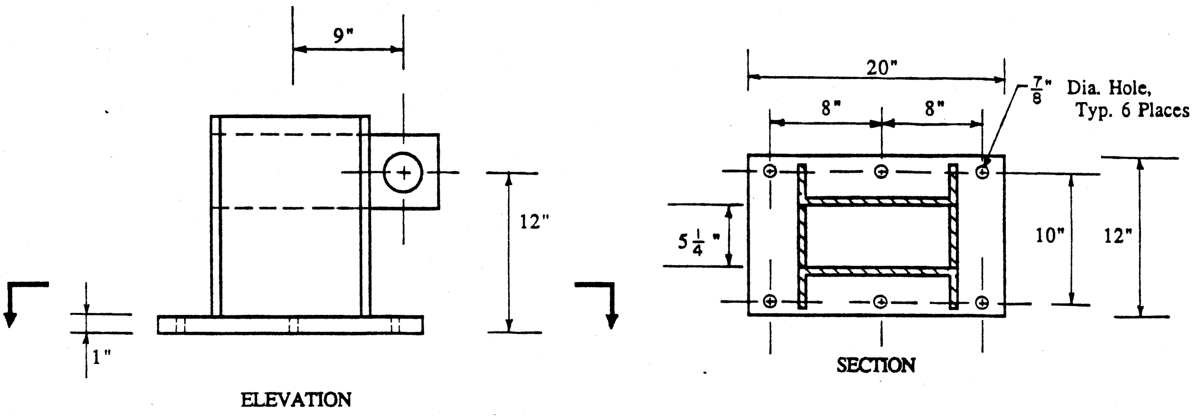

Figure 4.10 Steel attachment for flexible baseplate tests

The plate thickness was determined by assuming that at ultimate a force equal to the yield strength of the outer row of tension anchors would be applied to the baseplate at the tension anchor holes. The baseplate, acting as a tip-loaded cantilever, would have to be thick enough to avoid the formation of a plastic hinge at the edge of the tension flange of the attached member. The effective width of the cantilever was taken as the plate width, b. The design flexural strength of the baseplate, ϕM_p, was determined using the provisions of the AISC *LRFD Specification* [6]. Fig. 4.11

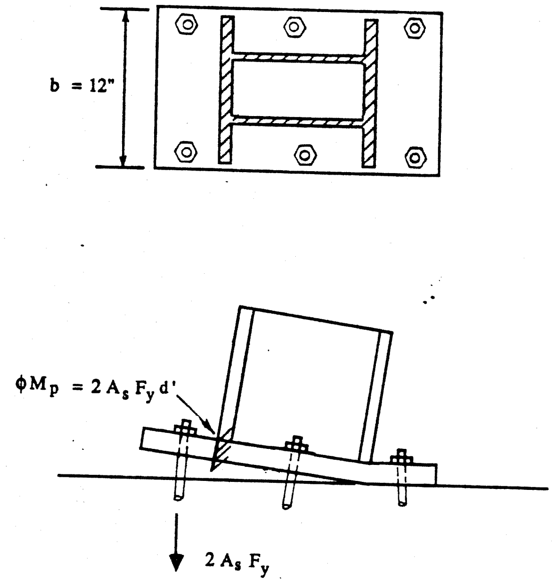

Figure 4.11 Design basis for flexible baseplate tests

shows the design basis for determining the thickness of the flexible baseplate. The flexible baseplate thickness was determined as:

$$\phi\ M_p \ \geq\ 2\ A_s\ F_y\ d'$$

$$\phi\ F_y \left(b\ t^2\ /\ 4\right) \ \geq\ 2\ A_s\ F_y\ d'$$

$$0.9\ (36)\ \Bigg(12\ t^2\ /\ 4Biggr) \ \geq\ 2\ (0.226)\ (105)\ (2)$$

$$t \ \geq\ 1 - inch$$

Since the actual tensile forces in the anchors were expected to exceed the yield strength of the anchors it was considered likely that yielding would occur on the tension side of the plate for the 1-inch plate thickness. If prying forces did not develop for this case, then baseplate thicknesses determined using the method described in Subsection 2.4.1 (based on the average strength of the anchors rather than the yield strength), could be considered sufficient to prevent significant prying forces.

Since the compressive resultant in the six-anchor test would be equal to the load in the four tension anchors, the 4 inch portion of the plate projecting past the compression flange was expected to yield. This compression- side yielding was not expected to degrade the performance of the attachment. As verified in the test program, this was in fact the case.

4.6 Development of Test Setup

The test setup was developed to apply shear loads to the steel attachment at various eccentricities, and to be capable of failing the anchors at all eccentricities.

4.6.1 Description of Test Setup. The test setup is shown schematically in Fig. 4.12. The test setup consisted of the following components:

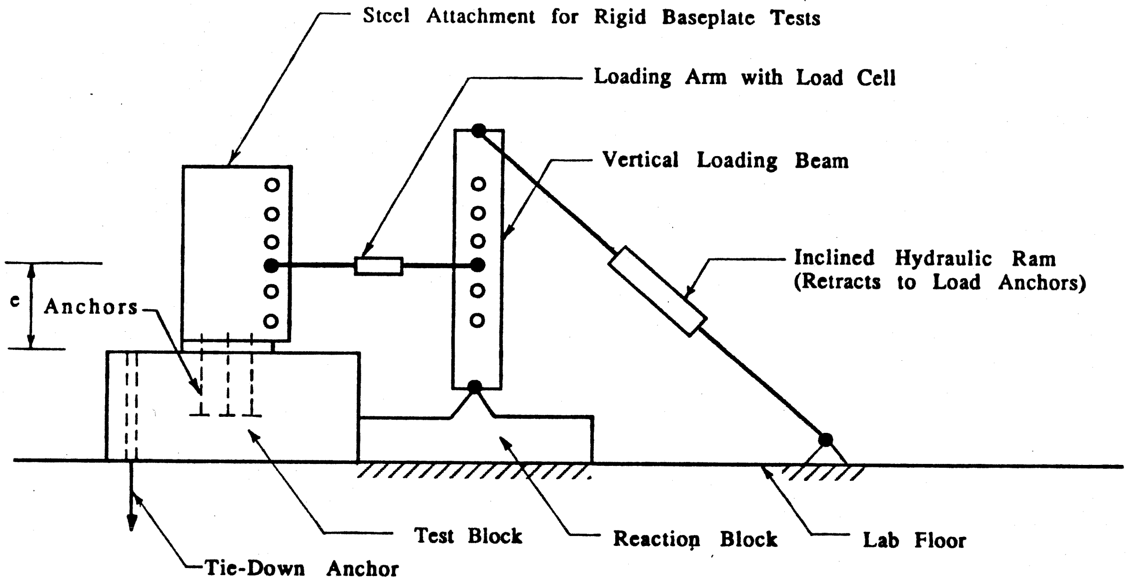
Steel Attachment for Rigid Baseplate Tests
Loading Arm with Load Cell
Vertical Loading Beam
Inclined Hydraulic Ram (Retracts to Load Anchors)
e
Anchors
Test Block
Reaction Block
Lab Floor
Tie-Down Anchor

Figure 4.12 Schematic Diagram of Test Setup

1) A test block, held in place by tie-down anchors in the lab floor and by the reaction block.

2) A steel attachment, connected to the test block by the anchors to be tested. The steel attachment contained holes (for hardened steel pins) at the desired shear load eccentricities. The holes used in this study were located over the toe of the baseplate.

3) A concrete and steel reaction block, fixed to the laboratory floor. The reaction block prevented the test block from slipping, and provided a pinned-end reaction point for the vertical loading beam.

4) A vertical loading beam, attached to the reaction block at the bottom of the beam and the inclined hydraulic ram at the top of the beam by pinned-end connections. Several holes were provided in the vertical loading beam at the elevations corresponding to the desired shear load eccentricities.

5) An inclined hydraulic ram, connected between the top of the vertical loading beam and a clevis on the laboratory floor by pinned-end connections.

6) A horizontal loading arm, connected between the vertical loading beam and the steel attachment by pinned-end connections. The horizontal loading arm could be moved up or down to provide the desired shear load eccentricity on the connection. The horizontal loading arm contained a load cell.

Loads were applied to the connection by retracting the inclined hydraulic ram using displacement control.

4.6.2 Shear Load Eccentricities. The shear load eccentricities chosen were based on the behavioral model for ductile multiple anchor connections presented in Chapter 8.

The shear load eccentricities used for the test setup were developed to cover the range of connection behavior that is least understood. In this range of shear load eccentricities, the frictional shear resistance of the connection, $\mu\ C$, is smaller than the applied shear, and the anchors are utilized for shear transfer. The range of eccentricities in which the frictional shear resistance of the connection, exceeds the applied shear was not of interest, since the anchors in the tension zone fail in pure tension in such cases.

To determine the range of shear load eccentricities in which shear is transferred by the anchors, it was necessary to assume a value for the coefficient of friction, μ, between steel and concrete. The value of the coefficient of friction, μ, was taken as 0.50. As noted in Subsection 2.3.3, this value represents the mean of previous test results.

The maximum eccentricity for testing was determined by Eq. (8-7) as:

$$e' = d / \mu$$

where: e' = the minimum eccentricity for multiple- anchor connections without shear anchors, i.e. the maximum eccentricity for testing

μ = the assumed value for the coefficient of friction between steel and concrete (taken as 0.50)

d = the distance from the compressive reaction to the centroid of the anchors in the tension zone, $d = 17$ inches for the two-anchor and four-anchor rigid baseplate tests, $d = (17 + 9) / 2 = 13$ inches for the six-anchor rigid baseplate tests

For the rigid baseplate, the minimum shear load eccentricity for no shear transfer in the anchors was determined to be around 34 inches for the two- anchor and four-anchor tests, and 26 inches for the six-anchor tests.

The maximum shear load eccentricity for the rigid baseplate tests was taken as 36 inches. Intermediate eccentricities were taken at 6 inch increments as limited by the hole spacing in the attachment loading plates.

The possible shear load eccentricities for the rigid baseplate tests were 6 inches, 12 inches, 18 inches, 24 inches, 30 inches, and 36 inches.

For the six-anchor flexible baseplate tests only one eccentricity was considered. The eccentricity was chosen so that all the anchors would contribute to the shear strength of the connection. This eccentricity was determined by using an eccentricity slightly less than the minimum eccentricity, e'', given by Eq. (8-10). This ensured that all anchors would contributed to the shear strength of the connection. The ratio of the shear strength of the anchor to the tensile strength of the anchor, τ, was taken as 0.65. As shown in Table 2.2, this is the largest value determined by previous experimental results.

The eccentricity, e'', was determined by Eq. (8-10) as:

$$e'' = n\,d \,/ \left(n\,\mu + \tau \right)$$

where: e'' = the minimum eccentricity for multiple- anchor connections without combined tension and shear in the anchors

n = the number of rows of anchors in the tension zone equal to 1 for the four-anchor pattern, and to 2 for the six- anchor pattern

μ = assumed value for the coefficient of friction between steel and concrete (taken as 0.50)

τ = assumed value for the ratio of the shear strength of the anchor to the tensile strength of the anchor (taken as 0.65)

d = the distance from the compressive reaction to the centroid of the tension anchors. For the six-anchor flexible baseplate this was taken as the same distance as for the six-anchor rigid baseplate: d = (17 + 9) / 2 = 13 inches

For the flexible baseplate, the minimum shear load eccentricity, e'', for which the anchors in the tension zone can be assumed to be at their full tensile strength was determined to be around 15 inches. A shear load eccentricity of 12 inches was used in the flexible baseplate tests to ensure that all anchors would contribute to the shear strength of the connection.

4.6.3 Test Frame and Loading System. The test frame and loading system were developed to transfer sufficient horizontal loads to the steel attachment to cause anchor failure for all types of connections. The six- anchor pattern was used as the design basis for the test frame and loading system.

The eccentric shear load required to fail the six-anchor connection was taken as the lesser of the load necessary to cause shear failure of all the anchors in the connection, or the load necessary to cause flexural failure of the connection with all the anchors in the tension zone attaining their maximum tensile strength. The load necessary to cause shear failure of the connection was determined by using the maximum shear strength of threaded anchors as reported in previous experimental studies. The load necessary to cause shear failure of a six-anchor connection was determined as:

$$V = 6\left(\tau\, T_{ut}\right)$$

$$V = 6\,(0.65)\,(31) = 121\ kips \qquad (4-5)$$

The load necessary to cause flexural failure of a six-anchor connection was determined using the behavioral model for ductile multiple anchor connections presented in Chapter 9. The load was determined using Eq. (9-4), with e substituted for e', as:

$$V = n\, T_{ut} d \,/\, e$$

$$V = 2\left((2)\,(31)\right)\left(13\right) / \, e$$

$$V = 1612 \,/\, e\ (in - kips) \qquad (4-6)$$

The design loads for the test frame and loading system were taken as the lesser of Eq. (4-5) or Eq. (4-6) multiplied by a load factor of 1.3. The design loads, including the load factor of 1.3, are shown in Table 4.1. The test frame was designed using the loads in Table 4.1 with the AISC *LRFD Specification* [6].

Table 4.1 Design Loads for Test Frame and Loading System

Shear Load Eccentricity e (in)	Design Load for Test Frame and Loading System (kips)
6	157
12	157
18	116
24	87
30	70
36	58

Note: The design loads include a load factor of 1.3

An important requirement of the test setup was to maintain the horizontal orientation of the load acting on the steel attachment. This was accomplished by locating the pivot points of the test frame and steel attachment to minimize the differential vertical displacement between the two ends of the horizontal loading arm. The maximum theoretical deviation of the horizontal loading arm from horizontal was limited to less than 0.1x. This corresponds to a vertical load component less than 0.2% of the horizontal load. This is insignificant.

4.7 Development of Test Instrumentation

In order to evaluate the behavior of the multiple-anchor connections it was necessary to develop means of measuring the eccentric shear load, V, the eccentricity of the shear load, e, the individual anchor tension, T, the baseplate slip, δ, and the baseplate rotation, Θ.

The eccentricity of the shear load, e, could vary from 6 inch through 36 inch eccentricities in 6 inch increments, because of the hole spacing.

The deviation of the shear load eccentricities from theoretical was kept to a minimum by specifying q 1/32 inch tolerances on the hole locations in the steel attachment and the vertical loading beam.

4.7.1 Load Measurement. The eccentric shear load, V, was measured by a commercially manufactured load cell installed in the horizontal loading arm.

The individual anchor tension loads were measured by specially constructed anchor load cells and anchor load cell adapters. The overall objective in the development of the anchor load cells and anchor load cell adapters was to measure the anchor tension without interfering with the anchor behavior.

Strain gages applied directly to the anchors were not considered since they would only give relative values for anchor tension and since their installation would reduce the net cross section of the anchor.

Fig. 4.13 shows a schematic diagram of an anchor load cell and anchor load cell adapter. The anchor load cells used in the experimental program were the same as those used by Armstrong, Klingner, and Steves [51] in their study of highway impact barriers. The anchor load cells were 2 inch high sections of high-strength steel tubing with a 1-inch inside diameter and a 1/4-inch wall thickness.

The anchor load cell adapters were developed to meet the following objectives:

1) Maintain the effective anchor projection above the surface of the concrete to what might be expected in a connection without load cells.
2) Provide the same restraint at the surface of the baseplate as provided by a standard nut.
3) Provide a means for preloading the anchors with a center-hole ram so that the residual preload could be measured by the anchor load cells in the friction tests.

As shown in Fig. 4.13 the anchor load cell adapters were developed to fit inside the load cells. The outside diameter of the anchor load cell adapters was slightly less than the inside diameter

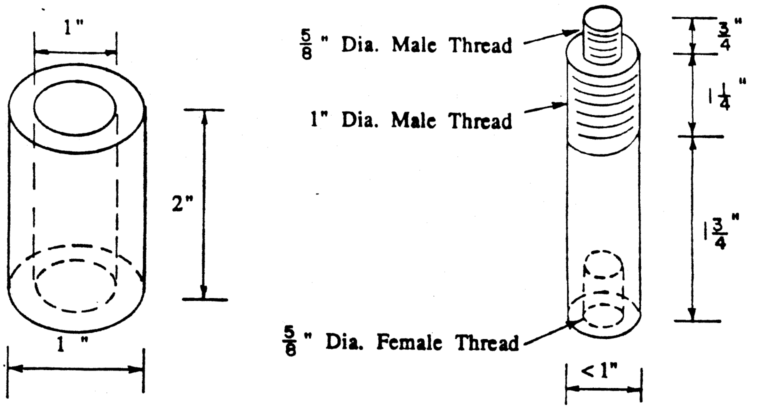
1"
2"
1 "
$\frac{5}{8}$ " Dia. Male Thread
1" Dia. Male Thread
$\frac{5}{8}$ " Dia. Female Thread
$\frac{3}{4}$ "
$1\frac{1}{4}$ "
$1\frac{3}{4}$ "
< 1"

(a) Anchor Load Cell

(b) Anchor Load Cell Adapter

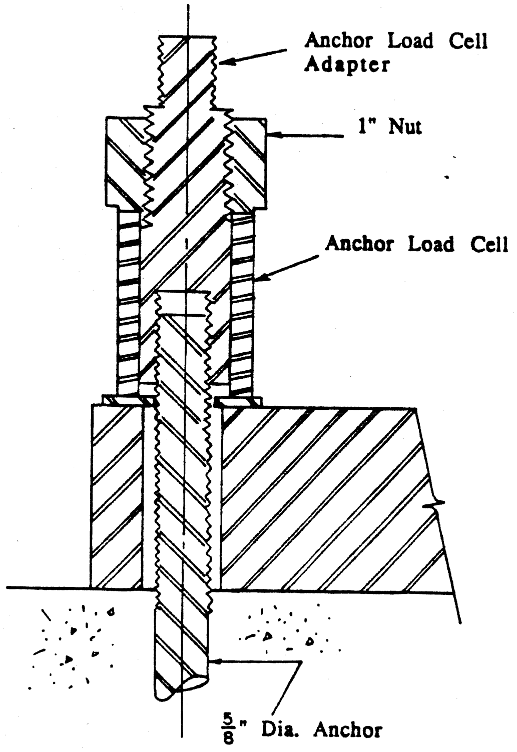
Anchor Load Cell Adapter
1" Nut
Anchor Load Cell
$\frac{5}{8}$" Dia. Anchor

(c) Installed Anchor Load Cell and Adapter

Figure 4.13 Schematic diagram of anchor load cell and adapter

first set of male threads accepted a standard 1-inch nut which bore on the load cell. The second set of male threads was 5/8-inches diameter and extended above the first. These threads provided a means of preloading the anchors with a center-hole ram in the friction tests.

The anchor load cell adapters limited the required projection of the anchors above the surface of the concrete. For the rigid baseplate tests, the effective projection of the anchors between the surface of the concrete and the base of the anchor load cell adapter was about 1-5/8-inches. For the flexible baseplate tests, the effective projection was about 1-1/8-inches. These effective anchor projections are what would be expected in a connection without the anchor load cells.

The anchor load cell adapters allowed the anchors to deform as in a connection without the anchor load cells.

4.7.2 Displacement and Rotation Measurement. Measurement of the baseplate slip, δ_h, was required for all tests. The important slip measurement was slip relative to the surface of the concrete. This is shown schematically in Fig. 4.14.

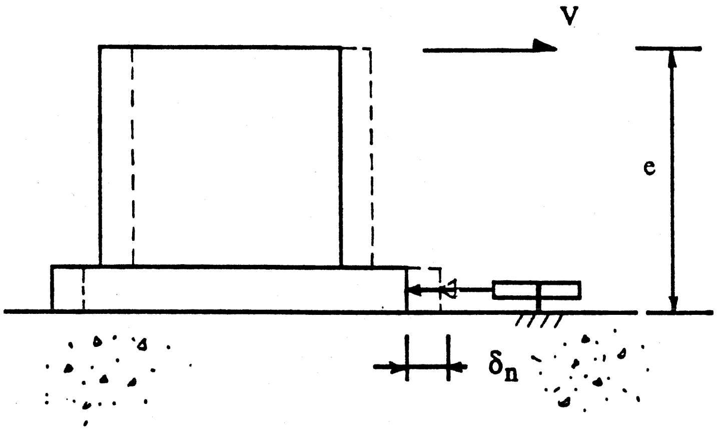

Figure 4.14 Schematic diagram of slip measurement

Baseplate rotation, Θ, for the rigid baseplate could be evaluated by measuring a single displacement since the plate was assumed to rotate as a rigid body on the concrete. This is shown schematically in Fig. 4.15. The plate rotation, Θ, could be evaluated as:

$$\Theta = \delta_v / h$$

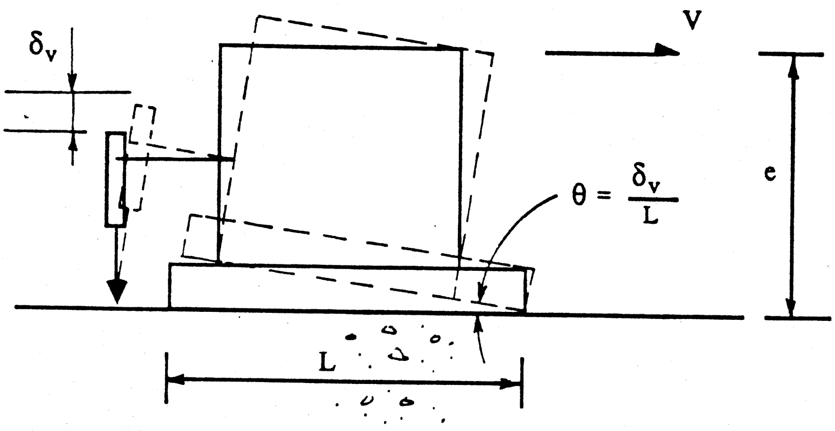

Figure 4.15 Schematic diagram of rotation measurement for rigid baseplate tests

Baseplate rotation, Θ, for the flexible baseplate was not measured directly. Instead, the vertical displacement along the centerline of the baseplate was measured at several locations. This is shown schematically in Fig. 4.16.

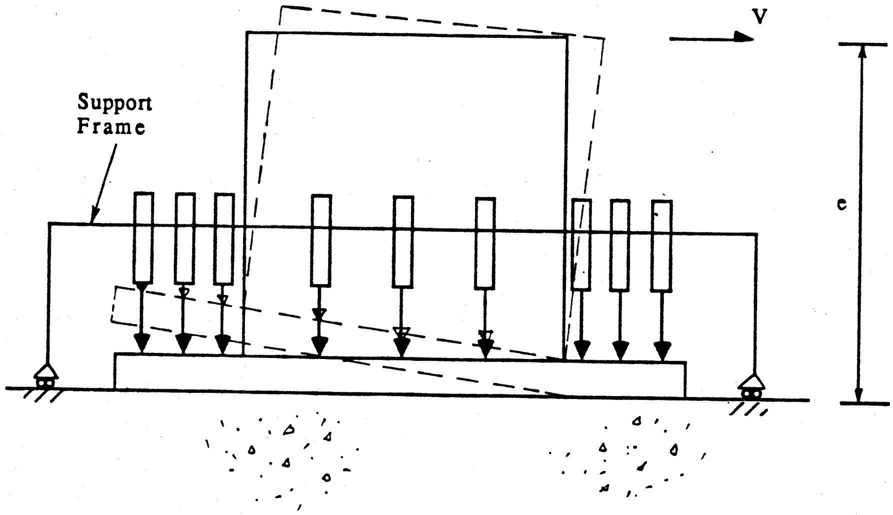
V
Support Frame
e

Figure 4.16 Schematic diagram of vertical displacement measurement for flexible baseplate tests

5. IMPLEMENTATION OF EXPERIMENTAL PROGRAM

5.1 Introduction

All tests were conducted on the testing floor of the Ferguson Structural Engineering Laboratory at the Balcones Research Center of the University of Texas at Austin. This chapter contains a discussion of the test matrix and test designations, the concrete casting procedures, the material properties, the anchor installation procedures, the testing equipment, and the testing procedures.

5.2 Test Matrix and Test Designations

5.2.1 Test Matrix. The test matrix is shown in Table 5.1. Three types of anchors were tested: cast-in-place (CIP); undercut (M1); and adhesive (A1-A6). Six different adhesives were included in the testing program: three epoxies (A1, A5, A6); two polyesters (A3, A4); and one vinylester (A2). The specific brand names of the undercut and adhesive anchors are shown in Table 5.1. The test matrix was developed to assess the behavior of all types of anchors, in the range of shear load eccentricities where connection behavior is least understood.

One epoxy adhesive and one polyester adhesive were tested for all the anchor patterns. The other four adhesives were tested only in the six-anchor pattern at 12 inch eccentricity with the rigid baseplate. This pattern and eccentricity were chosen to permit comparison of results for the six adhesives.

5.2.2 Test Designations. Each rigid baseplate test was designated by the number of anchors in the pattern, the type of anchor, and the eccentricity of the applied shear load. For example: Test 6 CIP 12 refers to a six-anchor rigid baseplate test with cast-in-place anchors, loaded at a 12 inch eccentricity. Test 4 A4 6 refers to a four-anchor rigid baseplate test with type A4 adhesive anchors, loaded at a 6 inch eccentricity.

The test number for a flexible baseplate test is followed by an “x”. For example: Test 6 M1 12x refers to a six-anchor flexible baseplate test with undercut anchors, loaded at a 12 inch eccentricity.

5.3 Concrete Casting

All test blocks were cast outdoors using ready-mix concrete (Fig. 5.1). Concrete was placed in three lifts, each consolidated with a mechanical vibrator. After the final lift, the surface was screeded, trowelled, and covered with polyethylene sheets to aid in curing. Cylinders were cured beside the formwork and under the same conditions as the test specimens. The formwork was stripped and the test blocks were moved within 7 days after casting. The blocks were not tested until at least 28 days after casting. Three test blocks were cast in each of nine separate concrete pours.

A form release agent was used on the forms but care was taken not to apply the release agent to the central portion of the bottom of the forms. This prevented contamination of the bottom surface of the test block in the area where the baseplate was to be attached.

Table 5.1 Test Matrix

TYPE OF TEST	*e* in.	TYPE OF ANCHOR (See Notes)								No. Tests
		CIP	M1	A1	A2	A3	A4	A5	A6	
Two-Anchor Rigid Baseplate	6	1	1	1	–	–	–	–	–	3
	12	1	1	1	–	–	1	–	–	4
	18	1	1	1	–	–	–	–	–	3
	24	1	1	–	–	–	1	–	–	3
	30	1	1	–	–	–	–	–	–	2
	36	1	1	–	–	–	1	–	–	3
										18
Four-Anchor Rigid Baseplate	6	1	1	1	–	–	1	–	–	4
	12	1	1	1	–	–	1	–	–	4
	18	1	1	1	–	–	1	–	–	4
	24	1	–	–	–	–	–	–	–	1
										13
Six–Anchor Rigid Baseplate	6	1	1	–	–	–	–	–	–	2
	12	1	1	1	1	1	1	1	1	8
	18	1	1	–	–	–	–	–	–	2
										12
Six–Anchor Flexible Baseplate	12	–	1	1	–	–	1	–	–	3
No. Tests		13	13	8	1	1	8	1	1	46

NOTES:
CIP = cast–in–place anchors
M1 = undercut anchor by Drillco (MAXIBOLT)
A1 = adhesive anchor by Ramset (EPCON)
A2 = adhesive anchor by Hilti (HIT)
A3 = adhesive anchor by Hilti (HVA)
A4 = adhesive anchor by Kelken (KELI-GROUT)
A5 = adhesive anchor by Sika (SIKA GEL)
A6 = adhesive anchor by Sika (SIKA INJECTION)

5.4 Materials

5.4.1 Concrete. The concrete used for the experimental program was a ready-mix concrete designed to meet Texas SDHPT Specifications for Class C concrete. The compressive strengths of 6-inch diameter x 12 inch cylinders are shown in Table 5.2. Since the three test blocks from each concrete pour were tested on different dates, the compressive strength at the time of testing is shown as a range in Table 5.2.

by Fel-Pro Incorporated of Skokie, Illinois. The lubricant had a specified coefficient of friction of $\mu_s = 0.10$.

3) Install the anchor load cell adapters, anchor load cells, and 1-inch nuts. Record the zero-load values for the anchor load cells.

4) Preload the anchors as required for the type of friction test being performed, using a center-hole hydraulic ram. This was accomplished by using an adapter with a female 5/8-inch diameter thread which fit through the center-hole ram and screwed onto the male 5/8-inch diameter thread of the anchor load cell adapter. The hydraulic ram was supported partially by the baseplate and partially by the concrete. The anchors were tensioned to about 80% of specified minimum yield. The 1-inch nuts were finger-tightened against the load cells, and the preload provided by the hydraulic ram was released. The residual preload in the anchors was recorded. The residual preload in the anchors was between 40% and 70% of the applied preload. Most of the preload loss appeared to be due to rocking of the baseplate on the surface of the concrete. Undercut anchors retained more preload than cast-in-place or adhesive anchors, due to their longer unrestrained length and more uniform cross section.

5) Install the horizontal displacement potentiometer and the horizontal loading arm with the main load cell. The horizontal loading arm was typically installed at the 6-inch eccentricity. Record the zero-displacement and zero-load values for the potentiometer and the main load cell.

6) Apply displacements increments to the attachment by retracting the inclined hydraulic ram. The eccentric shear load, the slip, and the anchor tension were measured continuously and/or immediately after each displacement increment.

7) Remove the horizontal loading arm, the anchor preload, the anchor load cells, and the anchor load cell adapters.

5.7.2 Ultimate Load Tests. A typical ultimate load test, with either a rigid baseplate or a flexible baseplate, involved the following steps:

1) Position the baseplate so that the anchors would contact the sides of the anchor holes away from the applied load. This ensured that some of the anchors would be in bearing at the start of the test.

2) Install the anchor load cell adapters, the anchor load cells, the 1-inch nuts, the horizontal loading arm, and the displacement potentiometers. Finger-tighten the 1-inch nuts. Record the zero-load and zero-displacement values for all load cells and potentiometers.

3) Apply displacement increments to the attachment by retracting the inclined hydraulic ram until an anchor fractured. The eccentric shear load, the anchor tension, and the horizontal and rotational displacements of the baseplate were measured immediately (less than 1 second), after each displacement increment. The displacement was incremented about every 30 seconds. Displacement increments were kept fairly constant throughout the test. A total of 40 to 50 displacement increments were applied in each test. In the latter portion of each test, the eccentric shear load was measured continuously as well as

after each displacement increment. Anchor failure was determined audibly, visually, and instrumentally.

4) Remove the horizontal loading arm, the anchor load cells, the anchor load cell adapters, the potentiometers, and the steel attachment.

5) Inspect the concrete surface and anchors. The concrete surface was inspected for spalling and crushing around the anchors and for the contact area between the baseplate and the concrete. The anchors which did not fracture were inspected for signs of yielding. A written and photographic record was made of each ultimate load test.

6. TEST RESULTS

6.1 Introduction

In this chapter, tabular summaries of test results, typical graphical results, and test observations for all tests are presented.

6.2 Friction Tests

Test results presented in this section are for the coefficient of friction, μ, between a steel baseplate and hardened concrete. Test results for the coefficient of friction, μ, were determined by the method discussed in Section 4.3.

Table 6.1 shows the maximum values of the coefficient of friction recorded by the HP Plotter and the HP DAS for tests in which both data acquisition systems were used. Fig. 6.1 shows typical results for the coefficient of friction plotted against baseplate slip as recorded by the two data acquisition systems. As shown in Table 6.1 and Fig. 6.1, there was essentially no difference in the results recorded by the two systems. The results recorded by the HP DAS are used in the remainder of this section, and in the discussion of friction test results in Chapter 7.

The results of the 44 friction tests performed in this study are shown in Table 6.2. Fig. 6.2 shows typical high and low results for the coefficient of friction plotted against baseplate slip (Mu-vs-Slip diagram). Mu-vs-Slip diagrams for other friction tests are presented in Appendix B.

The maximum, mean, and minimum values of the coefficient of friction shown in Table 6.2 are based on the following:

1) The maximum value of the coefficient of friction is the peak value recorded during the friction test.

2) The "mean" value of the coefficient of friction is the average of all the data points after the first significant slip occurred. The first significant slip was defined as the point where the slope of the Mu-vs-Slip diagram became less than 5 /inch. This data point is circled in the Mu- vs-Slip diagrams of Fig. 6.2 and Appendix B. This somewhat arbitrary definition of first slip was necessary since several tests did not exhibit a distinct point of first slip. The "mean" value is not the average of the maximum and minimum values.

3) The minimum value of the coefficient of friction is the lowest value recorded after the first significant slip.

Table 6.2 also shows the test variables that were considered to have a possible effect on the coefficient of friction. These variables are the sequential number of the friction tests with the rigid baseplate, the test block surface, the magnitude of the compressive force, and the type of friction test. The effects of these variables are discussed in Chapter 7.

In all types of friction tests, application of the eccentric shear load forced the centroid of the compressive force toward the leading edge, or toe, of the baseplate. This was especially true for friction tests where the compressive force was intentionally concentrated toward the leading edge prior to applying the shear load (the "toe" and "toe*" tests as described in Subsection 5.7.1).

Table 6.1
Maximum Coefficent of Friction Recorded on Separate Data Acquisition Systems

Test No.	Maximum Recorded Coefficient of Friction		
	HP Plotter	HP DAS	Difference
2 CIP 6	.50	.50	.00
2 A1 6	.39	.39	.00
2 M1 6	.44	.42	.02
2 CIP 12	.41	.41	.00
2 A1 12	.38	.38	.00
2 A4 12	.49	.49	.00
2 M1 12	.38	.37	.01
2 CIP 18	.43	.43	.00
2 A1 18	.40	.38	.02
2 A4 24	.55	.55	.00
2 CIP 30	.48	.48	.00
2 CIP 36	.40	.39	.01
2 A4 36	.23	.22	.01
4 CIP 6	.48	.48	.00
4 CIP 12	.45	.44	.01
4 A1 12	.41	.40	.01
4 A4 12	.51	.51	.00
4 M1 12	.66	.63	.03
4 CIP 18	.36	.36	.00
4 A1 18	.59	.58	.01
4 A4 18	.36	.36	.00
4 CIP 24	.59	.61	.02
6 CIP 12	.51	.51	.00
6 A4 12	.63	.62	.01
6 A5 12	.37	.37	.00
6 A6 12	.51	.52	.01
6 CIP 18	.47	.47	.00
6 A1 12X	.49	.50	.01
6 A4 12X	.37	.38	.01
6 M1 12X	.32	.32	.00

6.3 Ultimate Load Tests

All ultimate-load specimens failed by yielding and fracture of the anchors. The strength of the connection was limited by the strength of the steel in all tests.

Table 6.3 shows the maximum values of the applied shear load recorded by the HP Plotter and the HP DAS for those tests in which both data acquisition systems were used. As shown in Table 6.3, the maximum shear loads recorded by the HP Plotter were slightly higher than those recorded by the HP DAS (6% in one test and less than 2% in the others). The loads recorded by the HP Plotter better represent the maximum shear load carried by the connections since this system recorded data continuously (3 readings per second) during the last displacement increment. For

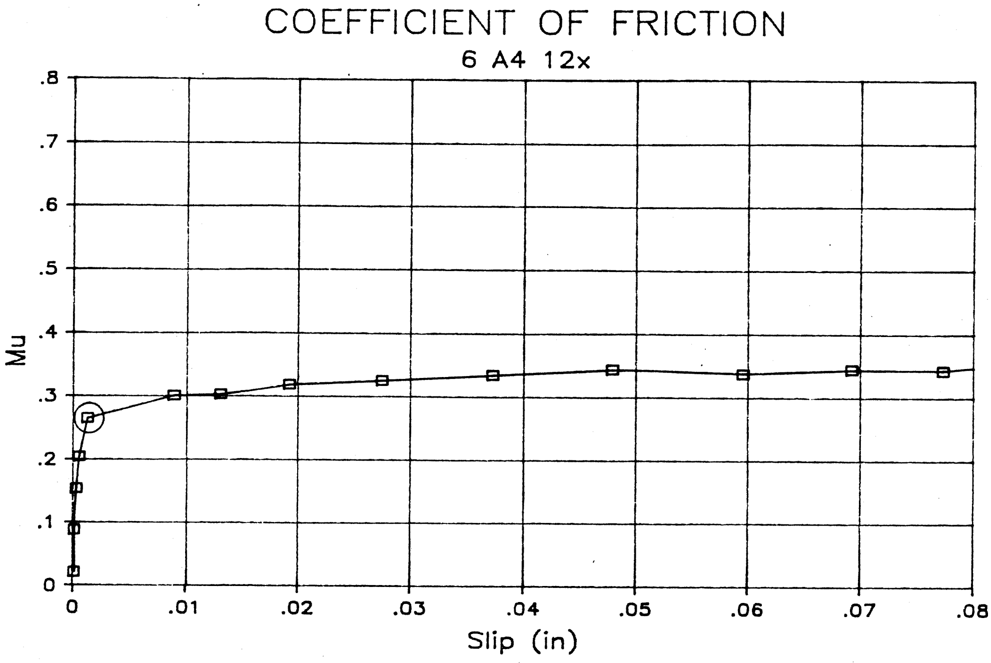

(a) Results Recorded by HP DAS

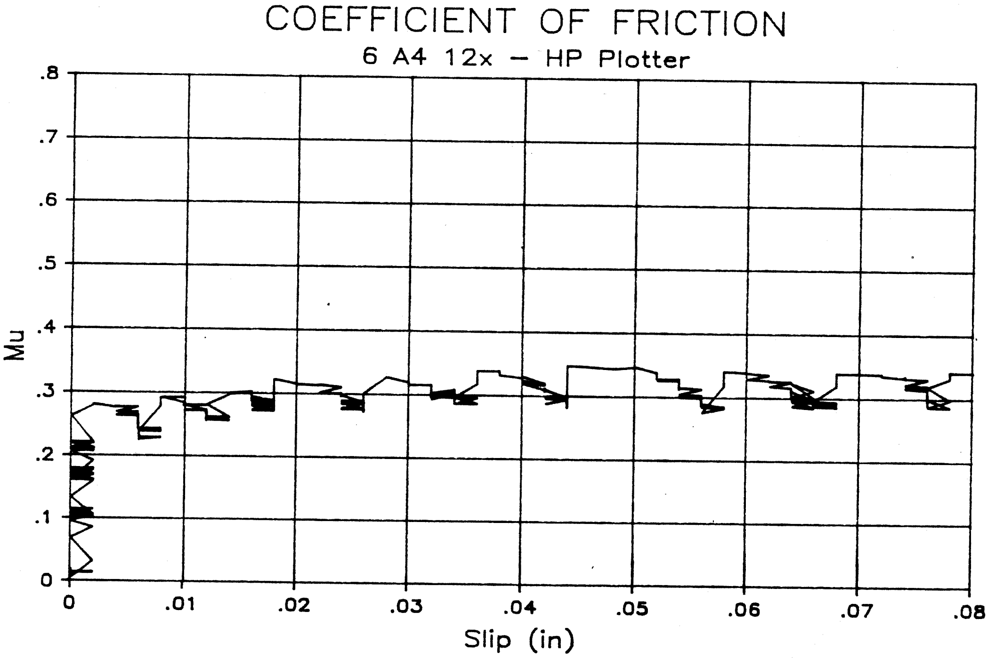

(b) Results Recorded by HP Plotter

Figure 6.1 Typical Results for Mu-vs-Slip Recorded by the HP DAS and by the HP Plotter Data Acquisition Systems

Table 6.2 Summary of Friction Tests

SUMMARY OF FRICTION TESTS

Test No.	Test Variables				Coefficient of Friction, μ		
	Seq. Test No.	Test Block Surf.	Comp. Force kips	Type of Test^1	max	min	mean
2 CIP 6	8	Top	18	All	.50	.46	.48
2 A1 6	24	Btm	18	All	.39	.35	.38
2 M1 6	28	Btm	28	All	.42	.34	.36
2 CIP 12	3	Top	18	All	.41	.35	.38
2 A1 12	25	Btm	16	All	.38	.35	.36
2 A4 12	26	Btm	16	All	.49	.37	.43
2 M1 12	27	Btm	25	All	.37	.30	.32
2 CIP 18	14	Top	11	All	.43	.38	.39
2 A1 18	12	Btm	9	All	.38	.37	.38
2 M1 18	37	Btm	39	Toe*	.42	.42	.42
2 CIP 24	1	Top	16	All	.39	.36	.38
2 A4 24	29	Btm	16	All	.55	.43	.50
	30	Btm	31	Toe*	.43	.43	.43
2 M1 24	38	Btm	36	Toe*	.48	.48	.48
2 CIP 30	2	Top	17	All	.48	.43	.47
2 M1 30		Btm		6 M1 18			
2 CIP 36	4	Top	18	All	.39	.34	.37
2 A4 36	23	Top	18	All	.22	.20	.21
2 M1 36		Btm		4 M1 18			
4 CIP 6	9	Top	20	All	.48	.44	.46
	10	Top	15	Toe*	.41	.41	.41
4 A1 6	7	Top	23	All	.41	.34	.37
4 A4 6	32	Top	20	Toe	.57	.47	.53
4 M1 6	31	Btm	28	Toe	.37	.34	.35
4 CIP 12	15	Top	29	All	.44	.39	.41
4 A1 12	6	Top	31	All	.40	.34	.37
4 A4 12	20	Top	20	All	.51	.46	.47
4 M1 12	33	Btm	40	Toe	.63	.53	.58
4 CIP 18	13	Top	29	All	.36	.32	.34
4 A1 18	11	Btm	22	All	.58	.50	.54
4 A4 18	21	Top	26	All	.36	.30	.32
4 M1 18	34	Btm	34	Toe	.62	.51	.57
4 CIP 24	5	Top	24	All	.61	.51	.56
6 CIP 6	36	Top	40	All	.32	.26	.27
6 M1 6	41	Btm	27	Toe	.61	.53	.57
6 CIP 12	17	Top	22	All	.51	.47	.50
6 A1 12	35	Top	40	All	.33	.28	.31
6 A2 12		Top		No Test			
6 A3 12		Top		No Test			
6 A4 12	22	Top	30	All	.62	.53	.58
6 A5 12	19	Btm	15	All	.37	.36	.36
6 A6 12	18	Btm	16	All	.52	.46	.49
6 M1 12	40	Btm	40	Toe	.60	.54	.58
6 CIP 18	16	Top	20	All	.47	.41	.44
6 M1 18	39	Btm	29	Toe	.51	.45	.47
6 A1 12X		Top	18	All	.50	.42	.48
6 A4 12X		Btm	16	All	.38	.26	.33
6 M1 12X		Top	40	All	.32	.28	.30
Total Number of Friction Tests = 44				Average	.46	.39	.43
				Std. Dev.	.10	.09	.09

Note: "All" represents tests with all the corner anchors preloaded, "Toe" represents tests with only the anchors on the leading edge preloaded, "Toe*" represents tests at high eccentricities without preload, and a reference to another test means that both tests were conducted on the same surface of the same block.

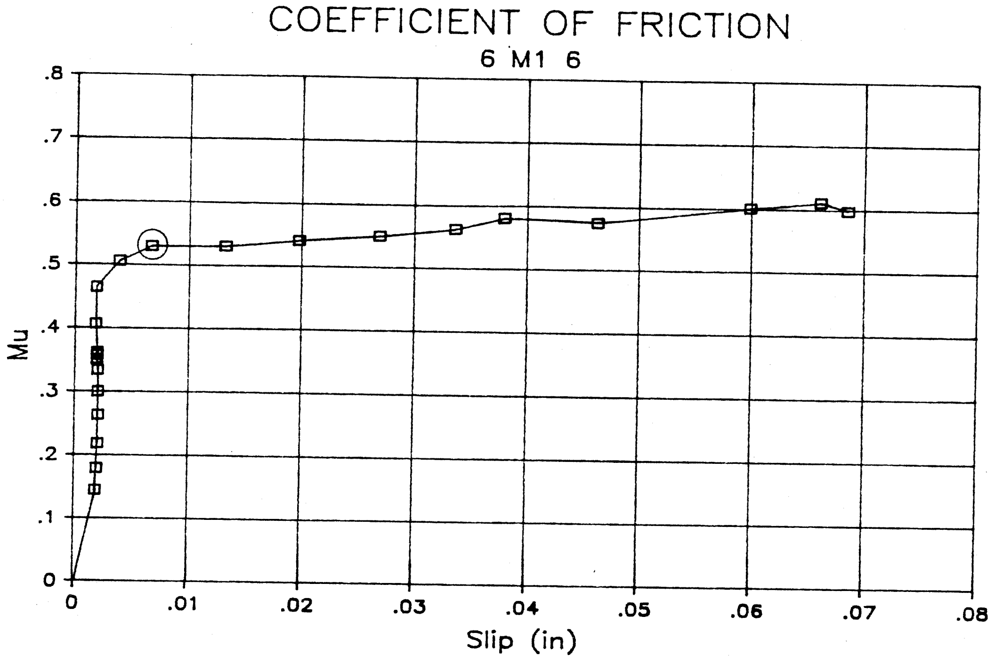

(a) Typical "high" value

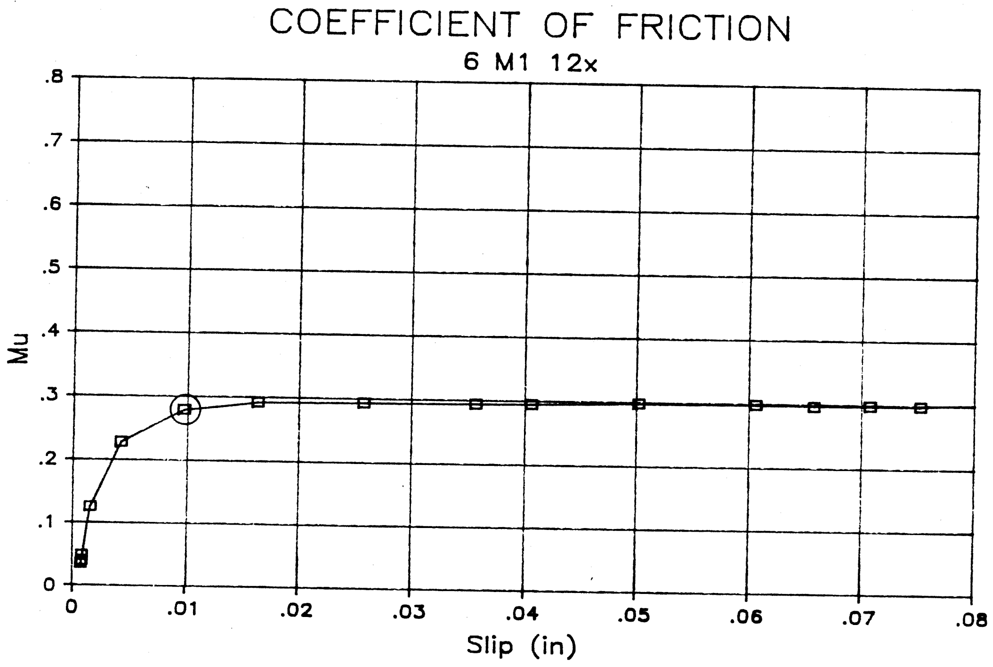

(b) Typical "low" value

Figure 6.2 Typical High and Low Values for the Coefficient of Friction

Table 6.3
Maximum Recorded Applied Load on Separate Data Acquisition Systems

Test No.	Maximum Recorded Applied Load, V (kips)		
	HP Plotter	HP DAS	Difference
2 M1 6	49.1	49.0	0.1
2 CIP 12	41.1	40.8	0.3
2 A1 12	52.2	52.2	0.0
2 M1 12	55.5	55.4	0.1
2 A1 18	47.1	46.2	0.9
2 M1 18	53.9	53.6	0.3
2 M1 24	44.9	44.6	0.3
2 A4 36	29.2	29.2	0.0
2 M1 36	31.1	31.1	0.0
4 CIP 6	74.4	70.0	4.4
4 A4 6	81.8	81.3	0.5
4 M1 6	86.9	86.6	0.3
4 A4 12	77.1	76.6	0.5
4 M1 12	85.9	85.7	0.2
4 CIP 18	58.3	57.9	0.4
4 A4 18	58.3	58.1	0.2
4 M1 18	63.9	63.3	0.6
6 CIP 6	107.8	107.2	0.6
6 M1 6	137.0	136.3	0.7
6 CIP 12	123.6	123.5	0.1
6 A1 12	110.6	109.6	1.0
6 A2 12	118.6	116.3	2.3
6 A3 12	125.3	124.5	0.8
6 A4 12	120.7	119.7	1.0
6 A5 12	104.7	104.5	0.2
6 A6 12	113.8	113.7	0.1
6 M1 12	130.5	129.8	0.7
6 CIP 18	86.8	86.4	0.4
6 A1 12X	107.7	105.5	2.2
6 A4 12X	104.8	103.8	1.0
6 M1 12X	110.4	109.7	0.7

tests in which both systems were used, the maximum shear loads recorded by the HP Plotter are used in the remainder of this section and in succeeding chapters. The maximum shear load for other tests, the anchor tensile forces, and displacements were recorded with the HP DAS.

Load-vs-Displacement diagrams are presented in this section and in Appendix C. Their only purpose is to show the ductile behavior of connections dominated by anchor shear and also by anchor tension. The displacement shown in those diagrams is the total displacement at the location of the outer row of tension anchors. The total displacement was determined as the square root of the sum of the squares of the horizontal slip, δ_h, and the vertical displacement, δ_v, at the location of the outer row of tension anchors. This particular displacement was chosen since it was applicable to all tests. The applied shear load shown in those diagrams is the actual applied shear load, divided by

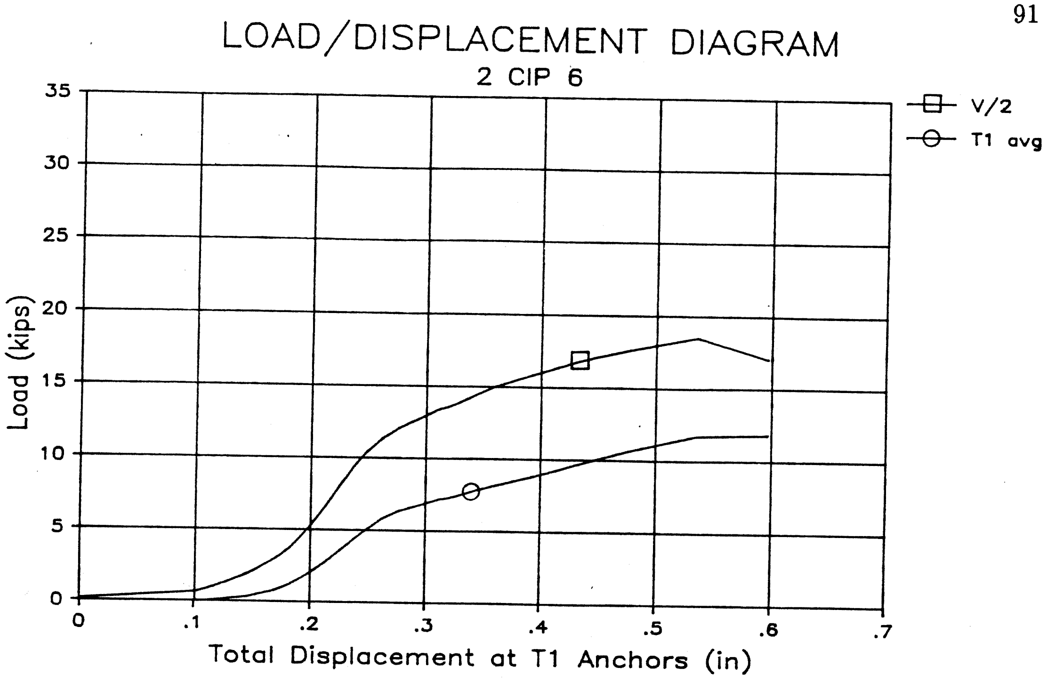

Figure 6.7 Typical Load-Displacement Diagram for Two-Anchor Rigid Baseplate Test Dominated by Anchor Shear

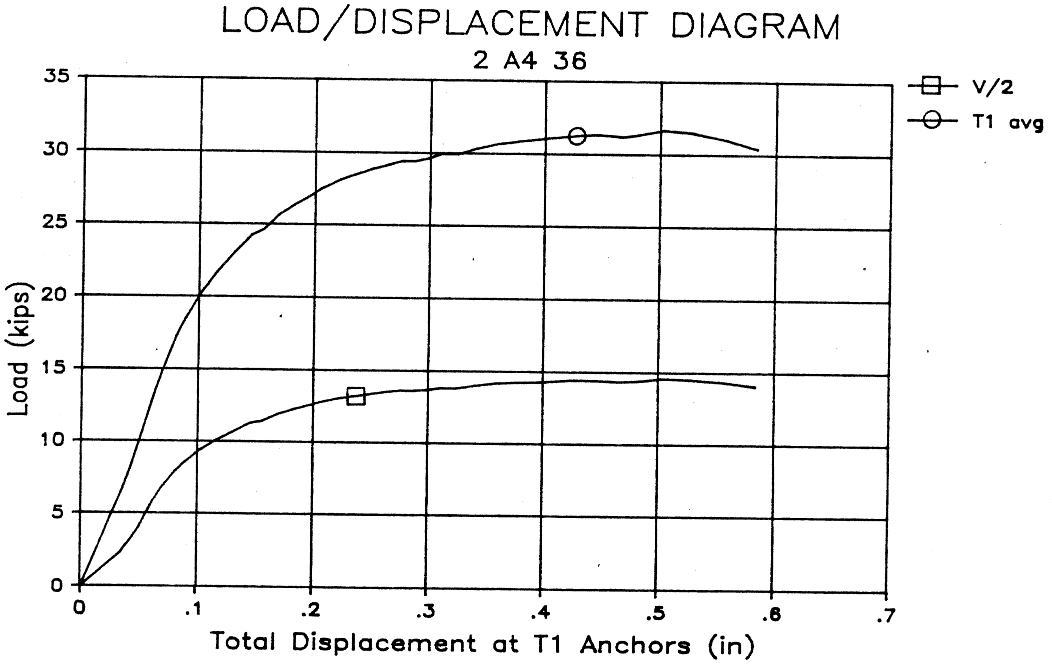

Figure 6.8 Typical Load-Displacement Diagram for Two-Anchor Rigid Baseplate Test Dominated by Anchor Tension

Table 6.5 Four-Anchor Rigid Baseplate Test Results

ANCHOR TENSION AND DISPLACEMENTS AT ULTIMATE LOAD							
Test No.	Ultimate Load V kips	Anchor Tension[1]				Displ.[2]	
		T_{1a} kips	T_{1b} kips	T_{3a} kips	T_{3b} kips	δ_h in.	δ_v in.
4 CIP 6	74.4	16.8	12.5	**3.2**	1.5	.23	.07
4 A1 6	75.2	17.8	15.6	**5.1**	3.3	.47	.08
4 A4 6	81.8	17.2	**16.6**	**3.5**	**6.4**	.60	.14
4 M1 6	86.9	16.3	16.3	**3.1**	**2.4**	.24	.09
4 CIP 12	76.7	31.4	26.0	**5.7**	**1.8**	.30	.19
4 A1 12	80.5	29.9	22.6	**4.0**	**4.4**	.49	.14
4 A4 12	77.1	27.6	28.2	**1.2**	**0.9**	.34	.13
4 M1 12	85.9	29.4	29.0	**1.8**	**3.6**	.37	.25
4 CIP 18	58.3	**34.4**	**28.3**	1.3	1.1	.24	.40
4 A1 18	59.9	**33.3**	28.3	3.4	2.7	.21	.33
4 A4 18	58.3	26.8	**30.6**	0.0	0.3	.26	.66
4 M1 18	63.9	30.2	**31.6**	5.9	2.9	.21	.79
4 CIP 24[3]	40.5	31.2	**30.3**	0.8	0.0	.07	.20

Note:

1) T_{1a} and T_{1b} are the tensile forces in the anchors in the tension zone. T_{3a} and T_{3b} are the tensile forces in the anchors in the compression zone. Anchor tensile forces shown in bold face type represent the anchor or anchors which failed.

2) δ_h is the horizontal slip, and δ_v is the vertical displacement at the location of the anchors in the tension zone, T_1.

3) Anchor failed by stripping of threads.

6.3.4 Six-Anchor Flexible Baseplate Tests. Table 6.6 shows values of shear load, V; anchor tensile forces, T_{1a} and T_{1b}, T_{2a} and T_{2b}, and T_{3a} and T_{3b}; horizontal slip, δ_h; and vertical displacement, δ_v (at the location of the outer row of tension anchors); corresponding to the ultimate shear load. The anchor tensile forces shown in bold face type in Table 6.7 represent the anchor or anchors which failed. Table 6.7 shows that of the 3 six-anchor flexible baseplate tests performed, 2 tests failed one anchor and 1 test failed two anchors simultaneously.

Fig. 6.13 shows a typical load-vs-displacement diagram for a six-anchor flexible baseplate test. Load-vs-Displacement diagrams for other six-anchor tests flexible baseplate tests are shown in Appendix C.

Fig. 6.14 shows the vertical displacements along the centerline of the baseplate for a typical flexible baseplate test. As shown by Fig. 6.14, the flexible baseplates rotated about a point very

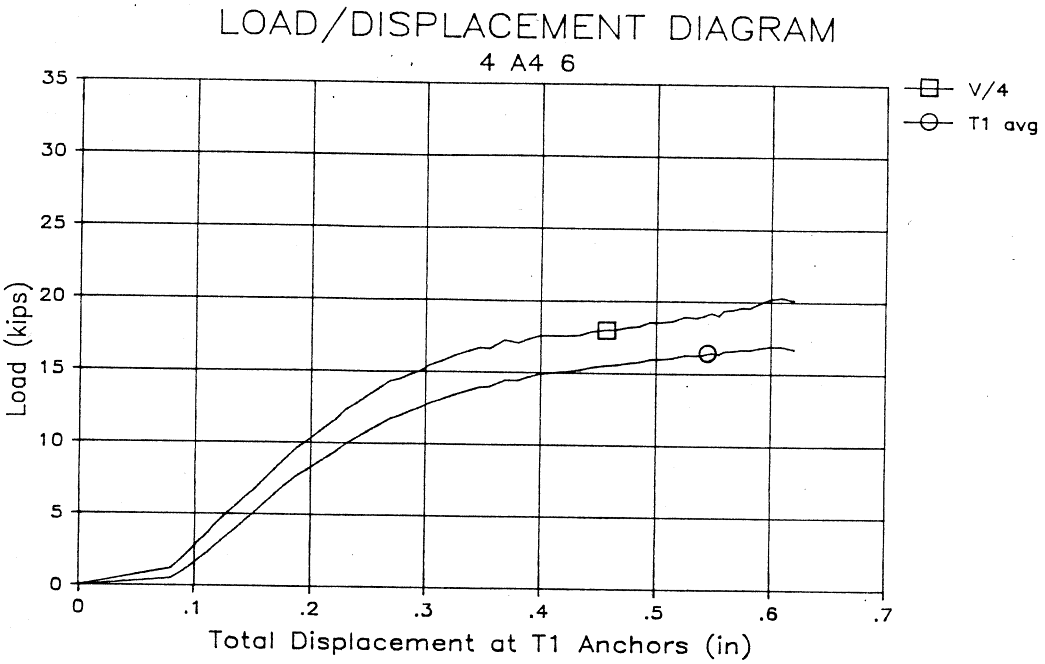

Figure 6.9 Typical Load-Displacement Diagram for Four-Anchor Rigid Baseplate Test Dominated by Anchor Shear

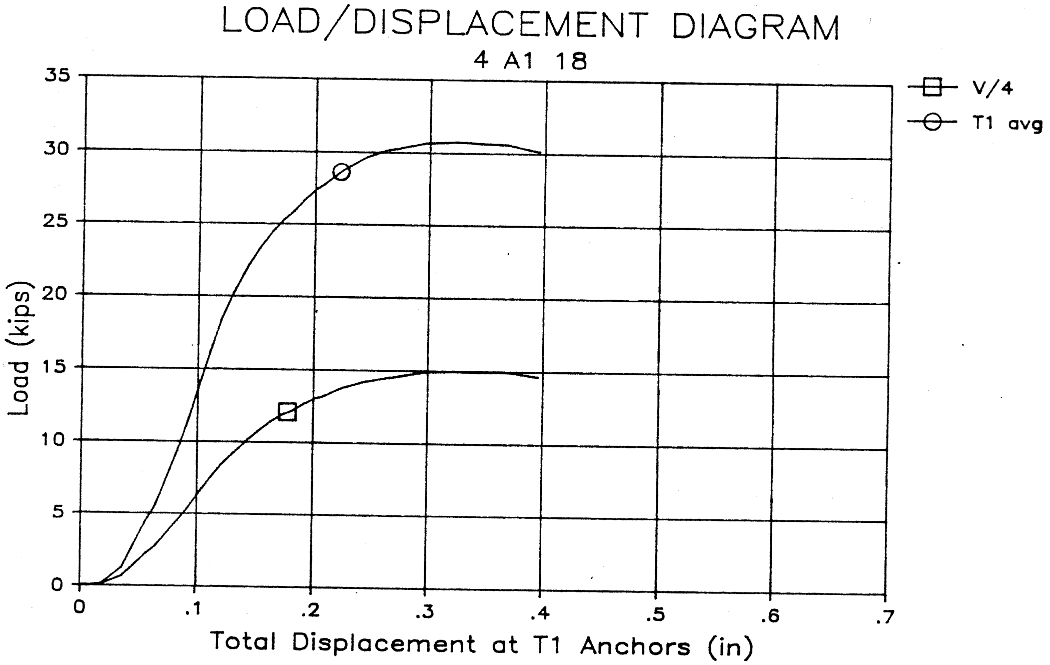

Figure 6.10 Typical Load-Displacement Diagram for Four-Anchor Rigid Baseplate Test Dominated by Anchor Tension

Table 6.6 Six-Anchor Rigid Baseplate Test Results

ANCHOR TENSION AND DISPLACEMENTS AT ULTIMATE LOAD									
Test No.	Ult. Load V kips	Anchor Tension[1]						Displ.[2]	
		T_{1a} kips	T_{1b} kips	T_{2a} kips	T_{2b} kips	T_{3a} kips	T_{3b} kips	δ_h in.	δ_v in.
6 CIP 6	107.8	18.1	22.1	3.9	**7.6**	0.4	**1.0**	.39	.11
6 M1 6	137.0	22.2	18.0	**12.2**	**12.5**	**3.7**	**1.7**	.27	.11
6 CIP 12[3]	123.6	31.5	**30.8**	26.8	24.7	1.1	2.1	.33	.38
6 A1 12	110.6	25.8	**27.9**	24.4	27.1	0.0	5.1	.30	.28
6 A2 12	118.6	**29.9**	25.7	25.2	23.3	0.0	2.2	.44	.46
6 A3 12	125.3	**28.5**	**26.3**	30.5	24.5	0.7	0.5	.28	.27
6 A4 12	120.7	30.4	29.7	25.0	24.1	**2.3**	**2.6**	.48	.41
6 A5 12	104.7	29.6	28.3	19.8	13.6	**5.0**	**2.4**	.40	.21
6 A6 12	113.8	30.0	**26.4**	20.9	22.8	3.6	2.5	.41	.25
6 M1 12	130.5	27.5	33.1	27.7	26.7	**1.4**	**2.5**	.35	.36
6 CIP 18	86.8	**30.9**	**31.1**	27.4	29.7	0.4	0.0	.22	.46
6 M1 18	94.0	**34.3**	31.5	33.3	33.5	2.7	3.7	.29	.72

Note:

1) T_{1a} and T_{1b} are the tensile forces in the outer row of anchors in the tension zone. T_{2a} and T_{2b} are the tensile forces in the middle row of anchors. T_{3a} and T_{3b} are the tensile forces in the anchors in the compression zone. Anchor tensile forces shown in bold face type represent the anchor or anchors which failed.

2) δ_h is the horizontal slip, and δ_v is the vertical displacement at the location of the outer row of anchors in the tension zone, T_1.

3) Anchor failed by stripping of threads.

near the compression flange of the attached member (the compression flange was 4 inches from the leading edge).

Fig. 6.15 shows a typical contact zone for the flexible baseplate tests. As indicated by Fig. 6.15, the actual contact zone is dependent on surface irregularities in the concrete finish.

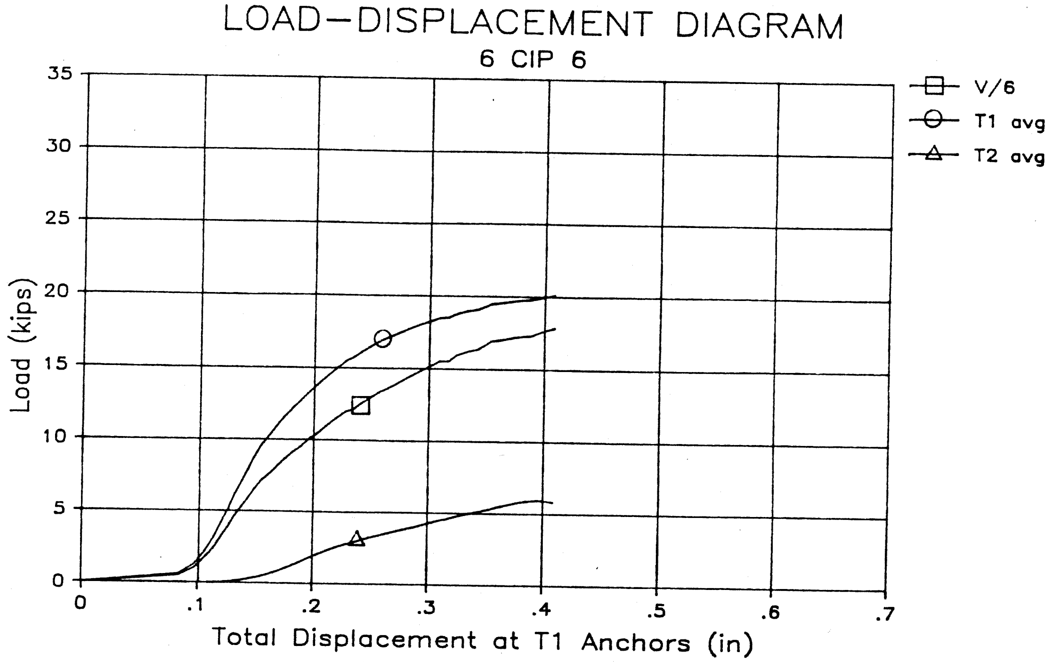

Figure 6.11 Typical Load-Displacement Diagram for Six-Anchor Rigid Baseplate Test Dominated by Anchor Shear

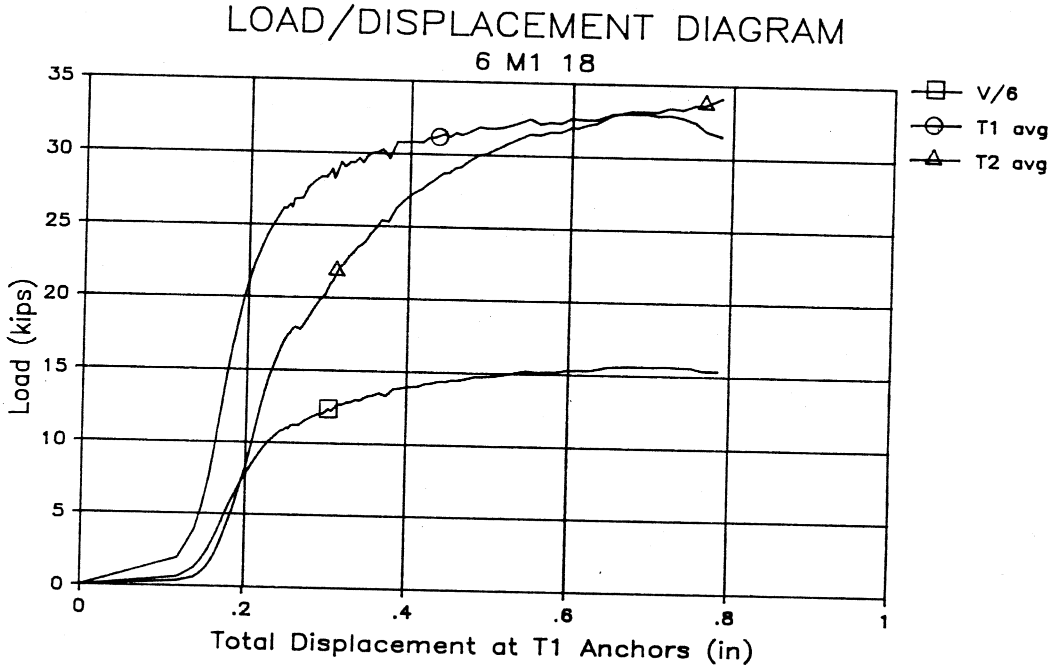

Figure 6.12 Typical Load-Displacement Diagram for Six-Anchor Rigid Baseplate Test Dominated by Anchor Tension

Table 6.7 Six-Anchor Flexible Baseplate Test Results

ANCHOR TENSION AND DISPLACEMENTS AT ULTIMATE LOAD									
Test No.	Ult. Load V kips	Anchor Tension[1]						Displ.[2]	
		T_{1a} kips	T_{1b} kips	T_{2a} kips	T_{2b} kips	T_{3a} kips	T_{3b} kips	δ_h in.	δ_v in.
6 A1 12x	107.7	31.8	28.3	21.1	21.0	**5.3**	**5.7**	.27	.20
6 A4 12x	104.8	32.1	**24.4**	20.7	21.4	1.8	5.9	.44	.32
6 M1 12x	110.4	32.6	29.3	19.9	24.3	0.8	**1.4**	.21	.28

Note:

1) T_{1a} and T_{1b} are the tensile forces in the outer row of anchors in the tension zone. T_{2a} and T_{2b} are the tensile forces in the middle row of anchors. T_{3a} and T_{3b} are the tensile forces in the anchors in the compression zone. Anchor tensile forces shown in bold face type represent the anchor or anchors which failed.

2) δ_h is the horizontal slip, and δ_v is the vertical displacement at the location of the outer row of anchors in the tension zone, T_1.

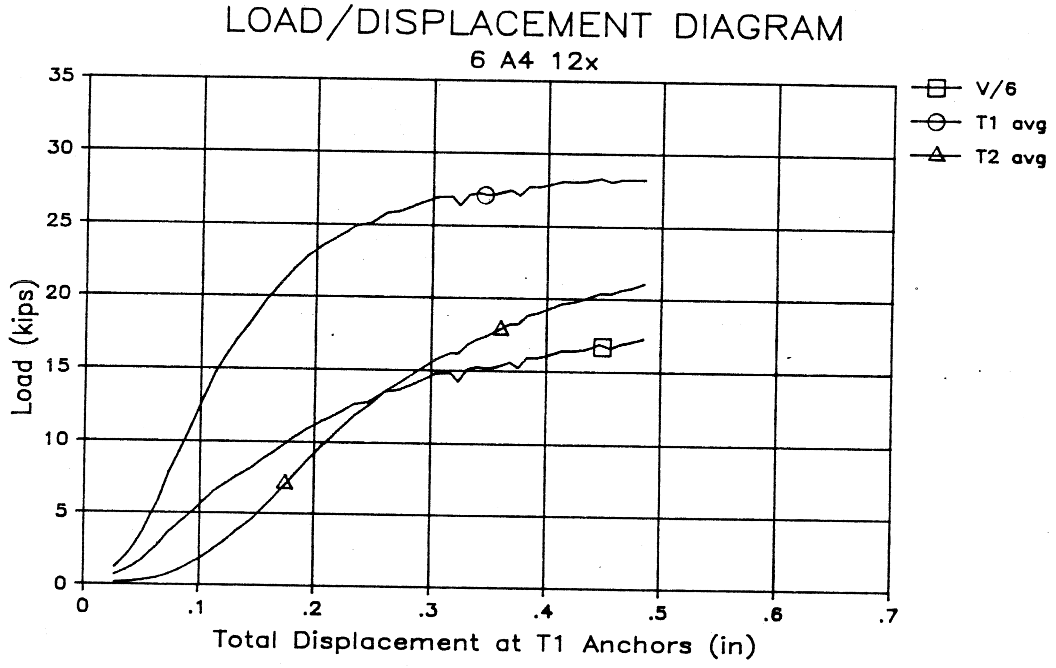

Figure 6.13 Typical Load-Displacement Diagram for Six-Anchor Flexible Baseplate Test

7. DISCUSSION OF TEST RESULTS

7.1 Introduction

In this chapter, the results of the experimental program are discussed. The discussion is organized according to the objectives of the experimental program as described in Section 4.1:

1) To determine the coefficient of friction between a surface mounted steel baseplate and hardened concrete in multiple- anchor connections.
2) To determine tension/shear interaction relationships for cast- in-place anchors, undercut anchors, and adhesive anchors in multiple-anchor connections.
3) To determine the distribution of tension and shear forces in multiple-anchor connections.
4) To determine the effect of baseplate flexibility on the behavior and design of multiple-anchor connections.

7.2 Coefficient of Friction

The purpose of the friction tests was to determine the coefficient of friction, μ, between a surface mounted steel baseplate and concrete.

7.2.1 Comparison and Analysis of Test Results. The effective coefficient of friction for the connection is best represented by the "mean" coefficient of friction described in Section 6.2, for the following reasons: The maximum and minimum values are based on single data points, while the "mean" value is based on a series of data points recorded after the first significant slip of the baseplate. The "mean" value filters out the effects of abnormally high or low data points, and provides a means for evaluating the coefficient of friction for specimens that did not exhibit linear Mu-vs-Slip behavior. As shown in Table 6.2, there is less than 10% difference between the average "mean" value and the average maximum and minimum values. For the above reasons the "mean" coefficient of friction value of Table 6.2 is used in this section.

The frequency distribution of the "mean" coefficient of friction for the 44 friction tests is shown in Fig. 7.1. As indicated in Table 6.2, the average "mean" value is 0.43 with a standard deviation of 0.09.

The following test variables may have affected the friction test results:

1) **Effect of the Concrete Surface**: Tests were performed on both the top and bottom surface of the test blocks. The top surface was hand finished, while the bottom surface was cast against formwork. No significant difference was observed between the results obtained for the 24 tests on the top surface of the blocks (average coefficient of friction = 0.41), and the 20 tests performed on the bottom surface of the blocks (average coefficient of friction = 0.44).
2) **Effect of the Compressive Force**: The compressive force applied in the friction tests ranged from 9 to 40 kips. Fig 7.2 shows that the magnitude of the compressive force had no discernable effect on the coefficient of friction.

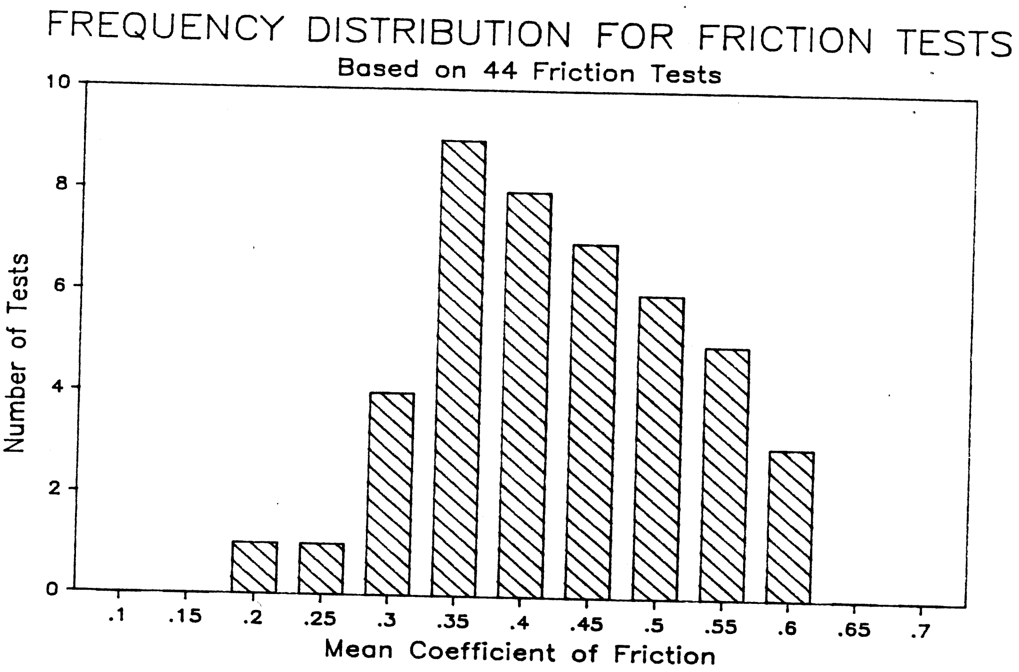

Figure 7.1 Frequency Distribution for Friction Tests

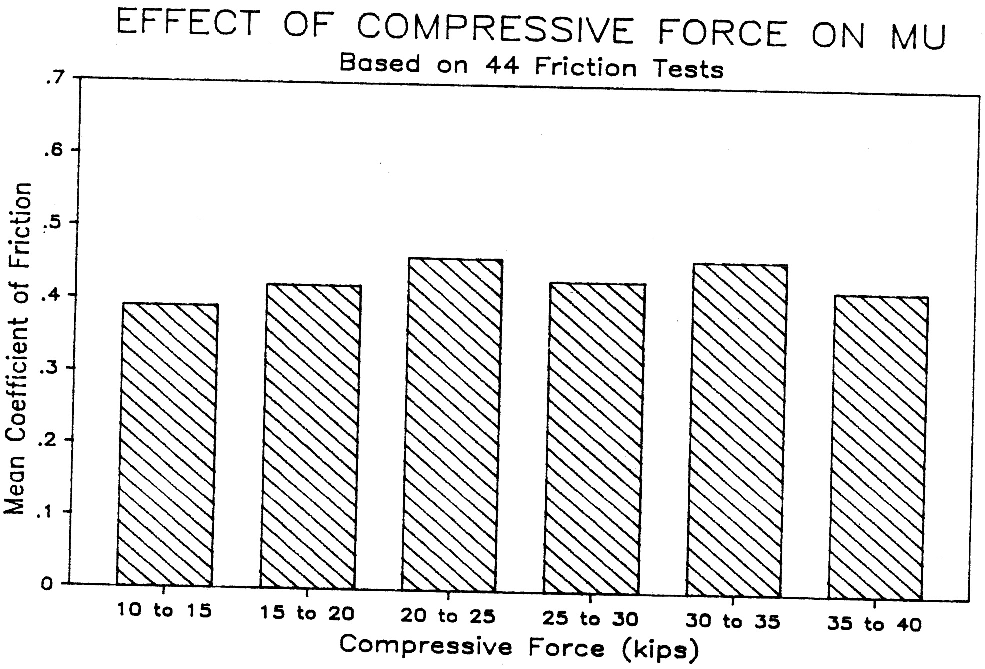

Figure 7.2 Effect of Compressive Force on the Coefficient of Friction

3) **Effect of Previous Testing**: During the course of the testing program, the contact surface of the rigid baseplate showed signs of wear, particularly at the toe of the plate. Fig. 7.3 shows a slight increase in the coefficient of friction for the last 11 friction tests with the rigid baseplate. The average coefficient of friction was 0.42 for the first 30 tests with the rigid baseplate, increasing to 0.47 for the last 11 tests. As shown by Fig. 7.3, the overall effect is minimal.

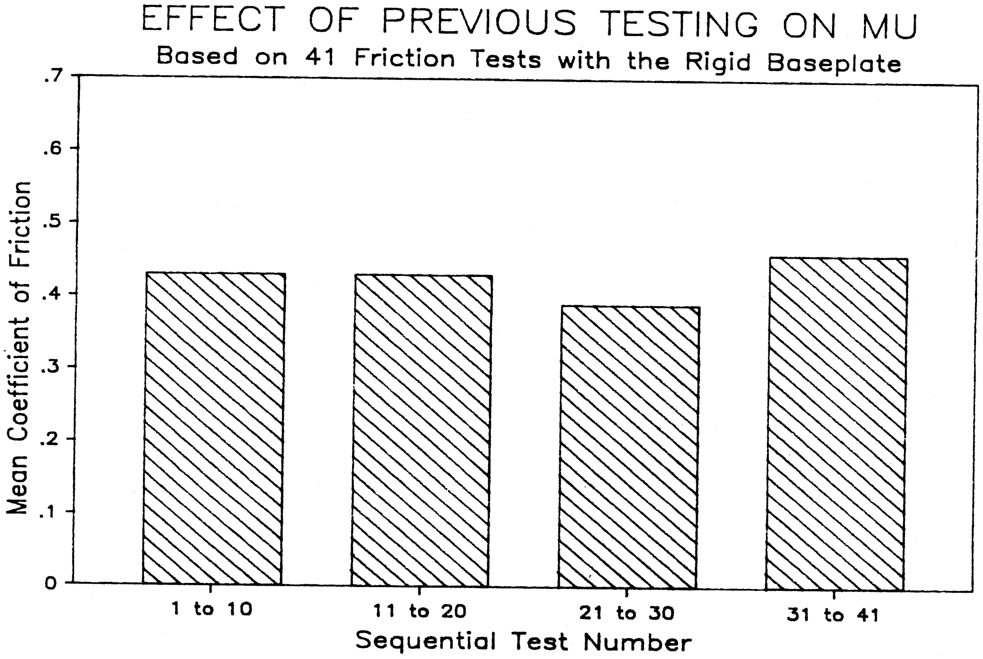

Figure 7.3 Effect of Previous Testing on the Coefficient of Friction

4) **Effect of Type of Friction Test**: Of the 44 friction tests performed, 33 had the compressive force spread over the baseplate and 11 had the compressive force concentrated on the toe of the baseplate. The average coefficient of friction for the 33 tests with the compressive force spread over the baseplate was 0.41 with a standard deviation of 0.08. The average coefficient of friction for the 11 tests with the compressive force concentrated on the toe of the baseplate was 0.49 with a standard deviation of 0.09.

However, in two cases (2 A4 24 and 4 CIP 6) in which both types of friction tests were performed prior to the ultimate load test, the coefficient of friction was less when the compressive force was concentrated on the toe of the plate.

It is not clear whether the generally higher values recorded for the coefficient of friction in tests with the compressive force concentrated on the toe of the plate were due to the type of test or to the effect of previous testing with the rigid baseplate. Most (9 out of 11) of the tests with the compressive force concentrated on the toe of the plate were in the last 11 tests with the rigid baseplate. In either case the difference is minimal, the average "mean" value of the coefficient of friction for each type of test lies within one standard deviation of the "mean" value obtained in the other type of test.

7.2.2 Summary: Coefficient of Friction. The coefficient of friction results of this testing program are in close agreement with previous test results for a steel plate installed on hardened concrete. As indicated by Table 2.4, the results of 15 previous friction tests [54,72] had an average value of 0.41 for the coefficient of friction for a steel plate installed on hardened concrete. The average "mean" coefficient of friction for the 44 friction tests conducted in this study was 0.43.

The surface condition of the concrete and the magnitude of the compressive force had no discernible effect on the coefficient of friction.

The effect of the toe of the rigid baseplate digging into the concrete appears to be minimal (average "mean" coefficient of friction = 0.49 for 11 tests). The exact effect is inconclusive since most of the friction tests with the compressive force concentrated on the toe of the plate were performed toward the end of the testing program, when the toe of the rigid baseplate showed signs of wear. In two cases in which both types of friction tests were performed prior to the ultimate load test, the measured value for the coefficient of friction was lower when the compressive force was concentrated on the toe of the plate.

For design purposes, the coefficient of friction, μ, should be taken as 0.40 with a strength reduction factor, ϕ, of 0.65. Based on the results of the 44 friction tests conducted in this study, the actual strength will then exceed the calculated design strength 98% of the time. This is considered acceptable.

7.3 Tension/Shear Interaction Relationships

The purpose of the two-anchor rigid baseplate tests was to determine the tension/shear interaction relationship for various types of anchors in a multiple-anchor connection.

7.3.1 Comparison and Analysis of Test Results. The results of the two-anchor rigid baseplate tests were used to construct tension/shear interaction diagrams for the three types of anchors studied in the experimental program. The anchor tensile forces were measured directly. The anchor shear forces presented in this subsection were calculated by the procedure discussed in Subsection 4.4.1.

As discussed in Subsection 4.4.1, the calculated anchor shear force is dependent on the coefficient of friction. In order to determine the most appropriate tension/shear interaction relationship, the following values for the coefficient of friction were considered:

1) The actual "mean" coefficient of friction measured in the friction test which preceded the ultimate load test.

2) The "mean" coefficient of friction for the friction tests with the compressive force concentrated on the toe of the rigid baseplate ($\mu = 0.49 \approx 0.50$). This value of the coefficient of friction represents a upper-bound to the friction tests results. The use of the upper bound value for the coefficient of friction produces a minimum calculated value for the shear force transferred by the anchors.

The combined anchor tensile and shear forces calculated using the different coefficients of friction are shown in Figs. 7.4-7.6. Figs. 7.4-7.6 also show how the test data compare to an elliptical tension/shear interaction relationship. The only test which indicates a significant underestimate of anchor strength using the upper bound coefficient of friction with an elliptical tension/shear interaction is Test No. 2 CIP 24. This was the very first test performed with the rigid baseplate. For this test, the upper bound coefficient of friction does not seem appropriate since there was no wear on the leading edge of the baseplate.

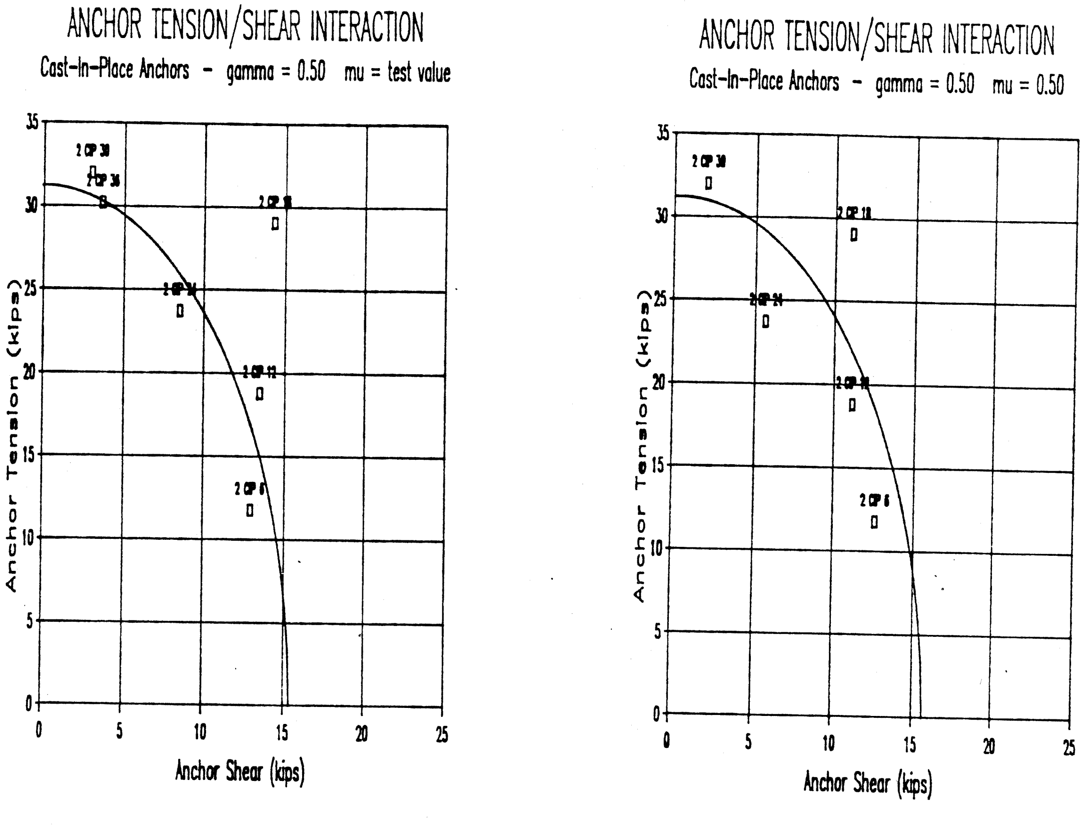

Figure 7.4 Tension/Shear Interaction for Cast-in-Place Anchors

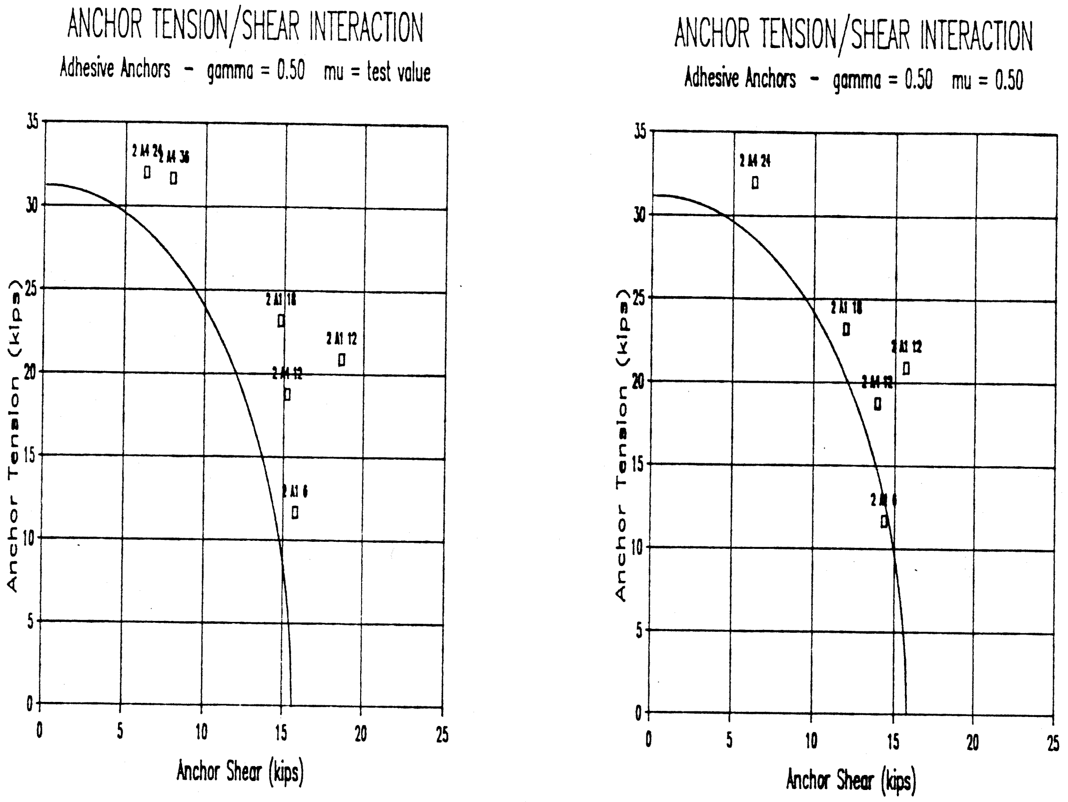

Figure 7.5 Tension/Shear Interaction for Adhesive Anchors

As shown by Figs. 7.4-7.6, an elliptical tension/shear interaction relationship provides a reasonable and generally conservative fit to the test data. As discussed in Subsection 2.3.3, an elliptical tension/shear interaction represents the most liberal tension/shear interaction established by previous research and existing design standards.

For cast-in-place and adhesive anchors the ratio, γ, between the shear strength and the tensile strength of an anchor should be taken as 0.50 in multiple-anchor connections. This value is slightly less than the corresponding value used in a steel-to-steel connection ($\gamma = 0.60$ [6]). The lower value for γ is due to the large flexural deformations which occur in steel-to-concrete anchors due to surface spalls in the concrete (1/2 to 1-1/2 inches). Fig. 2.4 shows the effect of surface spalling on flexural deformations in the anchors due to shear forces.

Undercut mechanical anchors show a marked increase in shear strength over cast-in-place and adhesive anchors of the same diameter. This is due to the embedded steel sleeve of the undercut anchors, which helps prevent flexural deformations in the anchor and reduces concrete surface spalling (1/4 to 1/2 inch). Based on the results of this testing program, for undercut anchors, the ratio, γ (shear strength to tensile strength), should be taken as 0.60, and might be even higher. Due to the limited test data, it is imprudent to assume a value of γ higher than that given in existing

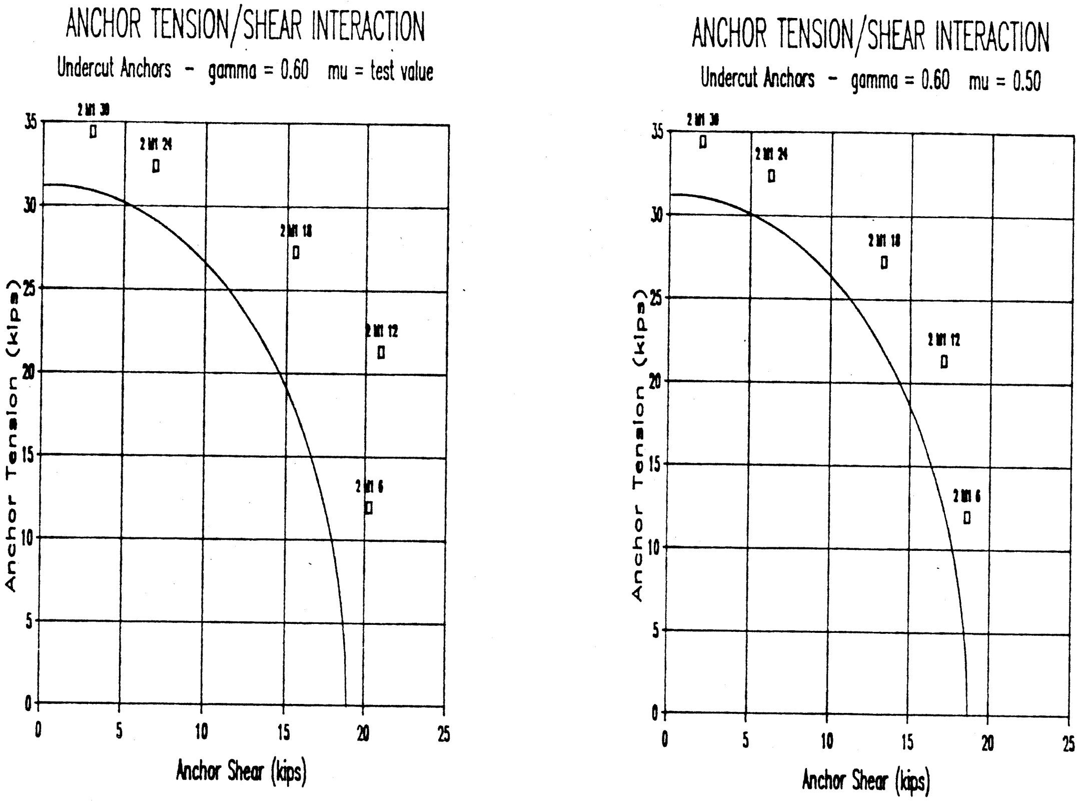

Figure 7.6 Tension/Shear Interaction for Undercut Anchors

design standards for anchors in steel-to-steel connections (γ = 0.60 [6]). Anchor flexural deformations, which reduce the shear strength of an anchor, will always be more severe in a steel-to-concrete connection since some amount of concrete spalling or crushing occurs.

7.3.2 Summary: Tension/Shear Interaction Relationships. The results of the two-anchor rigid baseplate tests indicate the following tension/shear interaction relationships as governed by steel failure.

1) An elliptical tension/shear interaction relationship is justified. A linear tension/shear interaction relationship is conservative.

2) The shear strength (steel failure) of cast-in-place and adhesive anchors are the same. The shear strength of these anchors in a multiple-anchor connection should be taken as 50% of the tensile strength ($V_O/T_O = \gamma = 0.50$).

3) The shear strength (steel failure) of undercut anchors in a multiple-anchor connection should be taken as 60% of the tensile strength ($V_O/T_O = \gamma = 0.60$).

7.4 Distribution of Tension and Shear among Anchors

The four-anchor rigid baseplate tests were developed to determine the distribution of shear forces in multiple-anchor connections. The six-anchor tests were developed to determine the distribution of both tension and shear forces in multiple-anchor connections.

As discussed in Section 2.3, the distribution of tension and shear forces in multiple-anchor connections subjected to moment and shear is not adequately covered by existing design procedures. This section provides a general discussion of the distribution of tension and shear forces noted in the four-anchor and six-anchor tests.

7.4.1 Comparison and Analysis of Results. Results of the four-anchor and six-anchor ultimate load tests indicated the following:

1) Tension and shear forces redistributed among the anchors as required to maintain equilibrium with the applied loading.
    a) At low eccentricities of the applied load (6 and 12 inches), the anchors near the toe of the baseplate underwent significant inelastic shear deformation, and the anchors away from the toe of the baseplate underwent significant inelastic deformation in combined tension and shear.
    b) At higher eccentricities of the applied load (18 and 24 inches), the anchors near the toe of the baseplate effectively stopped the connection from slipping, thereby allowing the anchors away from the toe to attain their full tensile strength.
2) For connections with more than one row of anchors in tension the distribution of tension at the ultimate load varied considerably at low eccentricities of the applied load (6 and 12 inches). However, this distribution had little effect on the ultimate strength of the connection. Table 7.1 shows the ratio, (T_2/T_1), of the tensile force in the middle row of anchors, T_2, to the tensile force in the outer row of anchors, T_1, at the ultimate load for all the six-anchor tests. As shown in Table 7.1, the ratio of (T_2/T_1) varied between 0.29 and 1.00 at ultimate for tests at the 6 and 12 inch eccentricities. The ultimate load for the test with $(T_2/T_1) = 0.29$ was 108 kips, and the ultimate load for the test with $(T_2/T_1) = 1.00$ was 125 kips. An increase of 250% in the ratio (T_2/T_1) corresponded to an increase of only 16% in the ultimate load. This indicates that at low eccentricities of the applied load the ultimate strength of the connection is not very sensitive to the assumed distribution of tension. This seems reasonable, since connections loaded at low eccentricities (low M/V ratios) are dominated by the applied shear rather than by the applied moment.
3) As the applied load was increased from zero to its ultimate value, the distribution of tensile forces among anchors varied, but this did not affect the ultimate strength of the connection. Fig. 7.7 shows a typical variation of the ratio of the tensile force in the middle row of anchors, T_2, to tensile force in the outer row of anchors, T_1, as a function of the applied shear load, V. The tests of Fig. 7.7 were both conducted at the same 12-inch load eccentricity, had essentially the same (T_2/T_1) ratio at the ultimate load, and failed at nearly the same ultimate load.

Table 7.1 Maximum Anchor Tension in Six-Anchor Tests

Test No.	Anchor Tension[1] (kips)		T_2 / T_1
	T_1	T_2	
6 CIP 6	40.2	11.5	0.29
6 M1 6	40.2	24.7	0.61
6 CIP 12	62.3	51.5	0.83
6 A1 12	53.7	51.5	0.96
6 A2 12	55.6	48.5	0.87
6 A3 12	54.8	55.0	1.00
6 A4 12	60.1	49.1	0.82
6 A5 12	57.9	33.4	0.57
6 A6 12	56.4	43.7	0.77
6 M1 12	60.6	54.4	0.90
6 CIP 18	62.0	57.1	0.92
6 M1 18	65.8	66.8	1.02
6 A1 12X	60.1	42.1	0.70
6 A4 12X	56.5	42.1	0.75
6 M1 12X	61.9	44.2	0.71

Note:

1) T_1 is the total tensile force in the outer row of anchors in the tension zone at failure. T_2 is the total tensile force in the middle row of anchors at failure.

7.4.2 Summary: Distribution of Tension and Shear. The results of the testing program indicate that:

1) Tension and shear forces in the anchors redistribute inelastically as required to maintain equilibrium with the applied loading.
2) For connections dominated by moment (high eccentricity of the applied load) the anchors away from the toe of the baseplate attain their full tensile strength.
3) For connections dominated by shear (low eccentricity of the applied load) the ultimate strength of the connection is not sensitive to the distribution of tension in the anchors.
4) The initial distribution of anchor tension (prior to inelastic redistribution) has no effect on the ultimate strength of the connection.

Based on these observations, a limit design approach appears to be appropriate for ductile multiple-anchor connections. Limit design requires that forces redistribute prior to failure and that the distribution of forces prior to redistribution not effect the ultimate strength. Chapter 8 presents

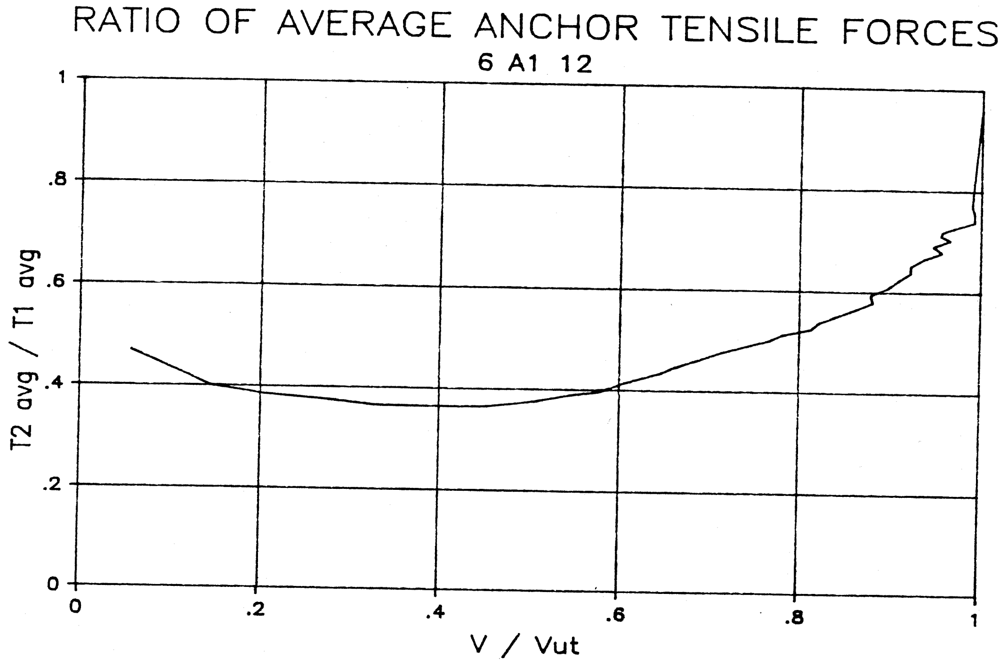

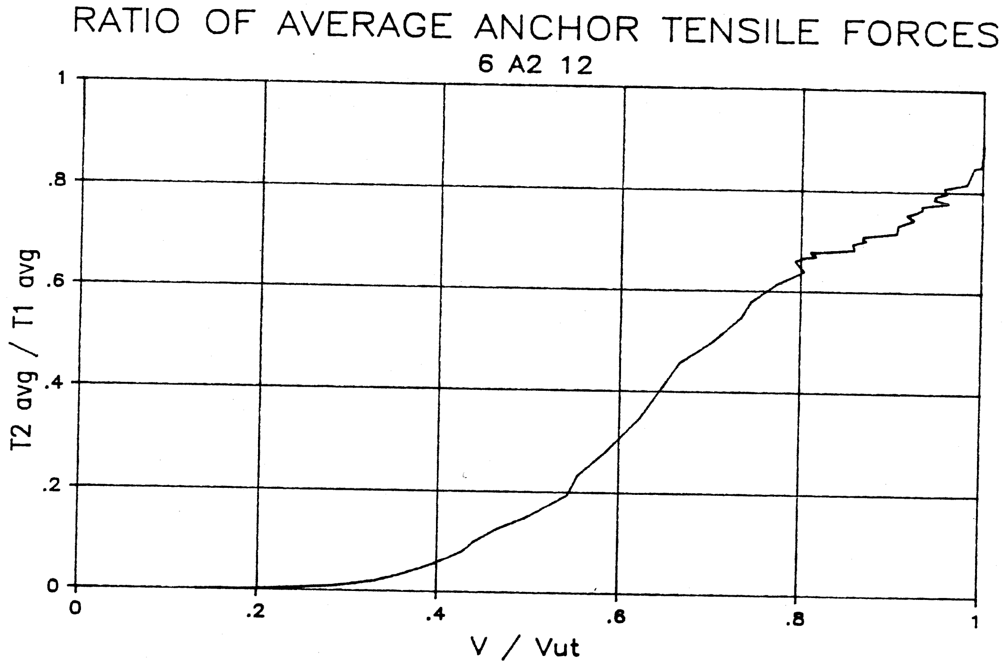

Figure 7.7 Typical Results for Distribution of Tensile Forces Prior to Redistribution

and assesses a behavioral model, based on limit design theory, for multiple-anchor connections to concrete.

7.5 Effect of Baseplate Flexibility

This section addresses the location of the compressive reaction, based on the results of the rigid baseplate tests and the flexible baseplate tests. As discussed in Section 2.3, the compressive reaction should be located in a conservative manner since it directly effects the calculated tensile forces in the anchors.

7.5.1 Comparison and Analysis of Test Results. As noted in Section 6.3, for the rigid baseplate tests the compressive reaction was located at the toe of the baseplate. The contact zone was typically a 1/4- to 1/2-inch strip at the toe of the baseplate. There was no measurable difference in the width of the strip for the two-, four-, or six-anchor rigid baseplate tests. This behavior cannot be explained by any of the procedures discussed in Subsection 2.3.1, but does agree with the probable location of the compressive reaction for rigid baseplate rotation shown in Fig. 2.12. For the six-anchor rigid baseplate tests the bearing stress at the toe of the plate was between 4 and 8 times the 28-day compressive strength of the concrete. These high bearing stresses had no influence on the strength of the connection, since the baseplate was not close to any free edge of the supporting concrete.

Fig. 7.8 shows the calculated location of the compressive reaction for the flexible baseplate tests over the entire load range of the tests. The location of the compressive reaction was determined by the condition of moment equilibrium as discussed in Subsection 4.4.4. As shown in Fig. 7.8, the calculated location of the compressive reaction changed during the course of the test. At low loads, it was near the toe of the plate; as the load increased, the reaction shifted inward from the toe until it was about 1/2 inch from the edge of the compression element of the attached member; with further increase in load, the reaction moved back toward the toe of the plate. In two of the flexible baseplate tests (6 A1 12x and 6 M1 12x), the compressive reaction moved back inward toward the edge of the compression element of the attached member with a further increase in load. This behavior cannot be explained by any of the procedures discussed in Subsection 2.3.1, but generally agrees with the probable location of the compressive reaction for a flexible baseplate shown in Fig. 2.12. As indicated by Fig. 6.15, for a flexible baseplate, the actual distribution and magnitude of bearing stresses is impossible to determine due to surface irregularities in the concrete finish.

The effect of baseplate flexibility on the location of the compressive reaction can be explained if the relative stiffnesses of the baseplate and the concrete are considered. For all practical purposes the concrete can be assumed to be rigid, as can that portion of the baseplate welded to the attached member. Any overhanging projection of the baseplate beyond the compression element of the attached member can be considered flexible.

The overhanging projection of the plate is essentially a cantilever beam fixed at its intersection with the compressive element of the attached member, and loaded with a movable concentrated load (the compressive reaction). The boundary conditions for this cantilever require that the fixed support rotate and displace. The free end can rotate but not displace if the compressive reaction

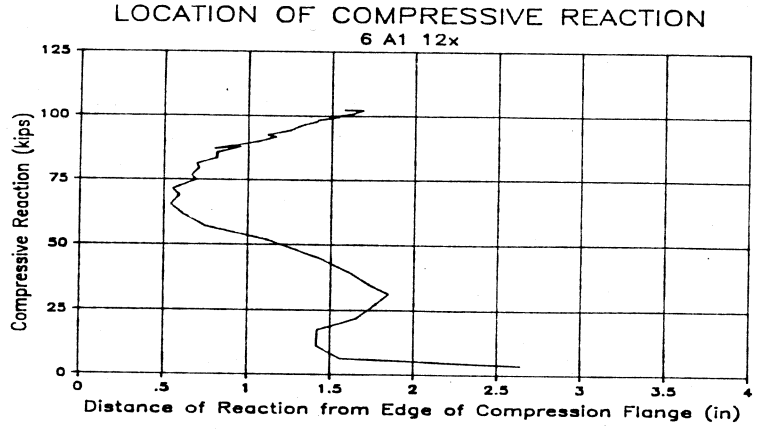

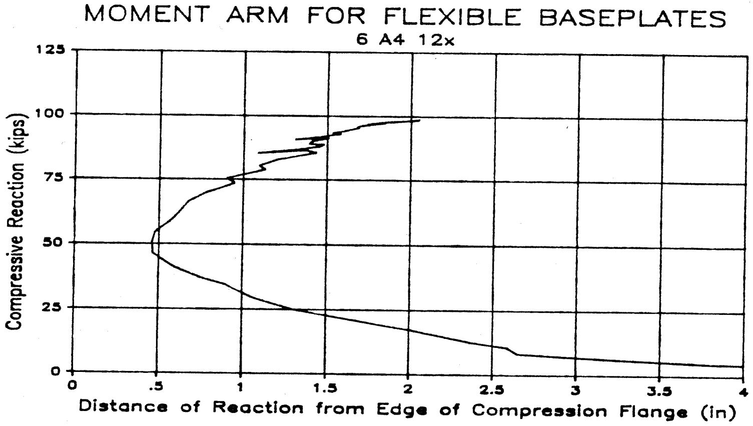

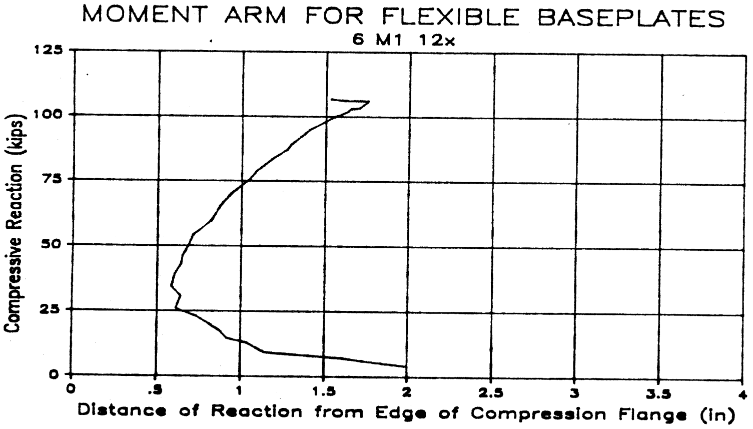

Figure 7.8 Calculated Location of the Compressive Reaction for Flexible Baseplate Tests

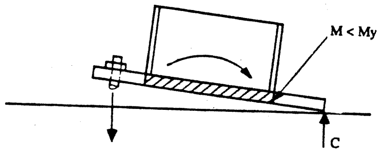

(a) Compressive Reaction at Toe

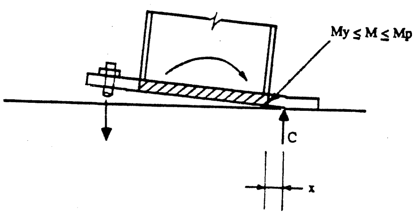

(b) Compressive Reaction Shifted in from Toe

Figure 7.9 Effect of Baseplate Flexibility on the Location of the Compressive Reaction

is at the toe of the plate, and can neither rotate nor displace if the compressive reaction moves in from the toe of the baseplate. This is shown in Fig. 7.9.

The behavior of a flexible baseplate can be described as follows:

1) Initially, the baseplate rotates as a rigid body pivoting about the toe of the plate.

2) As the compressive load increases, the portion of the baseplate adjacent to the compressive element of the attached member reaches the yield moment, M_y, of the baseplate. This causes the compressive reaction, C, to move inward toward the compression element. This inward movement, shown in Fig. 7.9, is required to prevent the formation of a hinge at the edge of the compression element of the attached member. If a hinge forms, the overhanging projection of the baseplate becomes a mechanism.

3) Eventually, the compressive reaction moves as close to the compression element of the attached member as it can without exceeding the yield moment, M_y, of the plate adjacent to the compression element. The smallest distance, x_{min}, between the compressive reaction and the compression element of the attached member can be determined by:

$$C\, x_{min} = M_y$$

$$x_{min} = M_y \,/\, C \qquad (7-1)$$

4) With a further increase in the compressive reaction, the baseplate begins to form a plastic hinge, M_p, and the compressive reaction, C, moves away from the compression element. The furthest distance that the compressive reaction moves away from the support is determined by:

$$C\, x_p \;=\; M_p$$

$$x_p \;=\; M_p \;/\; C \tag{7-2}$$

5) At this point, the overhanging projection of the baseplate becomes a mechanism. With a further increase in the magnitude of the compressive reaction, the location of the reaction will again approach the compression element of the attached member. This shift is indicated by tests 6 A1 12x and 6 M1 12x in Fig. 7.8.

The smallest distance, x_{min}, between the compressive reaction and the compression element of the attached member, is given by Eq. (7-1). This will give a conservative location for the compressive reaction. For the flexible baseplate tests, x_{min} can be determined from Eq.(7-1) as:

$$x_{min} \;=\; M_y \;/\; C$$

$$x_{min} \;=\; (b\, t^2\, F_y) \;/\; (6\; \Sigma T)$$

$$x_{min} \;=\; ((12)(1^2)(36))/((6)(4)(31))$$

$$x_{min} \;=\; 0.58\; inches$$

This agrees with the test results shown in Fig.7.8.

7.5.2 Summary: Effect of Baseplate Flexibility. The effect of baseplate flexibility on the location of the compressive reaction can be determined by considering the concrete to be a rigid bearing surface, and the portions of the baseplate projecting beyond the compression flange of the attached member to be flexible. The portion of the baseplate welded to the attached member should be considered to rotate as a rigid body.

To locate the compressive reaction in a conservative manner, the reaction can be considered to be at a distance, x_{min}, determined by Eq. (7-1) from the edge of the compression element of the attached member.

8. THEORETICAL STRENGTH OF DUCTILE MULTIPLE-ANCHOR CONNECTIONS

8.1 Introduction

In this chapter, a behavioral model developed to predict the strength of ductile multiple-anchor connections is presented and assessed. The behavioral model is based on limit design theory. Results of the ultimate load tests provide the basis for assessing the model.

8.2 Behavioral Model for Ductile Multiple-Anchor Connections

The behavioral model presented in this section is similar to the "plastic distribution" method proposed by Hawkins, Mitchell, and Roeder [56] for connections with welded studs. However, it includes the contribution of the frictional force between the baseplate and the concrete, and is applicable to connections with multiple rows of anchors. The model assumes that anchors transfer shear by bearing on the anchor, and that tensile and shear forces in the anchors redistribute prior to failure.

Fig. 8.1 shows the forces on a typical multiple-anchor connection. The connection shown in Fig. 8.1 has one row of anchors in the compression zone and two rows of anchors in the tension zone.

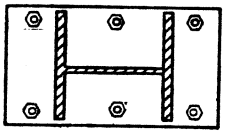

(a) PLAN VIEW

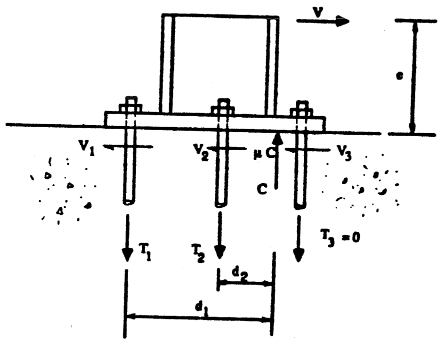

(b) SECTIONAL FREE BODY

Figure 8.1 Possible Distribution of Forces on a Multiple-Anchor Connection

The behavior of a ductile multiple-anchor connection can be separated into three distinct ranges:

1) If the shear strength provided by the frictional force (developed from the compressive reaction produced by the applied moment) is larger than the applied shear, then anchors are not required for shear. The anchors in the tension zone can be assumed to develop their full tensile strength for moment resistance.
2) If the shear strength provided by the frictional force and by the anchors in the compression zone exceeds the applied shear, the anchors in the tension zone can be assumed to develop their full tensile strength for moment resistance.
3) If the shear strength provided by the frictional force and by the anchors in the compression zone is less than the applied shear, the anchors in the tension zone must transfer the remaining shear load. The strength of the anchors in the tension zone is limited by their tension/shear interaction.

The transitions between these three ranges of behavior can be determined by considering two critical values of shear load eccentricity, e. The shear load eccentricity, e, is equal to the moment to shear ratio, (M/V), of the applied loading at the surface of the concrete.

The first critical eccentricity, e', corresponds to the point at which the applied shear load is equal to the frictional force. For eccentricities larger than e', the connection does not slip and no shear anchors are required. For eccentricities smaller than e', the connection slips and shear anchors must be provided. The first critical eccentricity, e', represents the transition between Range 1 behavior and Range 2 behavior as described above.

The second critical eccentricity, e'', corresponds to the point at which the applied shear load is equal to the sum of the frictional force and the shear strength of the anchors in the compression zone. For eccentricities larger than e'', the anchors in the tension zone can be assumed to develop their full tensile strength for moment resistance. For eccentricities smaller than e'', the anchors in the tension zone carry both tension and shear. The second critical eccentricity, e'', represents the transition between Range 2 behavior and Range 3 behavior as described above.

The three ranges of behavior are shown in Fig. 8.2. Note that if no anchors are provided in the compression zone, Range 2 behavior is not applicable, and e'' is the same as e'.

The strength of a ductile multiple-anchor connection can be summarized by considering two distinct areas of connection strength:

1) **Strength Dominated by Moment**: For $e \geq e''$, the strength of the connection is controlled by the tensile strength of the anchors in the tension zone. The connection has identical strength in Ranges 1 and 2. For connections without anchors in the compression zone, Range 2 does not exist, and the strength is dominated by moment when e r e'.
2) Strength Dominated by Shear: For $e < e''$, the strength of the connection is controlled by the shear strength of the anchors in the compression zone and the combined tensile and shear strength of the anchors in the tension zone. For connections without anchors in the compression zone, Range 2 does not exist, and the strength is dominated by shear when $e < e'$.

RANGE 3	RANGE 2	RANGE 1
Connection slips	Connection slips	Connection does not slip
Anchors in the compression zone are at their maximum shear strength, $\gamma\ T_0$	Anchors in the compression zone transfer shear and can achieve their maximum shear strength, $\gamma\ T_0$	Anchors are not required for shear
Anchors in the tension zone are in combined tension and shear and can achieve their maximum strength in combined tension and shear	Anchors in the tension zone can achieve their maximum tensile strength, T_0	Anchors in the tension zone can achieve their maximum tensile strength, T_0

0 e” e’ ∞

Shear Load Eccentricity (e) or Moment/Shear Ratio (M/V)
Note: e’ is defined by Eq. (8-7), e” is defined by Eq. (8-10)

Figure 8.2 Ranges of Behavior for Ductile Multiple-Anchor Connections

8.3 Analytical Development of the Behavioral Model

In this section, the analytical development of the behavioral model is presented.

The strength of connections dominated by shear is dependent on the tension/shear interaction of the anchors. As noted in Chapter 7, an elliptical interaction curve best describes the strength of a single anchor in combined tension and shear. A linear interaction is more conservative. An elliptical tension/shear interaction is used in the analytical development presented in this section. Since an elliptical interaction is difficult to apply in practice the corresponding linear formulations are also presented. The elliptical and linear tension/shear interactions are as given below:

1) For elliptical tension/shear interaction, the anchor shear strength is given by:

$$V_n = \gamma \sqrt{T_o^2 - T_n^2} \qquad (8-1)$$

2) For the more conservative linear tension/shear interaction, the anchor shear strength is given by:

2) For the more conservative linear tension/shear interaction, the anchor shear strength is given by:

$$V_n = \gamma (T_o - T_n) \qquad (8-2)$$

where: V_n = the shear strength of an anchor in combined tension and shear

γ = the ratio of the shear strength of the anchor to the tensile strength of the anchor

T_o = the tensile strength of the anchor

T_n = the tensile force in the anchor

8.3.1 Critical Eccentricities. The critical eccentricities, e' and e'', can be determined by the conditions of equilibrium. Fig. 8.3 shows the forces on a typical multiple-anchor connection with a shear load eccentricity equal to e'. Fig. 8.4 shows the forces on a typical multiple-anchor connection with the shear load eccentricity equal to e''.

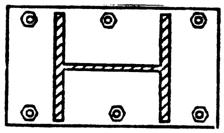

(a) PLAN VIEW

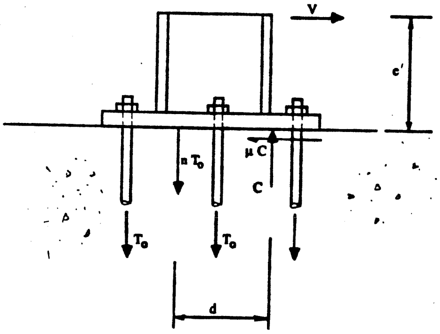

(b) SECTIONAL FREE BODY

Figure 8.3 Forces on a Multiple-Anchor Connection with Shear Load Eccentricity Equal to e'

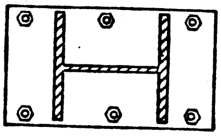

(a) PLAN VIEW

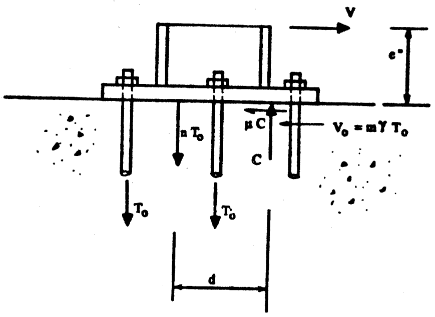

(b) SECTIONAL FREE BODY

Figure 8.4 Forces on a Multiple-Anchor Connection with Shear Load Eccentricity Equal to e''

The following formulations for the critical eccentricities, e' and e'', are applicable to connections with multiple rows of anchors if "d" is taken as the distance from the compressive reaction, C, to the centroid of the anchors in the tension zone, "n" is taken as the number of rows of anchors in the tension zone, "m" is taken as the number of rows of anchors in the compression zone, and "T_o" is taken as the tensile strength of a row of anchors.

The minimum eccentricity, e', for multiple-anchor connections without shear anchors can be determined by the conditions of equilibrium when the applied shear load, V, is equal to the frictional force, $\mu\,C$, (Fig. 8.3):

The condition of shear force equilibrium for the connection shown in Fig. 8.3 is given by:

$$V = \mu\,C \tag{8-3}$$

The condition of normal force equilibrium for the connection shown in Fig. 8.3 is given by:

$$C = n\,T_o \tag{8-4}$$

Substituting Eq. (8-3) into Eq. (8-4) yields the following:

$$V = \mu\,n\,T_o \tag{8-5}$$

$$e' = \frac{d}{\mu} \tag{8-7}$$

where: e' = the minimum eccentricity for multiple-anchor connections without shear anchors

μ = the coefficient of friction between steel and concrete

d = the distance from the compressive reaction to the centroid of the anchors in the tension zone

The minimum eccentricity, e'', for multiple-anchor connections without combined tension and shear in the anchors can be determined by the conditions of equilibrium when the applied shear load, V, is equal to the sum of the frictional force, $\mu\, C$, and the shear strength of the rows of anchors in the compression zone, $m\, \gamma\, T_o$. Fig. 8.4 only shows one row of anchors in the compression zone, ($m = 1$):

The condition of shear force equilibrium for the connection shown in Fig. 8.4 is given by:

$$V = \mu\, C + m\, \gamma\, T_o \tag{8-8}$$

Since the equation for normal force equilibrium is not changed by this formulation, Eq. (8-4) can be substituted into Eq. (8-8):

$$V = T_o\, (n\, \mu + m\, \gamma) \tag{8-9}$$

Since the equation for moment equilibrium, Eq. (8-6), is not changed by this formulation (e'' is substituted for e'), Eq. (8-9) can be set equal to Eq. (8-6) and the eccentricity, e'', can be determined as:

$$e'' = \frac{n\, d}{n\, \mu + m\, \gamma} \tag{8-10}$$

where: e'' = the minimum eccentricity for multiple-anchor connections without combined tension and shear in the anchors

n = the number of rows of anchors in the tension zone

m = the number of rows of anchors in the compression zone

μ = the coefficient of friction between steel and concrete

γ = the ratio of the shear strength of the anchor to the tensile strength of the anchor

d = the distance from the compressive reaction to the centroid of the tension anchors

Note that e'' reduces to e' when no anchors are provided in the compression zone.

8.3.2 Distribution of Tension. As noted in Chapter 7, for connections with more than one row of anchors in the tension zone the distribution of tension cannot be adequately predicted by traditional design methods. In limit design theory, the assumed distribution of tensile forces has no effect on the actual strength of the connection. Whatever distribution is assumed represents a lower bound to the actual strength of the connection. As long as sufficient anchors are provided to satisfy the conditions of equilibrium, the connection will perform satisfactorily.

In applying limit design theory, the issue of available inelastic deformation capacity must be addressed. Limit design theory is based on the assumption that materials have infinite plastic deformation capacity after yield. This is not the case. In a connection with two or more rows of anchors, subjected to an applied moment (Fig. 8.5), if the inner row of tension anchors is too close to the compressive reaction, anchors there will not be able to reach their tensile strength before the available deformation capacity is exceeded in the outer row of tension anchors.

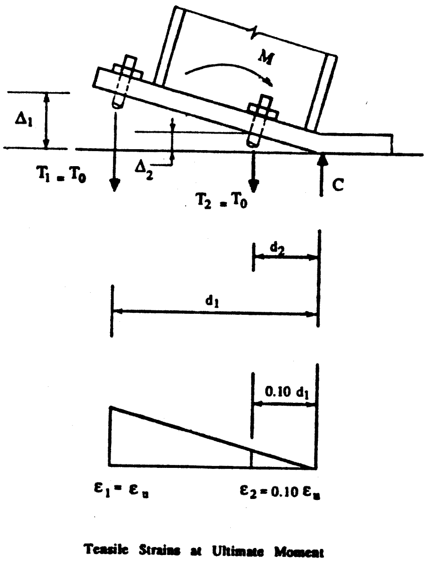
M
Δ_1
$T_1 = T_0$
Δ_2
$T_2 = T_0$
C
d_2
d_1
$0.10\ d_1$
$\varepsilon_1 = \varepsilon_u$
$\varepsilon_2 = 0.10\ \varepsilon_u$
Tensile Strains at Ultimate Moment

Figure 8.5 Limiting Location for Tension Anchors

Anchor materials typically have a specified minimum elongation requirement of at least 10% in 2 inches. This represents an ultimate strain, ϵ_u, of 0.10 or greater. To ensure that the tensile force in the inner row of anchors reaches the minimum specified tensile strength of the anchors, the distance between the inner row of anchors and the compressive reaction, d_2, should not be less than about 10% of the distance from the outer row of anchors to the compressive reaction, d_1 ($d_2 \geq 0.10$ d_1 in Fig. 8.5). The reason for this is as follows. When the inner row of anchors is so located, the tensile strain there, ϵ_2, will be at least 0.01 when the tensile strain in the outer row of anchors, ϵ_1, reaches its maximum value, ϵ_u. Since a tensile strain of 0.01 is roughly two to five times the yield strain for typical anchor materials, both rows of anchors will have yielded.

This somewhat arbitrary limit ensures that the innermost row of tension anchors will approach their tensile strength prior to tensile failure of the outermost row of tension anchors. This limit has little effect in a typical design situation, since greater flexural capacity of the connection is always achieved by locating the tension anchors as far as possible from the compressive reaction.

To properly assess the behavioral model, it was necessary to determine the assumed tension distribution which would give the highest predicted strength of the connection. This was accomplished by considering a connection with two rows of anchors in the tension zone and no anchors in the compression zone. Fig. 8.6 shows the connection used to determine the assumed tension distribution which produces the highest predicted strength.

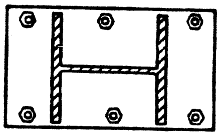

(a) PLAN VIEW

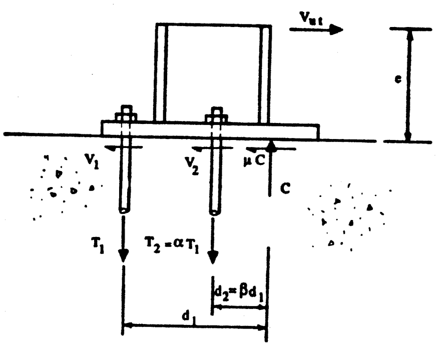

(b) SECTIONAL FREE BODY

Figure 8.6 Example of Connection Used to Assess the Maximum Predicted Strength

The type of connection shown in Fig. 8.6 covers both areas of connection strength. If the load eccentricity, e, is greater than or equal to e', the strength of the connection is dominated by moment and is controlled by the tensile strength of the anchors in the tension zone. For this condition it is obvious that the maximum predicted strength occurs when both rows of anchors reach their tensile strength, T_o. If the load eccentricity, e, is less than e', the strength of the connection is dominated by shear and is controlled by shear strength of the anchors in the compression zone and by the combined tensile and shear strength of the anchors in the tension zone. For this condition it is not obvious which distribution of tension in the anchors produces the maximum predicted strength.

The distribution of tension which produces the maximum predicted strength in a shear-dominated connection was determined by the conditions of equilibrium:

The moment equilibrium condition for the connection shown in Fig. 8.6 is given by:

$$V\, e \;=\; T_1\, d_1 \;+\; T_2\, d_2$$

$$V\,e \;=\; T_1\,d_1 \;+\; \alpha\,T_1\,\beta\,d_1$$

$$V\,e \;=\; T_1\,d_1\,(1 \;+\; \alpha\,\beta)$$

where: $\alpha =$ the ratio of the tensile force in the inner row of anchors, T_2, to the tensile force in the outer row of anchors, T_1; $0 < \alpha \leq 1$

$\beta =$ the ratio of the distance between the inner row of anchors and the compressive reaction, d_2, to the distance between the outer row of anchors and the compressive reaction, d_1; $0.10 \leq \beta \leq 1$

For a shear-dominated connection the tensile force in the outer row of anchors will be less than the tensile strength of the anchors, T_o:

$$V\,e \;=\; \delta\,T_0\,d_1\,(1 \;+\; \alpha\,\beta)$$

where: $\delta =$ the ratio of the tensile force in the outer row of anchors, T_1, to the tensile strength of a row of anchors, $T_o; 0 < \delta \leq 1$

Rearranging terms yields the following:

$$\frac{e}{d_1} \;=\; \frac{\delta\,(1 \;+\; \alpha\,\beta)}{\frac{V}{T_0}} \qquad (8-11)$$

The condition of normal force equilibrium for the connection shown in Fig. 8.6 is given by:

$$C \;=\; T_1 \;+\; T_2$$

$$C \;=\; T_1\,(1 \;+\; \alpha) \qquad (8-12)$$

The condition of shear force equilibrium for the connection shown in Fig. 8.6 is given by:

$$V \;=\; \mu\,C \;+\; V_1 \;+\; V_2 \qquad (8-13)$$

Substituting Eq. (8-12) and Eq. (8-1) for elliptical tension/shear interaction into Eq. (8-13) gives:

$$V \;=\; \mu\,T_1(1 \;+\; \alpha) \;+\; \gamma\,\sqrt{T_o^2 - T_1^2} \;+\; \gamma\,\sqrt{T_o^2 - \alpha^2 T_1^2}$$

Substituting $\delta\,T_o$ for T_1 gives:

$$V/T_0 = \mu\,\delta\,(1 + \alpha) + \gamma\,\sqrt{1-\delta^2} + \gamma\,\sqrt{1-\delta^2\alpha^2} \qquad (8-14)$$

Eq. (8-14), which represents the condition of force equilibrium for a connection with $e < e'$ and with anchors having an elliptical tension/shear interaction; and Eq. (8-11), which represents the condition of moment equilibrium for the same connection, are interdependent. These two equations were solved by assuming values of δ between zero and unity, which represents the range of application of Eq. (8-14), for various assumed values of α and β. The value of (V/T_o) determined from Eq. (8-14) was used in Eq. (8-11) to find the corresponding value of (e/d_1). The results are shown in Fig. 8.7.

To show continuity between the area of behavior dominated by shear, $e < e'$, and the area of behavior dominated by moment, $e \geq e'$; Fig. 8.7 includes the area of behavior dominated by moment for the assumed values of α and β. This area of behavior was determined from Eq. (8-11) with δ equal to unity, that is, $T_1 = T_o$:

$$\frac{V}{T_0} = \frac{(1 + \alpha\,\beta)}{(\frac{e}{d_1})} \qquad (8-15)$$

where: $e \geq e'$

As shown by Fig. 8.7, the maximum predicted strength of the connection in the area dominated by shear, $(e < e')$, and the area of behavior dominated by moment, $(e \geq e')$, occurs when the tensile force in the inner row of anchors is equal to the tensile force in the outer row of anchors $(\alpha = 1)$. Fig. 8.7 shows that this is true for various locations of the inner row of anchors ($\beta = 0.25$, 0.50, and 0.75).

For the more conservative assumption of a linear tension/shear interaction of anchor strength the condition of force equilibrium is given by:

$$V / T_0 = \mu\,\delta\,(1 + \alpha) + \gamma\,(1 - \delta) + \gamma\,(1 - \delta\,\alpha) \qquad (8-16)$$

This equation was solved with Eq. (8-11) in the same manner as the elliptical formulation, and the results are shown in Fig. 8.8. As shown in that figure, the assumption of a linear tension/shear interaction leads to predictions of higher strength in the shear-dominated region $(e < e')$, when the tensile force in the inner row of anchors is assumed to be zero $(\alpha = 0)$. This is inconsistent with the results of the elliptical formulation. Since a linear tension/shear interaction is conservative, and since the difference in maximum strength for $\alpha = 0$ and $\alpha = 1$, as shown in Fig. 8.8, is minimal; it is reasonable to assume that the maximum predicted strength for the linear interaction can be based on the tension in the inner row of anchors being equal to the tension in the outer row of anchors $(\alpha = 1)$.

To summarize, the maximum predicted strength of a ductile connection with multiple rows of anchors in the tension zone can be determined by assuming equal tension in all the anchors in the tension zone. This is true for connections dominated by moment $(e \geq e'')$, and connections

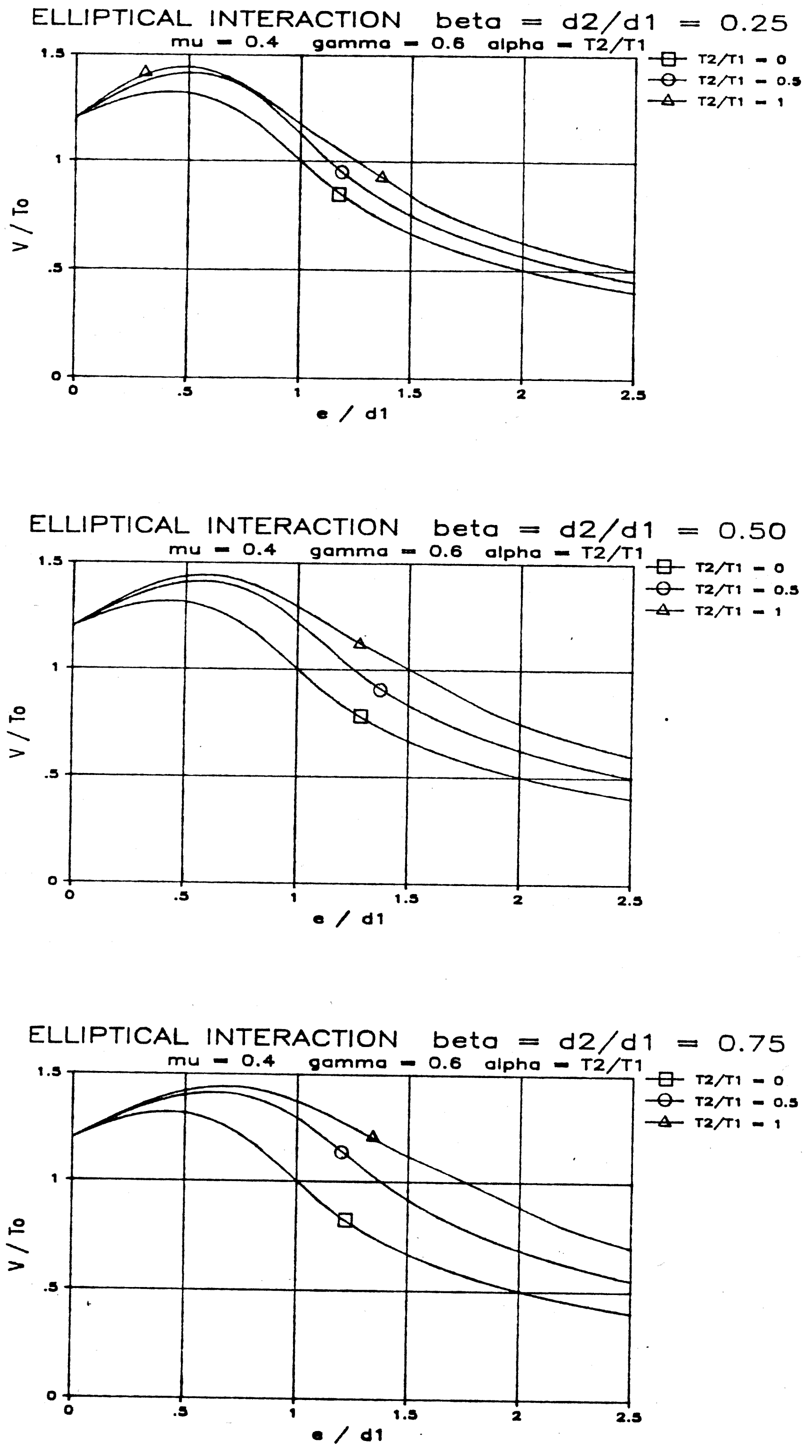

Figure 8.7 Comparison of Predicted Strengths with Elliptical Tension/Shear Interaction

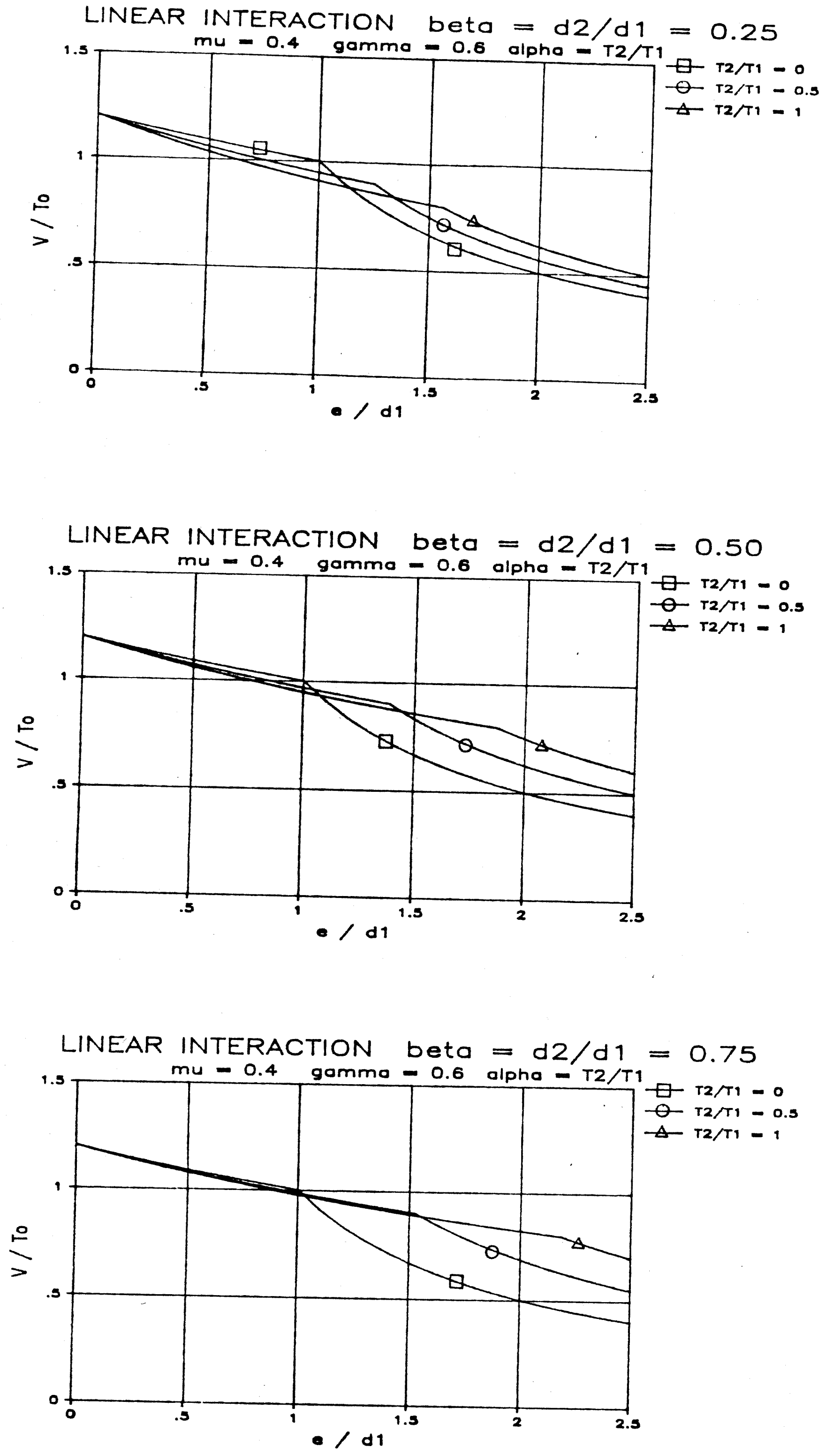

Figure 8.8 Comparison of Predicted Strengths with Linear Tension/Shear Interaction

dominated by shear ($e < e''$). The assumption of equal tension also implies equal shear in all the anchors in the tension zone for connections dominated by shear.

Analytically, the assumption of equal tension and shear in all the anchors in the tension zone is very convenient. The forces in all the anchors in the tension zone can be considered as a single force acting at the centroid, d, of the anchors in the tension zone. This is shown in Fig. 8.9.

8.3.3 Maximum Predicted Strength for Connections Dominated by Moment ($e \geq e''$). When the moment/shear ratio, e, of the applied loading is greater than or equal to the critical eccentricity, e'', the strength of the connection is controlled by the tensile strength of the anchors in the tension zone.

The moment equilibrium condition for the typical connection of Fig. 8.9, with $e > e''$ ($T_n = T_0$), gives the strength of the connection as controlled by the tensile strength of the anchors in the tension zone:

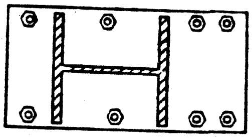

(a) PLAN VIEW

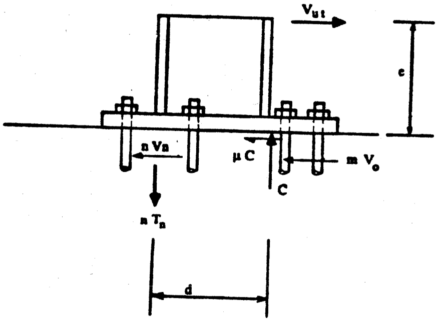

(b) SECTIONAL FREE BODY

Figure 8.9 Possible Distribution of Forces on a Multiple-Anchor Connection for Maximum Predicted Strength

$$V_{ut}\, e = n\, T_o\, d$$

$$V_{ut} = \frac{n\, T_o\, d}{e} \qquad (8-17)$$

where: V_{ut} = the maximum predicted strength of the connection when the moment/shear ratio, e, of the applied loading is greater than or equal to the critical eccentricity, e'', given by Eq. (8-10)

n = the number of rows of anchors in the tension zone

T_o = the tensile strength of a row of anchors in the tension zone

d = the distance from the compressive reaction to the centroid of the tension anchors

8.3.4 Maximum Predicted Strength for Connections Dominated by Shear ($e < e''$). When the moment/shear ratio, e, of the applied loading is less than the critical eccentricity, e'', the strength of the connection is controlled by the shear strength of the anchors in the compression zone, and by the combined tensile and shear strength of the anchors in the tension zone.

The condition of shear force equilibrium for the typical connection (shown in Fig. 8.9, with $e < e''$) is given by:

$$V_{ut} = \mu C + m V_o + n V_n \qquad (8-18)$$

The condition of normal force equilibrium for that same connection with $e < e''$ is given by:

$$C = n T_n \qquad (8-19)$$

Substituting Eq. (8-18) and Eq. (8-1) for elliptical tension/shear interaction into Eq. (8-18) yields the following:

$$V_{ut} = \mu n T_n + m \gamma T_0 + n \gamma \sqrt{T_0^2 - T_n^2} \qquad (8-20)$$

The condition of moment equilibrium for that same connection shown with $e < e''$ is given by:

$$V_{ut} e = n T_n d$$

$$T_n = \frac{V_{ut} e}{(n d)} \qquad (8-21)$$

Substituting Eq. (8-21) into Eq. (8-20) and solving the resulting quadratic equation for V_{ut} gives:

$$V_{ut} = \gamma T_0 \frac{m a + \sqrt{n^2(a^2 + b^2) - m^2 b^2}}{a^2 + b^2} \qquad (8-22)$$

where: V_{ut} = the maximum predicted strength of the connection when the moment/shear ratio, e, of the applied loading is less than the critical eccentricity, e'', given by Eq. (8-10)

γ = the ratio of the shear strength of the anchor to the tensile strength of the anchor

T_o = the tensile strength of a row of anchors in the tension zone

m = the number of rows of anchors in the compression zone

n = the number of rows of anchors in the tension zone

$a = 1 - \frac{\mu e}{d}$

$b = \frac{\gamma e}{d}$

μ = the coefficient of friction between steel and concrete

d = the distance from the compressive reaction to the centroid of the tension anchors

For the more conservative assumption of linear tension/shear interaction, the maximum predicted strength of the connection when $e < e''$ is given by:

$$V_{ut} = \gamma T_0 \frac{m + n}{1 + (\gamma - \mu) e / d} \qquad (8-23)$$

8.3.5 Summary: Analytical Development of Behavioral Model. The maximum predicted strength of any ductile multiple-anchor connection is given by Eq. (8-17) for connections dominated by moment ($e \geq e''$); and by Eq. (8-22) for connections dominated by shear ($e < e''$). The critical eccentricity, e'', is defined by Eq. (8-10). Eq. (8-22) is based on an elliptical tension/shear interaction. The maximum predicted strength using the more conservative linear tension/shear interaction is given by Eq. (8-23).

8.4 Assessment of Behavioral Model

In this section, the results of the ultimate load tests are compared to the connection strengths predicted by the behavioral model.

The ratio between the shear strength and the tensile strength of the anchor, γ, used in calculating the predicted strengths is taken from Chapter 7 ($\gamma = 0.50$ for cast-in-place and adhesive anchors, $\gamma = 0.60$ for undercut anchors). For both graphical and tabular comparisons of this section the coefficient of friction, μ, used in calculating the predicted strengths, is the design value in Chapter 7 ($\mu = 0.40$) . The tabular comparisons also include the predicted strengths calculated using a coefficient of friction, μ, of 0.50. As discussed in Chapter 7, this value for the coefficient of friction represents an upper bound to the results of the friction tests.

The predicted strength in the moment-dominated area of behavior ($e \geq e''$) is given by Eq. (8-17) for all tests. The values of n and d used in Eq. (8-17) for the different types of tests are discussed in the following subsections. The compressive reaction is assumed to act at the toe of the baseplate for the rigid baseplate tests, and at the location recommended in Chapter 7 for the flexible baseplate tests.

8.4.1 Two-Anchor Pattern. The two-anchor rigid baseplate tests did not require any redistribution of tension or shear among rows of anchors. In a sense, the comparison presented in this subsection represents the same results presented in Chapter 7 for the tension/shear interaction relationship of the anchors. The comparison is presented in this subsection in order to show that the test results of the two-anchor tests conform to the elliptical interaction relationship described in the behavioral model.

The two-anchor rigid baseplate specimens had no anchors in the compression zone ($m = 0$), one row of anchors in the tension zone ($n = 1$), and a value of d equal to 17 inches. The critical eccentricity, e'', given by Eq. (8-10), reduces to e' for this condition:

$$e'' = e' = \frac{d}{\mu}$$

Eq. (8-22), evaluated with $n = 1$ and $m = 0$, gives the predicted strength in the shear-dominated area of behavior:

$$V_{ut} = \gamma \, T_0 \, \frac{\sqrt{a^2 + b^2}}{a^2 + b^2}$$

In Fig. 8.10, the predicted strengths for both elliptical and linear tension/shear interaction are graphically compared to the test results for the two-anchor rigid baseplate specimens. In Table 8.1, the predicted strengths for elliptical tension/shear interaction are numerically compared to the test results.

As indicated by Fig. 8.10 and Table 8.1, the predicted strengths calculated using an elliptical tension/shear interaction with the recommended values of μ and γ are in close agreement with the test results. The only test which indicates a significant overestimate of the predicted strength calculated using the upper bound coefficient of friction is Test No. 2 CIP 24. As discussed in Chapter 7, this was the very first test performed with the rigid baseplate. For this test, the upper bound coefficient of friction is not appropriate.

8.4.2 Four-Anchor Pattern. The four-anchor rigid baseplate specimens had one row of anchors in the compression zone ($m = 1$), one row of anchors in the tension zone ($n = 1$), and a value of d equal to 17 inches. Eq. (8-10) gives the critical eccentricity, e'', for this condition:

$$e'' = \frac{d}{\mu + \gamma}$$

Eq. (8-22), evaluated with $n = 1$ and $m = 1$, gives the predicted strength in the shear-dominated area of behavior:

$$V_{ut} = 2 \, \gamma \, T_0 \, \frac{a}{a^2 + b^2}$$

In Fig. 8.11, the predicted strengths for both elliptical and linear tension/shear interaction are graphically compared to the test results for the four-anchor rigid baseplate specimens. In Table

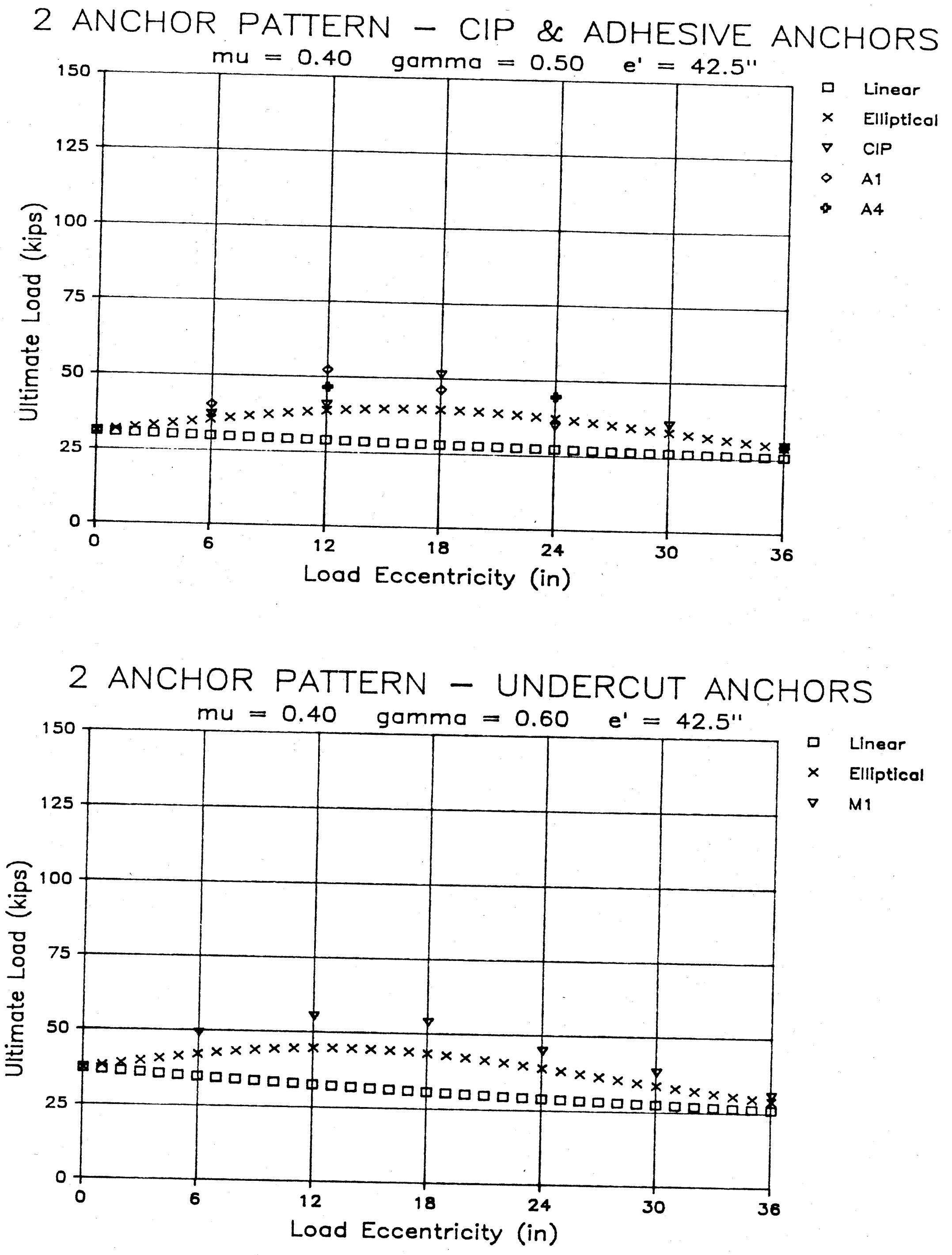

Figure 8.10 Test Results Versus Predicted Strengths for Two-Anchor Rigid Baseplate Specimens

Table 8.1 Test Results versus Predicted Strengths for Two- Anchor Specimens

Test No.	V_{test} kips	$\mu = 0.40$		$\mu = 0.50$	
		V_{ut} kips	$\frac{V_{test}}{V_{ut}}$	V_{ut} kips	$\frac{V_{test}}{V_{ut}}$
2 CIP 6	37.0	35.4	1.05	36.8	1.01
2 A1 6	40.3	35.4	1.14	36.8	1.10
2 M1 6	49.1	42.1	1.17	43.7	1.12
2 CIP 12	41.1	38.8	1.05	42.1	0.98
2 A1 12	52.2	38.8	1.34	42.1	1.24
2 A4 12	46.5	38.8	1.20	42.1	1.10
2 M1 12	55.5	44.6	1.24	48.1	1.15
2 CIP 18	51.2	39.6	1.29	43.8	1.17
2 A1 18	47.1	39.6	1.16	43.8	1.07
2 M1 18	53.9	43.4	1.24	47.1	1.14
2 CIP 24	35.0	37.4	0.94	40.5	0.86
2 A4 24	44.6	37.4	1.19	40.5	1.10
2 M1 24	44.9	39.1	1.15	41.5	1.08
2 CIP 30	36.0	33.3	1.08	34.8	1.03
2 M1 30	38.4	33.9	1.13	34.9	1.10
2 CIP 36	29.6	29.0	1.02	29.3	1.01
2 A4 36	29.2	29.0	1.01	29.3	1.00
2 M1 36	31.1	29.1	1.07	29.3	1.06

8.2, the predicted strengths for elliptical tension/shear interaction are numerically compared to the test results.

As indicated by Fig. 8.11 and Table 8.2, the predicted strengths calculated using an elliptical tension/shear interaction with the recommended values of γ and μ, agree closely with the test results. The only test which indicates an overestimate of the predicted strength is Test No. 4 CIP 24. This test failed by stripping of the anchor threads. As shown by Table 8.2, the predicted strengths for the four-anchor pattern are not particularly sensitive to the assumed value of the coefficient of friction ($\mu = 0.40$ or $\mu = 0.50$).

8.4.3 Six-Anchor Pattern. The six-anchor rigid baseplate specimens had one row of anchors in the compression zone ($m = 1$), two rows of anchors in the tension zone ($n = 2$), and a value of d equal to 13 inches. Eq. (8-10) gives the critical eccentricity, e'', for this condition:

$$e'' = \frac{2\,d}{2\mu + \gamma}$$

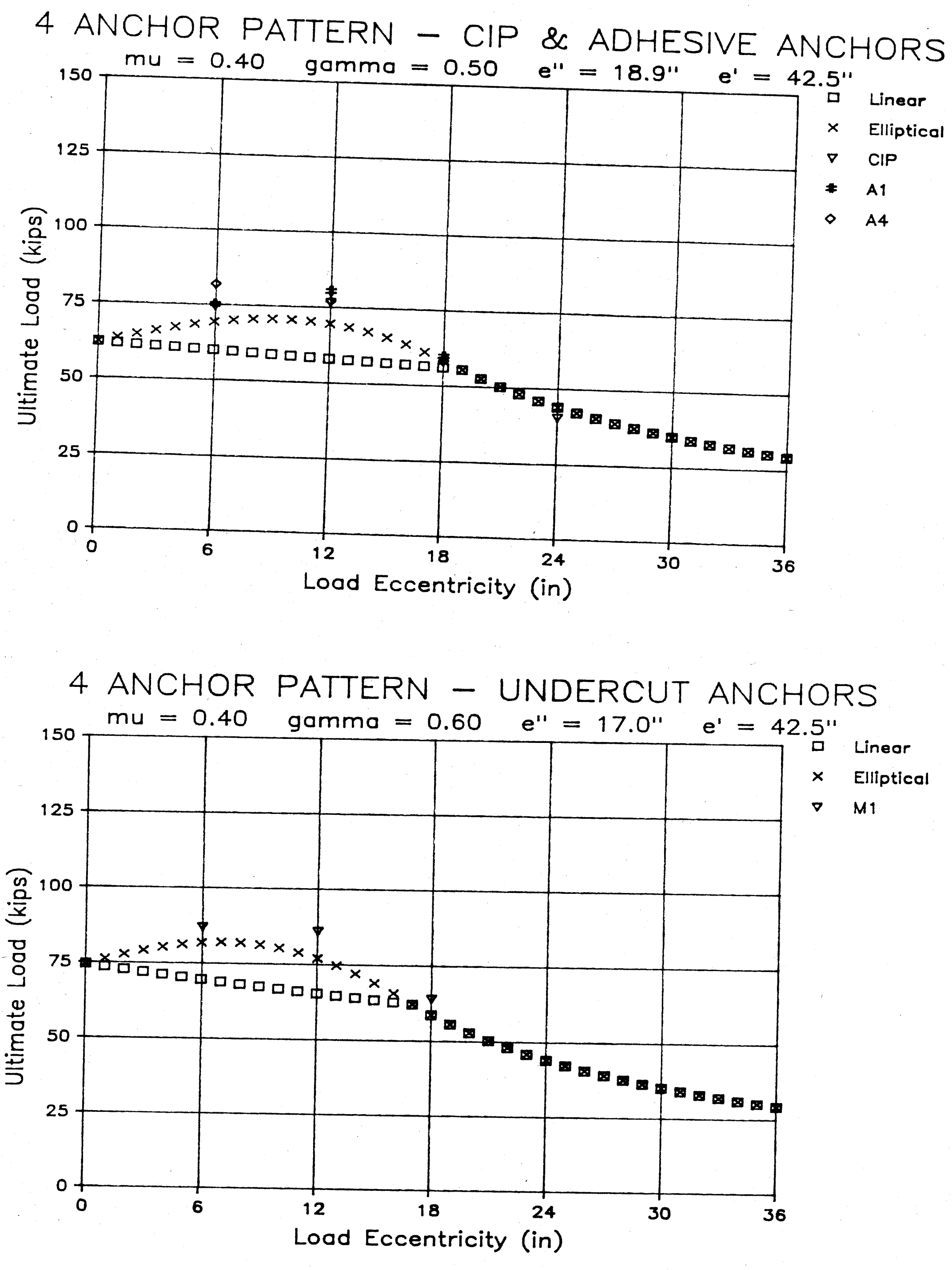

Figure 8.11 Test Results Versus Predicted Strengths for Four-Anchor Rigid Baseplate Specimens

Table 8.2 Test Results versus Predicted Strengths for Four- Anchor Specimens

Test No.	V_{test} kips	$\mu = 0.40$		$\mu = 0.50$	
		V_{ut} kips	$\frac{V_{test}}{V_{ut}}$	V_{ut} kips	$\frac{V_{test}}{V_{ut}}$
4 CIP 6	74.4	69.3	1.07	72.0	1.03
4 A1 6	75.2	69.3	1.08	72.0	1.04
4 A4 6	81.8	69.3	1.18	72.0	1.14
4 M1 6	86.9	81.7	1.06	84.7	1.03
4 CIP 12	76.7	69.6	1.10	73.8	1.04
4 A1 12	80.5	69.6	1.16	73.8	1.09
4 A4 12	77.1	69.6	1.11	73.8	1.04
4 M1 12	85.9	76.9	1.12	80.5	1.07
4 CIP 18	58.3	58.3	1.00	58.6	0.99
4 A1 18	59.9	58.3	1.03	58.6	1.02
4 A4 18	58.3	58.3	1.00	58.6	0.99
4 M1 18	63.9	58.6	1.09	58.6	1.09
4 CIP 24	40.5	43.9	0.92	43.9	0.92

Eq. (8-22), evaluated with $n = 2$ and $m = 1$, gives the predicted strength in the shear-dominated area of behavior:

$$V_{ut} = \gamma\, T_0\, \frac{a + \sqrt{4a^2 + 3b^2}}{a^2 + b^2}$$

In Fig. 8.12, the predicted strengths for both elliptical and linear tension/shear interaction are graphically compared to the test results for the six-anchor rigid baseplate specimens. In Table 8.3, the predicted strengths for elliptical tension/shear interaction are numerically compared to the test results for all six-anchor ultimate load tests.

As indicated by Fig. 8.12 and Table 8.3, the predicted strengths calculated using an elliptical tension/shear interaction with the recommended values of γ and μ, agree closely with the test results. As shown by Table 8.3, the predicted strengths for the six-anchor pattern are not particularly sensitive to the assumed value of the coefficient of friction ($\mu = 0.40$ or $\mu = 0.50$).

8.4.4 Summary: Assessment of Behavioral Model. As shown by the figures and tables in this section, the connection strengths predicted by the behavioral model compare quite well to the ultimate load test results. For the 46 ultimate load tests, the average test strength was 9% higher than the strength predicted using an elliptical tension/shear interaction with the recommended design values for the ratio of anchor shear strength to tensile strength ($\gamma = 0.50$ for cast-in-place and adhesive anchors, $\gamma = 0.60$ for undercut anchors) and using the recommended design value for

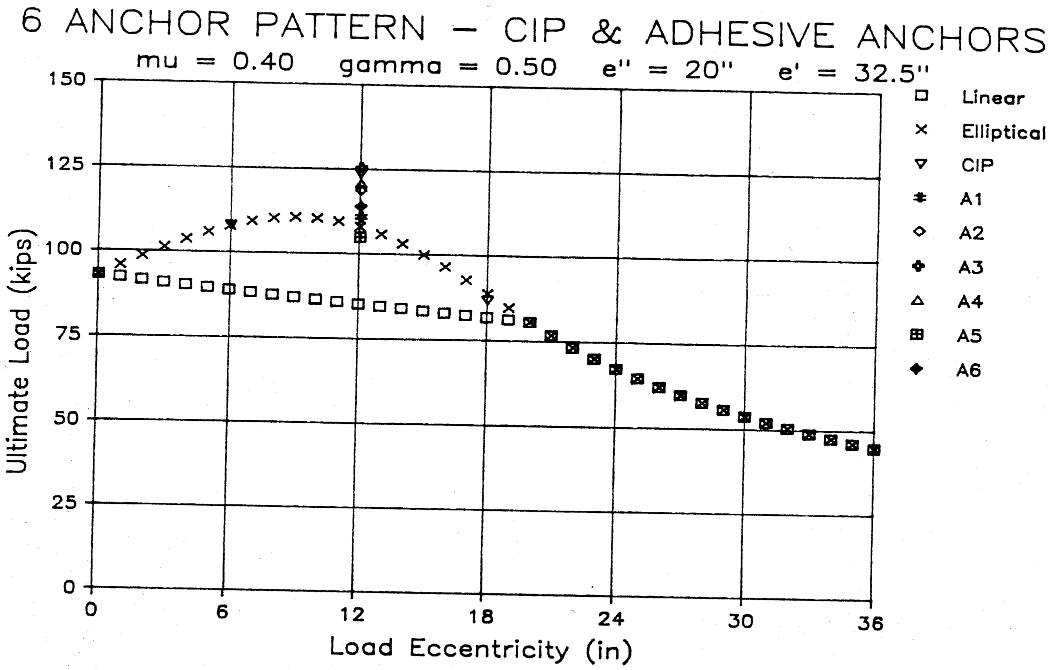

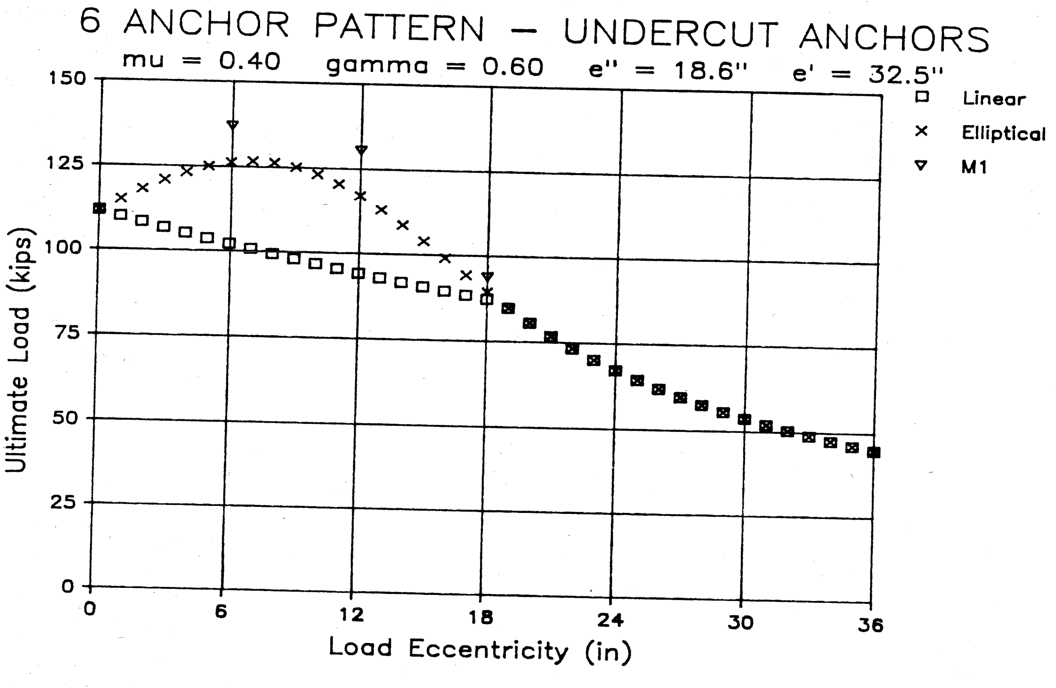

Figure 8.12 Test Results Versus Predicted Strengths for Six-Anchor Rigid Baseplate Specimens

Table 8.3 Test Results versus Predicted Strengths for Six-Anchor Specimens

Test No.	V_{test} kips	$\mu = 0.40$		$\mu = 0.50$	
		V_{ut} kips	$\frac{V_{test}}{V_{ut}}$	V_{ut} kips	$\frac{V_{test}}{V_{ut}}$
6 CIP 6	107.8	107.7	1.00	113.3	0.95
6 M1 6	137.0	126.2	1.09	132.5	1.03
6 CIP 12	123.6	107.8	1.15	115.9	1.07
6 A1 12	110.6	107.8	1.03	115.9	0.95
6 A2 12	118.6	107.8	1.10	115.9	1.02
6 A3 12	125.3	107.8	1.16	115.9	1.08
6 A4 12	120.7	107.8	1.12	115.9	1.04
6 A5 12	104.7	107.8	0.97	115.9	0.90
6 A6 12	113.8	107.8	1.06	115.9	0.98
6 M1 12	130.5	117.0	1.12	123.5	1.06
6 CIP 18	86.8	88.7	0.98	89.6	0.97
6 M1 18	94.0	89.5	1.05	89.6	1.05
6 A1 12x	107.7	100.8	1.07	106.1	1.02
6 A4 12x	104.8	100.8	1.04	106.1	0.99
6 M1 12x	110.4	105.2	1.05	108.4	1.02

the coefficient of friction ($\mu = 0.40$). Using the same elliptical tension/shear interaction relationship and the upper-bound value for the coefficient of friction ($\mu = 0.50$), the average test strength was 4% higher than the predicted value.

For the 28 four-anchor and six-anchor ultimate load tests, which required redistribution of tension and/or shear, the average test strength was 7% higher than the strength predicted using an elliptical tension/shear interaction with the recommended design values for the ratio of anchor shear strength to tensile strength ($\gamma = 0.50$ for cast-in-place and adhesive anchors, $\gamma = 0.60$ for undercut anchors) and using the recommended design value for the coefficient of friction ($\mu = 0.40$). Using the same elliptical tension/shear interaction relationship and the upper-bound value for the coefficient of friction ($\mu = 0.50$), the average test strength was 2% higher than the predicted value.

In conclusion, the behavioral model presented in this chapter provides a viable method for assessing the strength of ductile multiple-anchor connections to concrete.

9. SUMMARY, CONCLUSIONS, AND RECOMMENDATIONS

9.1 Summary

The overall objectives of this study were:

1) To determine the characteristic behavior of ductile multiple-anchor steel-to-concrete connections.

2) To develop a rational design procedure for calculating the strength of the steel in multiple-anchor steel-to-concrete connections.

For the purposes of this study, ductility was defined as the ability of a structural component to undergo significant inelastic deformation at predictable loads, and without significant loss of strength. A steel-to-concrete connection is ductile if its ultimate strength is controlled by the strength of the steel. A ductile connection to concrete fails by yielding and fracture of the anchors. A steel-to-concrete connection is non-ductile if its ultimate strength is controlled by the strength of the embedment. Non-ductile connections fail by brittle fracture of the concrete in tension, and by unpredictable concrete-related failure modes such as anchor slip without steel fracture.

To evaluate the behavior of ductile multiple-anchor steel-to-concrete connections, tests were performed to quantify and define the following variables affecting the strength of these connections:

1) The coefficient of friction between a surface mounted steel baseplate and hardened concrete in multiple-anchor connections.

2) The tension/shear interaction relationships for various types of anchors (cast-in-place, undercut, and adhesive) in multiple- anchor connections.

3) The distribution of tensile and shear forces among anchors in multiple-anchor connections.

4) The effect of baseplate flexibility on the behavior of multiple-anchor connections.

The study described in this report involved 44 friction tests and 46 ultimate load tests on multiple-anchor steel-to-concrete connections. The ultimate load tests were conducted on the following types of specimens: 18 two-anchor, 13 four-anchor, and 12 six-anchor specimens with a rigid baseplate; and 3 six-anchor specimens with a flexible baseplate. Test specimens were subjected to various combinations of moment and shear by applying an eccentric shear load to them at various eccentricities.

In the ultimate load tests, all specimens failed by yielding and fracture of the anchors. The strength of the anchor steel controlled the strength of the connections. For connections with cast-in-place and undercut anchors, embedment failure modes were precluded by designing the connections in accordance with the embedment criteria of ACI 349-85 Appendix B [4]. For connections with adhesive anchors, embedment failure modes were precluded by designing the connections in accordance with test results reported by Collins and Klingner [1]. Other failure modes associated with the concrete (such as bearing, flexural, or shear failure) were precluded by designing the test specimens in accordance with the criteria of ACI 349-85 [4].

The following general modes of behavior were observed in the testing program:

1) The frictional force which developed between the baseplate and the concrete, due to the compressive reaction from the applied moment, made a significant contribution to the shear strength of the connections.
2) Anchors transferred shear primarily by bearing. The shear- friction mechanism discussed in Subsection 2.2.2 was not observed. Anchors in shear failed by kinking and bending. Anchors in combined tension and shear failed by kinking, bending, and stretching.
3) Tension and shear forces in the anchors redistributed inelastically as required to maintain equilibrium with the applied loading.
4) Flexibility in the portion of the baseplate extending past the outermost compression element of the attached member caused the compressive reaction from the applied moment to shift inward from the leading edge, or toe, of the baseplate toward the outer edge of the compression element.
5) High bearing stresses between the baseplate and the concrete had no effect on the strength of the connections. For some tests with a rigid baseplate, the actual bearing stress at the toe of the plate was 5 times higher than the maximum permissible stress given by current design procedures. For tests with a flexible baseplate, the actual distribution and magnitude of bearing stresses was impossible to determine due to surface irregularities in the concrete finish. For these same tests, the actual location of the compressive reaction was not affected by the surface irregularities in the concrete finish.

9.2 Conclusions

9.2.1 Conclusions from Friction Tests. The purpose of the 44 friction tests was to determine the coefficient of friction between a surface mounted steel baseplate and hardened concrete in multiple-anchor connections.

Coefficient of Friction between a Surface Mounted Steel Baseplate and Hardened Concrete. The results of this testing program are in close agreement with previous test results for steel plates installed on hardened concrete. As indicated by Table 2.4, the results of 15 previous friction tests [54,72] had an average value of 0.41 for the coefficient of friction for a steel plate installed on hardened concrete. The average coefficient of friction for the 44 friction tests conducted in this study was 0.43.

For design purposes, the coefficient of friction, μ, should be taken as 0.40 with a strength reduction factor, ϕ, of 0.65. Based on the results of the 44 friction tests conducted in this study, the actual strength will then exceed the calculated design strength 98% of the time.

9.2.2 Conclusions from Ultimate-Load Tests. The 46 ultimate load tests served three purposes:

1) To determine the tension/shear interaction relationship for the anchors in multiple-anchor connections.
2) To determine the distribution of tensile and shear forces among anchors in multiple-anchor connections.

3) To determine the effect of baseplate flexibility on the behavior of multiple-anchor connections.

Tension/Shear Interaction for Anchors. The results of the two- anchor ultimate-load tests indicate that an elliptical tension/shear interaction relationship is appropriate for anchors in steel-to-concrete connections. A linear tension/shear interaction relationship is conservative. This agrees with previous test results for anchors in steel-to-steel connections [6].

The shear strength of cast-in-place and adhesive anchors in a multiple-anchor connection should be taken as 50% of the tensile strength ($V_0/T_o = \gamma = 0.50$). The shear strength of undercut anchors in a multiple-anchor connection should be taken as 60% of the tensile strength ($V_0/T_o = \gamma = 0.60$).

Distribution of Tensile and Shear Forces among Anchors. The results of the ultimate load tests indicate that a design procedure based on limit design theory is appropriate for ductile multiple-anchor steel-to-concrete connections. The application of limit design theory to multiple-anchor steel-to-concrete connections is presented and assessed in Chapter 8.

Steel-to-concrete connections can be divided into two distinct areas of behavior depending on the moment-to-shear ratio of the applied loading: an area dominated by the applied moment; and an area dominated by the applied shear. The distinction between these two areas of behavior is presented in Chapter 8.

For connections in the moment-dominated area of behavior, the anchors in the tension zone can be assumed to attain their tensile strength prior to failure of the connection. In this case, the combined shear strength provided by the frictional force at the steel/concrete interface (due to the compressive reaction from the applied moment) and by the shear strength of anchors in the compression zone, exceeds the applied shear. The strength of these connections is controlled by the tensile strength of the anchors in the tension zone.

For connections in the shear-dominated area of behavior, the anchors in the tension zone can be assumed to act as a single composite anchor acting at the centroid of the anchors in the tension zone. The strength of this composite anchor is limited by the anchors' tension/shear interaction relationship. In this case, anchors in the compression zone can be assumed to be at their maximum shear strength. The strength of these connections is controlled by the shear strength of the anchors in the compression zone, coupled with the combined tensile and shear strength of the anchors in the tension zone.

Effect of Baseplate Flexibility. Baseplate flexibility affects the assumed location of the compressive reaction from the applied moment. The compressive reaction should be located in a conservative manner since it directly affects the calculated tensile forces in the anchors.

The compressive reaction can be located in a conservative manner by considering the concrete surface to be rigid and the portion of the baseplate projecting beyond the outermost compression element of the attached member to be flexible. The portion of the baseplate welded to the attached member can be assumed to rotate as a rigid body.

To locate the compressive reaction from the applied moment in a conservative manner, the reaction can be considered to be located at a distance, x_{min}, determined by Eq. (7-1), from the outer edge of the compression element of the attached member. If the baseplate thickness is unknown, it is conservative to consider the compressive reaction to be located directly under the outer edge of the outermost compression element of the attached member.

9.3 Design Recommendations

The design recommendations resulting from this study are incorporated into a *Design Guide for Steel-to-Concrete Connections* [3]. The *Design Guide* is the final report on Texas SDHPT Project 1126.

9.4 Recommendations for Further Research

The results of this study indicate that a limit design approach is appropriate for ductile multiple-anchor steel-to-concrete connections. The most important goal of future research should be to determine the limits of applicability of this design approach. A limit design approach requires the following:

1) The strength of the connection must be controlled by the strength of the anchor steel. Non-ductile embedment failure modes associated with the concrete must not occur prior to failure of the anchor steel.

2) Anchors must be able to undergo sufficient inelastic deformation in both shear and tension so that tensile and shear forces are redistributed to other anchors in the connection prior to failure of any one anchor.

To ensure that these two requirements can be achieved in a multiple- anchor steel-to-concrete connection, the following additional research is recommended:

1) Investigate and define the embedded length requirements for anchors in multiple-anchor steel-to-concrete connections. Although the embedment criteria used to determine the embedded length of the anchors in this study were sufficient to produce designs whose capacities were governed by anchor steel failure, more research is needed to determine the embedment requirements for groups of anchors in tension, shear, and combined tension and shear. This is particularly true for adhesive anchors.

2) Investigate the bearing and shear strength of the supporting concrete for multiple-anchor steel-to-concrete connections (subjected to moment and shear, or to moment, shear, and axial load), as limited by free edges of the concrete. This should include rigid-baseplate tests with a single row of tension anchors and no anchors in the compression zone. The toe of the baseplate should be located near a free edge of concrete.

3) Investigate the flexural and shear strength of the supporting concrete for multiple-anchor steel-to-concrete connections (subjected to moment and shear, or to moment, shear, and axial load), as limited by the thickness of the concrete. Current design procedures for combined flexure and "punching" shear, resulting from localized loadings on a concrete slab, are based on test results for concrete column-to-slab connections. These design procedures may not be appropriate for multiple-anchor steel-to-concrete connections.

4) Investigate and define the maximum baseplate hole oversize that will permit redistribution of shear among the anchors in multiple-anchor steel-to-concrete connections. The baseplate hole oversize used in this study was 40% larger than the nominal diameter of the anchors. Studies should be performed on larger diameter anchors to determine if the proportionate hole oversize used in this study can be extrapolated to larger diameter anchors.

5) Investigate the strength and behavior of ductile multiple-anchor steel-to-concrete connections (subjected to moment and shear, or to moment, shear, and axial load), for reversible cyclic loads.

The limited flexible baseplate test results of this study indicate that a relatively simple design approach can be used for flexible baseplates. Additional tests of ductile multiple-anchor steel-to-concrete connections using flexible baseplates should be performed to verify the proposed method for locating the compressive reaction given in this study and the *Design Guide.*

APPENDIX A

APPROXIMATE METHOD FOR CALCULATING THE PROJECTED AREA WITH OVERLAPPING FAILURE CONES

The exact calculation of the actual projected area for overlapping failure cones (shown in Fig. 3.5) is difficult and unjustifiable given the inexact nature of other parameters in the embedment design (such as the concrete tensile strength and the shape of the failure cones). Marsh and Burdette [74] and Siddiqui and Beseler [75] provide design aids for calculating the projected area for overlapping failure cones.

The approximate method given here is generally conservative, and in the few situations where it is unconservative the error is less than 2%.

The approximate method is based on connecting the overlapping failure cones by tangents, calculating the resulting approximate projected area, A_{pa}, by relatively simple formulas, and then modifying that projected area by a reduction factor, β. Fig. A.1 shows approximate projected areas, A_{pa}, for overlapping cones. The reduction factor β is given by:

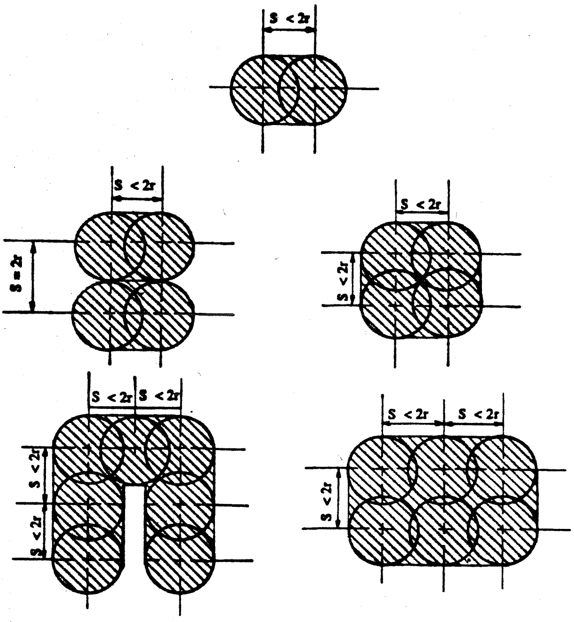

Figure A.1 Approximate Projected Areas for Overlapping Cones

$$\beta = 1 - 0.05\,\alpha^2 \qquad (A-1)$$

where: $\alpha =$ the ratio of the largest anchor spacing between adjacent anchors in a group of anchors with overlapping failure cones, to the radius of an individual failure cone. The factor α will always be less than 2 for overlapping failure cones (when α is greater than or equal to 2 the failure cones do not overlap).

For design purposes the projected area for groups of anchors, A_p, may be taken as:

$$A_p = \beta\, A_{pa} \qquad (A-2)$$

The reduction factor, β, given by Eq. (A-1), was determined as follows:

1) A conservative value for the reduction factor, β, can be determined by considering a typical quadrant of overlap for the most widely spaced anchors in a group of anchors with overlapping failure cones. Fig. A.2 shows a typical quadrant of overlap for the simple case of two anchors with overlapping failure cones.

2) The actual reduction factor, β, (which represents the ratio between the actual projected area and the approximate projected area) for the typical quadrant of overlap shown in Fig. A.2 was determined by geometry as follows:

The actual projected area, A_p, for the typical quadrant of overlap is given by:

$$A_p = \frac{\alpha\, r^2}{4}\sqrt{1-(\frac{\alpha}{2})^2} + \frac{r^2}{2} Sin^{-1}(\frac{\alpha}{2})$$

The approximate projected area, A_{pa}, for the typical quadrant of overlap is given by:

$$A_{pa} = \frac{\alpha r^2}{2}$$

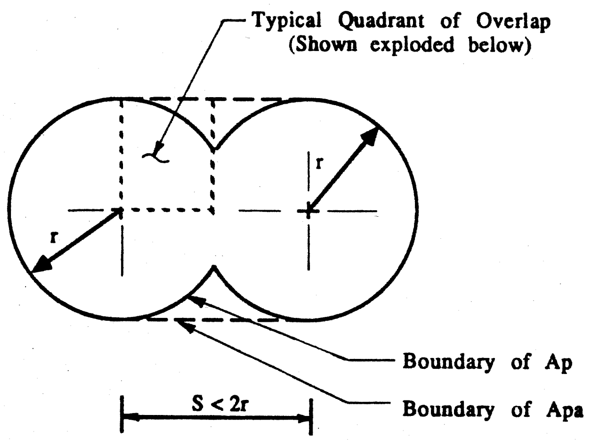
Typical Quadrant of Overlap
(Shown exploded below)
r
r
Boundary of Ap
Boundary of Apa
S < 2r

(a) Actual and Approximate Projected Areas for Two Anchors with Overlapping Failure Cones

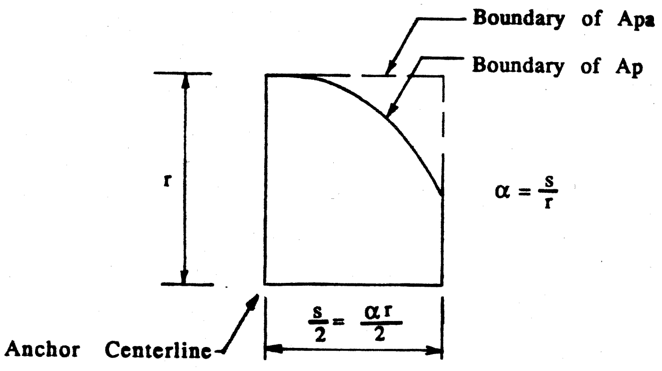
Boundary of Apa
Boundary of Ap
r
α = s/r
s/2 = αr/2
Anchor Centerline

(b) Typical Quadrant of Overlap

Figure A.2 Typical Quadrant of Overlap for Closely Spaced Anchors

The actual value of β is determined as:

$$\beta = \frac{A_p}{A_{pa}}$$

$$\beta = \frac{1}{2}\sqrt{1-(\frac{\alpha}{2})^2} + \frac{1}{\alpha}\,Sin^{-1}(\frac{\alpha}{2}) \qquad (A-3)$$

where: $\alpha =$ the ratio of the anchor spacing, s, to the radius, r, of an individual failure cone

3) An approximate value of the reduction factor, β, given by Eq. (A-1), was determined by fitting a parabolic curve to the actual value, given by Eq. (A-3). Fig. A.3 shows a graphical comparison of these two equations.

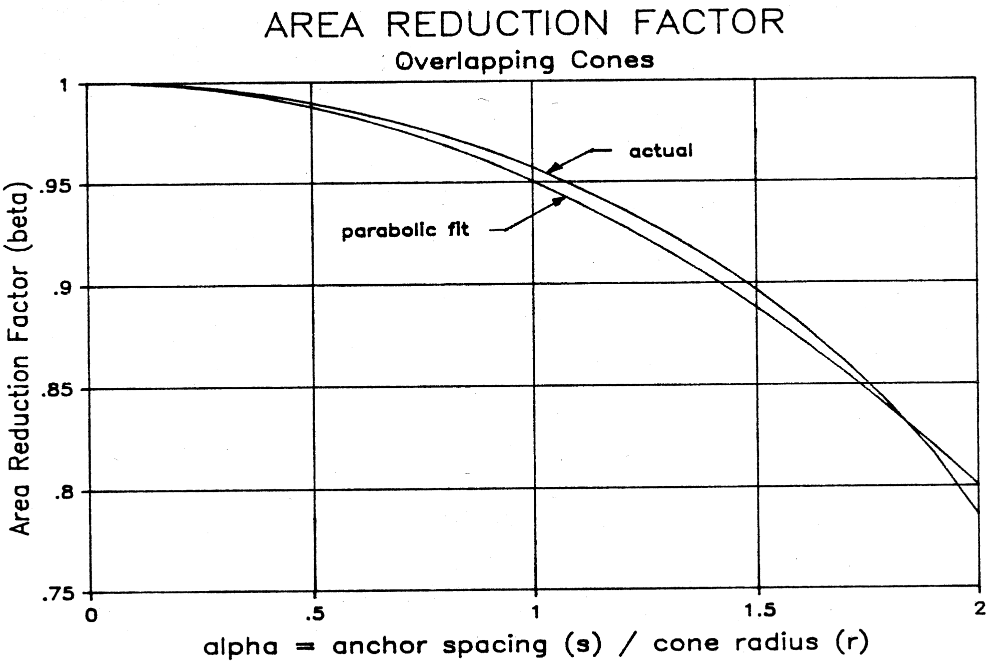

Figure A.3 Reduction Factor for Overlapping Failure Cones

4) For groups of anchors with overlapping failure cones a conservative value for the reduction factor, β, is determined by calculating a value for α based on the largest anchor spacing in the group.

APPENDIX B: GRAPHICAL RESULTS FOR FRICTION TESTS

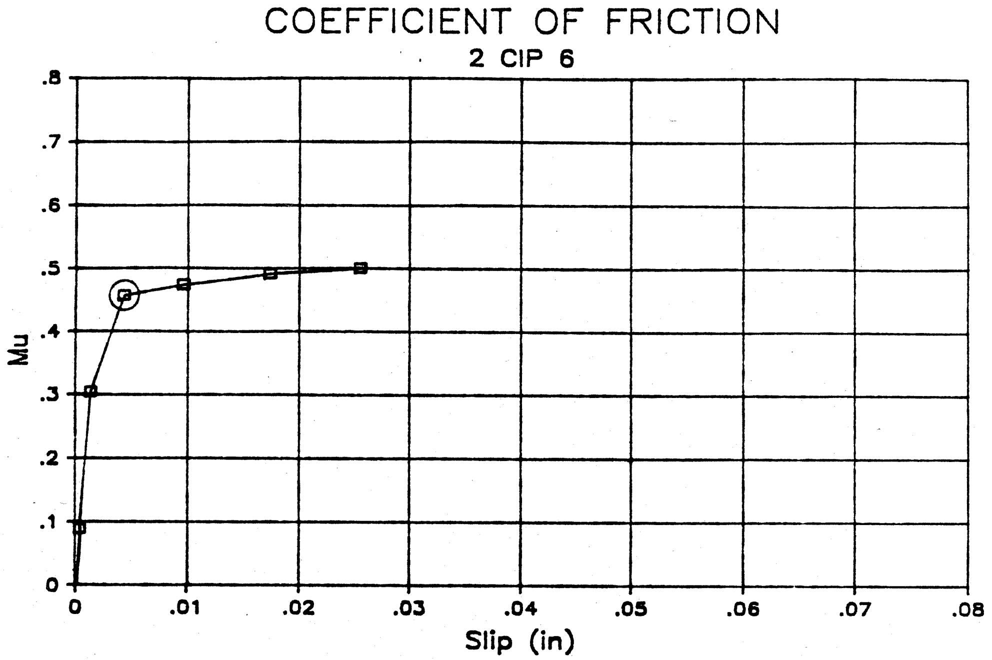
COEFFICIENT OF FRICTION
2 CIP 6
Mu
0
.1
.2
.3
.4
.5
.6
.7
.8
0
.01
.02
.03
.04
.05
.06
.07
.08
Slip (in)

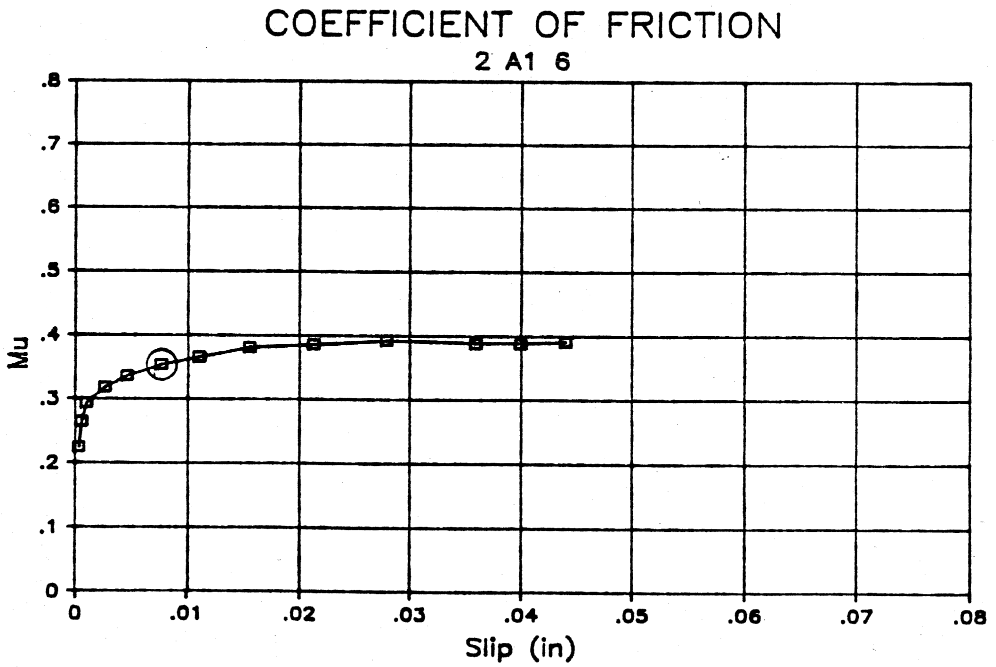
COEFFICIENT OF FRICTION
2 A1 6
Mu
0
.1
.2
.3
.4
.5
.6
.7
.8
0
.01
.02
.03
.04
.05
.06
.07
.08
Slip (in)

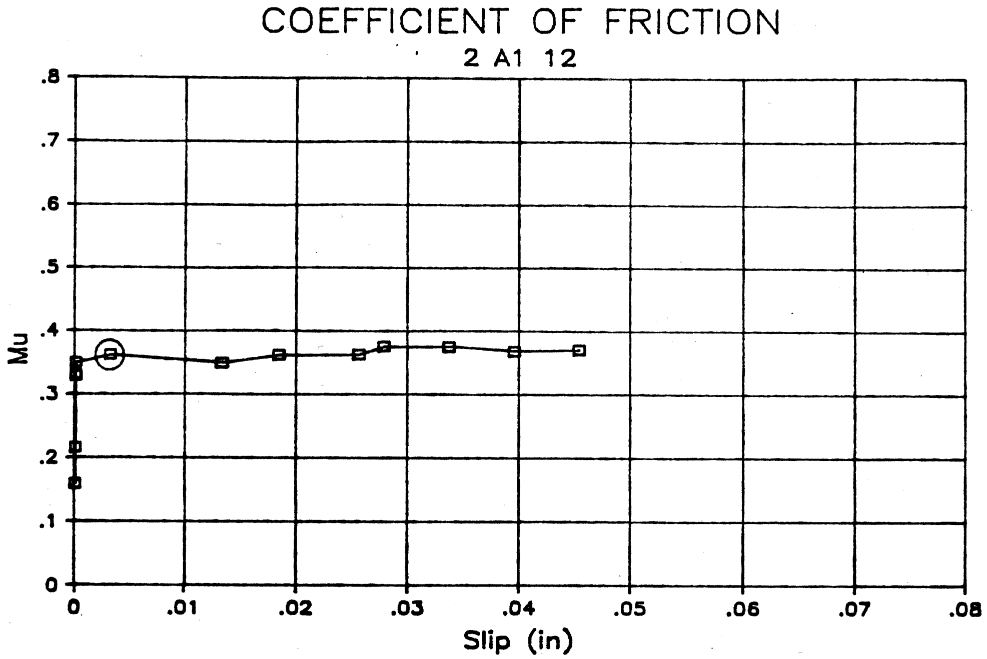
COEFFICIENT OF FRICTION
2 A1 12
Mu
Slip (in)
0
.1
.2
.3
.4
.5
.6
.7
.8
0
.01
.02
.03
.04
.05
.06
.07
.08

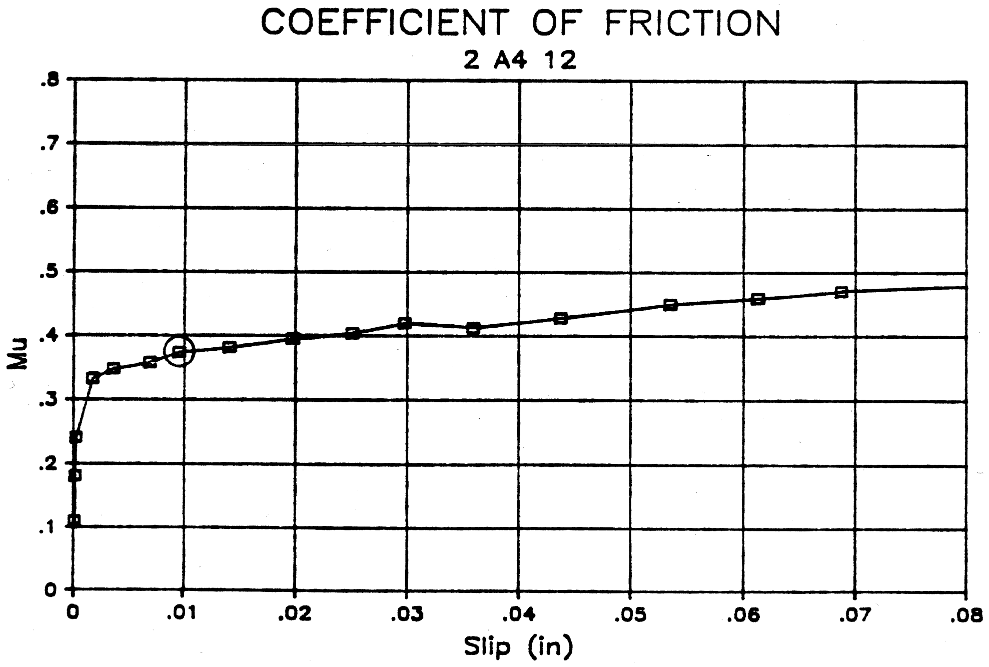
COEFFICIENT OF FRICTION
2 A4 12
Mu
Slip (in)
0
.1
.2
.3
.4
.5
.6
.7
.8
0
.01
.02
.03
.04
.05
.06
.07
.08

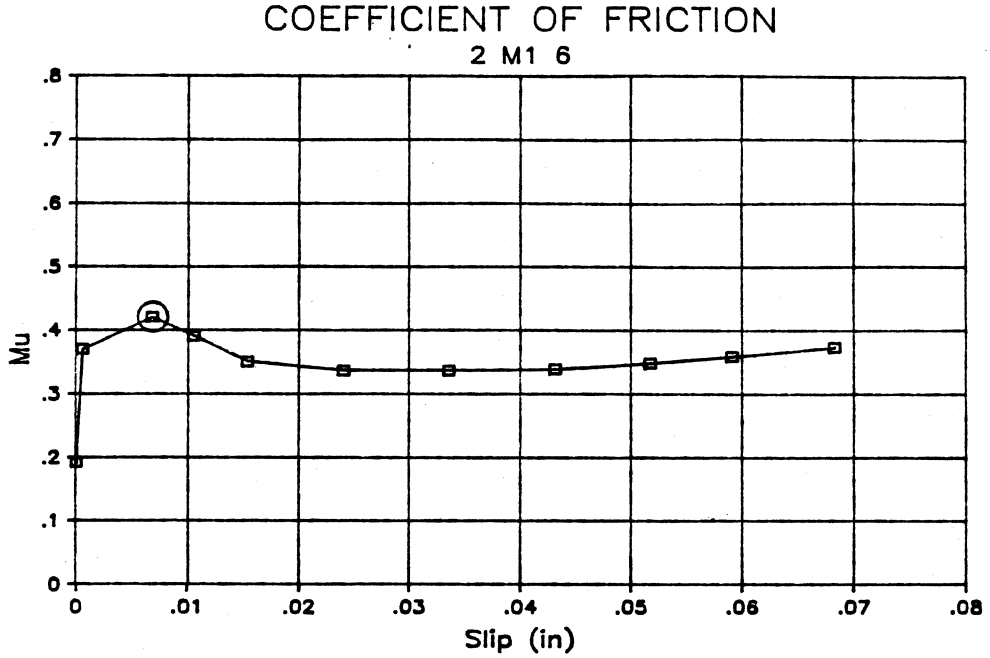
COEFFICIENT OF FRICTION
2 M1 6
Mu
.8
.7
.6
.5
.4
.3
.2
.1
0
.01
.02
.03
.04
.05
.06
.07
.08
Slip (in)

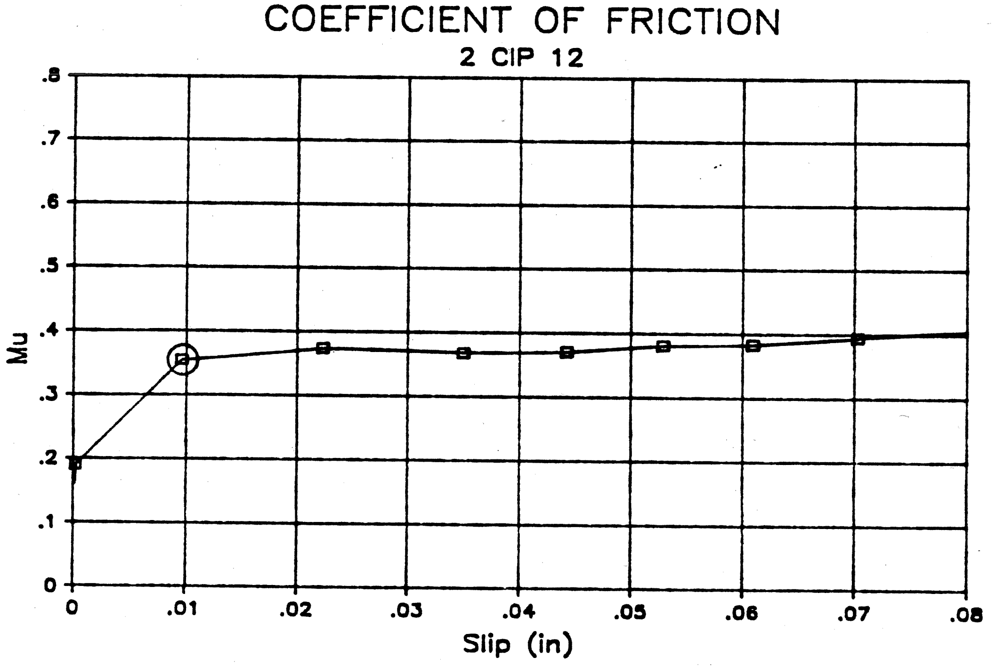
COEFFICIENT OF FRICTION
2 CIP 12
Mu
.8
.7
.6
.5
.4
.3
.2
.1
0
.01
.02
.03
.04
.05
.06
.07
.08
Slip (in)

COEFFICIENT OF FRICTION

2 M1 12

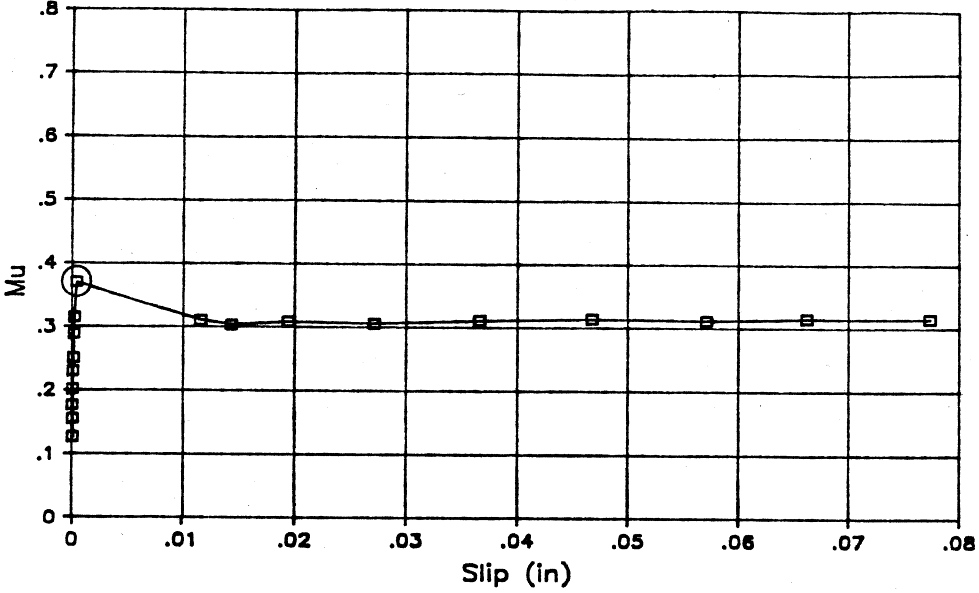

COEFFICIENT OF FRICTION

2 CIP 18

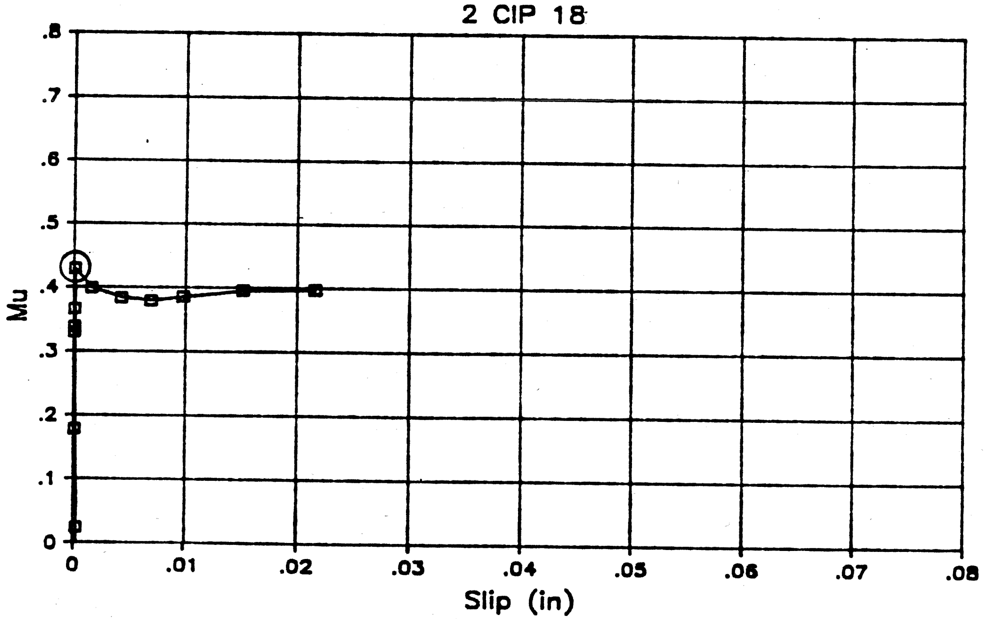

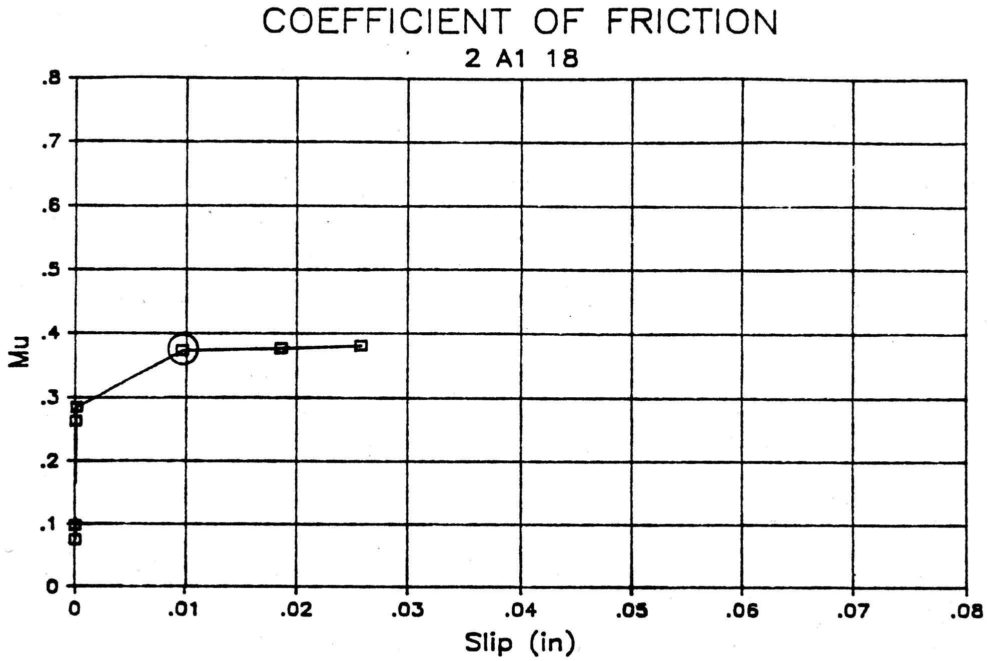

COEFFICIENT OF FRICTION

2 A1 18

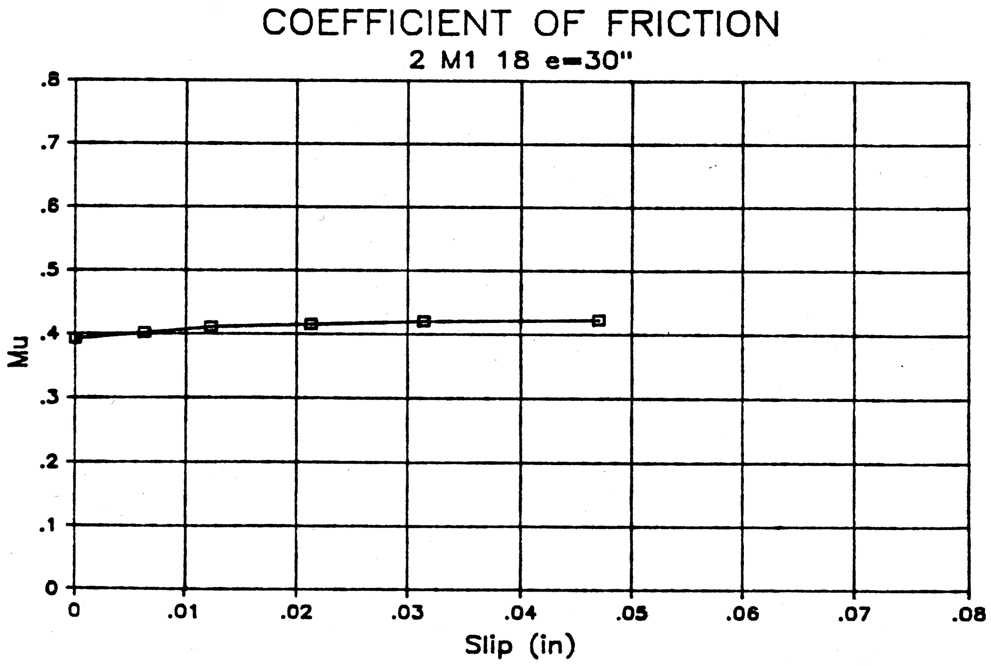

COEFFICIENT OF FRICTION

2 M1 18 e=30"

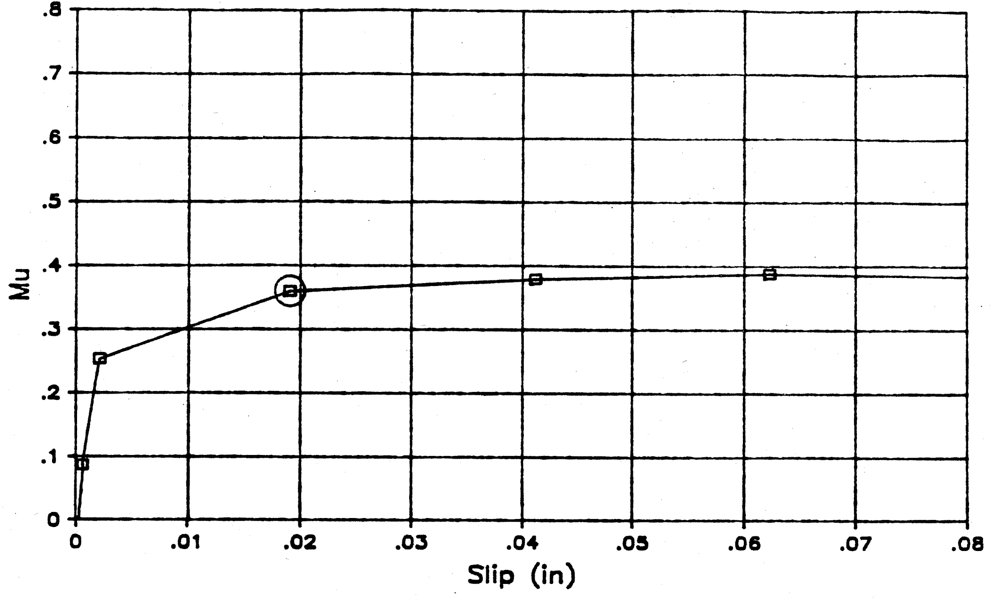
COEFFICIENT OF FRICTION
2 CIP 24

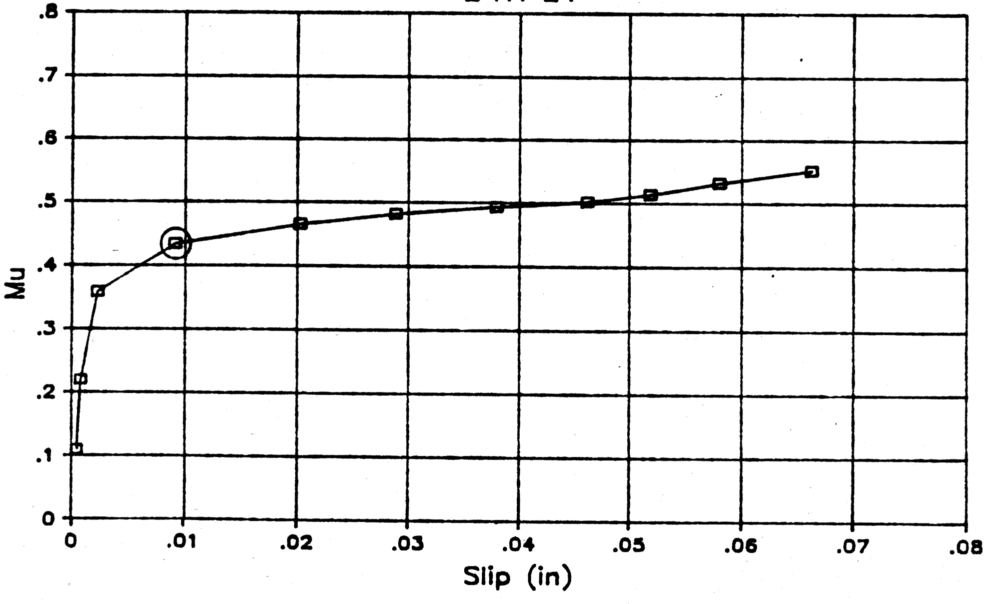
COEFFICIENT OF FRICTION
2 A4 24

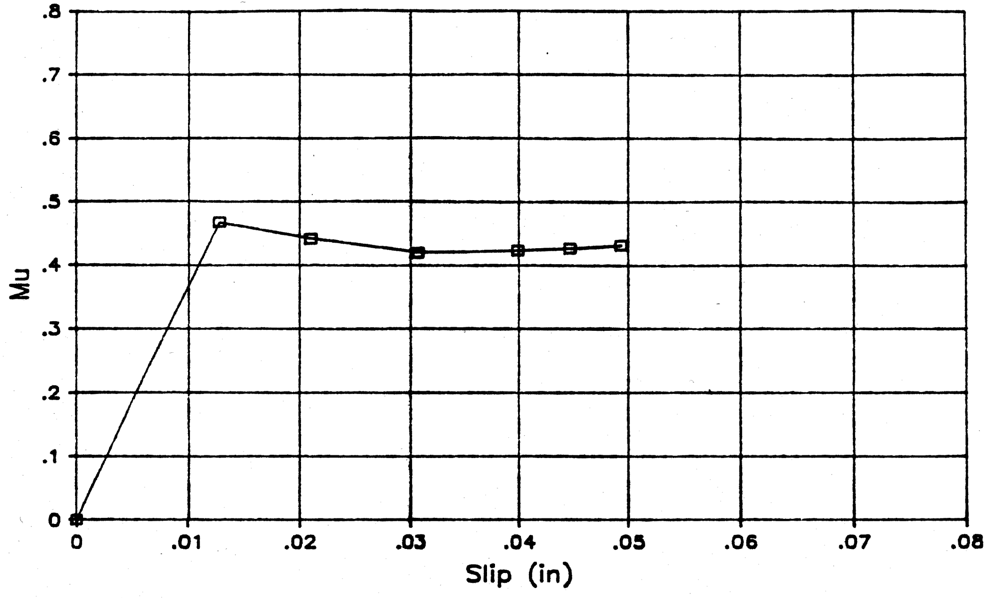

COEFFICIENT OF FRICTION
2 A4 24 e=36"

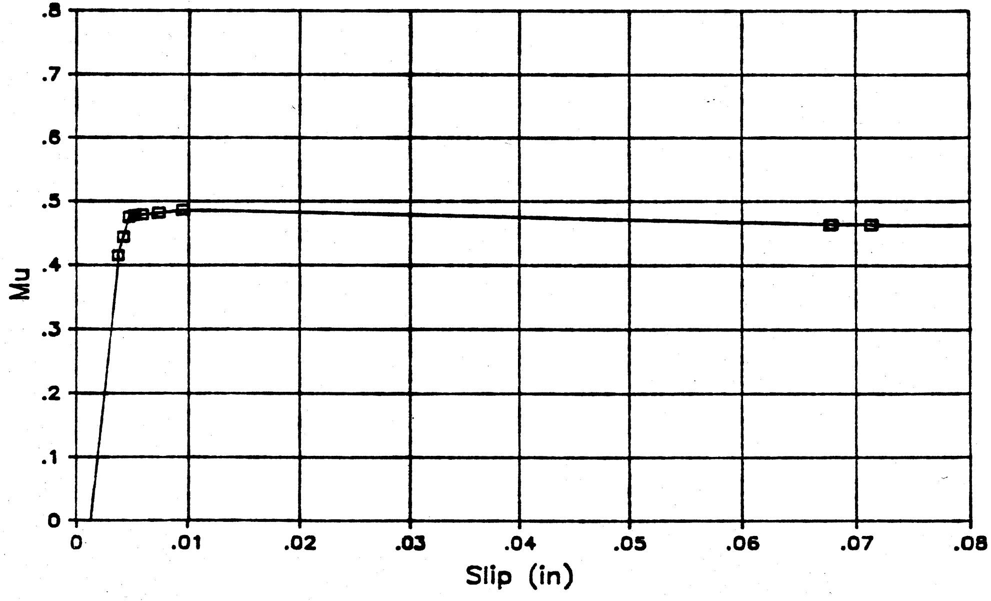

COEFFICIENT OF FRICTION
2 M1 24 e=30"

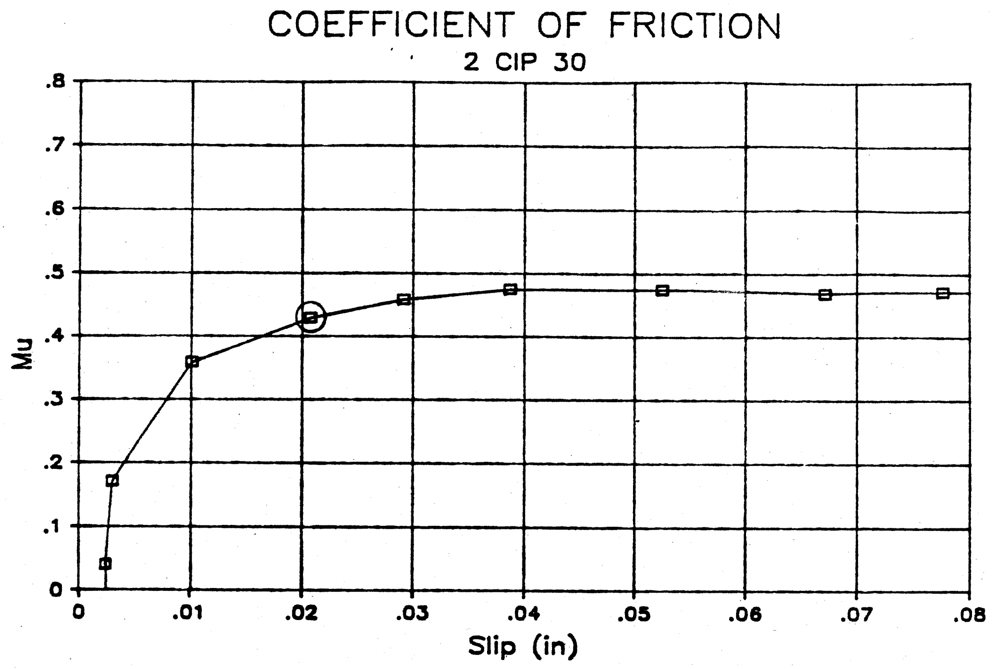
COEFFICIENT OF FRICTION
2 CIP 30
Mu
.8
.7
.6
.5
.4
.3
.2
.1
0
0
.01
.02
.03
.04
.05
.06
.07
.08
Slip (in)

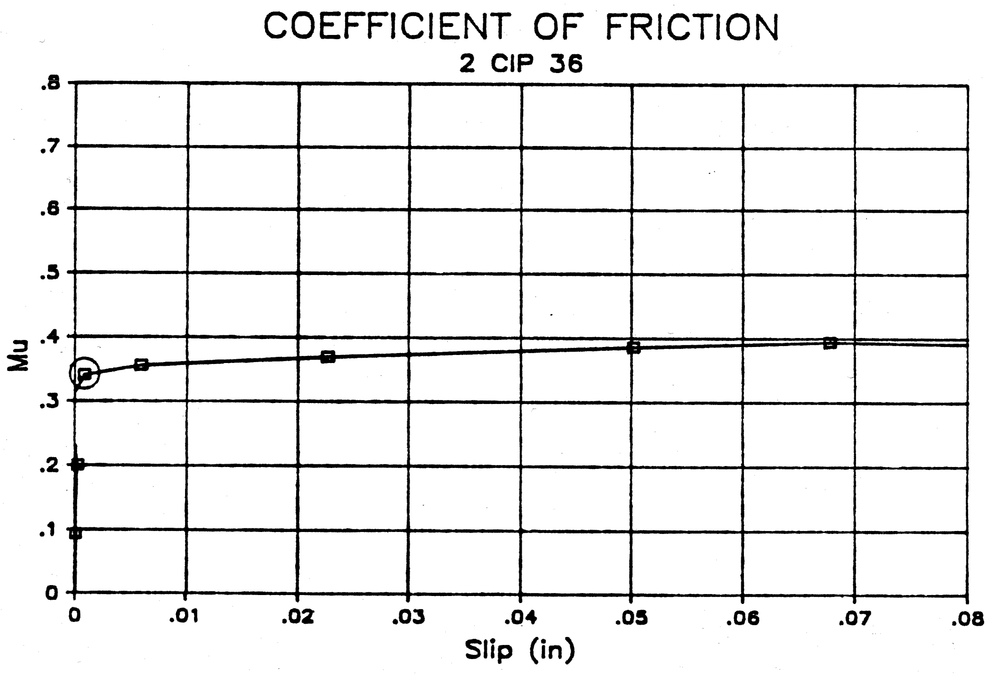
COEFFICIENT OF FRICTION
2 CIP 36
Mu
.8
.7
.6
.5
.4
.3
.2
.1
0
0
.01
.02
.03
.04
.05
.06
.07
.08
Slip (in)

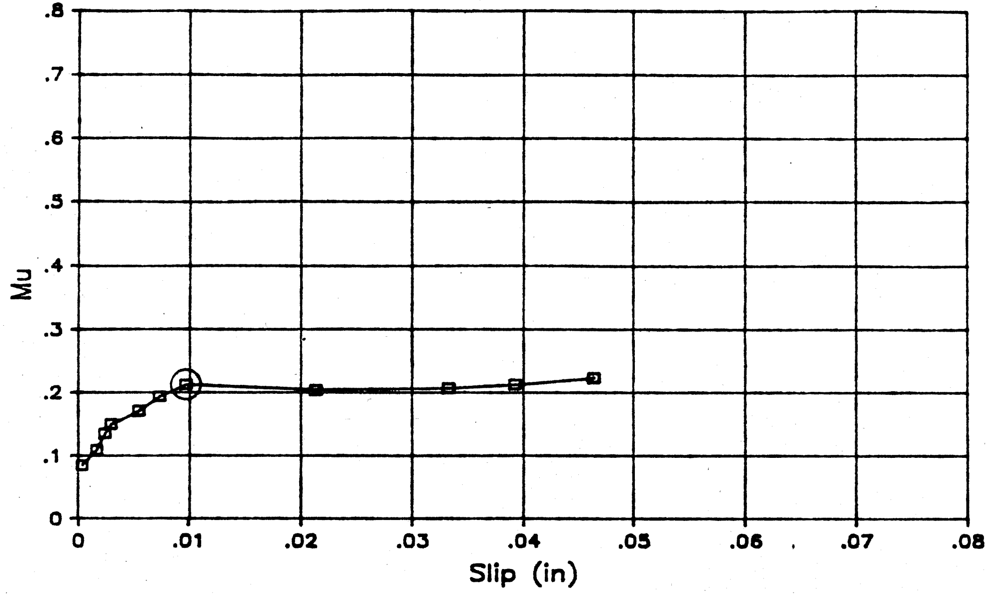

COEFFICIENT OF FRICTION
2 A4 36

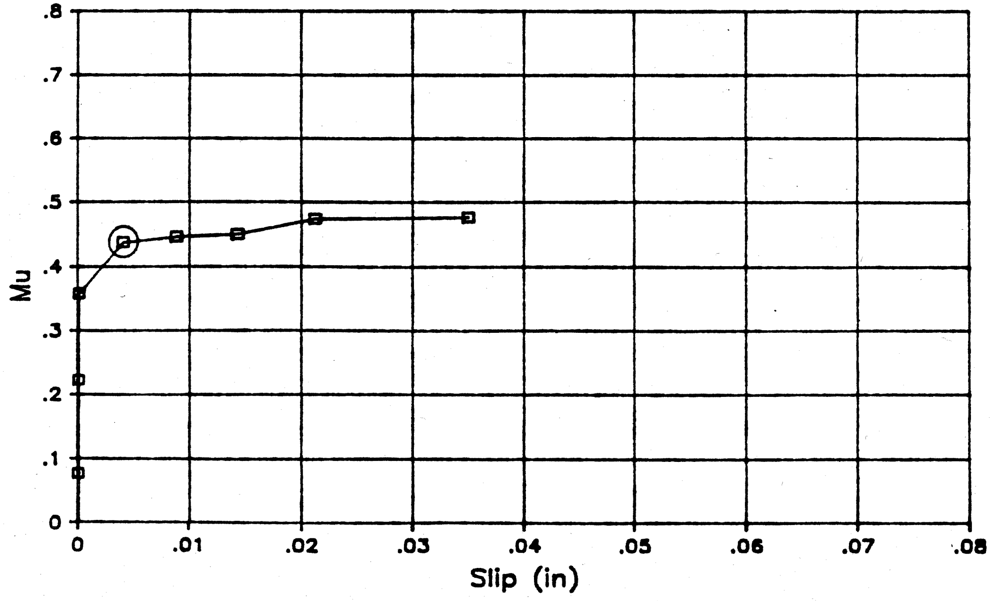

COEFFICIENT OF FRICTION
4 CIP 6

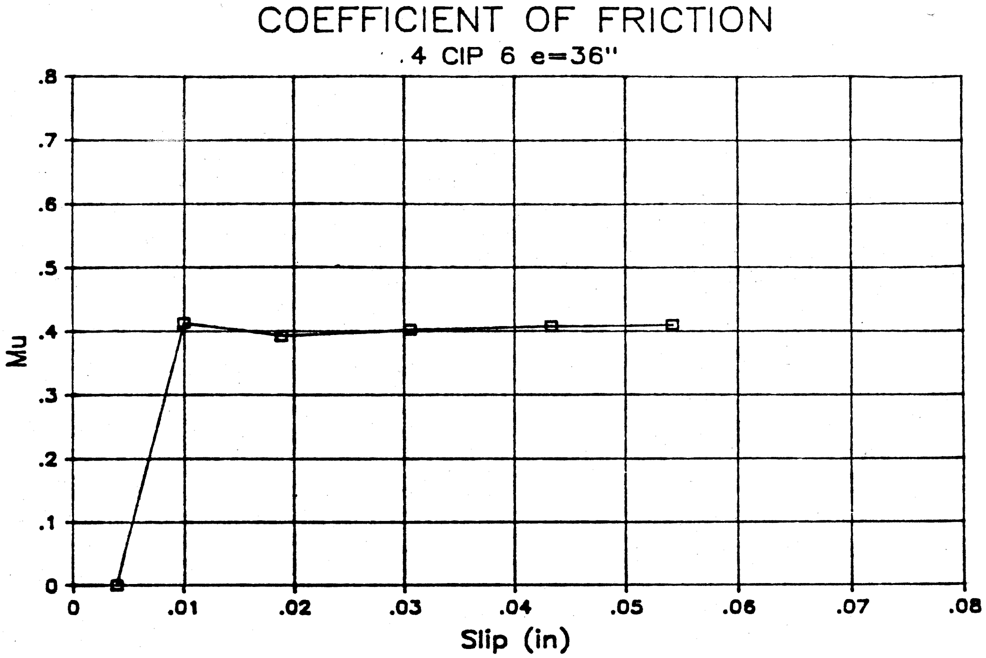
COEFFICIENT OF FRICTION
.4 CIP 6 e=36"
Mu
.8
.7
.6
.5
.4
.3
.2
.1
0
0
.01
.02
.03
.04
.05
.06
.07
.08
Slip (in)

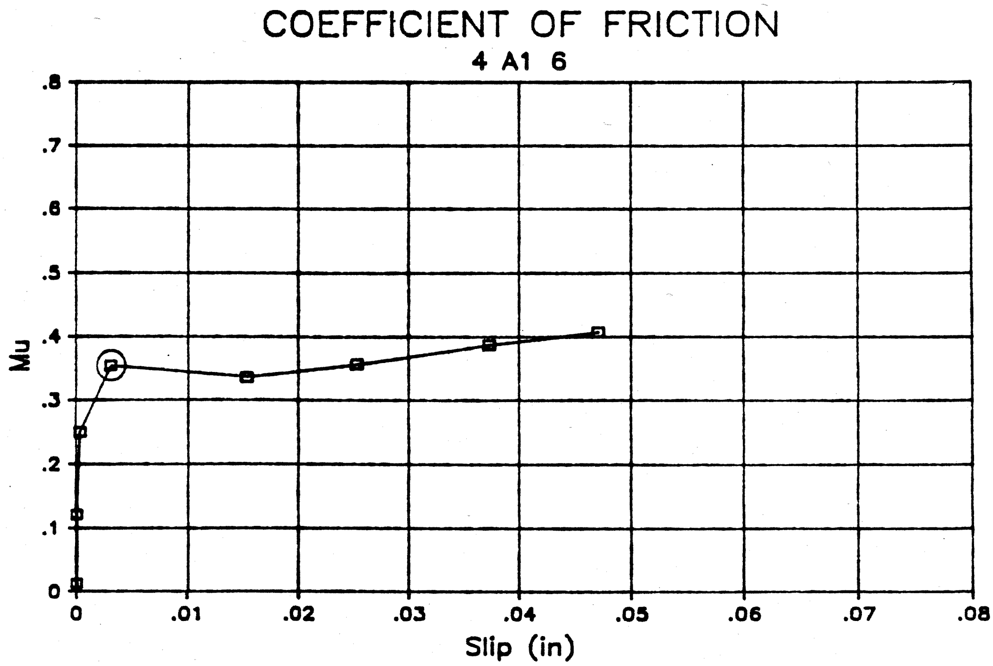
COEFFICIENT OF FRICTION
4 A1 6
Mu
.8
.7
.6
.5
.4
.3
.2
.1
0
0
.01
.02
.03
.04
.05
.06
.07
.08
Slip (in)

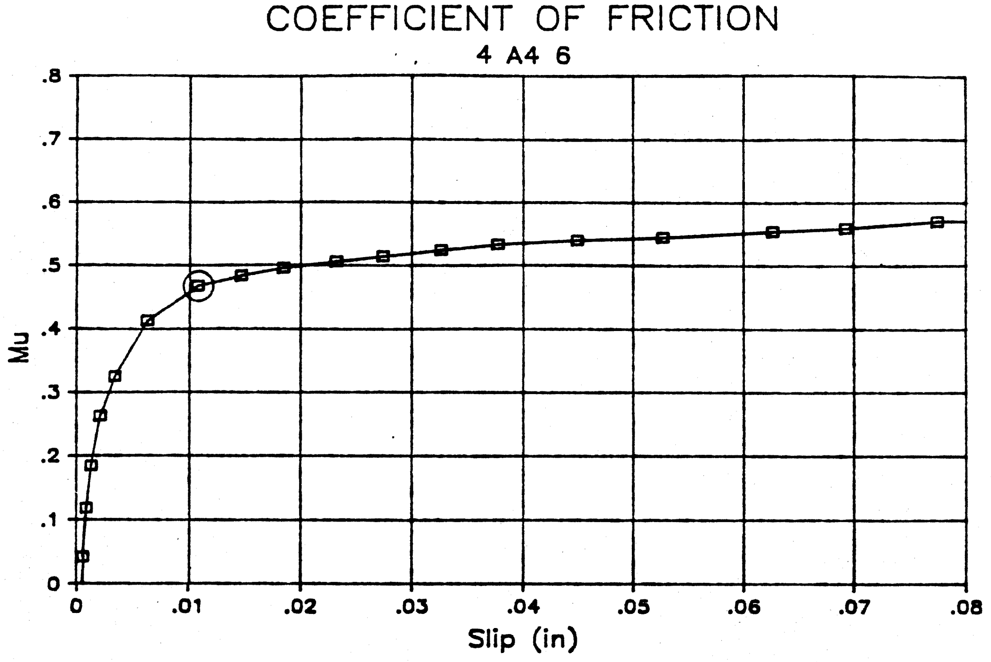
COEFFICIENT OF FRICTION
4 A4 6
Mu
0
.1
.2
.3
.4
.5
.6
.7
.8
0
.01
.02
.03
.04
.05
.06
.07
.08
Slip (in)

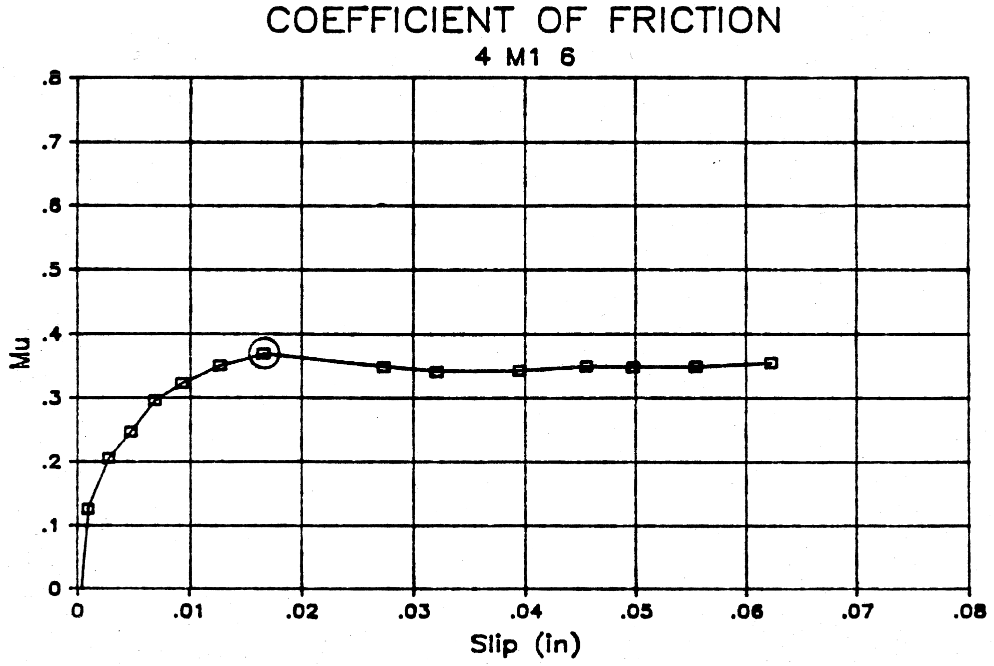
COEFFICIENT OF FRICTION
4 M1 6
Mu
0
.1
.2
.3
.4
.5
.6
.7
.8
0
.01
.02
.03
.04
.05
.06
.07
.08
Slip (in)

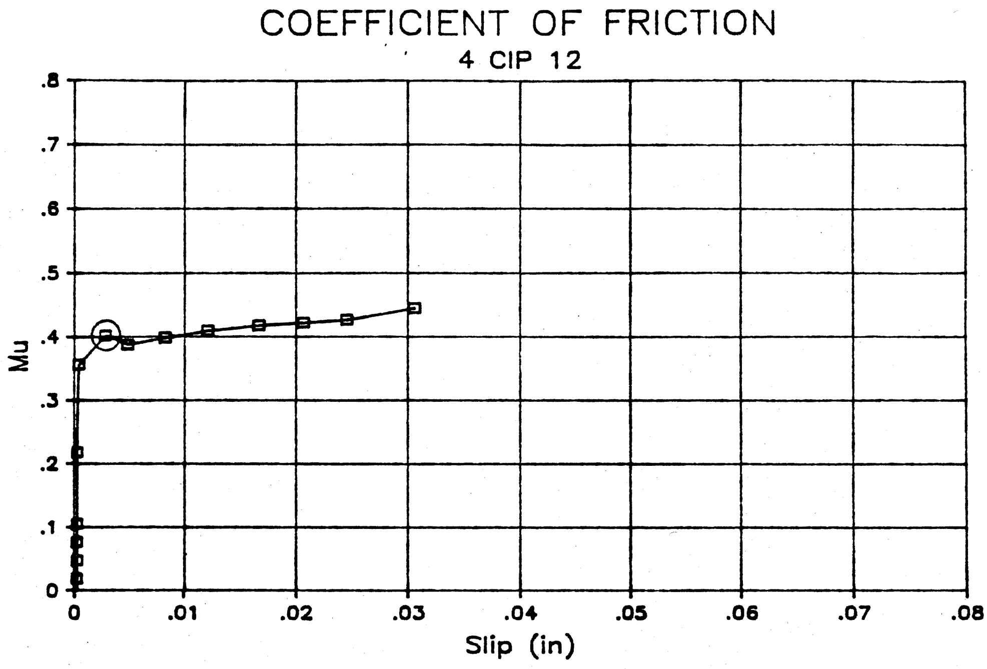
COEFFICIENT OF FRICTION
4 CIP 12
Mu
.8
.7
.6
.5
.4
.3
.2
.1
0
0
.01
.02
.03
.04
.05
.06
.07
.08
Slip (in)

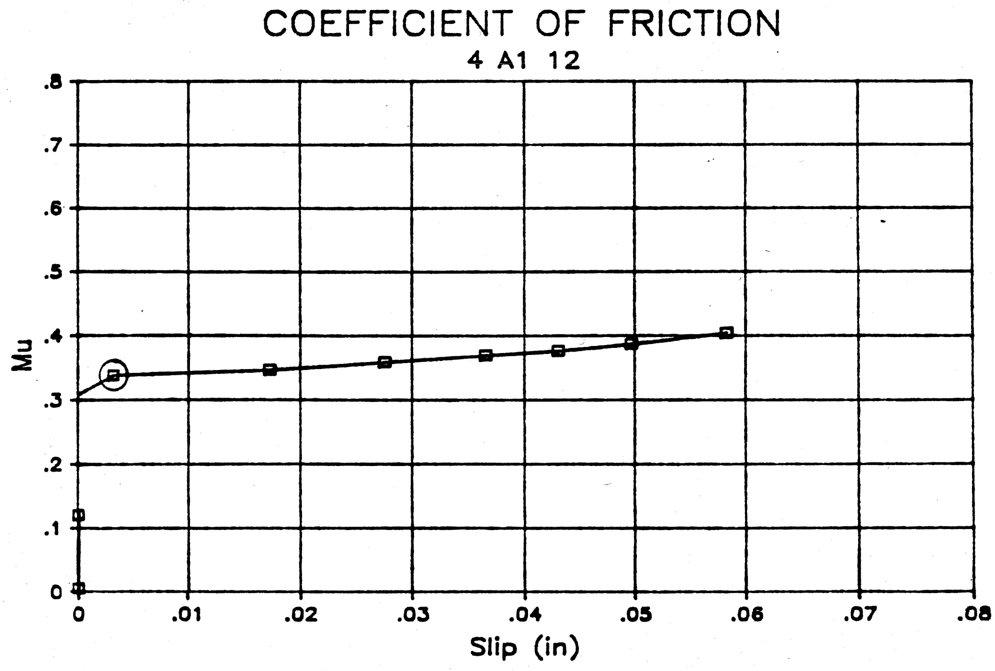
COEFFICIENT OF FRICTION
4 A1 12
Mu
.8
.7
.6
.5
.4
.3
.2
.1
0
0
.01
.02
.03
.04
.05
.06
.07
.08
Slip (in)

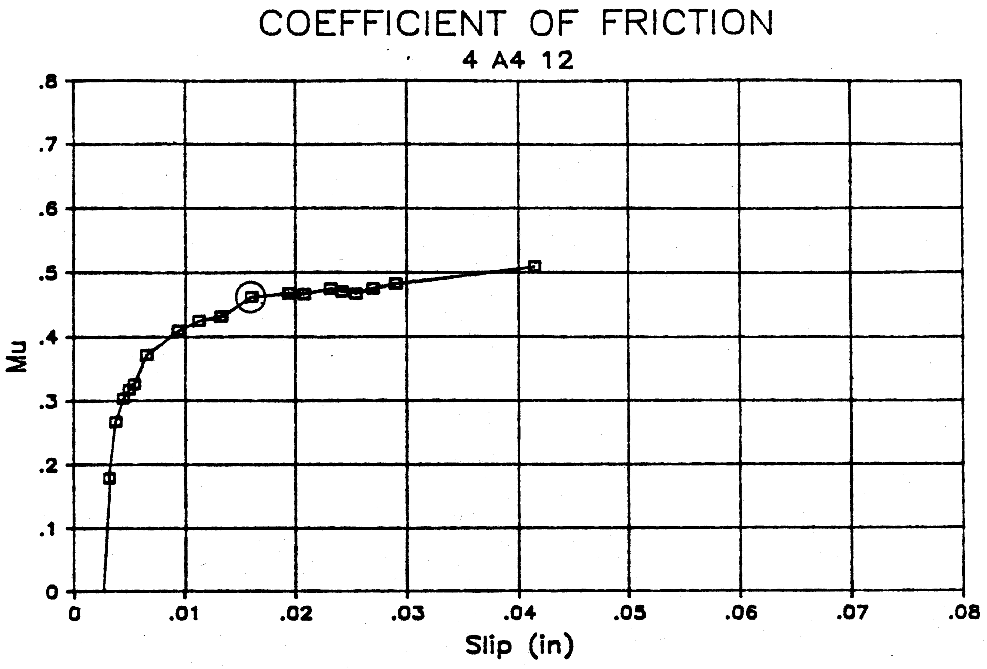
COEFFICIENT OF FRICTION
4 A4 12
Mu
.8
.7
.6
.5
.4
.3
.2
.1
0
0
.01
.02
.03
.04
.05
.06
.07
.08
Slip (in)

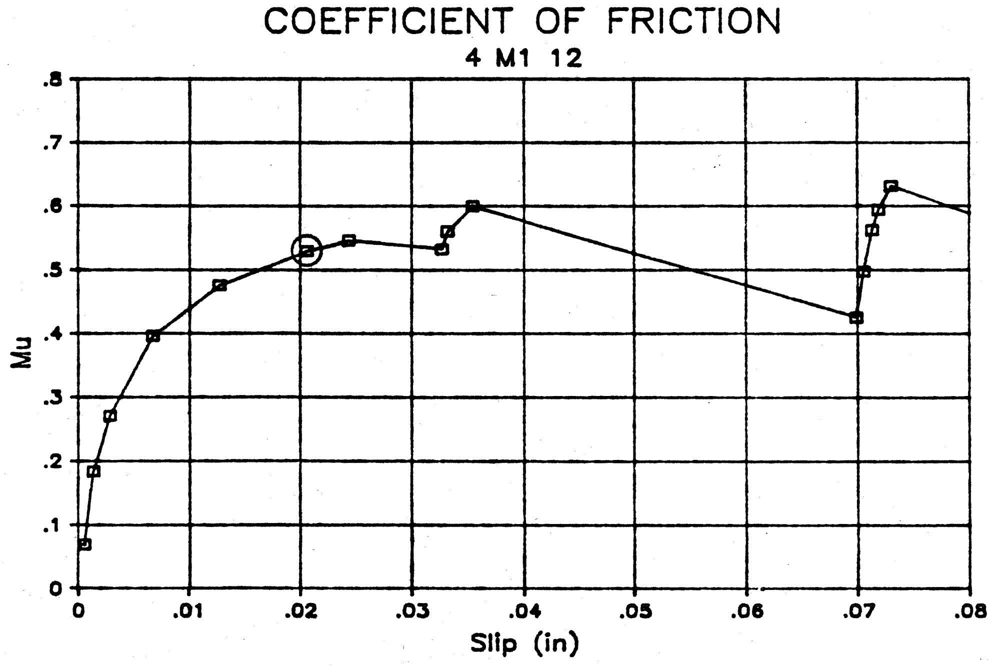
COEFFICIENT OF FRICTION
4 M1 12
Mu
.8
.7
.6
.5
.4
.3
.2
.1
0
0
.01
.02
.03
.04
.05
.06
.07
.08
Slip (in)

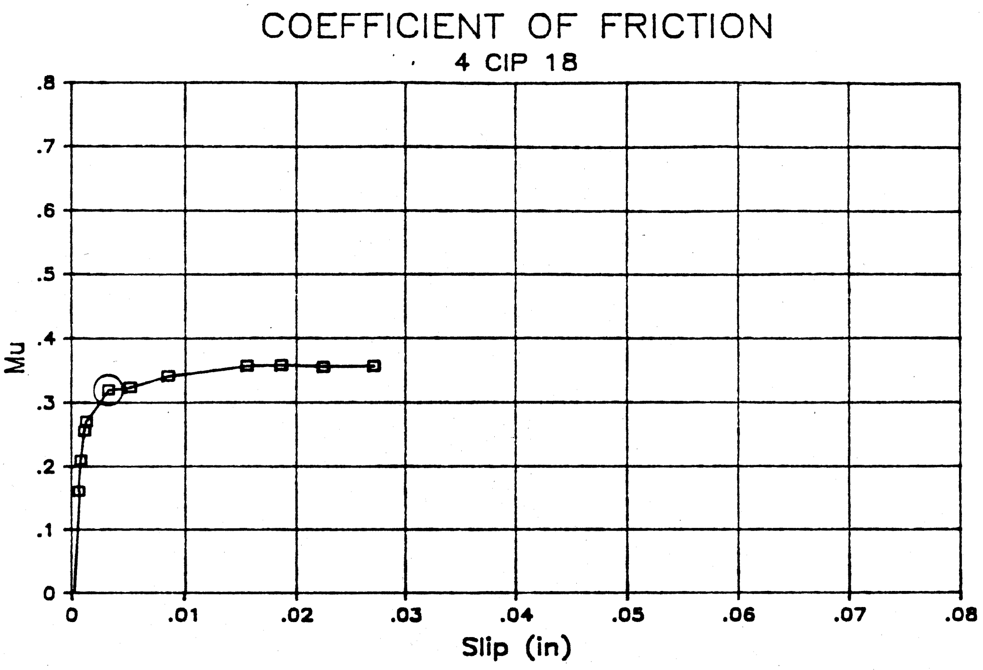
COEFFICIENT OF FRICTION
4 CIP 18
Mu
.8
.7
.6
.5
.4
.3
.2
.1
0
0
.01
.02
.03
.04
.05
.06
.07
.08
Slip (in)

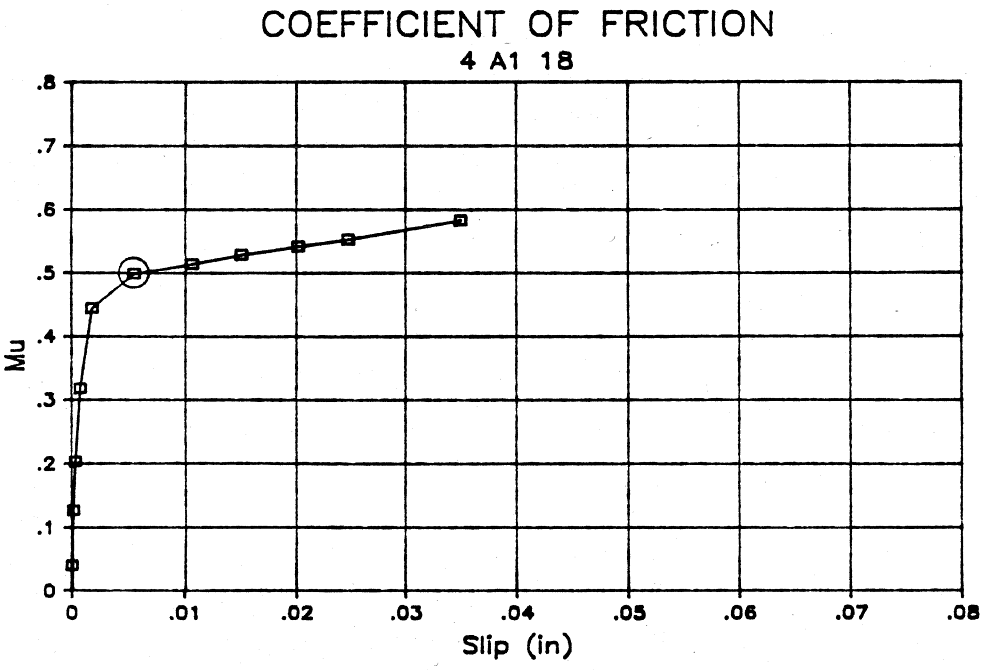
COEFFICIENT OF FRICTION
4 A1 18
Mu
.8
.7
.6
.5
.4
.3
.2
.1
0
0
.01
.02
.03
.04
.05
.06
.07
.08
Slip (in)

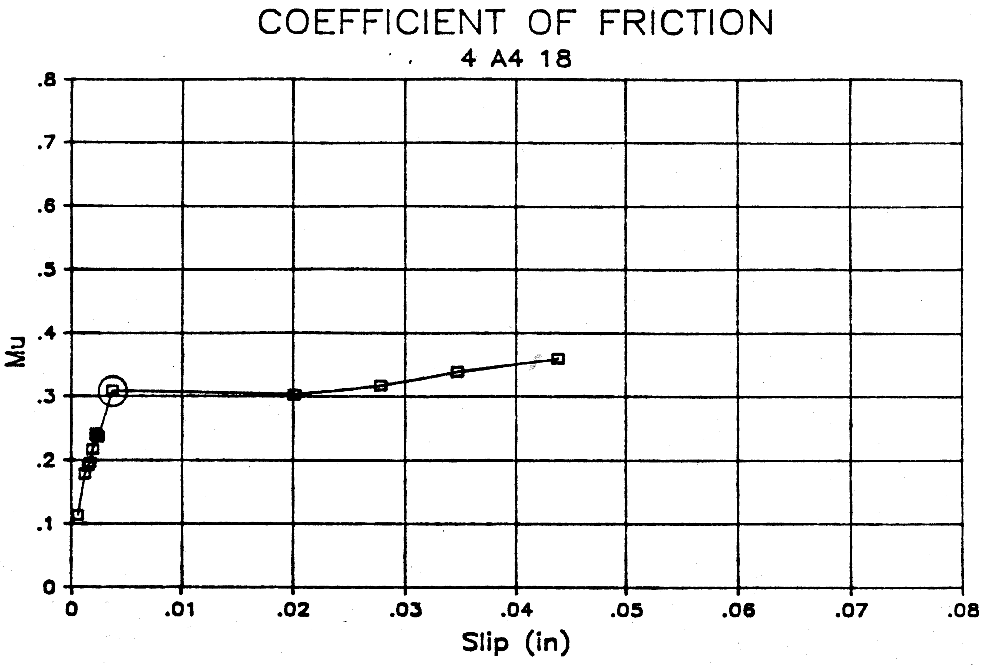
COEFFICIENT OF FRICTION
4 A4 18
Mu
Slip (in)
0
.1
.2
.3
.4
.5
.6
.7
.8
0
.01
.02
.03
.04
.05
.06
.07
.08

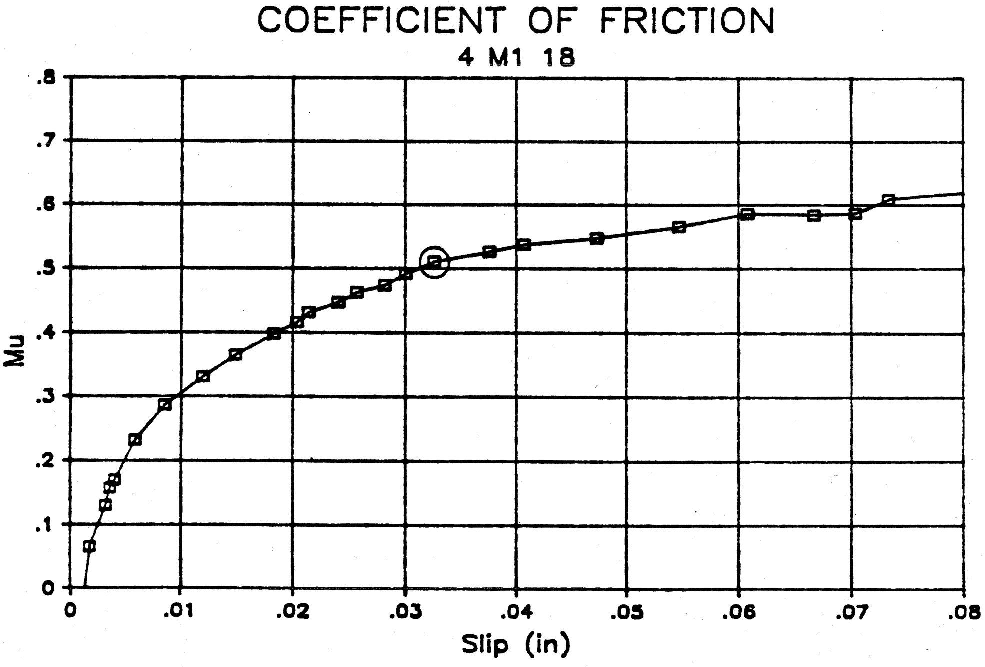
COEFFICIENT OF FRICTION
4 M1 18
Mu
Slip (in)
0
.1
.2
.3
.4
.5
.6
.7
.8
0
.01
.02
.03
.04
.05
.06
.07
.08

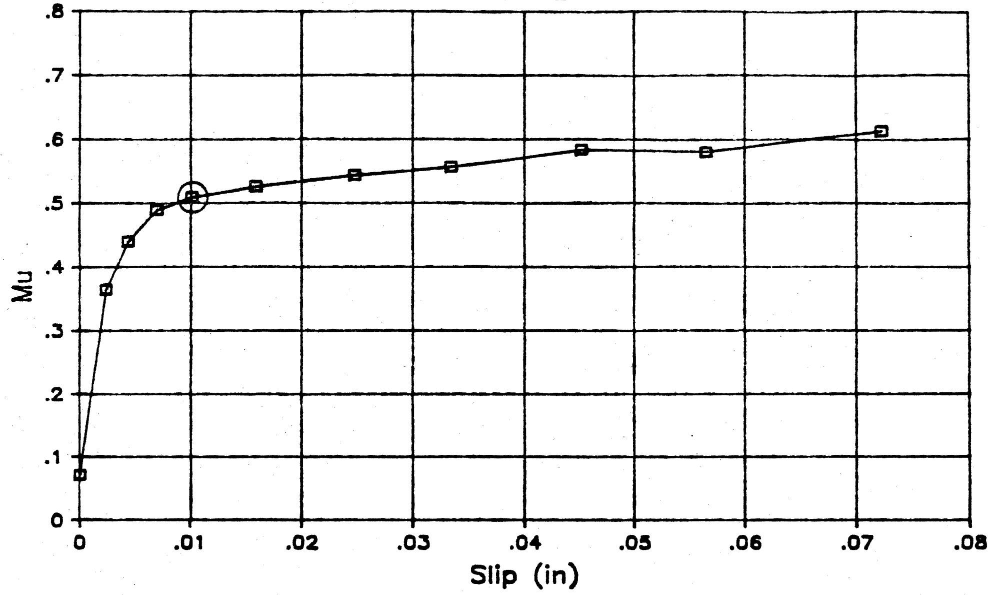
COEFFICIENT OF FRICTION
4 CIP 24

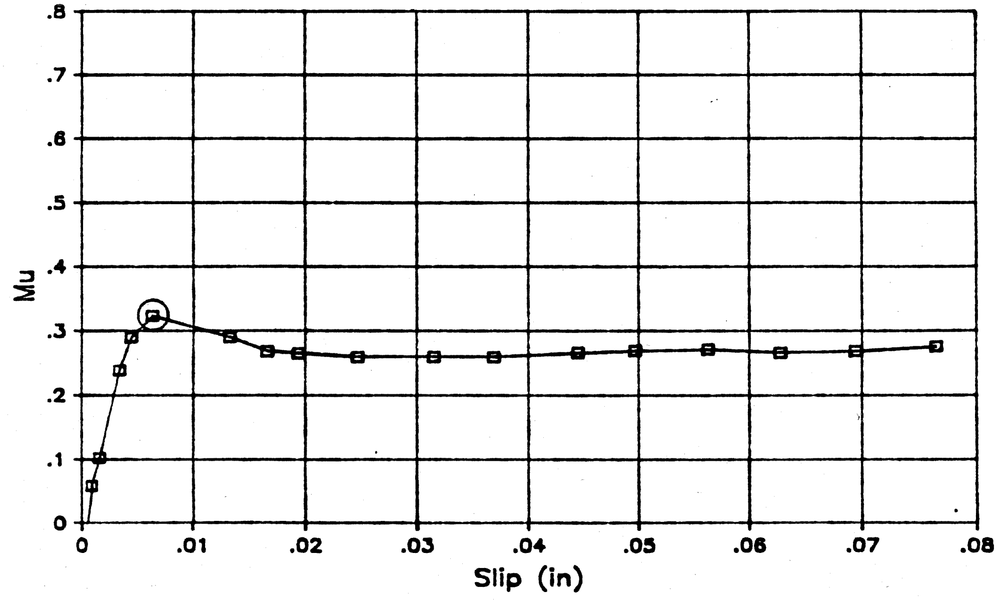
COEFFICIENT OF FRICTION
6 CIP 6

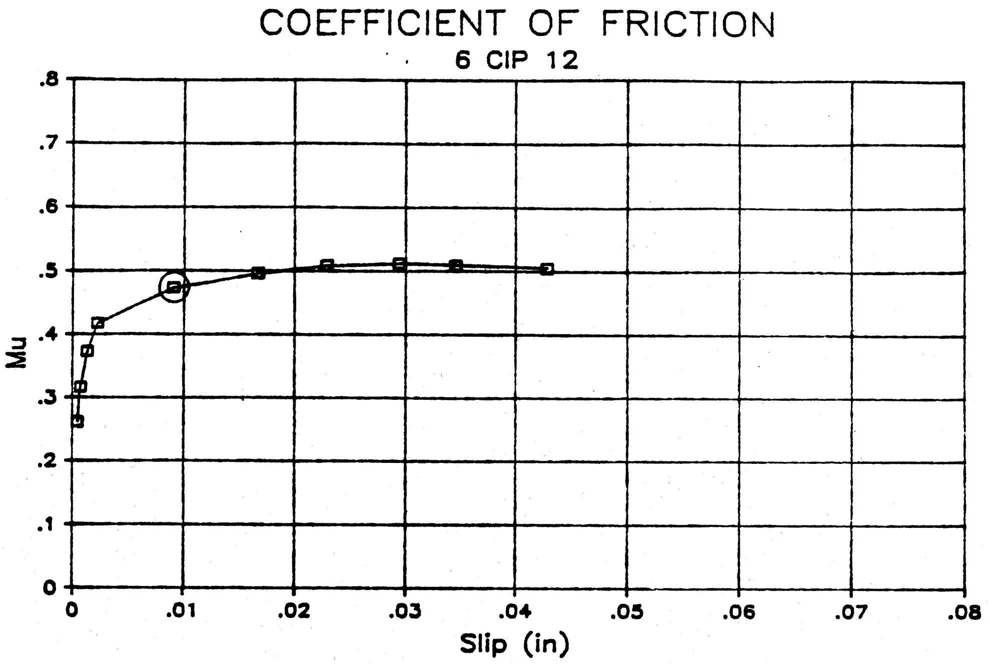
COEFFICIENT OF FRICTION
6 CIP 12
Mu
.8
.7
.6
.5
.4
.3
.2
.1
0
0
.01
.02
.03
.04
.05
.06
.07
.08
Slip (in)

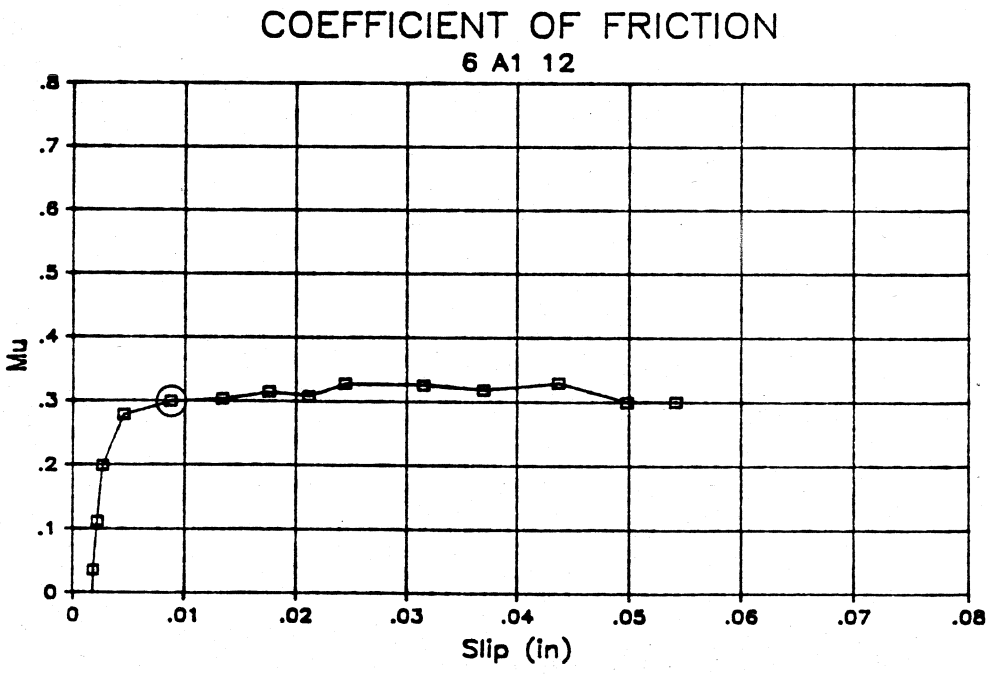
COEFFICIENT OF FRICTION
6 A1 12
Mu
.8
.7
.6
.5
.4
.3
.2
.1
0
0
.01
.02
.03
.04
.05
.06
.07
.08
Slip (in)

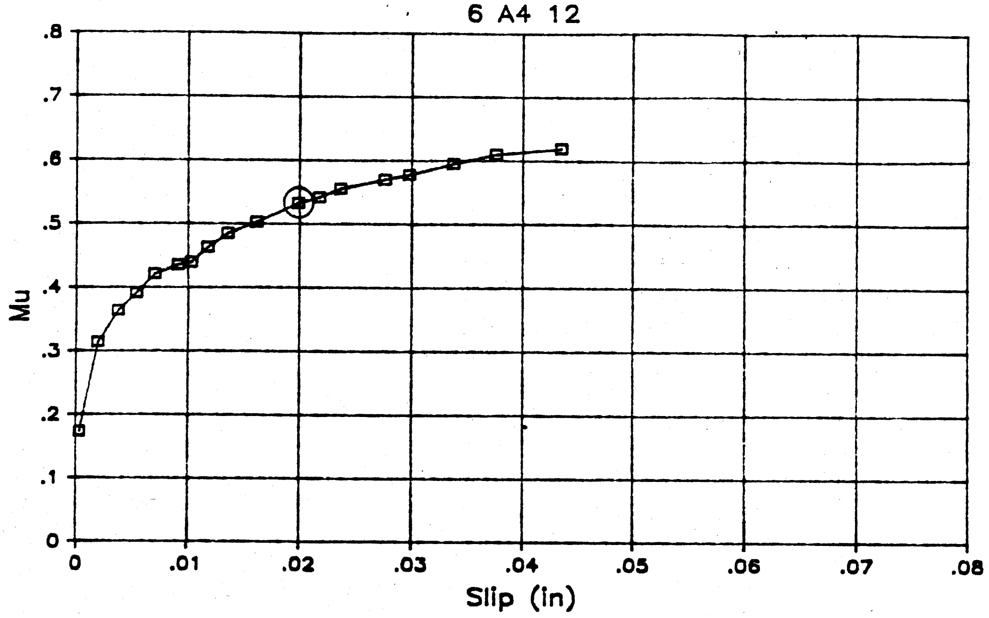

COEFFICIENT OF FRICTION

6 A4 12

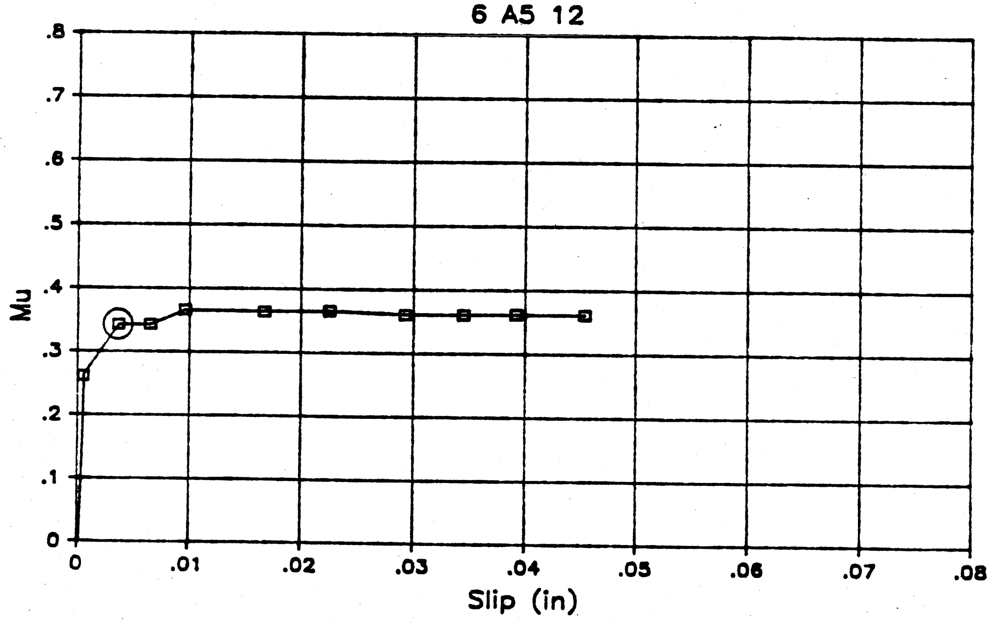

COEFFICIENT OF FRICTION

6 A5 12

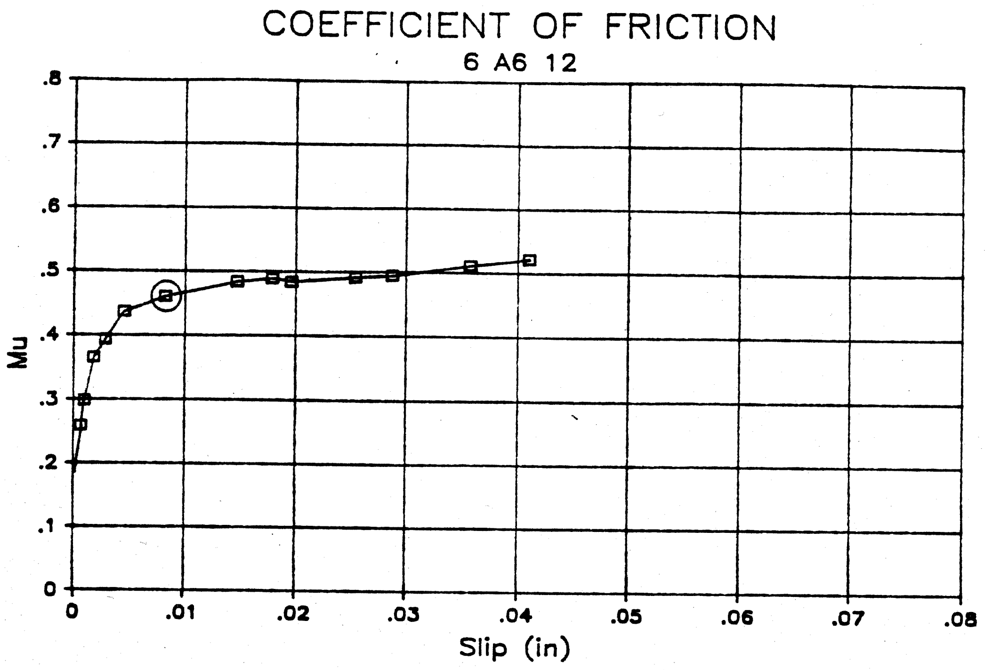
COEFFICIENT OF FRICTION
6 A6 12
Mu
.8
.7
.6
.5
.4
.3
.2
.1
0
0
.01
.02
.03
.04
.05
.06
.07
.08
Slip (in)

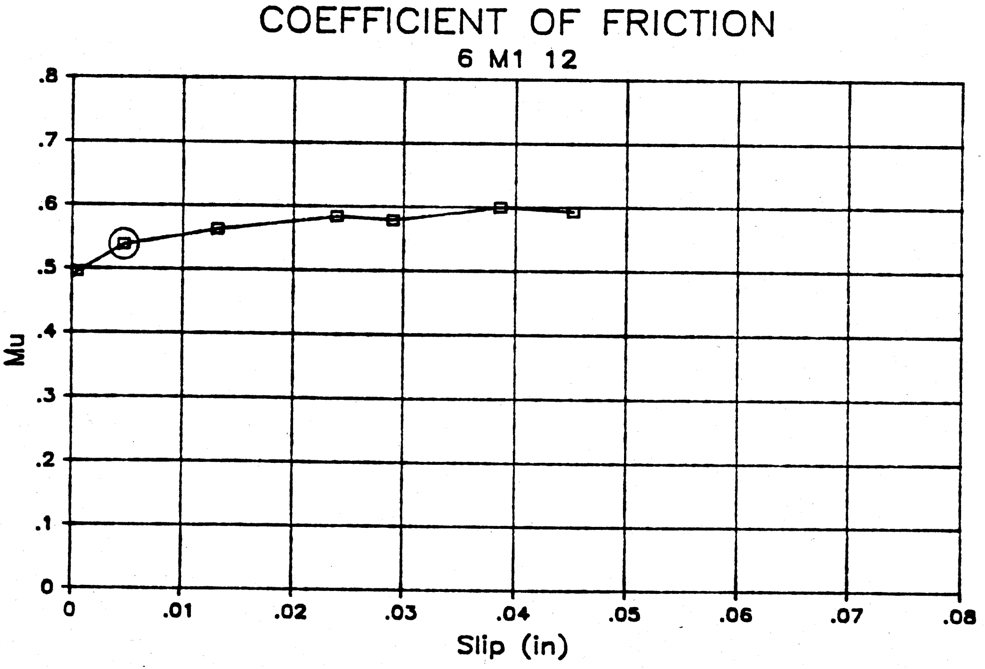
COEFFICIENT OF FRICTION
6 M1 12
Mu
.8
.7
.6
.5
.4
.3
.2
.1
0
0
.01
.02
.03
.04
.05
.06
.07
.08
Slip (in)

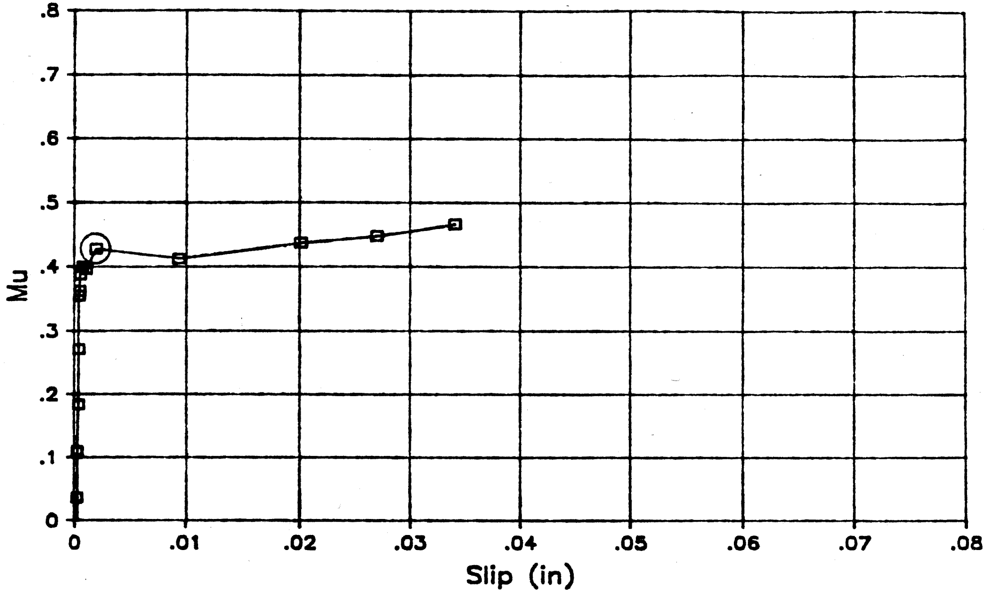

COEFFICIENT OF FRICTION
6 CIP 18

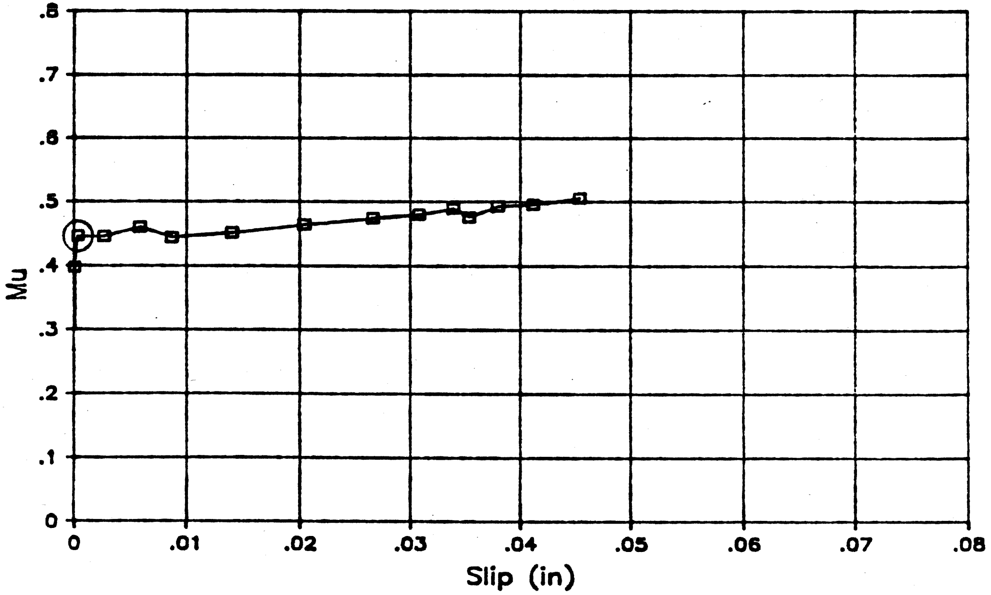

COEFFICIENT OF FRICTION
6 M1 18

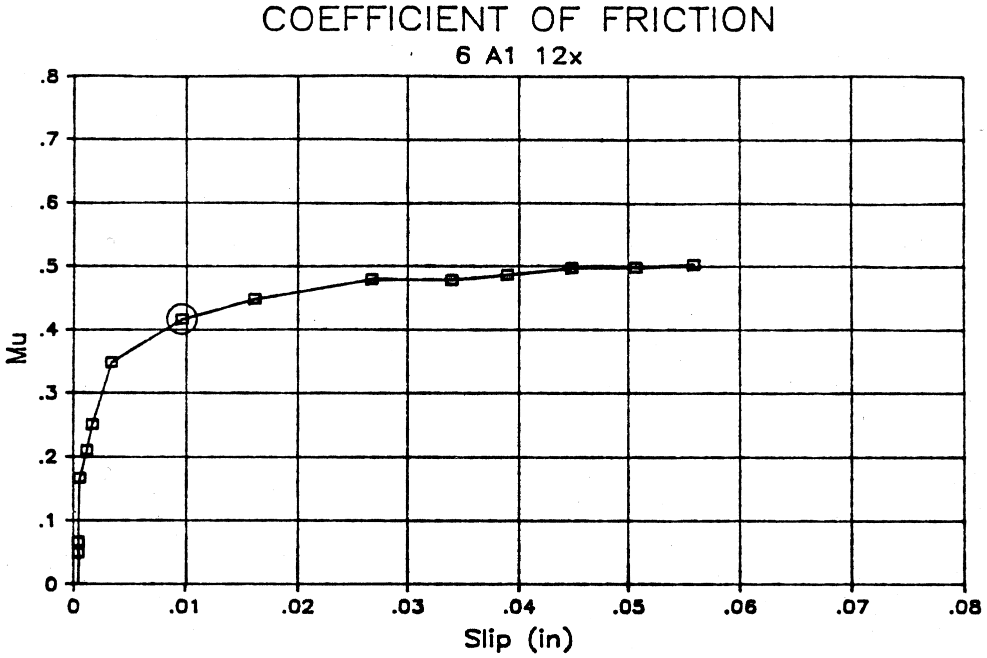
COEFFICIENT OF FRICTION
6 A1 12x
Mu
Slip (in)
0
.1
.2
.3
.4
.5
.6
.7
.8
0
.01
.02
.03
.04
.05
.06
.07
.08

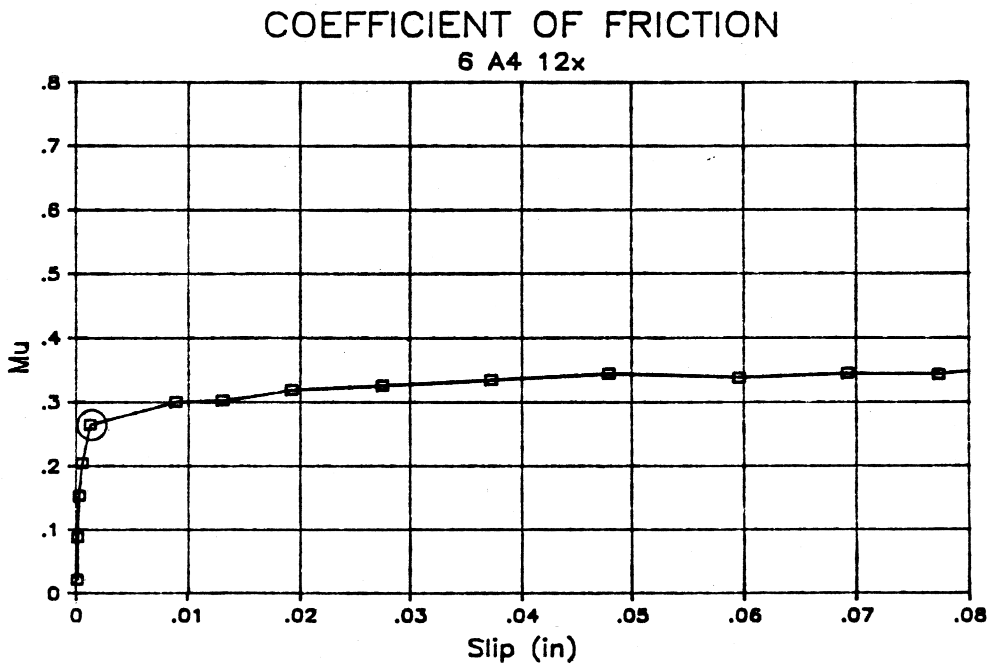
COEFFICIENT OF FRICTION
6 A4 12x
Mu
Slip (in)
0
.1
.2
.3
.4
.5
.6
.7
.8
0
.01
.02
.03
.04
.05
.06
.07
.08

APPENDIX C: GRAPHICAL RESULTS FOR ULTIMATE-LOAD TESTS

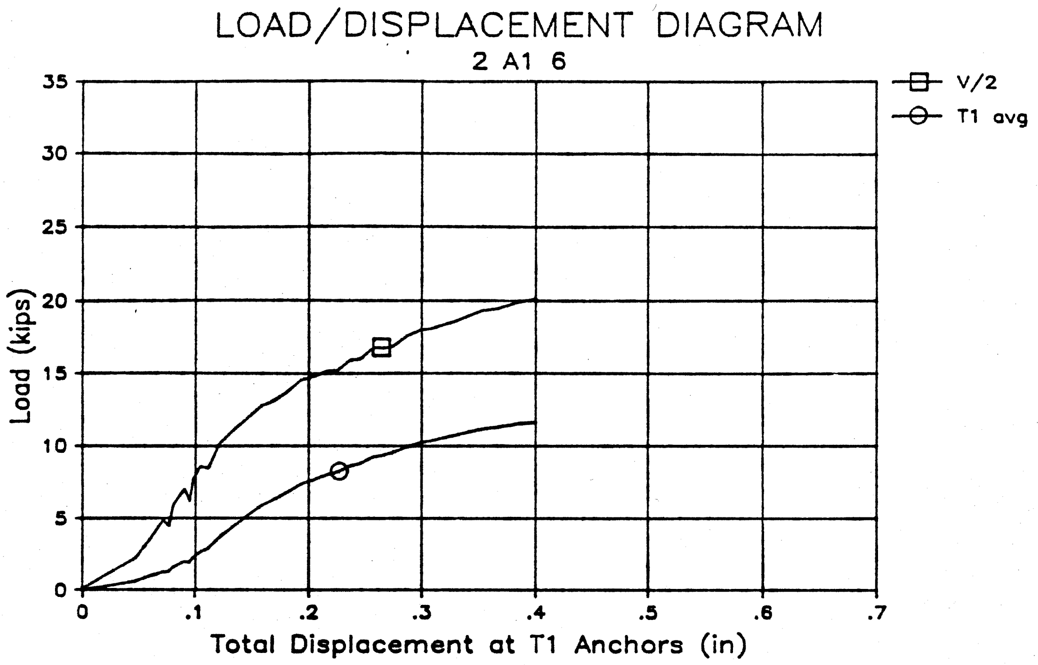
LOAD/DISPLACEMENT DIAGRAM
2 A1 6
V/2
T1 avg
Load (kips)
35
30
25
20
15
10
5
0
0
.1
.2
.3
.4
.5
.6
.7
Total Displacement at T1 Anchors (in)

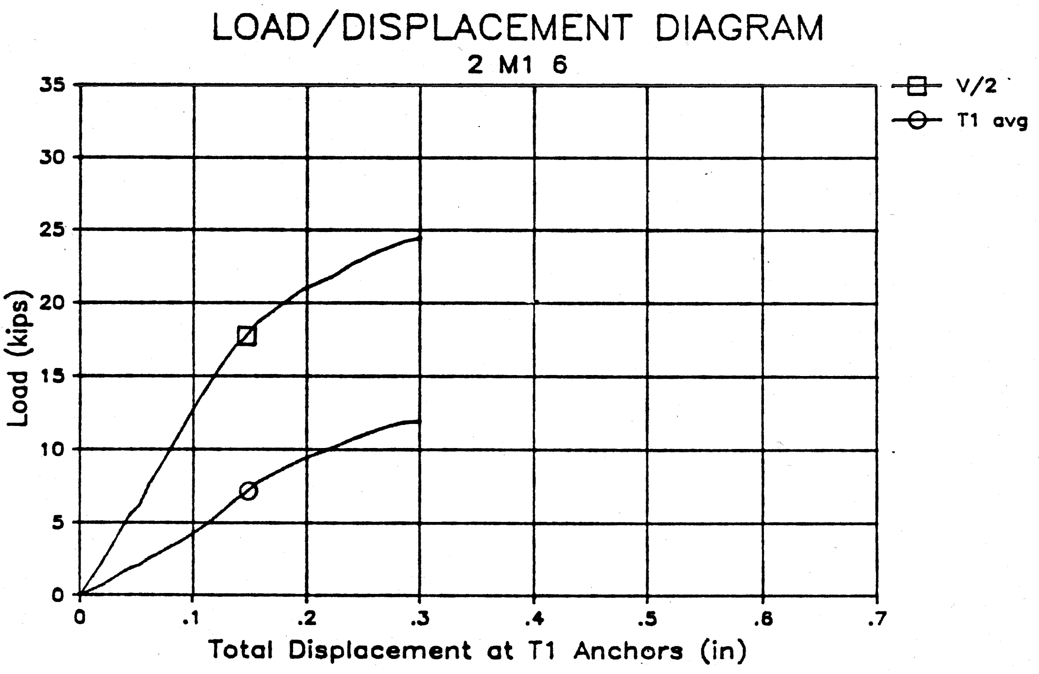
LOAD/DISPLACEMENT DIAGRAM
2 M1 6
V/2
T1 avg
Load (kips)
35
30
25
20
15
10
5
0
0
.1
.2
.3
.4
.5
.6
.7
Total Displacement at T1 Anchors (in)

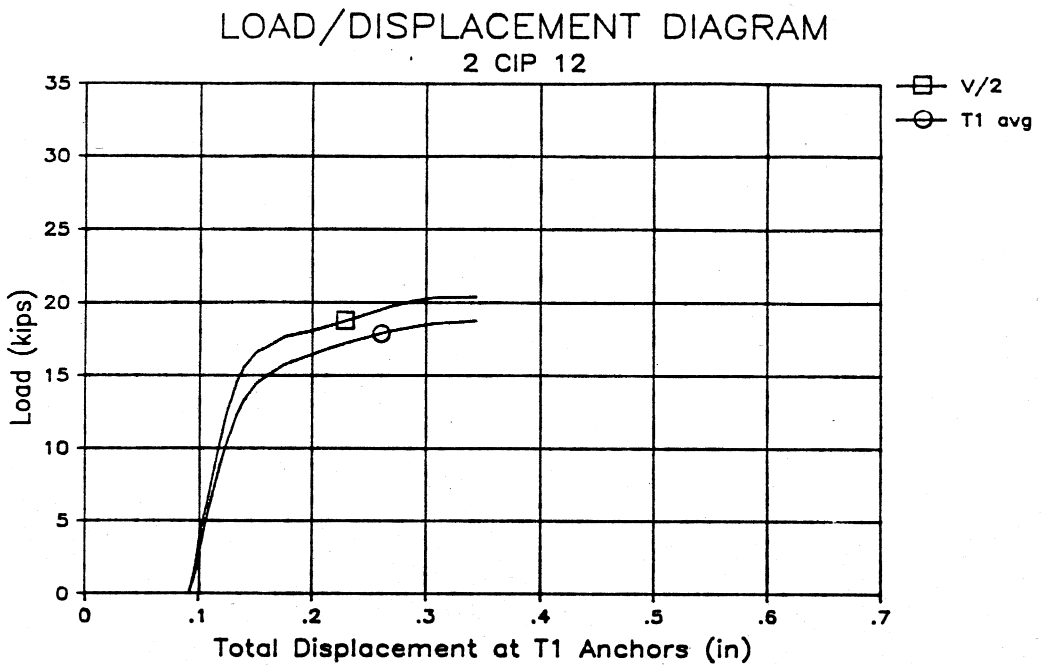
LOAD/DISPLACEMENT DIAGRAM
2 CIP 12
V/2
T1 avg
Load (kips)
0
5
10
15
20
25
30
35
0
.1
.2
.3
.4
.5
.6
.7
Total Displacement at T1 Anchors (in)

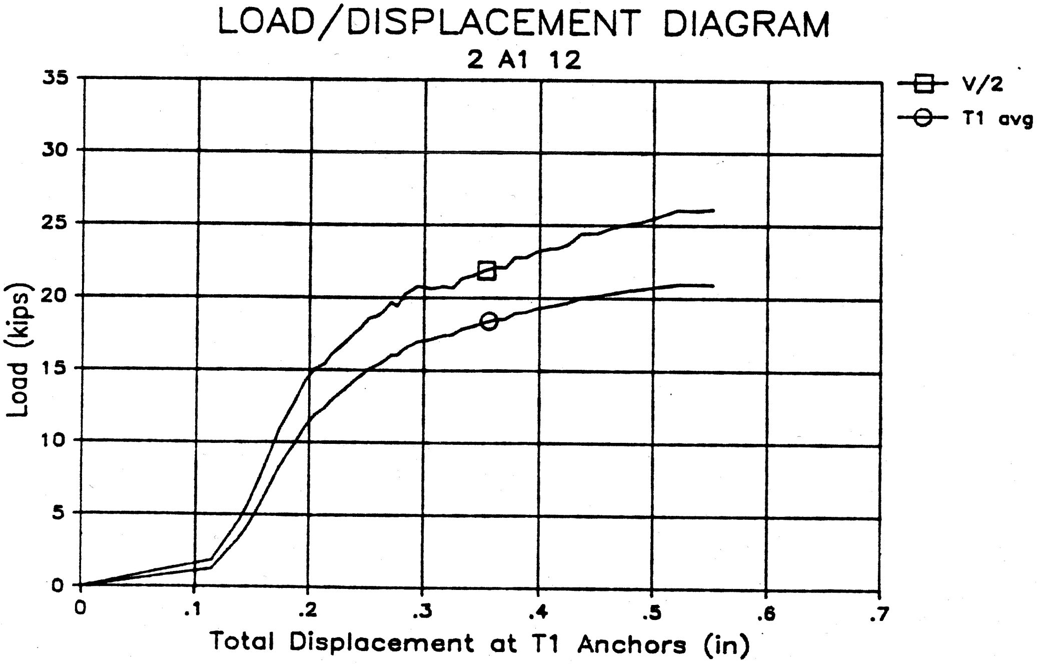
LOAD/DISPLACEMENT DIAGRAM
2 A1 12
V/2
T1 avg
Load (kips)
0
5
10
15
20
25
30
35
0
.1
.2
.3
.4
.5
.6
.7
Total Displacement at T1 Anchors (in)

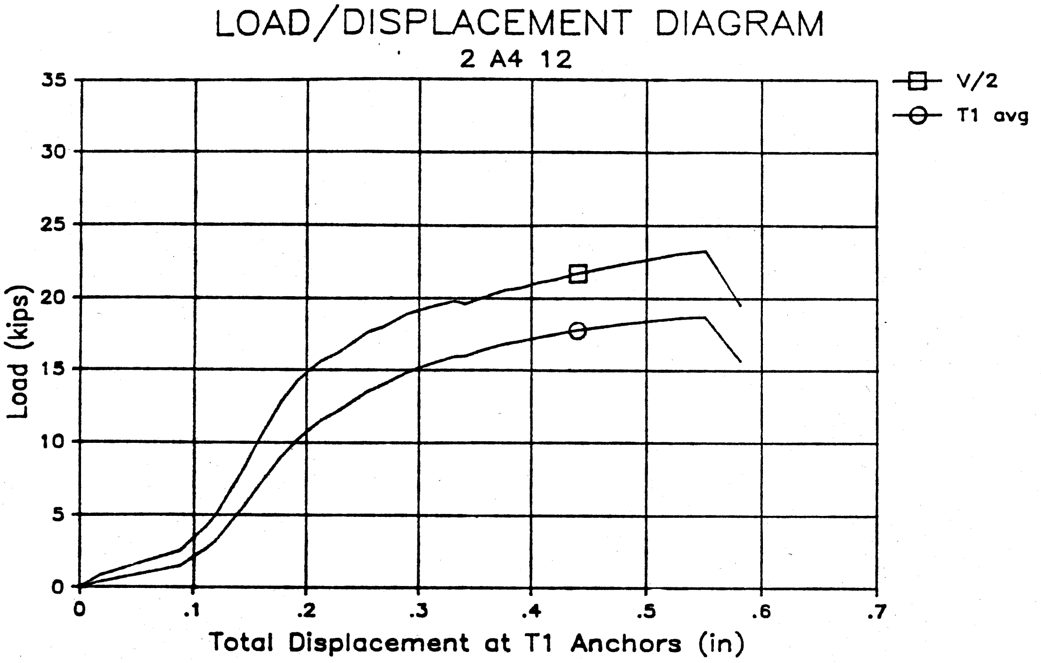
LOAD/DISPLACEMENT DIAGRAM
2 A4 12
V/2
T1 avg
Load (kips)
35
30
25
20
15
10
5
0
0
.1
.2
.3
.4
.5
.6
.7
Total Displacement at T1 Anchors (in)

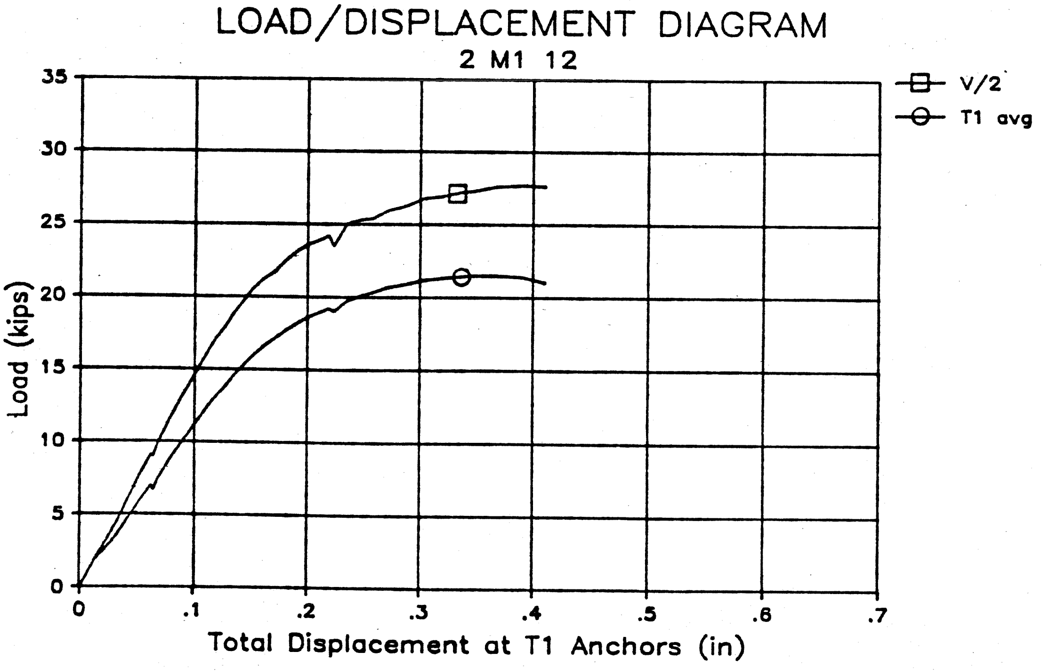
LOAD/DISPLACEMENT DIAGRAM
2 M1 12
V/2
T1 avg
Load (kips)
35
30
25
20
15
10
5
0
0
.1
.2
.3
.4
.5
.6
.7
Total Displacement at T1 Anchors (in)

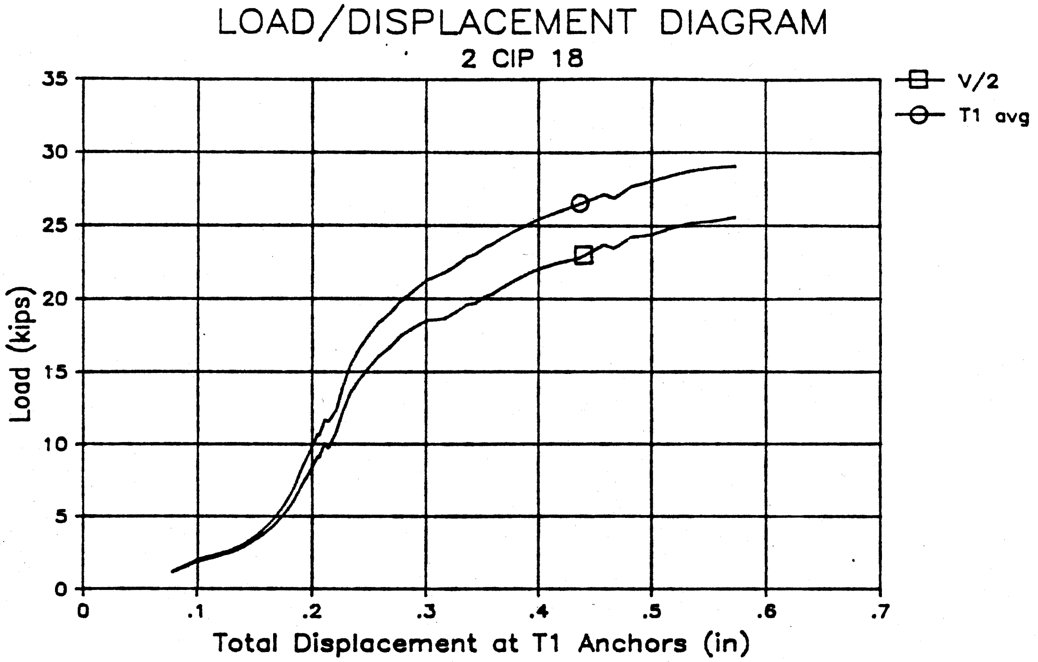
LOAD/DISPLACEMENT DIAGRAM
2 CIP 18
V/2
T1 avg
Load (kips)
35
30
25
20
15
10
5
0
0
.1
.2
.3
.4
.5
.6
.7
Total Displacement at T1 Anchors (in)

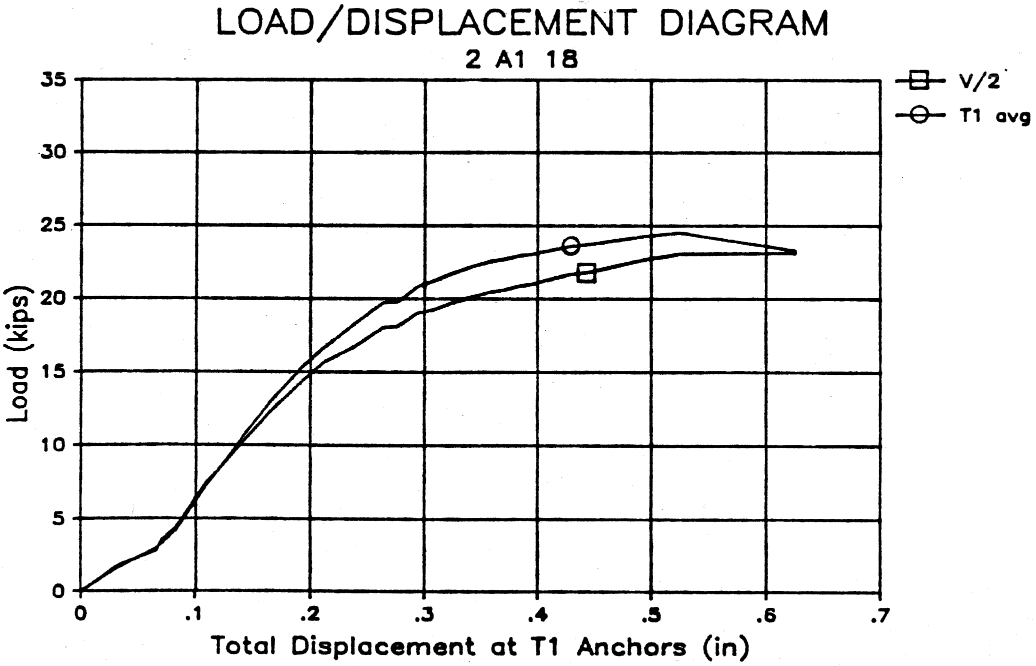
LOAD/DISPLACEMENT DIAGRAM
2 A1 18
V/2
T1 avg
Load (kips)
35
30
25
20
15
10
5
0
0
.1
.2
.3
.4
.5
.6
.7
Total Displacement at T1 Anchors (in)

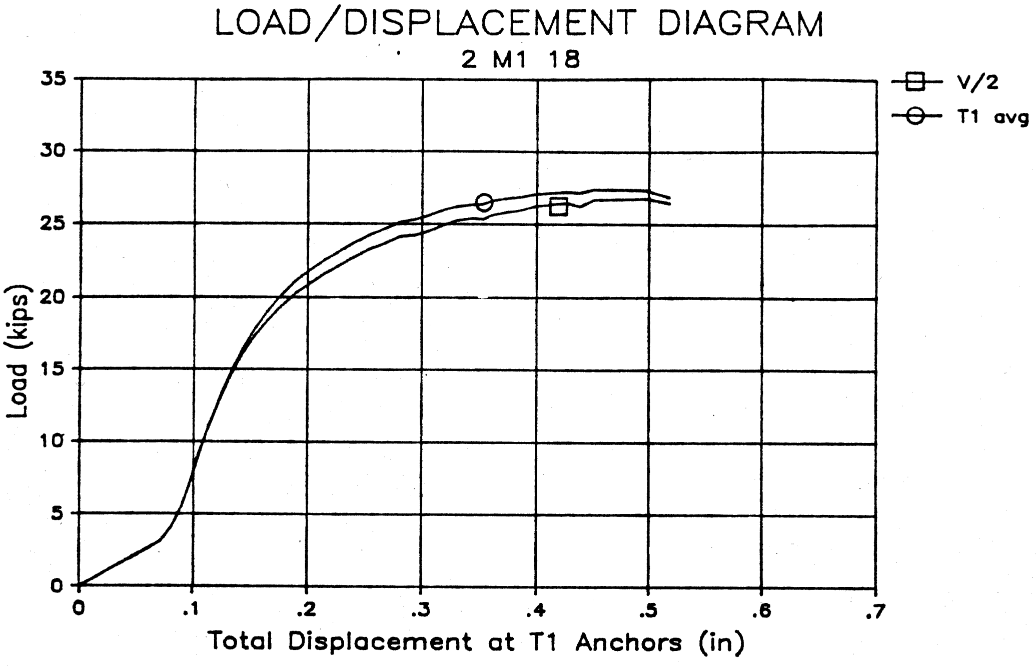
LOAD/DISPLACEMENT DIAGRAM
2 M1 18
V/2
T1 avg
Load (kips)
35
30
25
20
15
10
5
0
0
.1
.2
.3
.4
.5
.6
.7
Total Displacement at T1 Anchors (in)

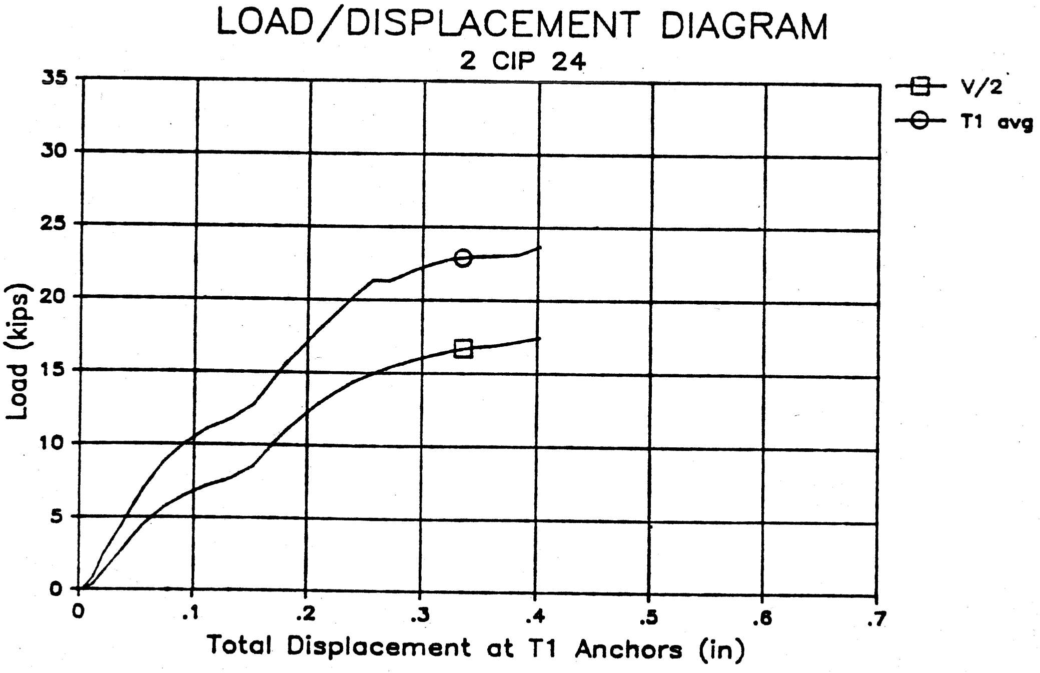
LOAD/DISPLACEMENT DIAGRAM
2 CIP 24
V/2
T1 avg
Load (kips)
35
30
25
20
15
10
5
0
0
.1
.2
.3
.4
.5
.6
.7
Total Displacement at T1 Anchors (in)

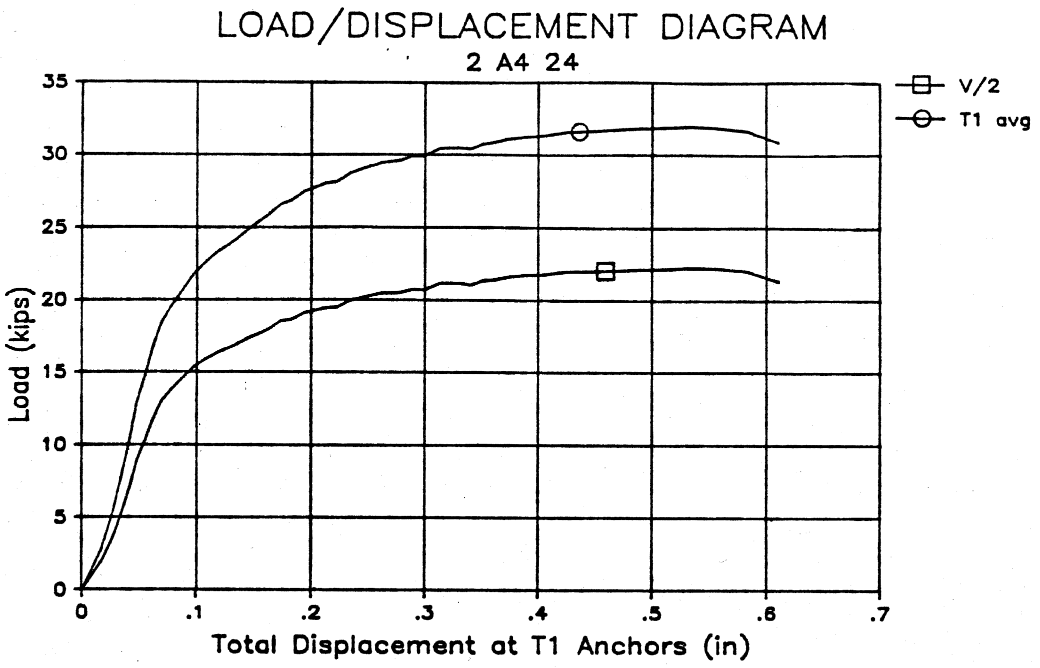
LOAD/DISPLACEMENT DIAGRAM
2 A4 24
V/2
T1 avg
Load (kips)
0
5
10
15
20
25
30
35
Total Displacement at T1 Anchors (in)
0
.1
.2
.3
.4
.5
.6
.7

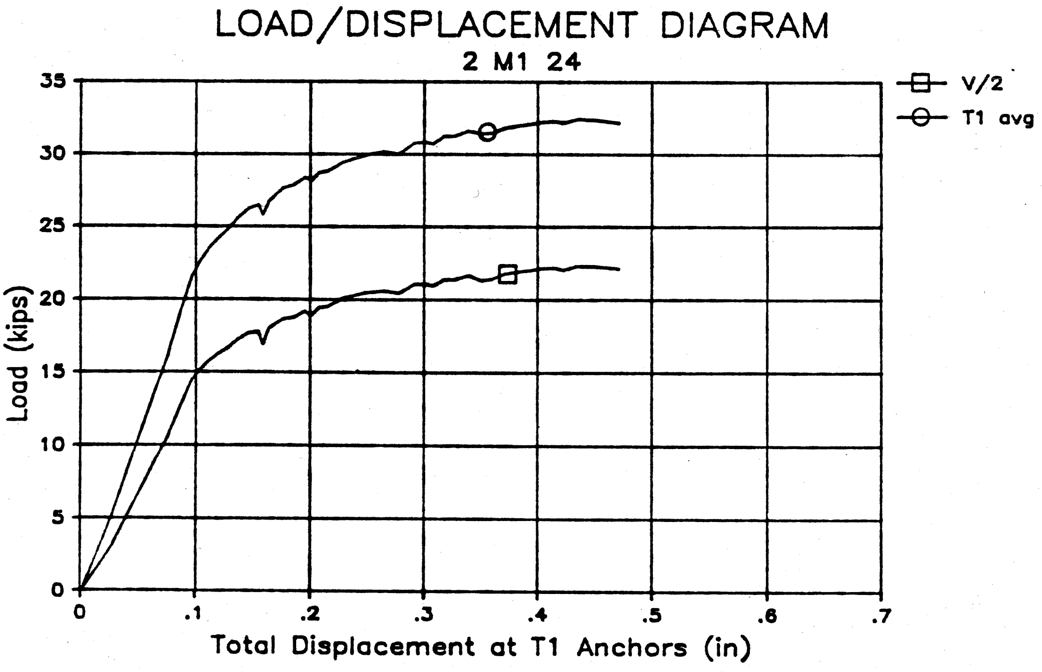
LOAD/DISPLACEMENT DIAGRAM
2 M1 24
V/2
T1 avg
Load (kips)
0
5
10
15
20
25
30
35
Total Displacement at T1 Anchors (in)
0
.1
.2
.3
.4
.5
.6
.7

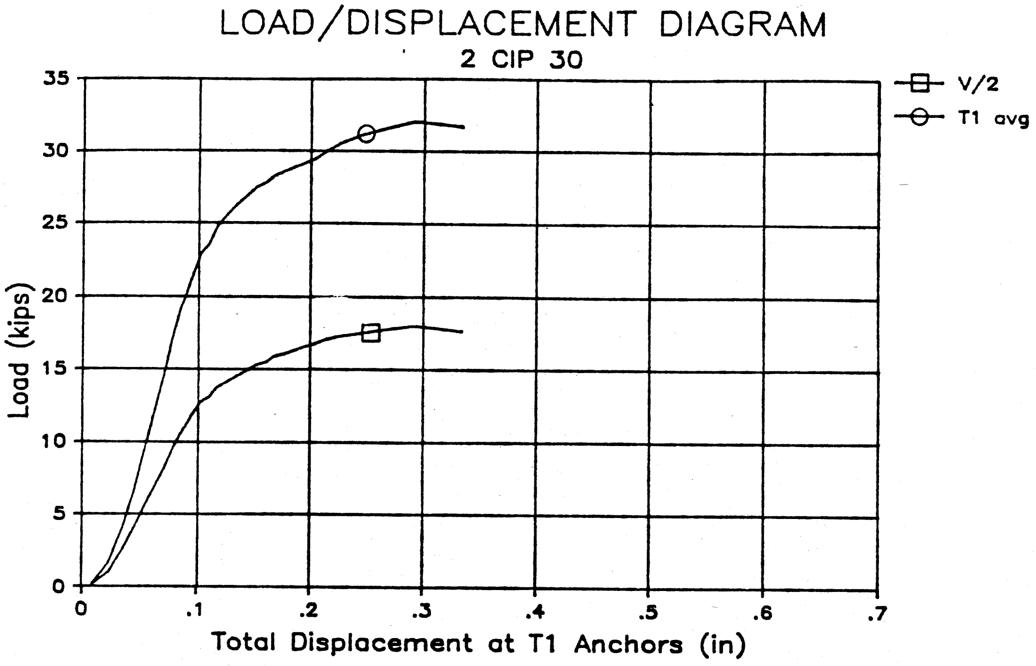
LOAD/DISPLACEMENT DIAGRAM
2 CIP 30
V/2
T1 avg
Load (kips)
35
30
25
20
15
10
5
0
0
.1
.2
.3
.4
.5
.6
.7
Total Displacement at T1 Anchors (in)

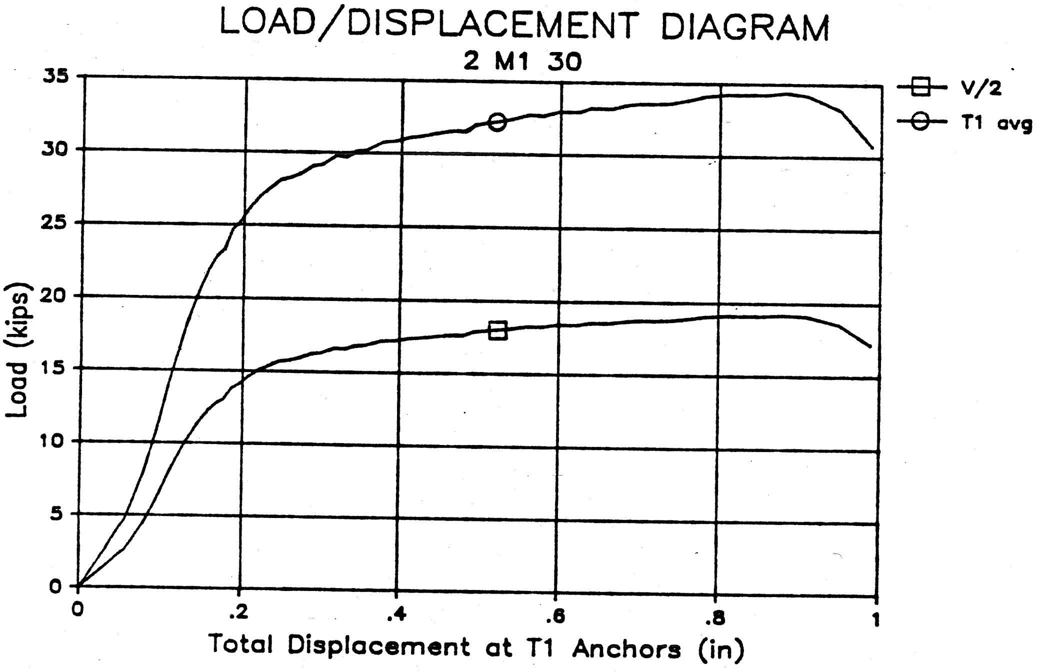
LOAD/DISPLACEMENT DIAGRAM
2 M1 30
V/2
T1 avg
Load (kips)
35
30
25
20
15
10
5
0
0
.2
.4
.6
.8
1
Total Displacement at T1 Anchors (in)

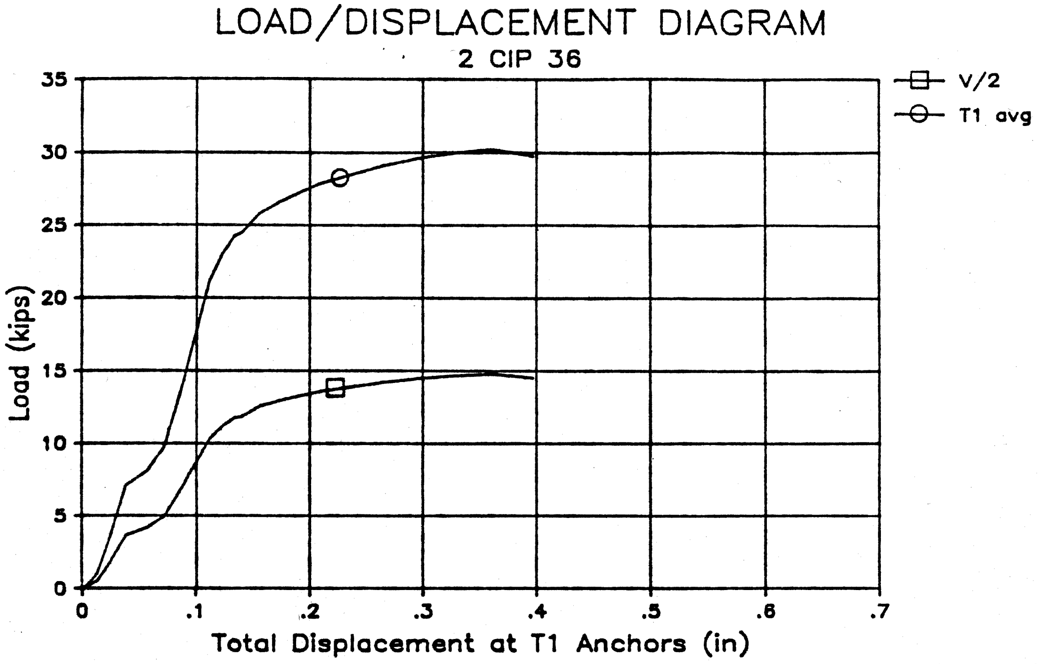
LOAD/DISPLACEMENT DIAGRAM
2 CIP 36
V/2
T1 avg
Load (kips)
0
5
10
15
20
25
30
35
Total Displacement at T1 Anchors (in)
0
.1
.2
.3
.4
.5
.6
.7

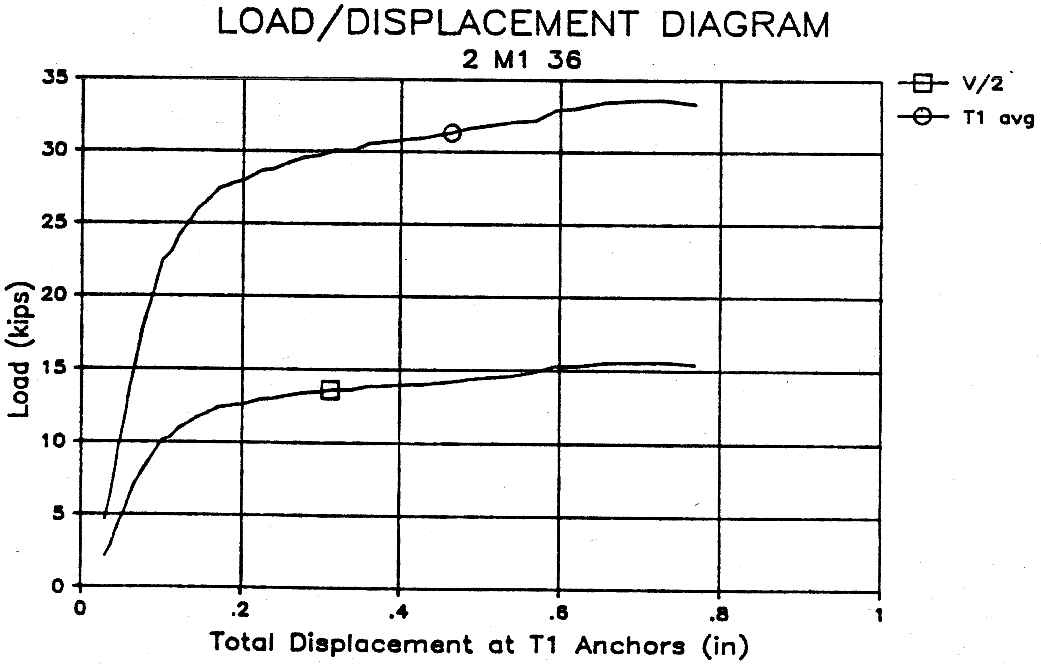
LOAD/DISPLACEMENT DIAGRAM
2 M1 36
V/2
T1 avg
Load (kips)
0
5
10
15
20
25
30
35
Total Displacement at T1 Anchors (in)
0
.2
.4
.6
.8
1

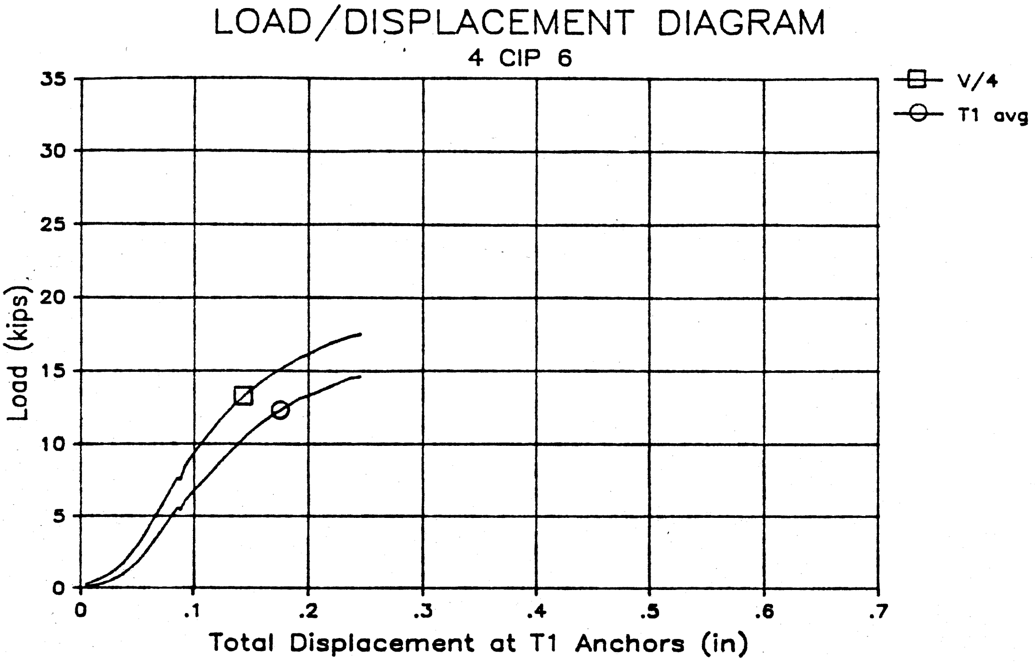
LOAD/DISPLACEMENT DIAGRAM
4 CIP 6
V/4
T1 avg
Load (kips)
0
5
10
15
20
25
30
35
0
.1
.2
.3
.4
.5
.6
.7
Total Displacement at T1 Anchors (in)

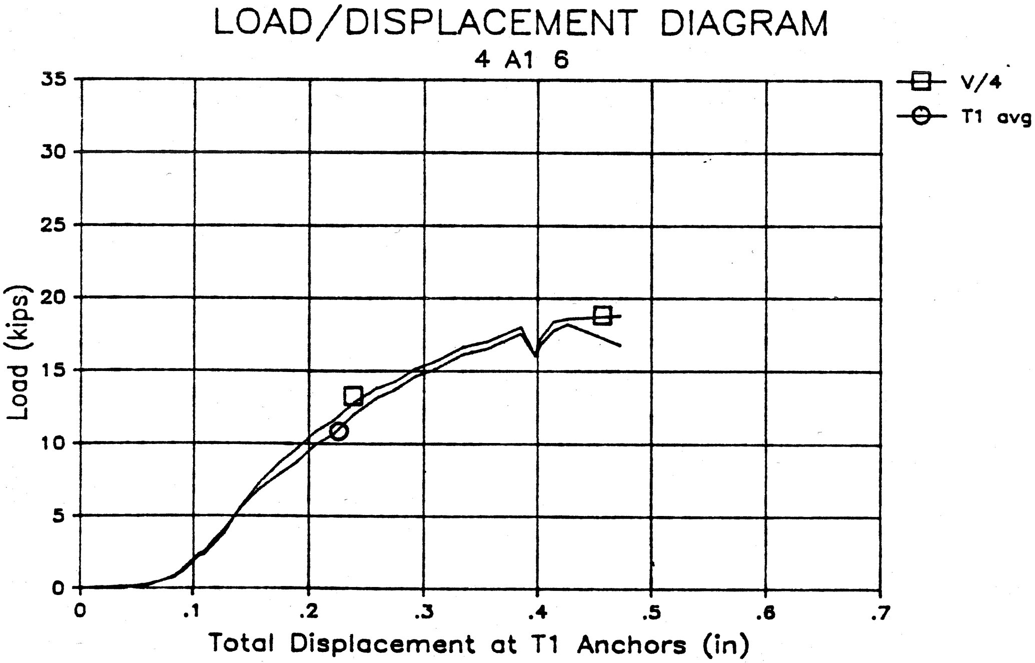
LOAD/DISPLACEMENT DIAGRAM
4 A1 6
V/4
T1 avg
Load (kips)
0
5
10
15
20
25
30
35
0
.1
.2
.3
.4
.5
.6
.7
Total Displacement at T1 Anchors (in)

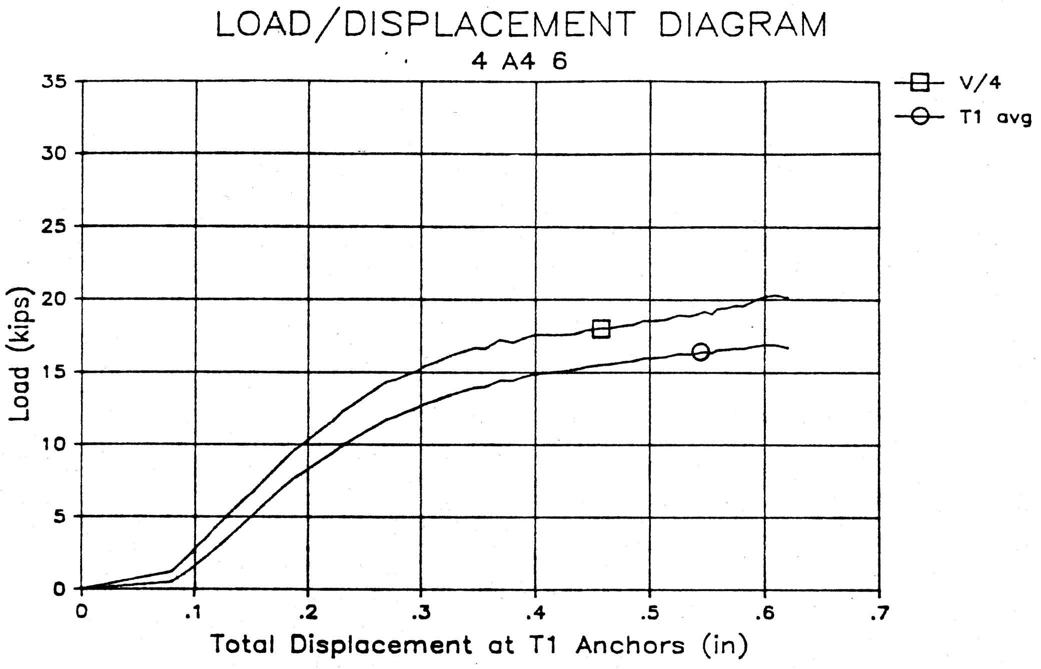
LOAD/DISPLACEMENT DIAGRAM
4 A4 6
V/4
T1 avg
Load (kips)
0
5
10
15
20
25
30
35
0
.1
.2
.3
.4
.5
.6
.7
Total Displacement at T1 Anchors (in)

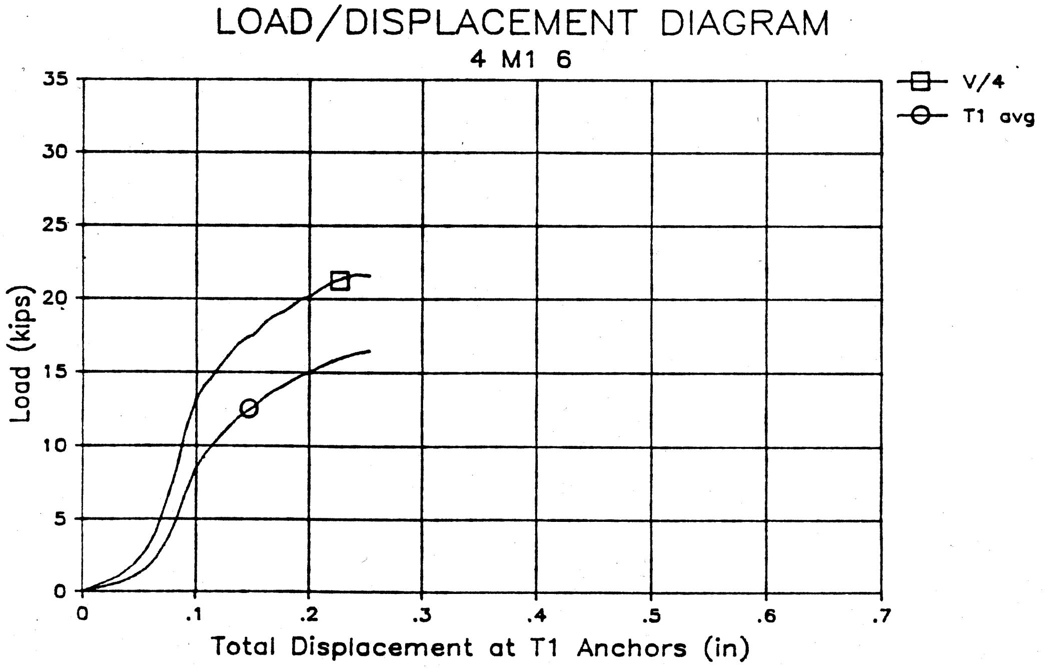
LOAD/DISPLACEMENT DIAGRAM
4 M1 6
V/4
T1 avg
Load (kips)
0
5
10
15
20
25
30
35
0
.1
.2
.3
.4
.5
.6
.7
Total Displacement at T1 Anchors (in)

LOAD/DISPLACEMENT DIAGRAM

4 CIP 12

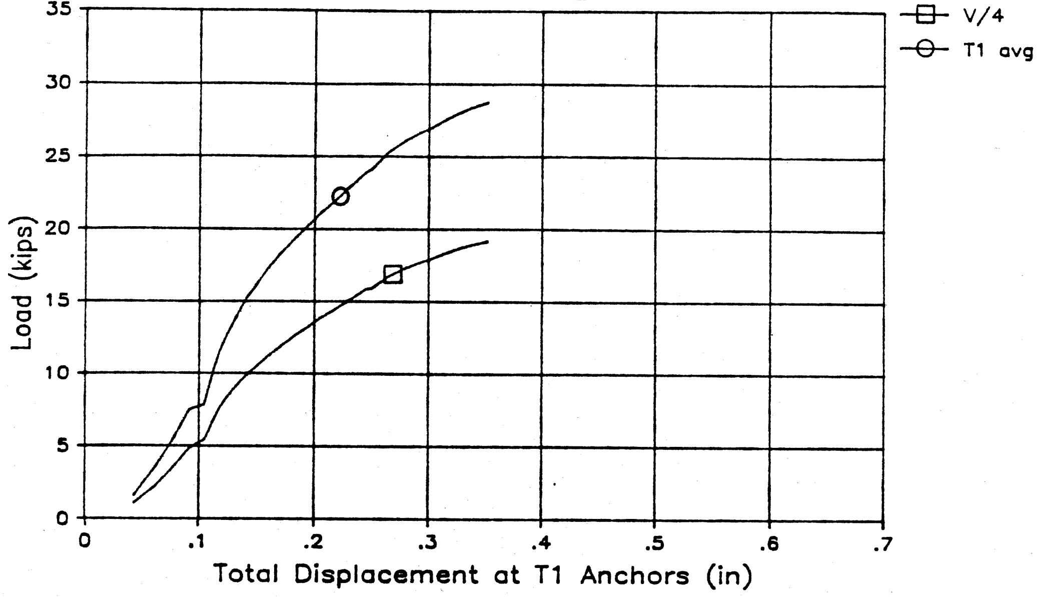

LOAD/DISPLACEMENT DIAGRAM

4 A1 12

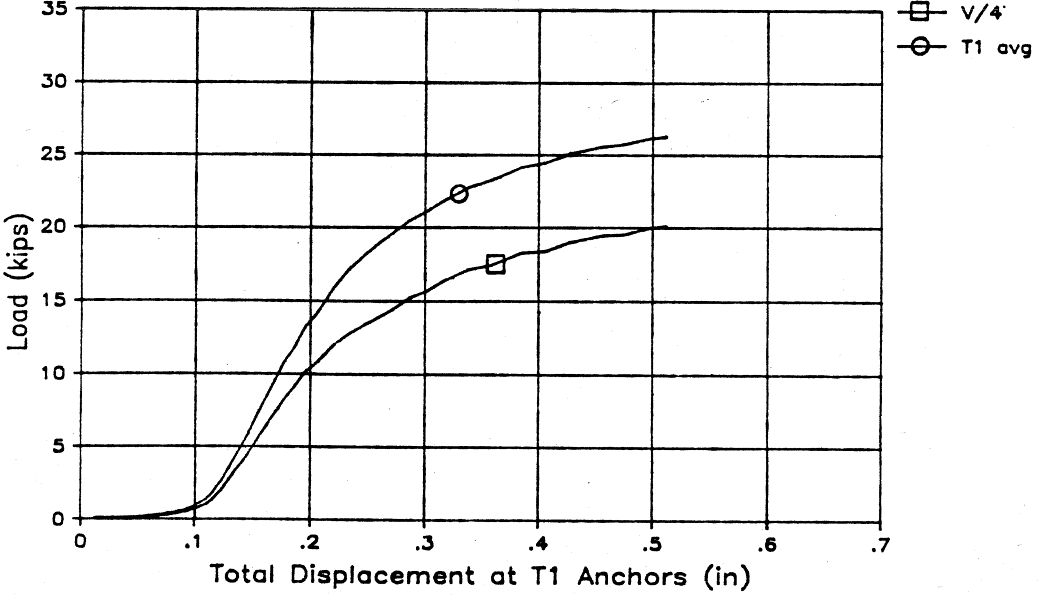

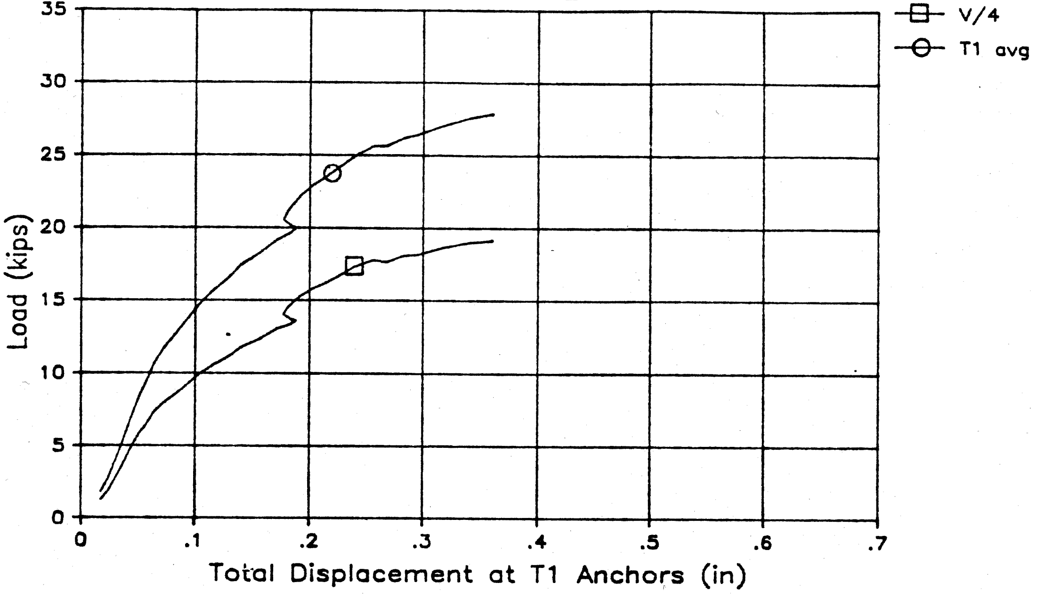

LOAD/DISPLACEMENT DIAGRAM
4 A4 12

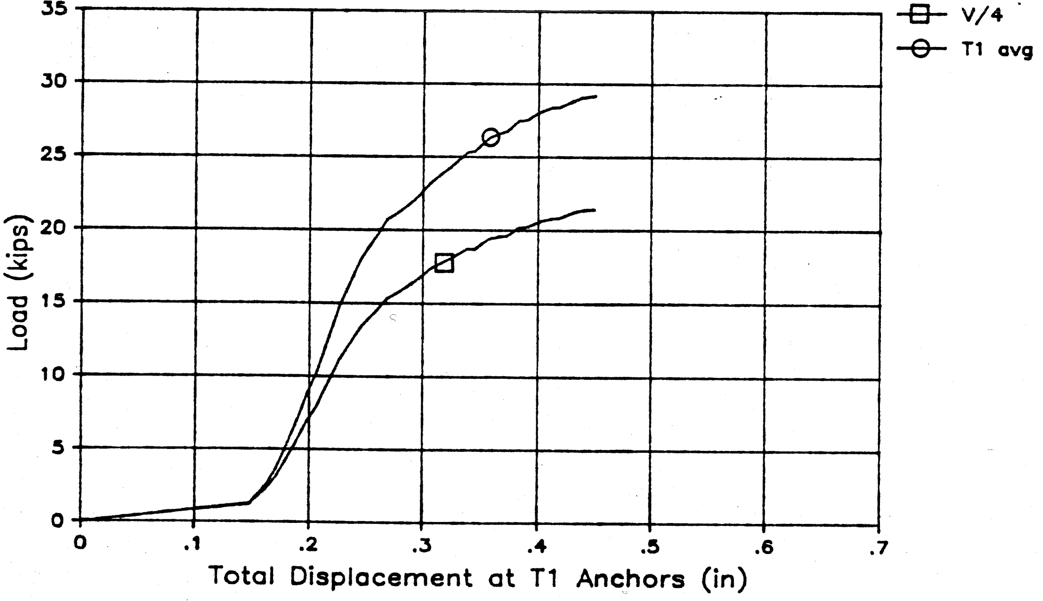

LOAD/DISPLACEMENT DIAGRAM
4 M1 12

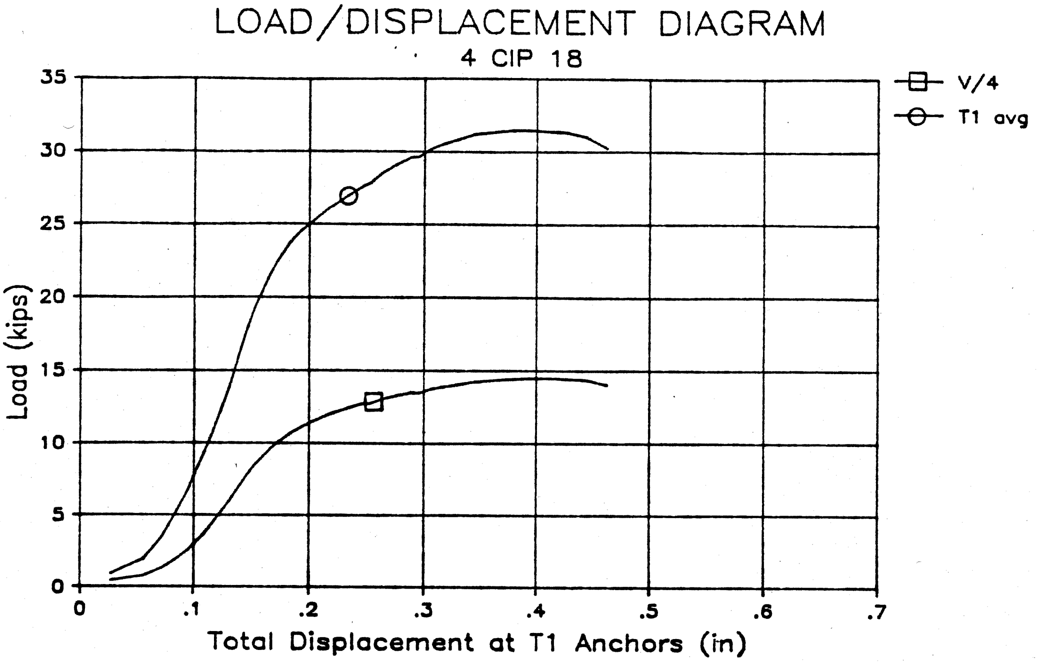
LOAD/DISPLACEMENT DIAGRAM
4 CIP 18
V/4
T1 avg
Load (kips)
35
30
25
20
15
10
5
0
0
.1
.2
.3
.4
.5
.6
.7
Total Displacement at T1 Anchors (in)

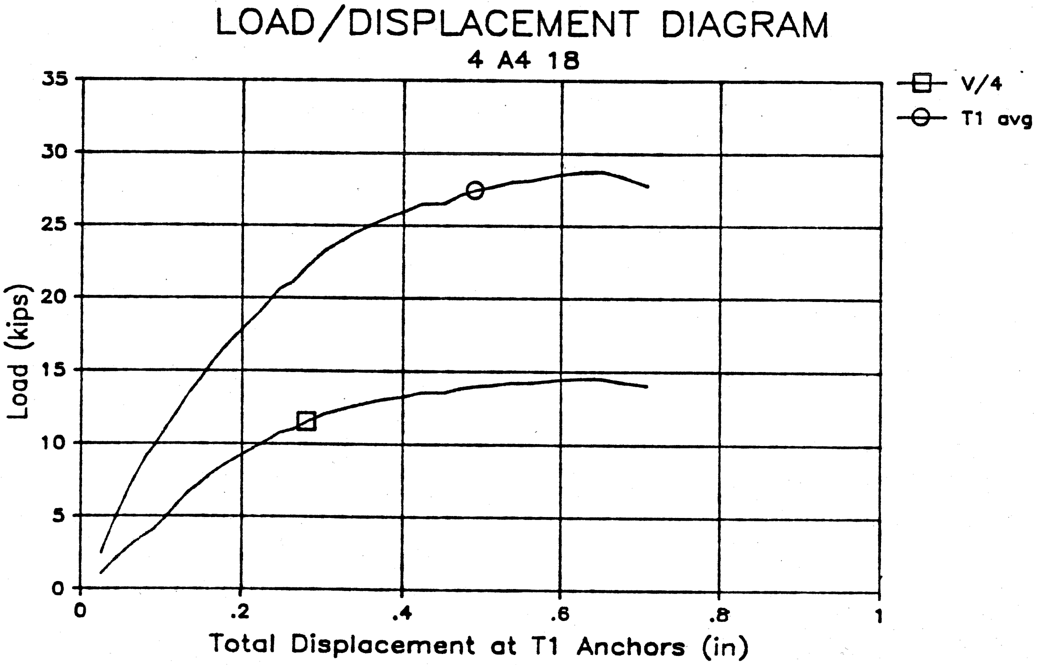
LOAD/DISPLACEMENT DIAGRAM
4 A4 18
V/4
T1 avg
Load (kips)
35
30
25
20
15
10
5
0
0
.2
.4
.6
.8
1
Total Displacement at T1 Anchors (in)

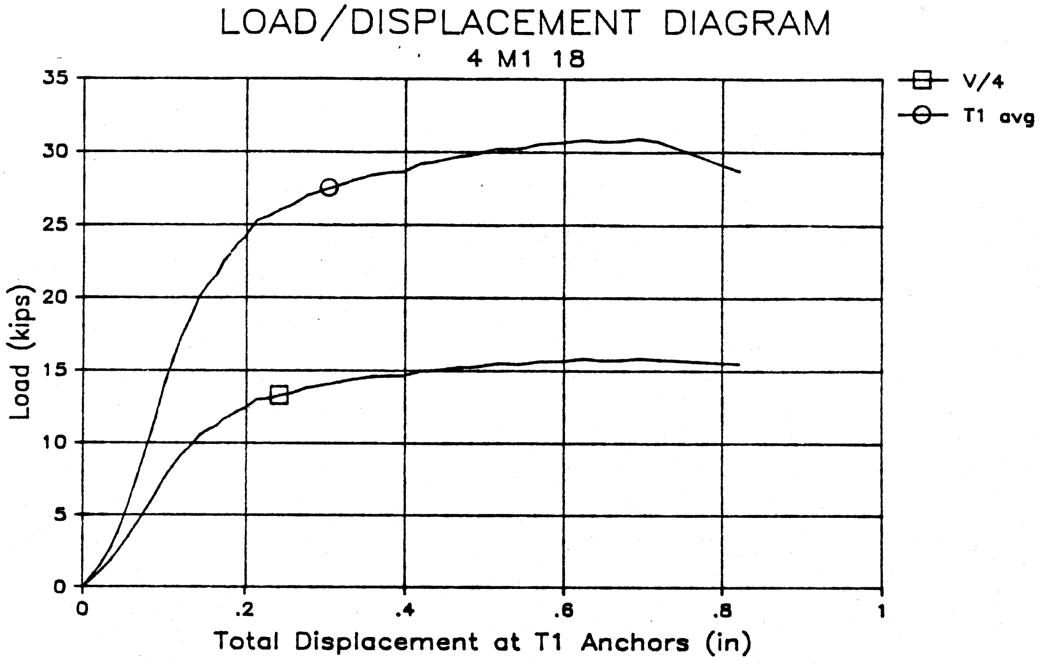
LOAD/DISPLACEMENT DIAGRAM
4 M1 18
V/4
T1 avg
Load (kips)
35
30
25
20
15
10
5
0
0
.2
.4
.6
.8
1
Total Displacement at T1 Anchors (in)

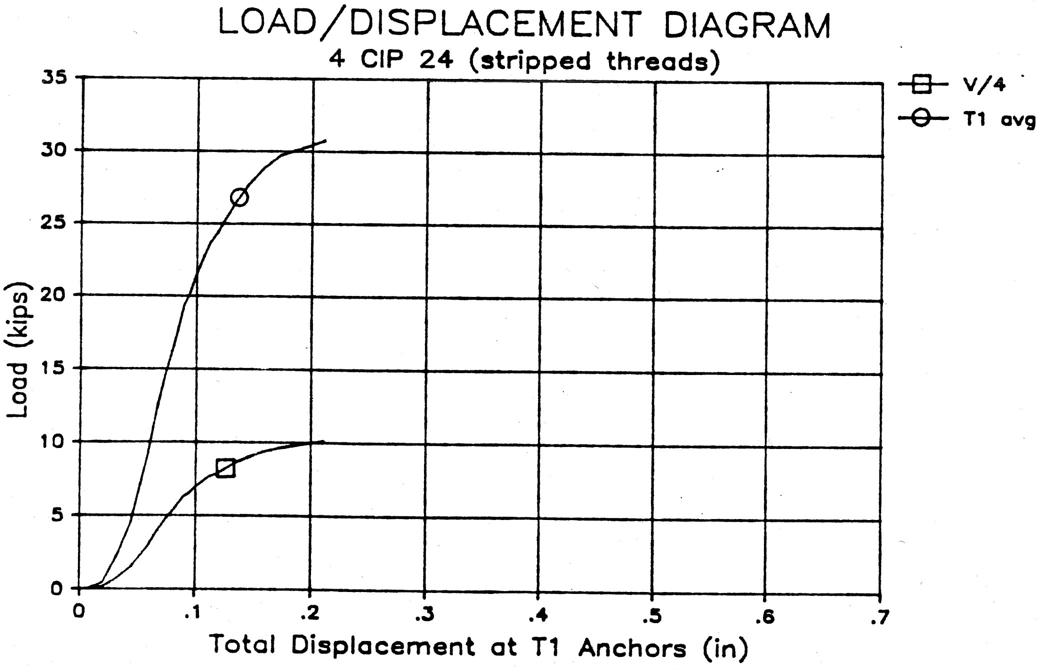
LOAD/DISPLACEMENT DIAGRAM
4 CIP 24 (stripped threads)
V/4
T1 avg
Load (kips)
35
30
25
20
15
10
5
0
0
.1
.2
.3
.4
.5
.6
.7
Total Displacement at T1 Anchors (in)

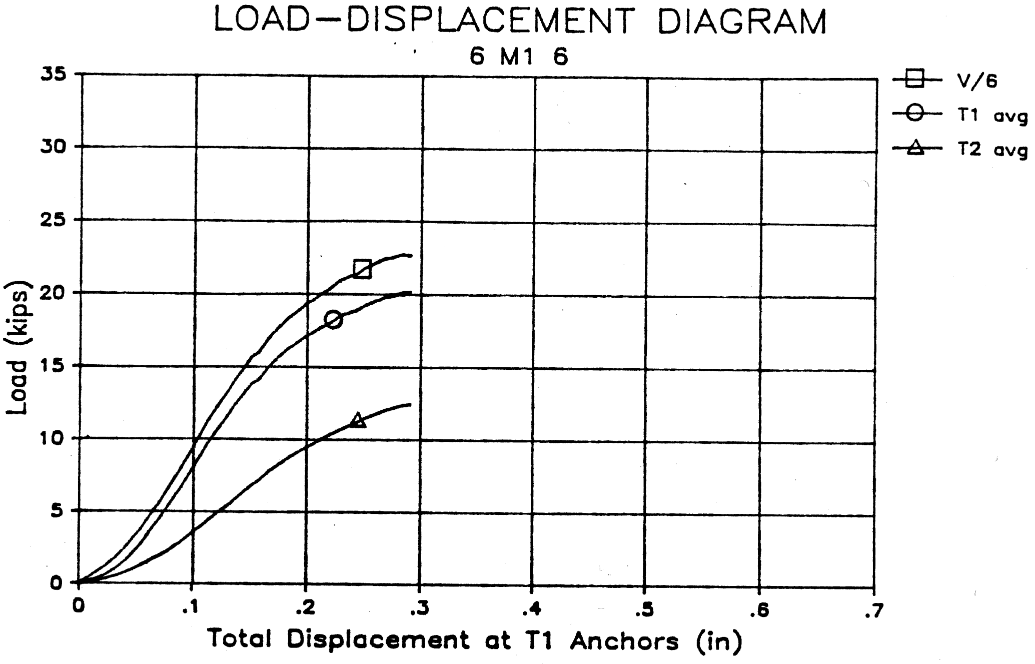
LOAD-DISPLACEMENT DIAGRAM
6 M1 6
Load (kips)
35
30
25
20
15
10
5
0
0
.1
.2
.3
.4
.5
.6
.7
Total Displacement at T1 Anchors (in)
V/6
T1 avg
T2 avg

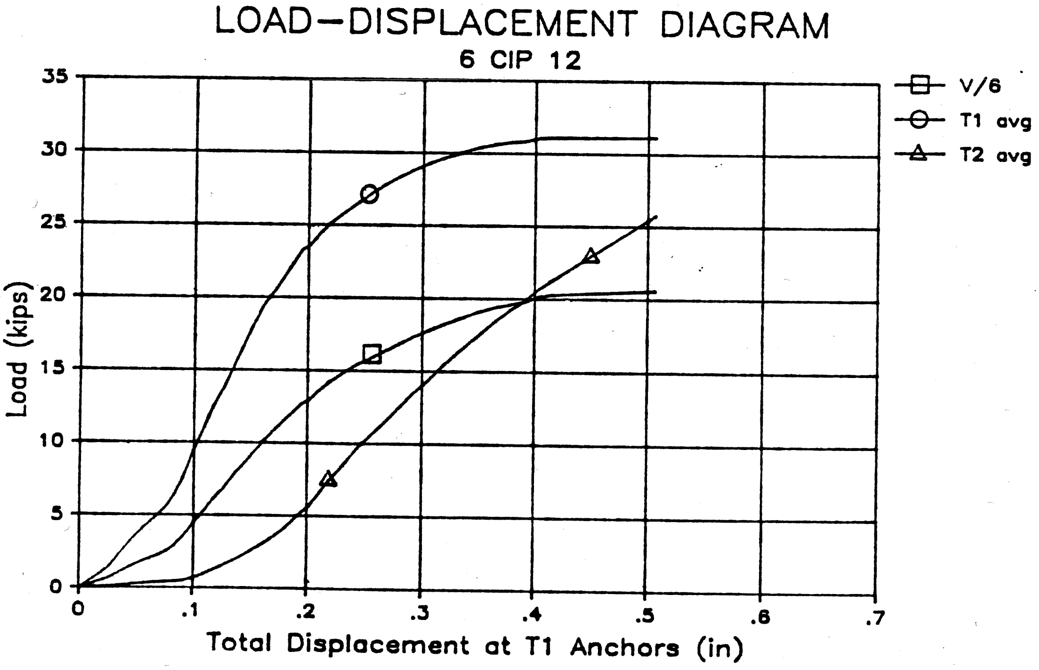
LOAD-DISPLACEMENT DIAGRAM
6 CIP 12
Load (kips)
35
30
25
20
15
10
5
0
0
.1
.2
.3
.4
.5
.6
.7
Total Displacement at T1 Anchors (in)
V/6
T1 avg
T2 avg

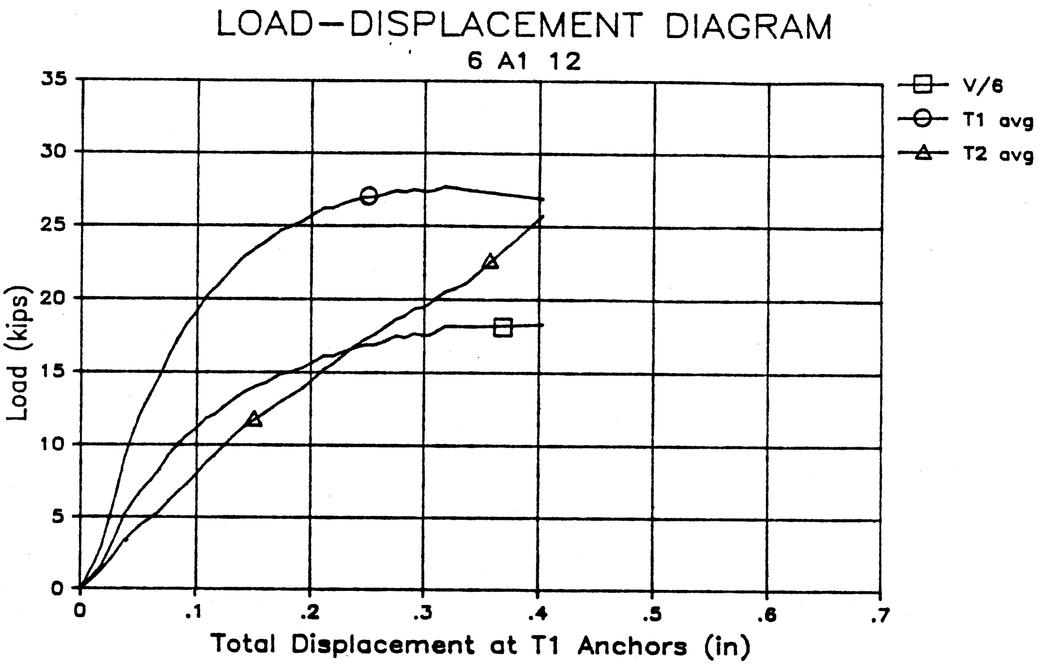
LOAD-DISPLACEMENT DIAGRAM
6 A1 12
V/6
T1 avg
T2 avg
Load (kips)
35
30
25
20
15
10
5
0
0
.1
.2
.3
.4
.5
.6
.7
Total Displacement at T1 Anchors (in)

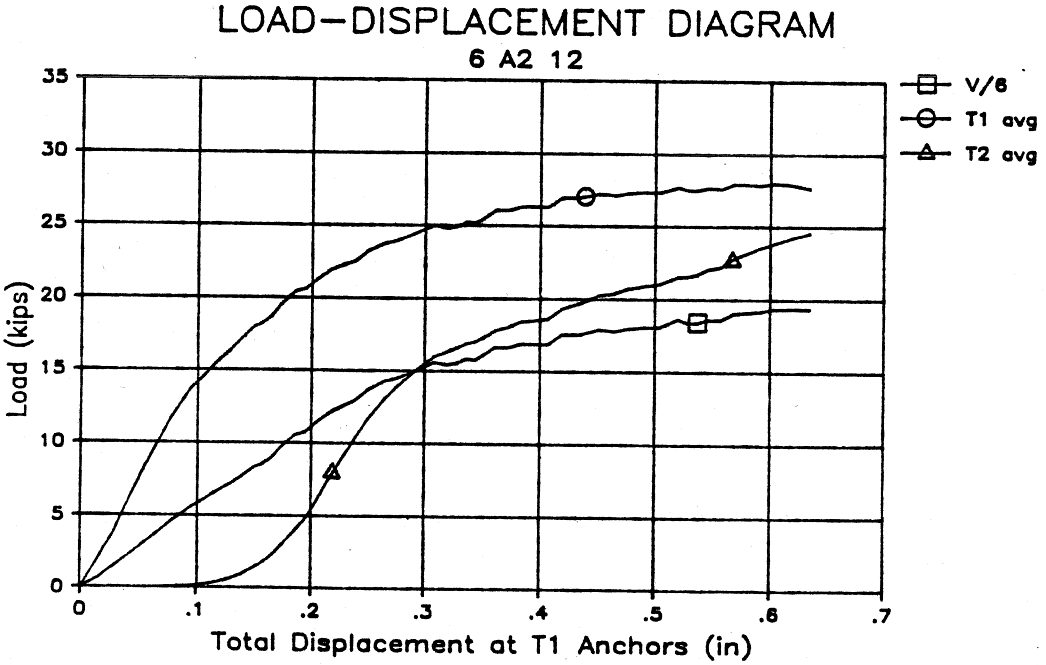
LOAD-DISPLACEMENT DIAGRAM
6 A2 12
V/6
T1 avg
T2 avg
Load (kips)
35
30
25
20
15
10
5
0
0
.1
.2
.3
.4
.5
.6
.7
Total Displacement at T1 Anchors (in)

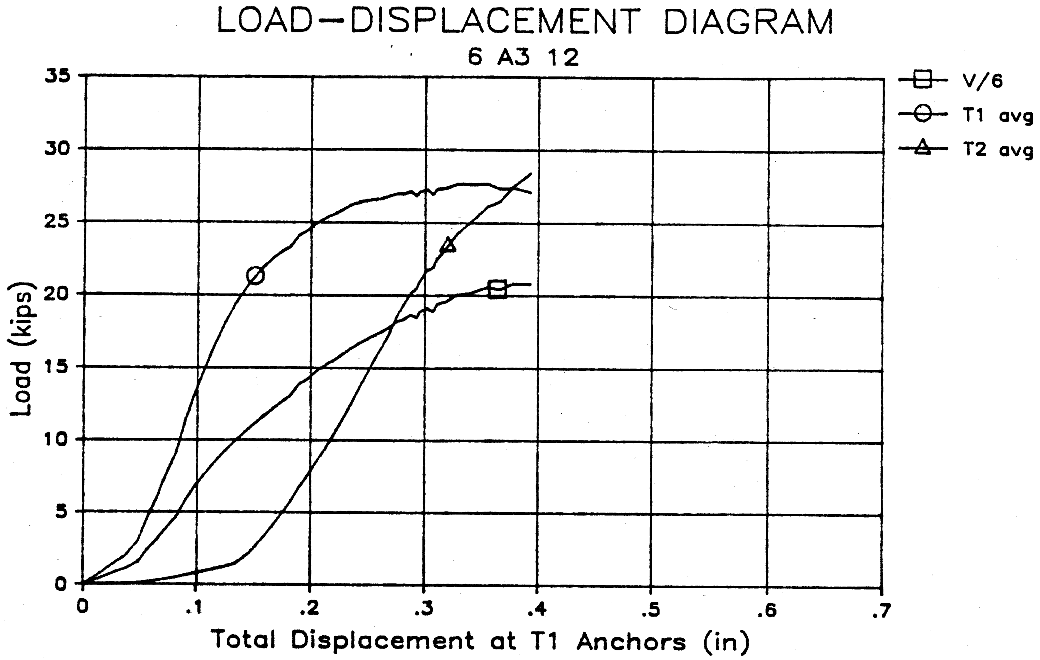
LOAD—DISPLACEMENT DIAGRAM

6 A3 12

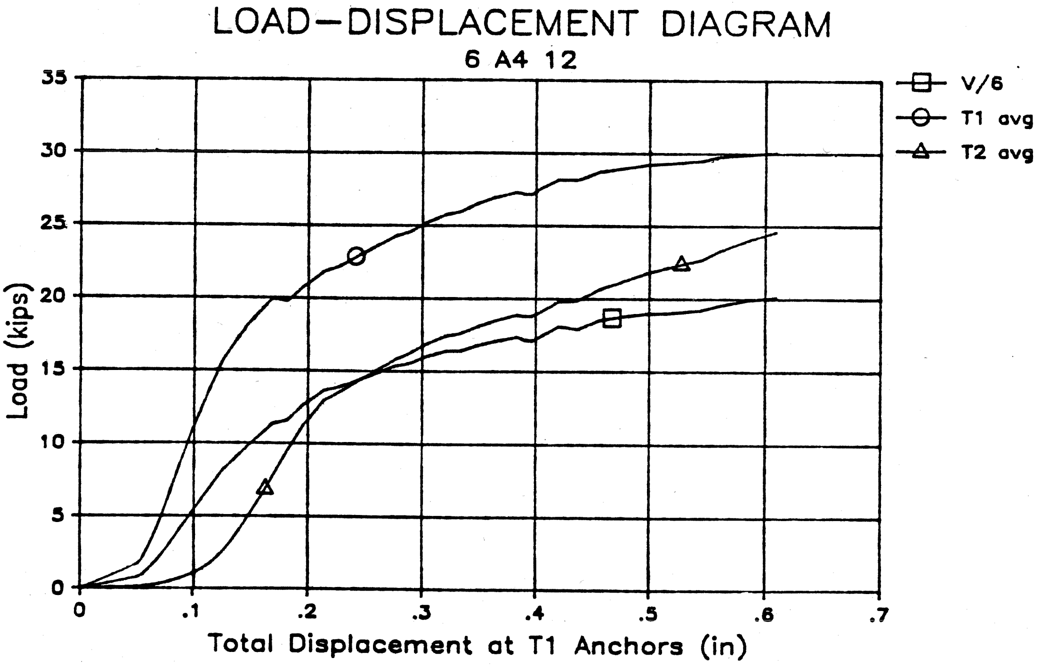
LOAD—DISPLACEMENT DIAGRAM

6 A4 12

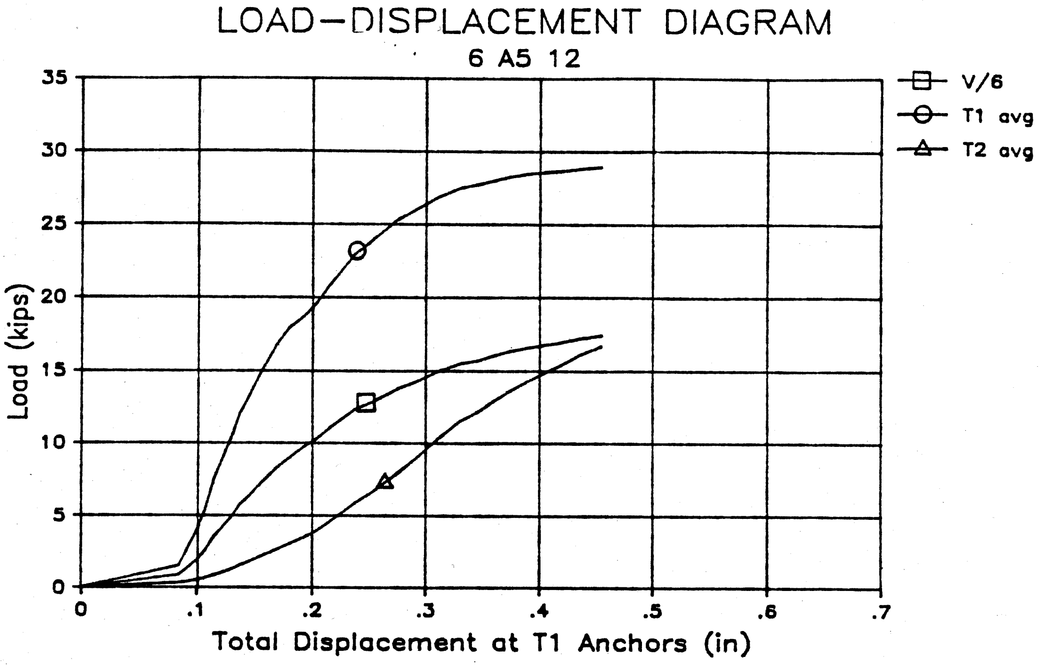
LOAD—DISPLACEMENT DIAGRAM
6 A5 12
V/6
T1 avg
T2 avg
Load (kips)
35
30
25
20
15
10
5
0
0
.1
.2
.3
.4
.5
.6
.7
Total Displacement at T1 Anchors (in)

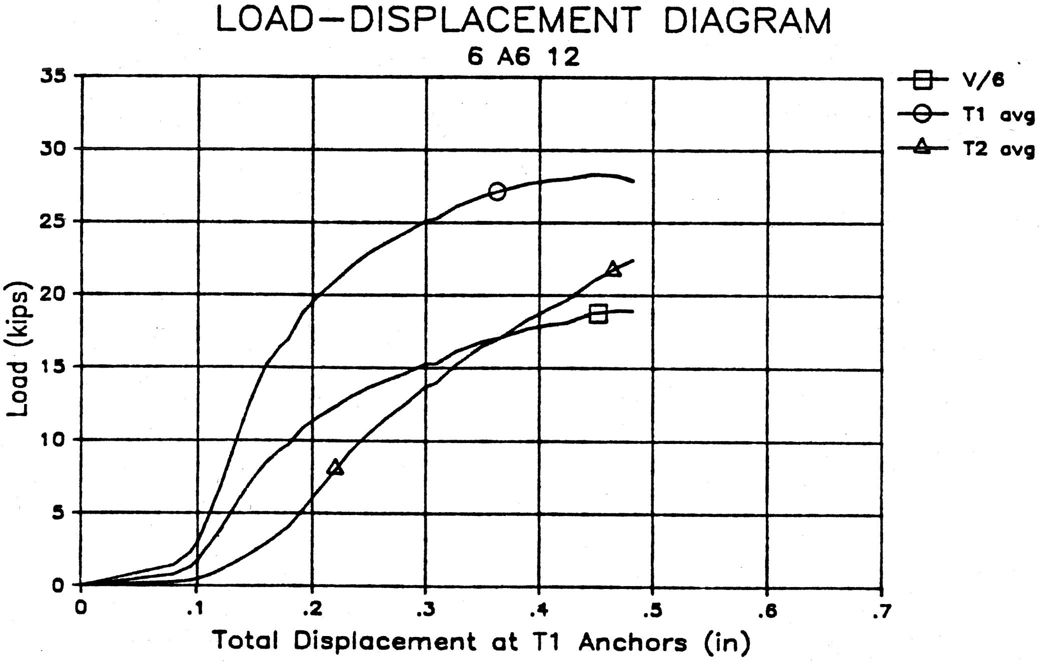
LOAD—DISPLACEMENT DIAGRAM
6 A6 12
V/6
T1 avg
T2 avg
Load (kips)
35
30
25
20
15
10
5
0
0
.1
.2
.3
.4
.5
.6
.7
Total Displacement at T1 Anchors (in)

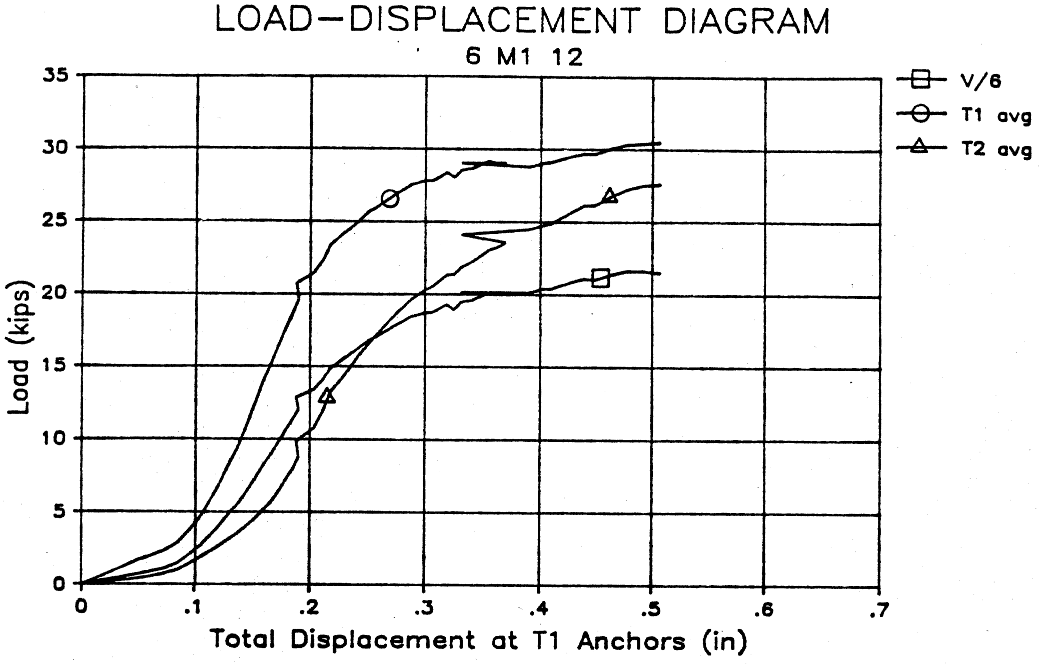
LOAD-DISPLACEMENT DIAGRAM
6 M1 12
V/6
T1 avg
T2 avg
Load (kips)
35
30
25
20
15
10
5
0
0
.1
.2
.3
.4
.5
.6
.7
Total Displacement at T1 Anchors (in)

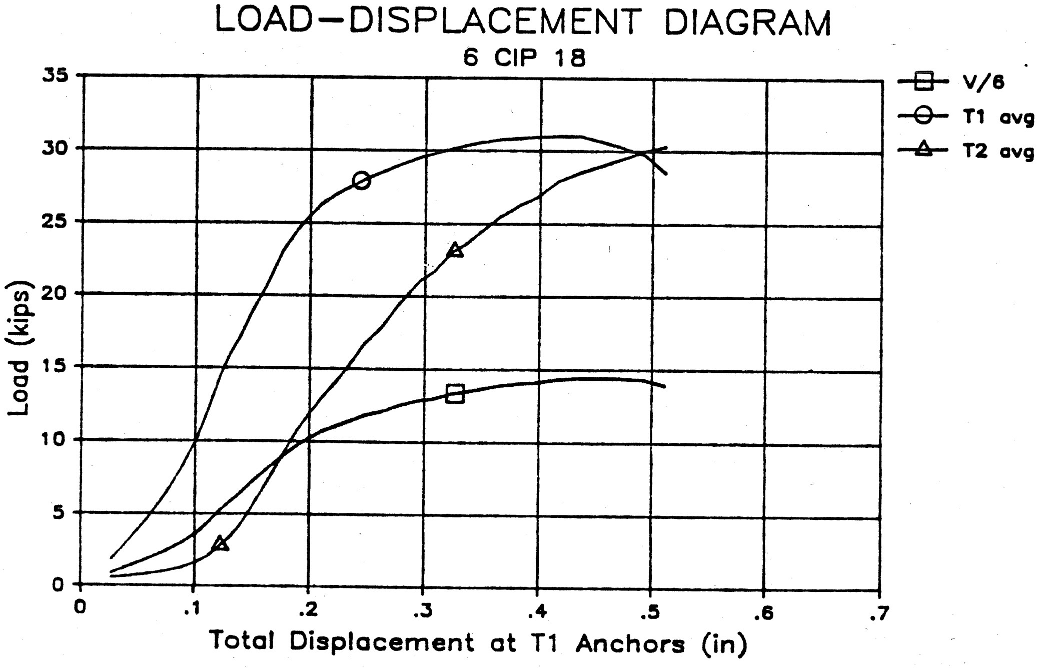
LOAD-DISPLACEMENT DIAGRAM
6 CIP 18
V/6
T1 avg
T2 avg
Load (kips)
35
30
25
20
15
10
5
0
0
.1
.2
.3
.4
.5
.6
.7
Total Displacement at T1 Anchors (in)

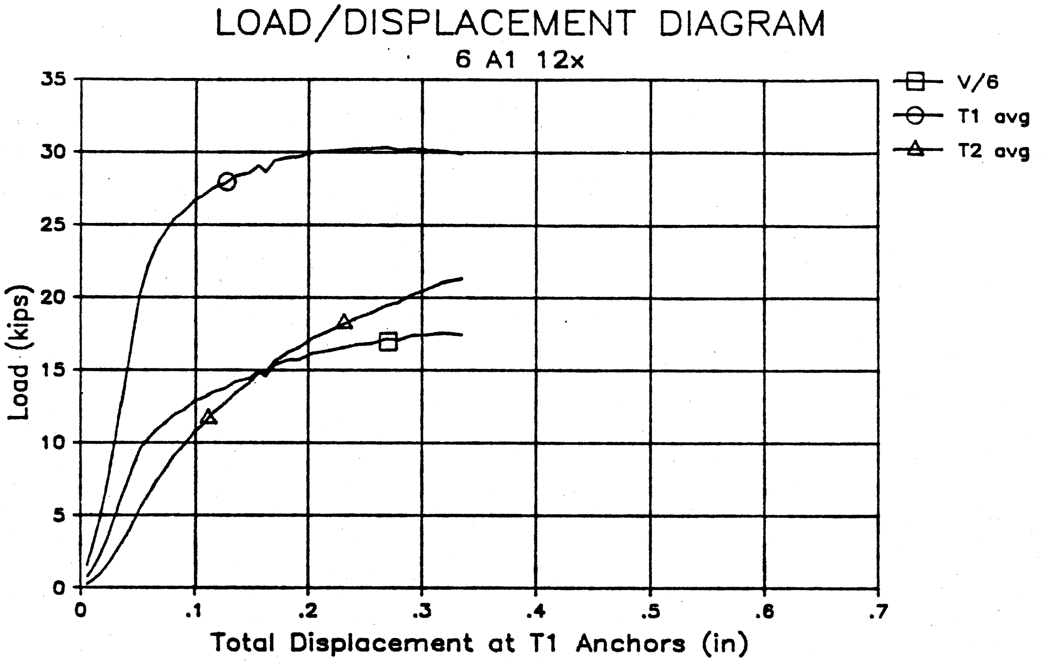
LOAD/DISPLACEMENT DIAGRAM
6 A1 12x
V/6
T1 avg
T2 avg
Load (kips)
0
5
10
15
20
25
30
35
0
.1
.2
.3
.4
.5
.6
.7
Total Displacement at T1 Anchors (in)

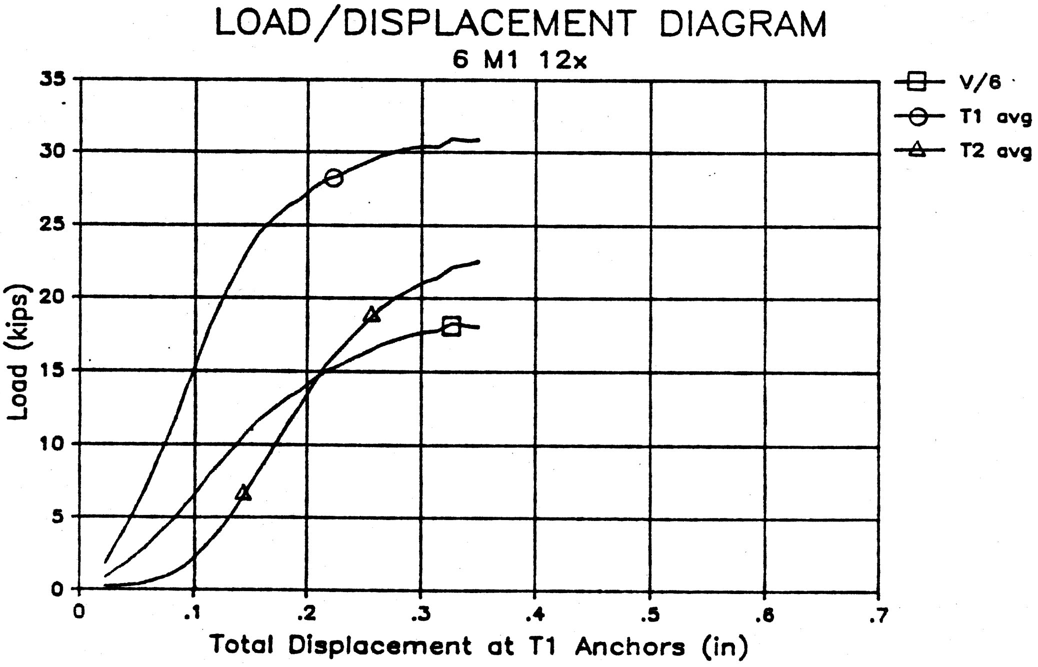
LOAD/DISPLACEMENT DIAGRAM
6 M1 12x
V/6
T1 avg
T2 avg
Load (kips)
0
5
10
15
20
25
30
35
0
.1
.2
.3
.4
.5
.6
.7
Total Displacement at T1 Anchors (in)

REFERENCES

1. Collins, D. M., Cook, R.A. and Klingner, R. E., "Load-Deflection Behavior of Cast-in-Place and Retrofit Concrete Anchors Subjected to Static, Fatigue, and Impact Tensile Loads," **Report No. 1126-1**, Center for Transportation Research, University of Texas at Austin, February 1989.

2. Doerr, G. T. and Klingner, R. E., "Behavior and Design of Adhesive Anchors," **Report No. 1126-2**, Center for Transportation Research, University of Texas at Austin, March 1989.

3. Cook, R. A., Doerr, G. T., Collins, D. M. and Klingner, R. E., "Design Guide for Steel-to-Concrete Connections," **Report No. 1126-4F**, Center for Transportation Research, University of Texas at Austin, March 1989.

4. ACI Committee 349, **Code Requirements for Nuclear Safety Related Structures (ACI 349-85)**, American Concrete Institute, Detroit, 1985.

5. "General Anchorage to Concrete," TVA **Civil Design Standard** No. DS-C1.7.1, Tennessee Valley Authority, Knoxville, TN, 1984.

6. **Manual of Steel Construction, Load and Resistance Factor Design**, 1st Edition, American Institute of Steel Construction, Chicago, Ill., 1986.

7. Abrams, D. A., "Tests of Bond Between Concrete and Steel," **University of Illinois Engineering Experiment Station Bulletin No. 71**, December 1913.

8. "Nelson Stud Project No. 8-Z," **Report No. 1960-16, Concrete Anchor Tests No. 5**, Nelson Stud Welding Company, Lorain, Ohio, 1960.

9. "Concrete Anchor Design Data," **Manual No. 21**, Nelson Stud Welding Company, Lorain, Ohio, 1961.

10. "Nelson Stud Project No. 802," **Report No. 1966-5, Concrete Anchor Tests No. 7**, Nelson Stud Welding Company, Lorain, Ohio, 1966.

11. Shoup, T. E. and Singleton, R. C., "Headed Concrete Anchors," **Proceedings of the American Concrete Institute**, Vol. 60, 1963.

12. **PCI Design Handbook - Precast and Prestressed Concrete**, 1st Edition, Prestressed Concrete Institute, Chicago, 1971.

13. **PCI Manual on Design of Connections for Precast Prestressed Concrete**, 1st Edition, Prestressed Concrete Institute, Chicago, 1973.

14. "Structural Engineering Aspects of Headed Concrete Anchors and Deformed Bar Anchors in the Concrete Industry," **Report No. SA 1-KSM 130- 5-970**, KSM Welding Systems, Omark Industries, Moorestown, New Jersey, 1971.

15. Breen, J. E., "Development Length for Anchor Bolts," **Research Report 55-1F**, Center for Highway Research, The University of Texas at Austin, April 1964.

16. Lee, D. W., and Breen, J. E., "Factors Affecting Anchor Bolt Development," **Research Report 88-1F**, Center for Highway Research, The University of Texas at Austin, August 1966.

17. Conrad, R. F., "Test of Grouted Anchor Bolts in Tension and Shear," **Proceedings of the American Concrete Institute**, Vol. 66, No. 9, September 1969.

18. Ollgaard, J. G., Slutter, R. G. and Fisher, J. W., "Shear Strength of Stud Connectors in Lightweight and Normal-Weight Concrete," **Engineering Journal, AISC**, Vol. 8, No. 2, April 1971.

19. McMackin, P. J., Slutter, R. G. and Fisher, J. W., "Headed Steel Anchors under Combined Loading," **Engineering Journal, AISC**, Second Quarter, 1973.

20. "Embedment Properties of Headed Studs," **Design Data 10**, TRW Nelson Division, Lorain, Ohio, 1974.

21. **PCI Manual for Structural Design of Architectural Precast Concrete**, First Edition, Prestressed Concrete Institute, Chicago, 1977.

22. **PCI Design Handbook - Precast and Prestressed Concrete**, 2nd Edition, Prestressed Concrete Institute, Chicago, 1978.

23. **PCI Design Handbook - Precast and Prestressed Concrete**, 3rd Edition, Prestressed Concrete Institute, Chicago, 1985.

24. "Anchorage to Concrete," TVA **CEB Report No. 75-32**, Tennessee Valley Authority, Knoxville, 1975.

25. Bailey, J. W. and Burdette, E. G., "Edge Effects on Anchorage to Concrete," **Civil Engineering Research Series No. 31**, The University of Tennessee at Knoxville, August 1977.

26. "General Anchorage to Concrete," TVA **Civil Design Standard** No. DS-C6.1, Tennessee Valley Authority, Knoxville, 1975.

27. ACI Committee 349, **Code Requirements for Nuclear Safety Related Structures (ACI 349-76 with 1979 Supplement)**, American Concrete Institute, Detroit, 1979.

28. Cannon, R. W., Godfrey, D. A., and Moreadith, F. L., "Guide to The Design of Anchor Bolts and Other Steel Embedments," **Concrete International**, Vol. 3, No. 7, July 1981.

29. Swirsky, R. A., Dusel, J. P., Crozier, W. F., Stoker, J. R., and Nordlin, E. F., "Lateral Resistance of Anchor Bolts Installed in Concrete," **Report No. FHWA-CA-ST-4167-77-12**, California Department of Transportation, Sacramento, May 1977.

30. Adihardjo, R. and Soltis, L., "Combined Shear and Tension on Grouted Base Details," **Engineering Journal, AISC**, Vol. 16, No. 1, 1979.

31. Klingner, R. E., Mendonca, J. A. and Malik, J. B., "Effect of Reinforcing Details on the Shear Resistance of Anchor Bolts Under Reversed Cyclic Loading," **Journal of the American Concrete Institute**, Vol. 79, No. 1, January-February 1982.

32. Klingner, R. E. and Mendonca, J. A., "Tensile Capacity of Short Anchor Bolts and Welded Studs: A Literature Review," **Journal of the American Concrete Institute**, Vol. 79, No. 4, July-August 1982.

33. Klingner, R. E. and Mendonca, J. A., "Shear Capacity of Short Anchor Bolts and Welded Studs - A Literature Review," **Journal of the American Concrete Institute**, Vol. 79, No. 5, September-October 1982.

34. "Testing of Special Anchors for Basic Data," TVA **CEB Report No. 80-64**, Tennessee Valley Authority, Knoxville, 1980.

35. Stethen, S. D. and Burdette, E. G., "Concrete Anchorage Performance in Cracked One-Way Slabs," **Civil Engineering Research Series No. 38**, The University of Tennessee at Knoxville, March 1981.

36. Burdette, E. G., "Tests of Drillco Maxi-Bolts in Combined Tension and Shear," Department of Civil Engineering, The University of Tennessee, Knoxville, August 1981.

37. Cones, M. A., "Analysis of Tests on Grouting of Anchor Bolts into Hardened Concrete," Paper presented at the 1982 Annual Convention, American Concrete Institute, Atlanta, 1982.

38. Ghodsi, F. and Breen, J. E., "Behavior and Design of Expansion Anchors Under Tension Pullout Force," Paper presented at the 1983 Annual Convention, American Concrete Institute, Los Angelos, 1983.

39. Elfgren, L., Broms, C., Cederwall, K., and Gylltoft, K., "Anchor Bolts in Reinforced Concrete Foundations," **Anchorage to Concrete (ACI SP-103)**, 1987.

40. Bode, H. and Roik, K., "Headed Studs - Embedded in Concrete and Loaded in Tension," **Anchorage to Concrete (ACI SP- 103)**, 1987.

41. Schwartz, F., "Wedge-Type Expansion Anchor Performance in Tension," **Anchorage to Concrete (ACI SP-103)**, 1987.

42. Burdette, E. G., Perry, T. and Funk, R., "Tests of Undercut Anchors," **Anchorage to Concrete (ACI SP-103)**, 1987.

43. Eligehausen, R., "Anchorage to Concrete by Metallic Expansion Anchors," **Anchorage to Concrete (ACI SP-103)**, 1987.

44. Hasselwander, G. B., Jirsa, J. O., and Breen, J. E., "Strength and Behavior of Single Cast-in-Place Anchor Bolts Subject to Tension," **Anchorage to Concrete (ACI SP-103)**, 1987.

45. Hawkins, N. M., "Strength in Shear and Tension of Cast-in- Place Anchor Bolts," **Anchorage to Concrete (ACI SP- 103)**, 1987.

46. Dusel, J. P., and Harrington, C. N., "The Evaluation of Mechanical Expansion Anchors," **Report No. FHWA/CA/TL- 86/09**, California Department of Transportation, Sacramento, July 1986.

47. Mahoney, E. H., Jr. and Burdette, E. G., "Moment Resistant Concrete Anchorages: A Parameter Study," **Civil Engineering Research Series No. 33**, The University of Tennessee at Knoxville, September 1978.

48. "Anchorage Tests of Load Transfer Through Flexible Plate: Interim Report," TVA **CEB Report No. 78-21**, Tennessee Valley Authority, Knoxville, 1978.

49. "Welded Stud Anchors - Effect of Plate Flexibility on Stud Capacity," TVA **CEB Report No. 79-18**, Tennessee Valley Authority, Knoxville, 1979.

50. "Welded Stud Anchors - Effect of Bending Studs on Capacity and Load-Deflection Behavior," TVA **CEB Report No. 80-1**, Tennessee Valley Authority, Knoxville, 1980.

51. Armstrong, K. S., Klingner, R. E. and Steves, M. A., "Response of Highway Barriers to Repeated Impact Loads: Steel Post Barriers," **Research Report 382-1**, Center for Transportation Research, The University of Texas at Austin, November 1985.

52. DeWolf, J. T. and Sarisley, E. F., "Column Base Plates with Axial Loads and Moments," **Journal of the Structural Division, ASCE**, Vol. 106, ST11, November 1980.

53. Thambiratnam, D. P. and Paramasivam, "Base Plates Under Axial Loads and Moments," **Journal of the Structural Division, ASCE**, Vol. 112, No. 5, May 1986.

54. "Eight-Bolt Base Plate Tests," **Report No. EQL 65/84 E**, Hilti Technical Center, 1984.

55. Picard, A. and Beaulieu, D., "Behaviour of a Simple Column Base Connection," **Canadian Journal of Civil Engineering**, Vol. 12, No. 1, March 1985.

56. Hawkins, N. M., Mitchell, D. and Roeder, C. W., "Moment Resisting Connections for Mixed Construction," **Engineering Journal, AISC**, First Quarter, January 1980.

57. Marsh, M. L. and Burdette, E. G., "Anchorage of Steel Building Components to Concrete," **Engineering Journal, AISC**, Vol. 22, No. 1, First Quarter, 1985.

58. DeWolf, J. T., "Column Anchorage Design," **Proceedings of the National Engineering Conference: Conference of Operating Personnel**, AISI, April 1987.

59. Slaughter, E. M., "Tests on Threaded Sections Show Exact Strengthening Effect of Threads," **Metal Progress**, Vol.23, No. 3, March 1933.

60. Kulak, G. L., Fisher, J. W., and Struik, J. H. A., **Guide to Design Criteria for Bolted and Riveted Joints**, 2nd Edition, John Wiley and Sons, New York, 1987.

61. Chesson, E., Jr., Faustino, N. L. and Munse, W. H., "High- Strength Bolts Subjected to Tension and Shear," **Journal of the Structural Division, ASCE**, Vol. 91, ST5, October 1965.

62. Birkeland, P. W. and Birkeland H. W., "Connections in Precast Concrete Construction," **Journal of the American Concrete Institute**, Vol. 63, No. 3, March 1966.

63. Hofbeck, J. A., Ibrahim, I. O. and Mattock, A. H., "Shear Transfer in Reinforced Concrete," **Journal of the American Concrete Institute**, Vol. 66, No. 2, February 1969.

64. Mattock, A. H. and Hawkins, N. M., "Shear Transfer in Reinforced Concrete - Recent Research," **Journal of the Prestressed Concrete Institute**, Vol. 17, No. 2, March-April 1972.

65. Blodgett, O. W., **Design of Welded Structures**, The James F. Lincoln Arc Welding Foundation, Cleveland, Ohio, 1966.

66. Gaylord, E. H. and Gaylord, C. N., **Design of Steel Structures**, 2nd Edition, McGraw-Hill Book Co., New York, 1972.

67. Tall, L. et al., **Structural Steel Design**, 2nd Edition, Ronald Press Company, New York, 1974.

68. Miatra, N., "Graphical Aid for Design of Base Plate Subjected to Moment," **Engineering Journal, AISC**, Vol. 15, No. 2, Second Quarter, 1978.

69. Salmon, C. G. and Johnson, J. E.,**Steel Structures**, 2nd Edition, Harper and Row, New York, 1980.

70. Shipp, J. G. and Haninger, E. R., "Design of Headed Anchor Bolts," **Engineering Journal, AISC**, Vol. 20, No. 2, Second Quarter, 1983.

71. Holmes, M. and Martin, L. H., **Analysis and Design of Structural Connections: Reinforced Concrete and Steel**, Ellis Horwood Limited, Chichester, England, 1983.

72. "All Projects, Steel to Concrete Coefficient of Friction, Preliminary Tests," TVA **CEB Report No. 77-46**, Tennessee Valley Authority, Knoxville, 1977.

73. Rabbat, B. G. and Russell, H. G., "Friction Coefficient of Steel on Concrete or Grout," **Journal of the Structural Division, ASCE**, Vol. 111, No. 3, March 1985.

74. Marsh, M. L. and Burdette, E. G., "Multiple Bolt Anchorages: Method for Determining the Effective Projected Area of Overlapping Stress Cones," **Engineering Journal, AISC**, Vol. 22, No. 1, First Quarter, 1985.

75. Siddiqui, M. A., and Beseler, J. W., "Computing Concrete Pullout Strength," **Concrete International**, February 1989.

76. Meinheit, D. F. and Heidbrink, F. D., "Behavior of Drilled-In Expansion Anchors," **Concrete International**, Vol. 7, No. 4, April 1985.

You are invited to share
in our wedding ceremony

Sunday, December 31, 1989, 12:15pm
at The Charles W. Moore House
2102 Quarry Road, Austin, TX

RSVP by December 10
By invitation only

You are invited to share
in our wedding ceremony

Sunday, December 31, 1989, 12:15pm
at The Charles W. Moore House
2102 Quarry Road, Austin, TX

RSVP by December 10
By invitation only

You are invited to share
in our wedding ceremony

Sunday, December 31, 1989, 12:15pm
at The Charles W. Moore House
2102 Quarry Road, Austin, TX

RSVP by December 10
By invitation only

You are invited to share
in our wedding ceremony

Sunday, December 31, 1989, 12:15pm
at The Charles W. Moore House
2102 Quarry Road, Austin, TX

RSVP by December 10
By invitation only

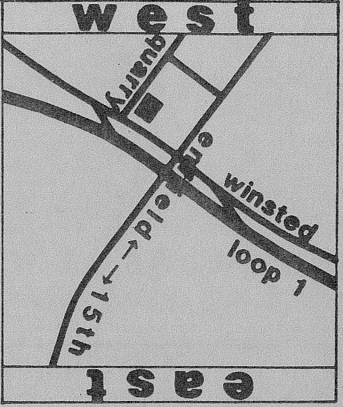

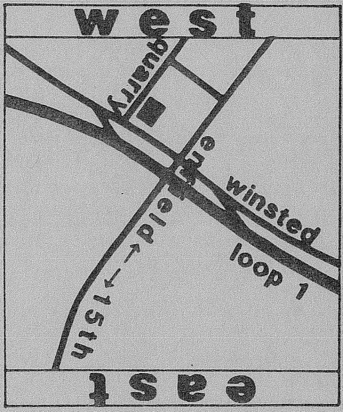

We're really sorry, but due to the nature of the location
Please do not bring your children
Thank You.

We're really sorry, but due to the nature of the location
Please do not bring your children
Thank You.

We're really sorry, but due to the nature of the location
Please do not bring your children
Thank You.

We're really sorry, but due to the nature of the location
Please do not bring your children
Thank You.

We're really sorry, but due to the nature of the location
Please do not bring your children
Thank You.

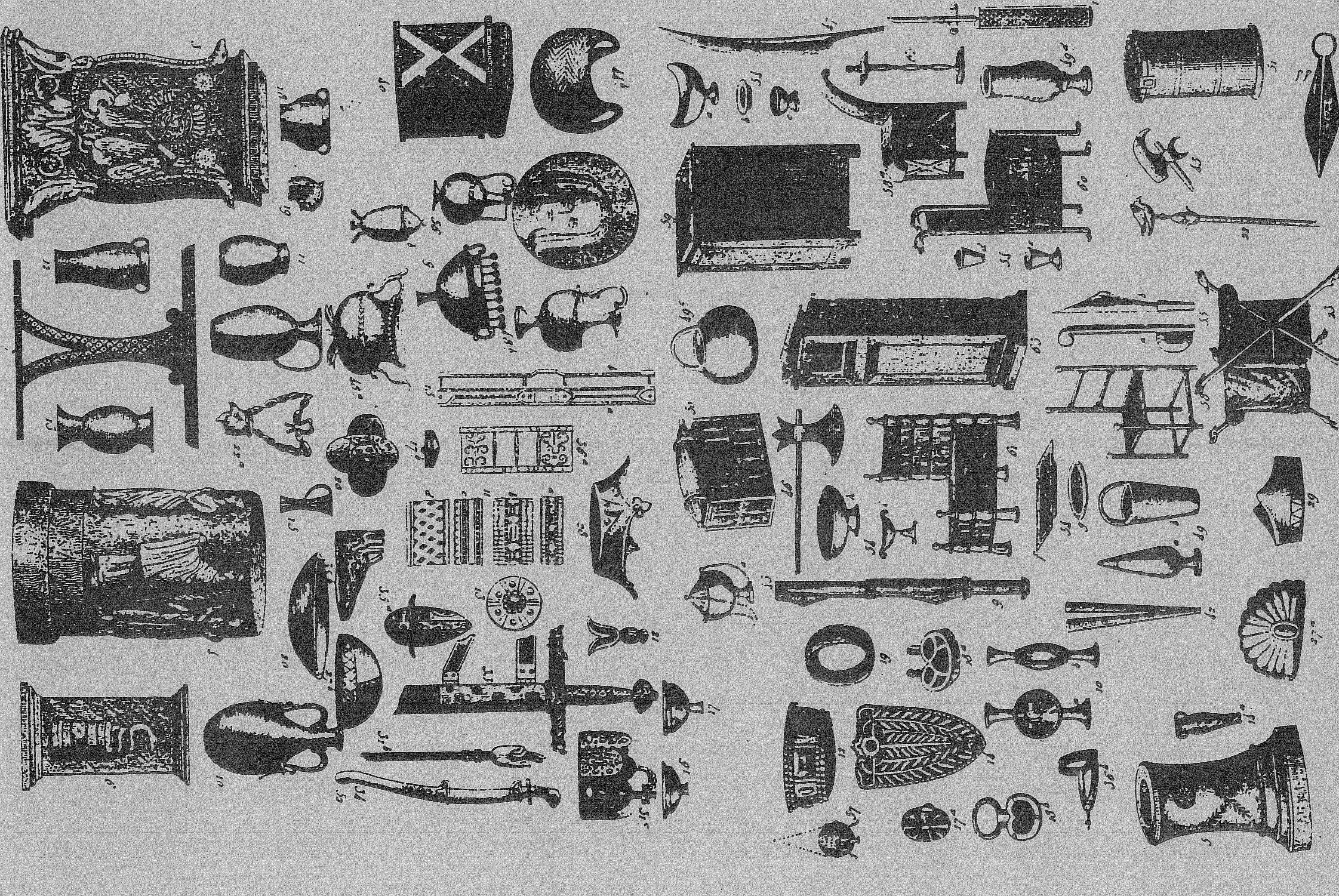We're really sorry, but due to the nature of the location
Please do not bring your children
Thank You.